



TECHNISCHE UNIVERSITÄT MÜNCHEN

Lehrstuhl für Technische Mikrobiologie

Identification of factors affecting the high pressure tolerance of *Clostridium botulinum* type E endospores

Juliane Schnabel

Vollständiger Abdruck der von der Fakultät Wissenschaftszentrum Weihenstephan für Ernährung, Landnutzung und Umwelt der Technischen Universität München zur Erlangung des akademischen Grades eines

Doktors der Naturwissenschaften

genehmigten Dissertation.

Vorsitzender: Univ.-Prof. Dr. H.-Chr. Langowski

Prüfer der Dissertation: 1. Univ.-Prof. Dr. R. F. Vogel

2. Univ.-Prof. Dr. W. Liebl

Die Dissertation wurde am 15.12.2014 bei der Technischen Universität München eingereicht und durch die Fakultät Wissenschaftszentrum Weihenstephan für Ernährung, Landnutzung und Umwelt am 24.02.2015 angenommen.

VORWORT UND DANKSAGUNG

Die vorliegende Arbeit entstand im Rahmen eines vom Bundesministerium für Ernährung, Landwirtschaft und Verbraucherschutz (BMELV) geförderten Projektes (PGI-0313849A).

Besonders möchte ich mich bei meinem Doktorvater, Herrn Prof. Dr. Rudi F. Vogel, für die Überlassung meines Promotionsthemas, die Bereitstellung aller nötigen Mittel, die kompetente wissenschaftliche Unterstützung und die herzliche Betreuung bedanken.

Mein Dank gilt auch Herrn Prof. Dr. Wolfgang Liebl für die Übernahme des Korreferats und Herrn Prof. Dr. Horst-Christian Langowski für die Übernahme des Prüfungsvorsitzes.

Des Weiteren möchte ich mich bei Christian A. Lenz für die kompetente und aktive Unterstützung, sowie für die unkomplizierte Zusammenarbeit bedanken, die maßgeblich zur Fertigstellung dieser Arbeit beigetragen hat.

Außerdem möchte ich mich herzlich bei Dr. Jürgen Behr für die zahlreichen, wissenschaftlichen Anregungen und Hilfestellungen, sowie für die tatkräftige Unterstützung im Bereich der bioinformatischen Datenverarbeitung bedanken. Zusätzlich möchte ich mich bei Julia C. Usbeck, Carola C. Kern und Dr. Patrick Preißler für Hilfestellungen im Bereich der Proteinanalytik bedanken.

Ich danke auch Prof. Dr. Matthias Ehrmann und Prof. Dr. Ludwig Niessen für die zahlreichen Ratschläge und Anregungen.

Ebenso danke ich Angela Seppeur, Monika Hadek, Margarete Schreiber und Andrea Pape für die stetige Hilfsbereitschaft sowohl in organisatorischen als auch in praktischen Bereichen.

Außerdem möchte ich mich bei der Abteilung für Lebensmittelbiotechnologie und Lebensmittelverfahrenstechnik der TU Berlin und seinem ehemaligen Leiter, Prof. Dr. Dietrich Knorr, für die Bereitstellung von Hochdruckanlagen und für die aktive Unterstützung durch seine Mitarbeiter Dipl.-Ing. Robert Sevenich und Stefan Boguslawski bedanken.

Des Weiteren möchte ich mich bei allen derzeitigen und ehemaligen Arbeitskollegen des Lehrstuhls für Technische Mikrobiologie für die kollegiale Zusammenarbeit und das angenehme Arbeitsklima bedanken.

Ganz besonders möchte ich mich bei meiner Familie für die stetige Unterstützung und den beachtlichen Rückhalt bedanken, den sie mir in jeglicher Situation entgegen gebracht hat.

CONTENTS

1	INTRODUCTION	1
1.1	High pressure processing of food	1
1.2	The food pathogen <i>Clostridium botulinum</i>	2
1.3	Bacterial endospores	5
1.3.1	Sporulation	5
1.3.2	Structure of bacterial endospores	6
1.3.3	Spore germination	7
1.4	High pressure/heat-induced inactivation of bacterial endospores	8
1.5	Objectives of this work	10
1.5.1	Generation of <i>C. botulinum</i> type E knock out mutants	10
1.5.2	Correlation of medium-induced endospore resistance and proteome pattern.....	11
1.5.3	High pressure/temperature-induced inactivation of endospores in emulsion matrices	11
2	MATERIAL AND METHODS	13
2.1	Material	13
2.1.1	Equipment	13
2.1.2	Chemicals.....	16
2.1.3	Enzymes.....	19
2.1.4	Consumables	20
2.1.5	Molecular biological kits	21
2.1.6	Primers	21
2.1.7	Vectors	22
2.1.8	Bacterial strains.....	23
2.2	Methods	24
2.2.1	Media, growth conditions and strain storage	24
2.2.2	Strain storage	26

2.2.3	Preparation and purification of endospore suspensions.....	26
2.2.4	Molecular biological methods.....	28
2.2.5	Clostron mutagenesis	33
2.2.6	Circumvention of putative restriction barriers of <i>C. botulinum</i> type E.....	37
2.2.7	Methods for protein analysis	40
2.2.8	Characterization of soybean oil emulsions and high pressure-induced endospore inactivation in emulsion matrices	44
3	RESULTS.....	50
3.1	Transformation of <i>C. botulinum</i> type E strains.....	50
3.1.1	Selection of <i>C. botulinum</i> type E strains for knock out and transformation experiments.....	50
3.1.2	Transformation of <i>C. botulinum</i> type E strains by <i>E. coli</i> mediated conjugation.....	51
3.1.3	Transformation of <i>C. botulinum</i> type E strains by electroporation	52
3.1.4	Circumvention of putative restriction barriers of <i>C. botulinum</i> type E.....	53
3.1.5	Plasmid methylation by employing the methyltransferase (CLO_1092) of <i>C. botulinum</i> (TMW 2.990)	55
3.1.6	Restriction assay and plasmid methylation by cell free extracts of <i>C. botulinum</i> (TMW 2.990).....	58
3.2	Influence of sporulation medium on spore proteomes of <i>C. botulinum</i> type E	60
3.2.1	Strain- and medium-dependent character of <i>C. botulinum</i> type E spore proteomes.....	60
3.2.2	Identification of predominant proteins in SFE-derived endospores by MALDI-TOF MS	61
3.2.3	Identification of predominant proteins in SFE-derived endospores by high resolution LC- MS/MS.....	63
3.3	Characterization of soybean oil emulsions and HPT-induced endospore inactivation in emulsion matrices	66
3.3.1	Characterization of soybean oil emulsions	66
3.3.2	Determination of endospore localization in heterogenic oil/buffer mixtures	79
3.3.3	Inactivation of <i>C. botulinum</i> type E endospores in emulsion matrices.....	84
4	DISCUSSION	92

4.1	Knock out generation of <i>C. botulinum</i> type E strains.....	92
4.1.1	Strain selection for Clostron mutagenesis	93
4.1.2	Choice of Clostron plasmids for <i>C. botulinum</i> type E mutagenesis.....	94
4.1.3	Transformation of <i>C. botulinum</i> type E strains.....	96
4.1.4	Transformation of <i>C. botulinum</i> type E strains by conjugation	96
4.1.5	Transformation of <i>C. botulinum</i> type E strains by electroporation.....	98
4.1.6	Restriction modification systems.....	101
4.1.7	Conclusion: Knock out generation of <i>C. botulinum</i> type E strains.....	110
4.2	Influence of the sporulation medium on <i>C. botulinum</i> type E spore proteomes	111
4.2.1	MALDI-TOF MS analyses of medium-dependent spore proteomes.....	112
4.2.2	Identification of predominant proteins in SFE-derived endospores by high resolution LC-MS/MS.....	118
4.2.3	Conclusion: Influence of the sporulation medium on <i>C. botulinum</i> type E spore proteomes	120
4.3	HPT-induced inactivation of <i>C. botulinum</i> type E spores in model emulsion matrices.....	121
4.3.1	Characterization of model emulsions	121
4.3.2	Determination of endospore distribution in oily systems.....	126
4.3.3	Inactivation of <i>C. botulinum</i> type E endospores in emulsion matrices by heat treatment .	130
4.3.4	Inactivation of <i>C. botulinum type E</i> endospores in emulsion matrices by HPT treatment .	133
4.3.5	Conclusion: HPT-induced inactivation of <i>C. botulinum</i> type E spores in model emulsion systems	136
	SUMMARY	137
	ZUSAMMENFASSUNG	142
	REFERENCES.....	148
	APPENDIX	164

TABLE OF FIGURES

Figure 1: Structure of a bacterial endospore.....	7
Figure 2: Simplified model of the nutrient and pressure-induced endospore germination cascade	9
Figure 3: Plasmid map of pMTL007-E2.....	34
Figure 4: ClosTron mutagenesis by using ClosTron Plasmid pMTL007C-E2.....	35
Figure 5: Definition of oil-, inter- and buffer-phase.....	47
Figure 6: Gene detection in <i>C. botulinum</i> type E strains, by PCR amplification.	51
Figure 7: BspHI-mediated digestion of <i>E. coli</i> CA434-derived ClosTron plasmids	52
Figure 8: Digestion of ClosTron plasmids, reisolated from different <i>E. coli</i> strains	53
Figure 9: Evidence of double <i>E. coli</i> GM2163 transformation.....	55
Figure 10: Confirmation of pBAD/Myc-His A-Met.....	56
Figure 11: Methyltransferase expression in <i>E. coli</i> Top10	56
Figure 12: BspHI-mediated digestion of pBAD/Myc-His A-Met and ClosTron plasmids.....	57
Figure 13: Crude extract-mediated digestion of pMTL007C-E2:53144-Cbo-gpr	59
Figure 14: ClosTron plasmids after <i>in vitro</i> methylation	60
Figure 15: Cluster of MALDI-TOF MS endospore spectra	61
Figure 16: Venn diagram	63
Figure 17: SDS-PAGE of endospore proteins.....	63
Figure 18: Alignment of identified peptide fragments against the amino acid sequence of the putative surface/cell-adhesion protein/N-acetylmuramoyl-L-alanine amidase (WP_004461520.1) of <i>C. sporogenes</i>	65
Figure 19: Slopes of integral creaming kinetics, according to untreated soybean oil emulsions.....	67
Figure 20: Slopes of integral creaming kinetics according to heat-, pressure- and HPT-treated soybean oil emulsions	68
Figure 21: Particle-size distribution of soybean oil emulsions, prior and after heat-, pressure- and HPT-treatment.....	72
Figure 22: Diameters of soybean oil droplets during compression and decompression.....	74
Figure 23: Diameters of soybean oil droplets during compression and decompression.....	75
Figure 24: Diameters of soybean oil droplets during compression and decompression.....	75
Figure 25: Diameters of soybean oil droplets during compression and decompression.....	76
Figure 26: Diameters of soybean oil droplets during compression and decompression.....	76

Table of Figures

Figure 27: Micrographs of a 10% soybean oil emulsions during pressure generation and pressure reduction	77
Figure 28: Influence of the emulsifier concentration on heat-, pressure- and HPT-induced inactivation behavior of <i>C. botulinum</i> type E endospores (TMW 2.992).....	79
Figure 29: Percentage distribution of endospores in heterogenic soybean oil/IPB mixtures.....	80
Figure 30: Endospore distribution in the interface and in the top of the buffer phase, of heterogenic soybean oil/IPB mixtures, containing different fat contents (30, 50 and 70%)	81
Figure 31: Percental endospore arrangement (TMW. 2.992) in 50% soybean oil/IPB mixtures	82
Figure 32: Micrograph of a 50% soybean oil/IPB mixture, which was inoculated with 5×10^5 spores/ml (TMW 2.992), at 1000 fold of magnification.....	82
Figure 33: Percental endospore arrangement (TMW. 2.992) in 30, 50 and 70% soybean oil emulsions	83
Figure 34: Localization of SYTO 9 stained endospores in soybean oil emulsions	84
Figure 35: Temperature-dependent log reduction of TMW 2.992 endospores in soybean oil emulsions of different fat contents	85
Figure 36: HPT-dependent log reductions of <i>C. botulinum</i> type E endospores (TMW 2.992), in emulsion matrices with different fat contents.....	89
Figure 37: HPT-dependent log reductions of <i>C. botulinum</i> type E endospores (TMW 2.992), in emulsion matrices with different fat contents.....	91
Figure 38: Organization of RM systems encoding and flanking genes.	104
Figure 39: Transformation strategies of <i>C. botulinum</i> (TMW 2.990), by exploiting methylation patterns of different <i>E. coli</i> strains.	105
Figure 40: Transformation strategies of <i>C. botulinum</i> (TMW 2.990), by taking advantages of the methyltransferase CLO_1092 and by cell free extracts.....	110
Figure 41: Model conceptions of endospore distributions in heterogenic oil/buffer mixtures	128
Figure 42: Electro micrographs of <i>C. botulinum</i> beluga endospores (Hodgkiss and Ordal, 1996).....	130

TABLE OF INDICES

Table 1: Grouping and characteristics of <i>C. botulinum</i> strains.....	3
Table 2. Overview of used devices	13
Table 3. Overview of used chemicals.....	16
Table 4. Overview of used enzymes	19
Table 5. Overview of used consumables	20
Table 6. Overview of used molecular biological kits.....	21
Table 7. Overview of used primers.....	21
Table 8: Overview of used plasmids	22
Table 9. Overview of used <i>C. botulinum</i> strains.....	23
Table 10. Overview of used <i>E. coli</i> strains	23
Table 11. Composition of LB medium	24
Table 12. Composition of TPYG medium.....	25
Table 13. Composition of AEY medium	25
Table 14. Composition of TPYC medium	25
Table 15. Composition of M140 medium.....	25
Table 16. Composition of SFE.....	26
Table 17. Preparation of IPB	27
Table 18. Composition of TAE buffer	29
Table 19. Composition of the digest reaction mixture	29
Table 20. Composition of the ligation reaction mixture	30
Table 21. Composition of PCR reaction mixtures	31
Table 22. Parameters of PCR cycles	32
Table 23. Compounds of 1x SDS-PAGE sample buffer.....	43
Table 24: Statistical parameters of particle-size distribution in soybean oil emulsions.....	73
Table 25: Genotype-dependent methylation patterns of <i>E. coli</i> strains	106

LIST OF ABBREVIATIONS

ACN	acetonitrile
ATP	adenosintriphosphate
AEY	anaerobic egg yolk agar
<i>B.</i>	<i>Bacillus</i>
BLAST	basic local alignment search tool
BoNT	botulinum neurotoxin
<i>C.</i>	<i>Clostridium</i>
°C	degree Celsius
ccc	covalently closed circular
CMC	critical micelle concentration
CRG	Clostridia Research Group
Da	dalton
DPA	dipicolinic acid
DTT	dithiothreitol
E	field strength
EDTA	ethylenediaminetetraacetic acid
F	faraday
g	gram
h	hour
HPP	high pressure processing
HPT	high pressure thermal
IBS	Intron-binding site
IEP	intron encoded protein
IPTG	Isopropyl β-D-1-thiogalactopyranoside
IPB	imidazole phosphate buffer
l	liter
LB	lysogeny broth
m	milli (10 ⁻³)
M	molar
MALDI-TOF MS	Matrix-assisted laser desorption/ionization Time of Flight Mass Spectrometry
MCS	multiple cloning sites
MDS	multidimensional scaling
min	minute
MPa	mega pascal
MTase	methyltransferase
m/z	mass-to-charge ratio
NCBI	National Center for Biotechnology Information
oc	open circular
OD	optical density
O/W	oil in water
p	pressure
PAGE	polyacrylamide gel electrophoresis
PCR	polymerase chain reaction
PEG	polyethylene glycol
pI	isoelectric point
PTM	posttranslational modifications
R	resistance
REase	restriction endonuclease
RAM	retransposition-activated marker

List of Abbreviations

RM	restriction-modification
RNA	ribonucleic acid
RT	room temperature
SAM	S-(5'-adenosyl)-L-methionine
SASPs	small acid soluble proteins
SDS	sodium n-dodecyl sulfate
SFE	sediment fish extract
T	temperature
TFA	trifluoroacetic acid
T _m	melting point
TMW	Technische Mikrobiologie Weihenstephan
TPYC	tryptone, peptone, yeast extract, sugar mix
TPYG	tryptone, peptone, yeast extract, glucose
v	volume
w	mass
μ	micro

1 INTRODUCTION

The spoilage of food is primarily caused by microbial degradation processes. The history of food preservation dates right back to 3000 before Christ. Traditionally, the shelf life of food is extended by salting, sugaring, drying, pickling, smoking, cooking, refrigerating or by preservation in alcohols, oils and acids. Since the 19th century, advanced technologies like pasteurization, canning and bottling were established. To date additional shelf life extending techniques such as the application of artificial additives, vacuum- and gas-packing are widely applied (Lück and Jager, 1995). The most common food preservation methods are based on heat treatment, which is often accompanied by a reduction in sensory and nutritional quality. Since the demand of consumers for fresh and healthy food is increasing, the food industry is looking for safe and alternative preservation technologies (Ahvenainen, 1996). In the past 40 years, non-thermal alternative technologies like irradiation, pulse electric field electroporation and high pressure processing (HPP) have been investigated (Farkas, 1998; Qin *et al.*, 1996, Farkas and Hoover, 2011).

1.1 High pressure processing of food

HPP represents an alternative non-thermal conservation method, which can provide safe products with fresh taste, true-to-life colors and high nutrient contents. In this technique pressures up to 1000 MPa are applied to inactivate food spoiling microorganisms. An additional advantage of HPP is based on the isostatic active principle. In comparison to thermal inactivation processes, where temperature gradients can be exceeded in food products, high pressure transmission is uniform (Patterson *et al.*, 2007). The first comprehensive study on HPP was already done in 1897, by Bert von Hite, who analyzed the influence of high pressure on milk, meat and fruit juices (Hite, 1899; Hite *et al.*, 1914). Nevertheless, based on lacks in technical feasibility, no major efforts were put into investigating HPP, until the end of 80s (Pfister *et al.*, 2000). Primarily the application of pressure facilitates reactions, which are accompanied by volume-reductions, according to Le Chatelier's principle. Accordingly phase transition of lipids, denaturation of proteins, increased ionization of dissociable molecules and changes in non-covalent bonds are results of pressurization. Finally, changes in chemical parameters can contribute to microbial inactivation (Bridgman, 1914; Hemley, 2000; Winter, 2001). A major problem for food safety is the presence of highly resistant bacterial endospores. Thermal-induced inactivation of spores require

high temperatures, long processing times and high energy input, which consequently leads to reduced food quality and high costs. Food technological research indicated that the combined application of high pressure and moderate heat represents a reliable and gentle technique for endospore inactivation (Eisenbrand, 2005). To date the availability of high pressure treated food is increasing and the global production of these products can be estimated to 500 million kg/year (Tonello-Samson, 2014). For example, high pressure-treated yoghurts, fruit preparations, jams, juices, guacamole, ham, oysters and lobster are currently available on the world market (Eisenbrand, 2005; Krzikalla, 2007). In Europe, the commercial launch of high pressure-treated foods is controlled by the regulation (EC) No 258/97 of the European Parliament and of the Council, since 1997 (Novel Food legislation). Accordingly, the commercial launch of novel food products is admissible, when harmlessness is ensured and when the character of ingredients is considered as equivalent to conventional produced foods. Generally, the SKLM (Senatskommission zur Beurteilung der gesundheitlichen Unbedenklichkeit von Lebensmitteln) considered that HPP of food represents a safe preservation method. Nevertheless, the success of pressure-induced inactivation of microorganisms is highly influenced by strain specificity, growth conditions of microorganisms, processing parameters and food matrix character. Finally, for investigation and evaluation of food safety, process- and matrix-dependent inactivation behavior of relevant organisms will be required (Eisenbrand, 2005).

1.2 The food pathogen *Clostridium botulinum*

The species (*C.*) *Clostridium botulinum* comprises anaerobe, gram positive, rod-shaped, spore-forming bacteria, which share the ability of botulinum neurotoxin (BoNT) production (Arnon *et al.*, 2001). Because the classification of *C. botulinum* is solely defined on the basis of BoNT production, this species includes microorganisms of high phenotypic and genotypic diversity (Collins and East, 1998). Based on the formation of different toxin types, members of this species can be divided into seven different serological groups (A - G). Especially the toxin types A, B, E and F are responsible for human botulism, including foodborne-, wound- and infant-botulism. While the toxin types C and D can cause animal botulism (Hatheway, 1993). For a long time, it was supposed that toxin type G is not associated to causes diseases. Nevertheless, recent studies indicated that toxin type G is also harmful to vertebrates (Zhou *et al.*, 1995). BoNTs are the most poisonous neurotoxins found in nature. Intravenous application of 0.09 - 0.15 µg, inhalation of 0.7 - 0.9 µg or oral intake of 70

μg of BoNT A have already lethal effects on human adults. BoNTs represent dichain polypeptides, which consist of a 100 kDa heavy- and a 50 kDa light chain. After intoxication, BoNTs enter into neurons by endocytosis. Inside of neuromuscular junctions, endopeptidase activity of the light chain permits the cleaving of SNARE proteins, which are parts of synaptic fusion proteins. The enzymatic degradation of these proteins prevents the fusion of synaptic vesicles and synaptic membranes. In turn, the release of the neurotransmitter acetylcholine is blocked and saltatory conduction is interrupted. This results in muscle paralyses, which finally cause death (Arnon *et al.*, 2001). Additionally, differences in physiological properties enable the classification in four characteristic groups (I - IV). The classification criteria of different *C. botulinum* strains are listed in Table 1 (Hatheway, 1993; Dodds and Austin, 1997). Members of the group I include proteolytic strains, which can produce toxin types A, B and F. Vegetative cells are able to grow in the range of 10 – 48 °C, while the optimal growth temperature is about 37 °C. Endospores of group I are also characterized by high heat resistance ($D_{100\text{ °C}} = 25$ min). The nonproteolytic *C. botulinum* strains, which produce toxin types E, B and F are divided into group II. The optimal growth temperature of group II strains is generally lower than for other strains (18 - 25 °C). Especially members of type E strains are able to grow at temperatures as low as 3.3 °C. Endospores of group II strains are generally more heat sensitive than group I strains ($D_{100\text{ °C}} = < 0.1$ min). The group III includes nonproteolytic strains, which can cause animal botulism (toxin types C and D). Vegetative cells are able to grow at 15 °C, while the optimal growth temperature is about 40 °C. The heat resistance of group III endospores is slightly higher than of group II endospores ($D_{100\text{ °C}} = 0.1 - 0.9$ min). *C. botulinum* strains which can produce toxins of type G are classified in group IV. Their optimal growth temperature is about 37 °C and corresponding endospores show slightly increased heat resistance in comparison to group III spores ($D_{100\text{ °C}} = 0.8 - 1.12$ min), (Dodds and Austin, 1997).

Table 1: Grouping and characteristics of *C. botulinum* strains (modified to Hatheway, 1993; Dodds and Austin, 1997). The table indicates the physiological grouping of *C. botulinum* strains as a function of toxin type, growth characteristics and endospore resistance. $D_{100\text{ °C}}$ (decimal reduction time at 100 °C) represents the required time, which is necessary to inactivate 9/10 of endospores at 100 °C. ND indicates that the corresponding parameter is not determined.

physiological group	I	II	III	IV
neurotoxin type	A, B, F	B, E, F	C, D	G
growth temperature _{min.} (°C)	10	3.3	15	ND
growth temperature _{opt.} (°C)	35 - 40	18 - 25	40	37
$D_{100\text{ °C}}$ of spores (min)	25	< 0.1	0.1 - 0.9	0.8 - 1.12

C. botulinum is strictly anaerobic but the ability to form endospores promote their environmental distribution. Based on the high resistance of bacterial endospores, contamination of food constitutes a threat for consumers. Particularly, insufficient sterilized food benefits spore germination, growth and thus toxin production (Macdonald *et al.*, 2011). First historical reports already published in 1793, linked botulism outbreaks with the consumption of contaminated meat (Erbguth, 2004). For a long time, botulism presented a major problem in thermally processed food. In 1922, the Botulism Commission of the United States Public Health Service requested sufficient heating of home-canned food products (Hartman, 1997).

According to infectious-epidemiological yearbooks of the Robert Koch institute, a total of 107 botulism infections were registered in Germany, between 2001 and 2013. A total of seven cases were attributed to infant botulism, 24 infections were caused by wound botulism and 76 persons went ill due to food-borne botulism. Food-borne botulism is frequently related to the consumption of home slaughtered liver sausage and other meat products, home canned beans, self-smoked fish and self-collected mushrooms. Nevertheless, scattered outbreaks were also caused by the consumption of commercial products such as conserves and olives.

C. botulinum type E strains are predominantly present in fresh water or salt water sediments, in regions north of the 40° parallel. Especially aquatic animals from the Pacific coast of North America and from the Great Lakes are contaminated with high levels of *C. botulinum* type E spores. Consequently food-borne botulism outbreaks, which were associated with *C. botulinum* type E, are primarily related to the consumption of contaminated fishery products. Based on anaerobic lifestyle and the cold tolerance of *C. botulinum* type E strains, especially members of these serological group present a risk for insufficiently preserved, refrigerated vacuum-packaged foods. Earliest reported cases of botulism, which were associated with type E strains, were caused by contaminated sturgeon from the Sea of Azov (1936), by salted seal meat of the Caspian Sea (1937) and by smoked salmon from Labrador (1938) (Gunnison *et al.*, 1936; Hazen, 1938; Kurochkin and Emelyanchik, 1937; Macdonald *et al.*, 2011; Dodds and Austin, 1997). For instance, during 1995 – 1997, in more than 7% of hot-smoked, vacuum-packaged rainbow trout and whitefish products marked in Finland, *C. botulinum* type E spores were present (Hyytiä *et al.*, 1998).

Finally, the cold tolerance of vegetative cells, the high incidence in aquatic environments, the ability for toxin production and the heat resistance of endospores indicates that *C. botulinum* type E strains represent serious food pathogens.

1.3 Bacterial endospores

Bacterial endospores represent dormant, highly resistant structures, which are formed by several anaerobic and aerobic bacteria, surviving harsh conditions and starvation. Clostridia and bacilli constitute the most common members of spore forming genera, while *B. subtilis* represents the best-studied species. Endospores are characterized by their enormous resistance against high temperatures, ionizing radiation, chemical solvents, detergents and hydrolytic enzymes. Based on the high spore resistance, the dormant structures can remain millions of years (Cano and Borucki, 1995; Errington, 2003).

1.3.1 Sporulation

Nutrient deficiency, increased cell density or limiting growth factors induce the complex process of sporulation. In *B. subtilis*, the morphological modification is regulated by more than 200 genes and the process can be endure for several hours. In *B. subtilis*, sporulation is initiated by extra- and intracellular signals that are conveyed by a phosphorelay system. The phosphorelay system accordingly triggers a highly regulated sporulation cascade. In contrast to bacilli, earliest sporulation genes, which encode proteins of the mentioned phosphorelay systems, are not conserved in clostridia. Nevertheless, key genes of the sporulation cascade are similar to those of *B. subtilis*. In bacilli and clostridia, sporulation is regulated in equal ways but tended to be not superimposable (Paredes *et al.*, 2005). After initiation of sporulation, asymmetric division of the cytoplasmic membrane is performed and leads to the development of two compartments, which differ in sizes (the spore protoplast and the mother cell). Subsequently, the smaller spore protoplast is engulfed by the cytoplasmic membrane of the mother cell and leads to formation of a double membrane engulfed forespore. Ensuing from the former spore protoplast membrane, the germ cell wall is synthesized outwardly, while ensuing from the former mother cell membrane. The cortex is synthesized inwardly. The cortex is composed of peptidoglycan, which is less cross linked than in vegetative cells. Simultaneously, spore dehydration takes place, which contributes to increased heat resistance. Following, the mother cell is responsible for the formation of the spore coat. In several species, for example in some

C. botulinum spores, an exosporium is formed, additionally. Simultaneously, the spore-specific substances dipicolinic acid (DPA) and small, acid-soluble spore proteins (SASPs) are synthesized, while Ca^{2+} -ions are accumulated. Chelates of Ca-DPA are stored in the core, which also contributes to increased heat resistance. SASPs are associated to spore DNA, which in turn permits protection against heat, UV radiation and toxic components. SASPs also serve as amino acid sources during spore germination. Finally, the mature endospore is released from the mother cell. (Errington, 1993; Fairhead *et al.* 1993; Schlegel, 1992; Setlow 1995; Paredes *et al.*, 2005; Raju *et al.*, 2006).

1.3.2 Structure of bacterial endospores

In Figure 1, the schematic structure of a bacterial endospore is depicted (Paredes-Sabja *et al.*, 2011). The center of the spore is formed by the core. This structure possesses low water content and contains DNA, RNA, SASPs, Ca-DPA chelates and enzymes. The core is surrounded by the weakly permeable inner membrane. Accordingly, this layer prevents the permeation of DNA damaging chemicals into the spore core. The inner membrane is surrounded by the germ cell wall. This layer is composed of peptidoglycan and exhibits equal structures to cell walls of vegetative cells. The cortex, which surrounds the germ cell wall, is also composed of peptidoglycan. Nevertheless, in comparison to conventional mureins, the level of crosslinks is reduced. The spore coat is largely formed by spore-specific proteins and permits protection against reactive chemicals and lytic enzymes. As already mentioned, in some endospore species, the outermost layer is formed by the exosporium. This layer is primarily composed of proteins, lipids and carbohydrates and presumably plays a role in interface phenomena (Paredes-Sabja *et al.*, 2011; Lequette *et al.*, 2011). Finally, the functional sum of different spore layers is responsible for high endospore resistance.

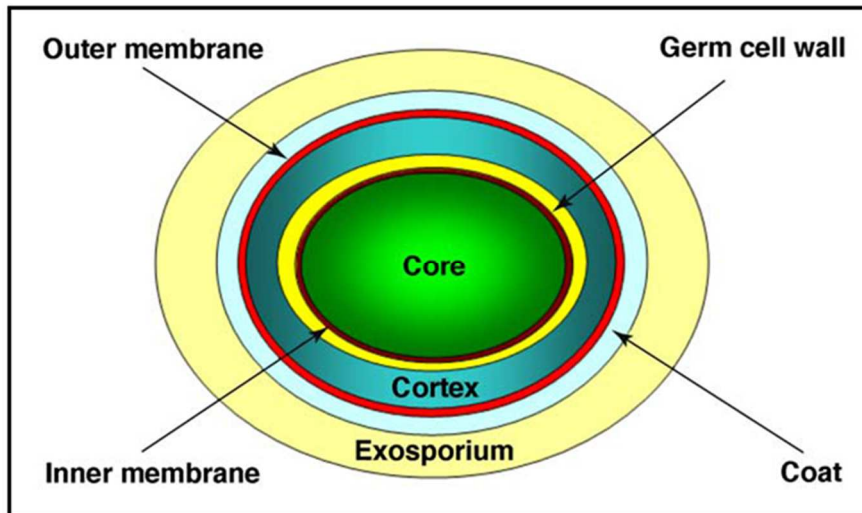


Figure 1: Structure of a bacterial endospore. The different spore layers (core, inner- and outer-membrane, germ cell wall, cortex, coat and exosporium) are visualized by different colors (Paredes-Sabja *et al.*, 2011).

1.3.3 Spore germination

When environmental conditions are favorable, germination of endospores can be induced and the dormant structures return to vegetative cells. Under natural conditions, germination is induced by germinants, which activate specific germination receptors in the inner membrane. Amino acids, purine nucleotides, and sugars present common germinants. In bacilli and clostridia, the mechanisms of germination are largely similar, nevertheless the kind of germination receptors, germinants and proteins, which are involved in signaling pathways, differ slightly. Similar to the process of sporulation, germination has been studied most extensively in *B. subtilis*. Through the activation of germination, the release of H^+ , Zn^{2+} and monovalent cations is induced. Based on this procedure, the pH in the spore core increases. Consequently, the increasing pH is required for functionality of enzymes. Afterwards, DPA-Ca chelates and divalent Ca^{2+} ions are discharged from the core by specific channels and are replaced by water. Subsequently, this events trigger the activity of cortex lytic enzymes, which are involved in the hydrolysis of cortex peptidoglycan. Especially the cortex lytic enzyme CwlJ is directly activated by the release of DPA. Based on cortex degradation, the rehydration of the spore core is further increased. The increased uptake of water permits swelling of the core and induces reactivation of enzymes and increased movement of proteins. Accordingly, SASPs are converted into amino acids and macromolecules, while the cell initiates ATP generation. Finally the mature spore is growing out of the spore coat (Setlow, 2003; Settlow *et al.*, 2008; Paredes-Sabja *et al.*, 2011).

1.4 High pressure/heat-induced inactivation of bacterial endospores

As already mentioned, HPP represents a promising, alternative tool for food preservation. For endospore inactivation, pressure treatment at ambient temperatures is not sufficient and requires the additional application of other inactivation processes (Sale, *et al.*, 1970). High pressure treatments induce the process of endospore germination. During this process, spore resistance and dormancy decrease rapidly and in turn enables spore inactivation either by an additional pressurization or by heat application. Whereas high pressure thermal (HPT)-induced inactivation requires also the additional application of high temperatures, this inactivation method requires much lower temperatures than in exclusive thermal inactivation processes (Nicholson *et al.*, 2000).

Generally, based on the pressure intensity, the processes of spore germination can be induced via two different mechanisms. In Figure 2, the nutrient- and pressure-induced germination cascade is depicted in a simplified, schematic model (Setlow, 2003, modified according to Setlow, 2007).

Until now, these two mechanisms are also mostly studied in *B. subtilis* spores. The application of relatively low pressure (50 - 300 MPa) leads to activation of nutrient receptors in the inner membrane, which finally trigger the complete germination cascade. To date, the pressure-induced mechanism of nutrient receptor activation is not understood in detail. Presumably, pressure application leads to changes in receptor conformation and in turn induces receptor activation. Otherwise, it is also possible that pressure application influences the fluidity and phase behavior of the inner membrane, which can also induce changes of receptor conformations (Setlow, 2003; Black *et al.*, 2005; Black *et al.*, 2007 B; Paredes-Sabja *et al.*, 2011).

The application of high pressure (300 - 800 MPa) induces the release of DPA from the spore core, without influencing earlier events of the natural sporulation cascade. The release of DPA induces the activation of the cortex lytic enzyme CwlJ, which in turn triggers subsequent events of the sporulation cascade. Until now, the pressure-induced release of DPA is not understood completely. Seemingly, pressure in the range of 300 - 800 MPa induces the opening of DPA-channels or leads to pore formation in the inner membrane, which finally enables DPA release (Paidhungat *et al.*, 2002; Black *et al.*, 2006; Black *et al.*, 2007 B; Wilson *et al.*, 2008). Since spores of *Clostridium* and *Bacillus* partly differ in signal transduction pathways and in

components of the germination machinery, mechanism of HPT-induced spore inactivation of both species tended to differ (Paredes-Sabja *et al.*, 2011; Sarker *et al.*, 2013).

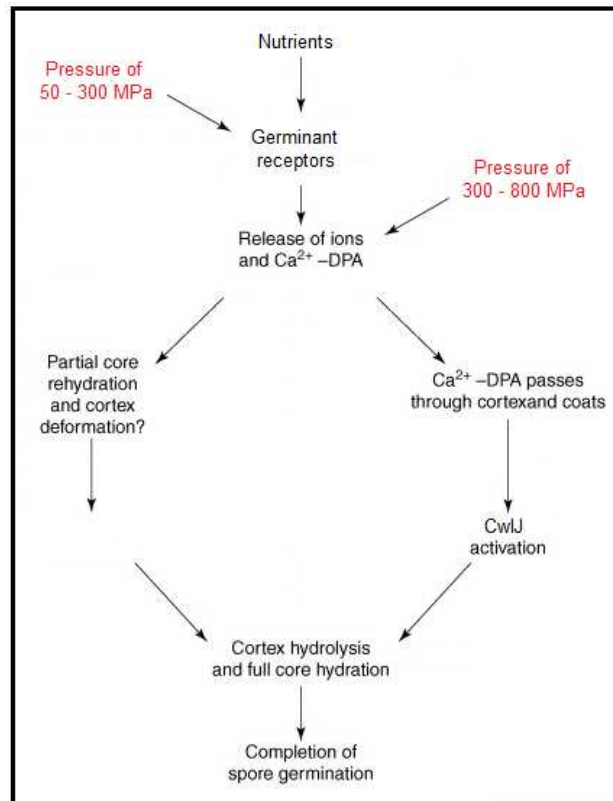


Figure 2: Simplified model of the nutrient- and pressure-induced endospore germination cascade (Setlow, 2003, modified according to Setlow, 2007). According to 1.3.3, the nutrient-induced germination cascade of endospores is depicted. Additionally, the pressure-induced activation of germination receptors (50 – 300 MPa) and the pressure-induced release of Ca²⁺-DPA (300 – 800 MPa) are indicated.

The HPT-induced inactivation behavior of endospores is not readily predictable. The high pressure/heat tolerance of endospores depends on strain specificity and is also influenced by sporulation conditions. Besides of sporulation medium composition, pH and salt concentrations, spore tolerance also depends on sporulation temperature (Black *et al.*, 2005; Black *et al.*, 2007, B; Wuytack and Michiels, 2001). Inactivation behavior of endospores additionally depends on processing parameters and on food matrix properties. Furthermore, spore populations are not completely homogeneous. They can contain super-dormant fractions, which are more difficult to inactivate than conventional spores of the population (Gänzle *et al.*, 2007). The efficiency of endospore inactivation does not necessarily correlate with increasing pressure and/or temperature parameters. At some defined pressure/temperature combinations,

endospores tend to be stabilized. For instance, Margosch *et al.* (2006) indicated that *C. botulinum* spores can be inactivated more efficiently by thermal treatment at 100 °C than by combined high pressure/heat application at 100 °C and 600 MPa. On the contrary, at parameters of 100 °C and 900 – 1400 MPa, the spore inactivation was more effective than at 100 °C and ambient pressure. Supposedly, the mentioned effect is caused by the simultaneous pressure-induced activation of nutrient receptors and DPA release, which probably leads to hindering of both mechanisms (Reineke *et al.*, 2011). During the process of compression, adiabatic heating is caused by the conversion of mechanical energy into thermal energy. The magnitude of pressure-induced temperature increase depends on matrix properties, final pressure level, initial temperature, pressure- temperature-time profile and by the type of high pressure vessel construction (Kessler, 2002; Ardia, 2004; Mathys and Knorr, 2009).

Finally, for the development of novel and safe HPT preserved food products, all mentioned facts that can influence endospore inactivation behavior have to be considered. The general target inactivation level for *C. botulinum* type E spores to provide a sufficient level of food safety is thought to be reached when inactivation processes enable the reduction of six orders of magnitude (Margosch, 2004 c).

1.5 Objectives of this work

The primary aim of this work was the identification of molecular and external factors, affecting the high pressure tolerance of *C. botulinum* type E spores.

1.5.1 Generation of *C. botulinum* type E knock out mutants

In contrast to the knowledge on sporulation, germination, spore structure and HPT-induced inactivation mechanism of *B. subtilis* spores, comparable information about the key food spoiling *C. botulinum* spores is rare. For the investigation of physiological and mechanistic processes, the generation of knock out mutants presents a promising tool. For ages, gene knock out generation in the genus *Clostridium* was extremely difficult, until the Clostridia Research Group (CRG) developed the promising ClosTron mutagenesis system (Heap *et al.*, 2009, B). To date, a broad spectrum of strain- and species-dependent ClosTron mutagenesis protocols are existent. Nevertheless, for a few *Clostridium* species, no established knock out mutagenesis strategies are available. Thus, within the context of this work, transformation and gene knock out generation in *C. botulinum* type E strains should be examined. As a representative

model for this investigation, genes of *C. botulinum* type E that encode SASPs (CLO_1237, CLO_3013 and CLO_3241) and a germination-specific protease, which is involved in rapid SASP degeneration, should be used. In clostridia predominantly α/β -types of the spore-specific proteins are present, while γ -types are absent. In dormant spores, SASPs of the α/β -type are associated with spore DNA and confer protective effects against heat, UV radiation and toxic components (Fairhead *et al.*, 1993; Setlow 1995; Raju *et al.*, 2006). *B. subtilis* spores with defects in α/β -type SASP encoding genes, showed reduced HPT resistance (Lee *et al.*, 2007). Hence, in a successful knock out mutant, a deficit of SASP should lead to HPT sensitive *C. botulinum* spores.

1.5.2 Correlation of medium-induced endospore resistance and proteome pattern

The composition of sporulation medium can directly influence the HPT resistance of endospores. In comparison to *C. botulinum* type E spores, which were derived from conventional sporulation media (TPYC, AEY, M140), SFE (sediment fish extract) derived spores showed significantly increased HPT tolerance (Lenz and Vogel 2014). Therefore, a second aim of this work was to identify and compare spore proteomes of three different *C. botulinum* type E strains, which were obtained from mentioned sporulation media. For proteome analyses and comparison, MALDI-TOF MS spectra should be acquired. Additionally, spore proteins that are probably involved in increased HPT resistance should be identified by SDS-PAGE coupled with high resolution LC-MS/MS.

1.5.3 High pressure/temperature-induced inactivation of endospores in emulsion matrices

In HPT-induced inactivation processes, the effectivity of microbial reduction strongly depends on matrix constitution. Until now, most matrix-dependent inactivation studies focused on simple aqueous buffer systems of complex food matrices like fruit juices, vegetables and meat. However, information concerning on inactivation kinetics in foods of high fat contents or emulsions are generally rare and completely missing for *C. botulinum* type E. Nevertheless, such required information would probably allow the commercial launch of novel, high quality products like mayonnaises, marinated meat, fish products and cocktail sauce, etc. Until now, some studies have indicated that microorganisms are generally more resistant to heat and pressure inactivation, when

they are embedded in fat containing matrices (Simpson and Gilmour, 1997; Miller 2006; Morales *et al.* 2006; Ananta *et al.* 2001). To date, the protective effect of fat has not completely been understood and several authors have proposed different, partly contradictory theories. To understand several unclear issues in this largely unexplored field, basic research is required.

Consequently, in this study, droplet size distribution and stability of soybean oil emulsions of different fat contents should be characterized at standard conditions and after/during pressure application. Additionally, spore distribution in inoculated model emulsions should be determined. Finally, as a function of different processing parameters, spore inactivation behavior in model emulsions of different fat contents should be investigated.

2 MATERIAL AND METHODS

2.1 Material

2.1.1 Equipment

Table 2. Overview of used devices

device	model	manufacturer
agarose gel chamber 13.8 x 12 cm	Easy Cast electrophoresis system	Thermo Fisher Scientific Inc., Waltham, MS, USA
autoclaves	2540 ELV VE-40	Systec GmbH, Wettenberg, Germany
	VX-150 Varioklav	H + P Labortechnik, Oberschleißheim, Germany
anaerobic chamber	WA 6200	Heraeus Instruments, Hanau, Germany
breeding/ incubation	Certomat BS-1	Systec GmbH, Wettenberg, Germany
	Hereaus B5042E	Hereaus Instruments, Hanau, Germany
	Memmert INB series	Memmert GmbH & C. KG, Schwabach, Germany
	Memmert ICP 500	Witeg Labortechnik GmbH, Wertheim, Germany
centrifuge	WiseCube® WIS-ML02	Witeg Labortechnik GmbH, Wertheim, Germany
	Sigma 1 K 15	Sigma Labortechnik, Osterode am Harz, Germany
	Sigma 6-16 K	Sigma Labortechnik, Osterode am Harz, Germany
	Hermle Z382 K	Hermle Labortechnik, Wehningen, Germany
	Hermle Z383 K	Hermle Labortechnik, Wehningen, Germany
Hermle Z216 MK	Hermle Labortechnik, Wehningen, Germany	
Mini Centrifuge MCF-1350	Laboratory Medical Supplies, Hongkong, China	
colony counter	WTW BZG 30 colony counter	WTW Wissenschaftlich-Technische Werkstätten GmbH, Weilheim, Germany
electroporator	Gene Pulser II Electroporation System	Bio-Rad Laboratories GmbH, Munich, Germany

high pressure unit	dual vessel HP unit	Knam Schneidetechnik GmbH, Langenargen, Germany
	high-pressure low-temperature vessel 1000 MPa, type U111	Unipress - Institute of High Pressure Physics of the Polish Academy of Sciences, Warszawa, Poland
	high pressure single vessel apparatus U4000	
high pressure microscope unit	HPDS-high pressure cell	SITEC-Sieber Engineering AG, Zürich, Switzerland (Hartmann <i>et al.</i> , 2003)
laser particle analyzer	Mastersizer 2000	Malvern Instruments GmbH, Herrenberg, Germany
incubation hood	Certomat H	B. Braun Biorech International, Melsungen, Germany
laminar flow sterile work bench	HERA safe	Heraeus Instruments, Hanau, Germany
MALDI-TOF-MS	microflex LT	Bruker Daltonics GmbH, Bremen, Germany
microscope	Axiostar plus	Carl Zeiss Microimaging GmbH, Munich, Germany
	BX51WI	Olympus Deutschland GmbH, Germany
nanodrop	Nanodrop 1000	Peqlab Biotechnologie GmbH, Erlangen, Germany
particle separation analyzer	LUMiFuge, LF110	LUM GmbH, Berlin, Germany
PCR cycler	Primus 96 plus	MWG Biotech, AG, Ebersberg, Germany
	Mastercycler gradient	Eppendorf AG, Hamburg, Germany
pH determination (electrode)	InLab 412, pH 0-14	Mettler-Toledo, Gießen, Germany
pH determination (measuring device)	Knick pH 761 Calimatic	Knick elektronische Geräte, Berlin, Germany
photometer	Novaspec	Pharmacia Biotech, Cambridge, England

pipettes	Pipeman	Gilson-Abomed, Langenfeld, Germany
power supplies	MPP 2 x 3000 Power Supply Electrophoresis Power Supply EPS 3000	MWG Biotech, AG, Ebersberg, Germany Pharmacia Biotech, Cambridge, England
pure water	Euro 25 and RS 90-4/ UF pure water system	SG Wasseraufbereitung GmbH, Barsbüttel, Germany
refrigerated/heating circulator	FC 600	JULABO Labortechnik GmbH, Seelbach, Germany
SDS-PAGE	Mini-PROTEAN Tetra System	Bio-Rad Laboratories GmbH, Munich, Germany
shaking	Vortex 2 Genie	Scientific Industries Inc., Bohemia, NY, USA
stirring	Wise Stir MSH-20A	Witeg Labortechnik GmbH, Wertheim, Germany
thermo block	Teche DRI-Blick DB3	Thermo-Dux Gesellschaft für Laborgerätebau mbH, Wertheim, Germany
two-dimensional gel electrophoresis	IEF100 First-dimension Isoelectric Focusing Unit SE900 Large Format Vertical Gel Electrophoresis Unit	Hoefer Inc., Holliston, MS, USA
ultrasonic water bath	Sonorex Super RK 103H	Bandelin electronic, Berlin, Germany
ultrasonic homogenizer	Sonopuls UW 2070	Bandelin electronic, Berlin, Germany
UV table	Herolab UVT 28M	Herlab GmbH Laborgeräte, Wiesloch, Germany
Ultra-Turrax	Micra D8	ART-Labortechnik, Müllheim, Germany
water bath	Lauda BD	LAUDA Dr. D. Wobser GmbH & Co., Lauda-Königshofen, Germany

2.1.2 Chemicals

Table 3. Overview of used chemicals

chemicals	purity	manufacturer
6 x DNA loading dye	-	Fermentas GmbH, St. Leon-Rot, Germany
acetic acid	99-100% (glacial)	Merck, Darmstadt
acetone	99.5%	Carl Roth GmbH & Co. KG, Karlsruhe, Germany
acetonitrile	99.5%	Carl Roth GmbH & Co. KG, Karlsruhe, Germany
acrylamide- bis solution	(19:1); 30% (w/v)	SERVA, Heidelberg, Germany
agar	technical quality	Difco, BD Sciences, Heidelberg
agarose	for gel electrophoresis	Biozym Scientific GmbH, Hessisch Oldendorf, Germany
ammonium bicarbonate	≤ 99.5%	SIGMA-Aldrich, Steinheim, Germany
ampicillin sodium salt	93.3%	Gerbu Biotechnik GmbH, Gaiberg, Germany
antifoam B emulsion	-	SIGMA-Aldrich, Steinheim, Germany
ammonium persulfate	electrophoresis grade	SERVA, Heidelberg, Germany
arabinose	99%	Carl Roth GmbH & Co. KG, Karlsruhe, Germany
β-mercaptoethanol	for electrophoresis	SIGMA-Aldrich, Steinheim, Germany
bacto peptone	for microbiology use	Becton, Dickinson and Company, Heidelberg, Germany
bromphenol blue	for electrophoresis	SIGMA-Aldrich, Steinheim, Germany
BSA	for biochemical use	Merck, Darmstadt, Germany
CaCO ₃	Reag. Ph Eur	Merck, Darmstadt, Germany
cellobiose	≤ 98%	SERVA, Heidelberg, Germany
CHAPS	≤ 98%	SIGMA-Aldrich, Steinheim, Germany
CHCA	-	Bruker Daltonic GmbH, Biburg, Germany
chloramphenicol	≥ 98.5%	Carl Roth GmbH & Co. KG, Karlsruhe, Germany

cysteine hydrochloride	≤ 98%	SIGMA-Aldrich, Steinheim, Germany
D-cycloserine	≥ 96%	SIGMA-Aldrich, Steinheim, Germany
dimidium bromide	≤ 98%	Carl Roth GmbH & Co. KG, Karlsruhe, Germany
DPA	99%	SIGMA-Aldrich, Steinheim, Germany
DRCM	for microbiology	Merck, Darmstadt, Germany
drystrip cover fluid	-	GE Healthcare Europe GmbH, Freiburg, Germany
ethanol, absolute	≥ 99.8%	VWR, Prolabo, Foutenay-sous-Bois, France
erythromycine	≥ 93%	Carl Roth GmbH & Co. KG, Karlsruhe, Germany
formic acid	~ 98%	SIGMA-Aldrich, Steinheim, Germany
forming gas	95% N ₂ , 5% H ₂	Westfalen AG, Münster, Germany
glucose	for biochemical use	Merck, Darmstadt, Germany
glycerol	99.5%, high purity	Gerbu Biotechnik GmbH, Gaiberg, Germany
glycine	p.a.	Merck, Darmstadt, Germany
HCl	p.a.	Merck, Darmstadt, Germany
imidazole	99%	SIGMA-Aldrich, Steinheim, Germany
iodoacetamide	for biochemical use	AppliChem GmbH, Darmstadt, Germany
isopropyl alcohol	≥ 99%	Carl Roth GmbH & Co. KG, Karlsruhe, Germany
kanamycin sulfate	98%	SIGMA-Aldrich, Steinheim, Germany
KCl	≥ 99%	Carl Roth GmbH & Co. KG, Karlsruhe, Germany
KH ₂ PO ₄	p.a.	Carl Roth GmbH & Co. KG, Karlsruhe, Germany
K ₂ HPO ₄ *2H ₂ O	p.a.	Merck, Darmstadt, Germany
maltose	for microbiology	Gerbu Biotechnik GmbH, Gaiberg, Germany

methanol	≥ 99.9%	Carl Roth GmbH & Co. KG, Karlsruhe, Germany
meat extract	for microbiology	Merck, Darmstadt, Germany
MgSO ₄ *7H ₂ O	p.a.	Merck, Darmstadt, Germany
N ₂	≥ 99.8%	Westfalen AG, Münster, Germany
NaCl	p.a.	Merck, Darmstadt, Germany
NaH ₂ PO ₄	p.a.	Merck, Darmstadt, Germany
NaOH	50%	J.T. Baker, Deventer, Netherlands
neutralized peptone from soybeans	for microbiology	Oxoid, Hampshire, England
n-hexadecane	-	J.T. Baker, Griesheim, germany
paraffin oil	Reag. Ph Eur	SIGMA-Aldrich, Steinheim, Germany
PEG 400	for laboratory use	Carl Roth GmbH & Co. KG, Karlsruhe, Germany
PEG 8000	for laboratory use	SIGMA-Aldrich, Steinheim, Germany
peptone from casein	for microbiology	Merck, Darmstadt, Germany
polymyxine B sulfate	GR grade	Gerbu Biotechnik GmbH, Gaiberg, Germany
polypeptone	for microbiology	Becton, Dickinson and Company, Heidelberg, Germany
Roti-Blue (5 x concentrare)	-	Carl Roth GmbH & Co. KG, Karlsruhe, Germany
S-(5'-adenosyl)-L-methionine	≤ 80%	SIGMA-Aldrich, Steinheim, Germany
SERVALYTE 3-10	analytical grade	SERVA, Heidelberg, Germany
silver nitrate	≥ 99.9%	Carl Roth GmbH & Co. KG, Karlsruhe, Germany
sodium carbonate	≥ 99.8%	Carl Roth GmbH & Co. KG, Karlsruhe, Germany
sodium thioglycolate	microbiology grade	AppliChem GmbH, Darmstadt, Germany
sodium thiosulfate pentahydrate	GR for analysis	Merck, Darmstadt, Germany

soybean lecithin	≥ 97%	Carl Roth GmbH & Co. KG, Karlsruhe, Germany
soybean oil	food quality	Vandemoortele Lipids Werke GmbH, Dresden, Germany
spectinomycin - dihydrochlorid - pentahydrat	≥ 98%	SIGMA-Aldrich, Steinheim, Germany
sucrose	for laboratory use	SIGMA-Aldrich, Steinheim, Germany
SYTO 9	-	Invitrogen GmbH, Darmstadt, Germany
TEMED	p.a.	Merck, Darmstadt, Germany
Tetracycline hydrochloride	≥ 98%	SIGMA-Aldrich, Steinheim, Germany
terbium(III) chloride hexahydrate	99%	SIGMA-Aldrich, Steinheim, Germany
TFA	99.9%	Carl Roth GmbH & Co. KG, Karlsruhe, Germany
thiamphenicol	R and D use	SIGMA-Aldrich, Steinheim, Germany
thiourea	≥ 99%	SIGMA-Aldrich, Steinheim, Germany
tris	ultra-pure	MP Biomedicals Solon, Ohio, USA
tris-HCl	p.a.	Merck, Darmstadt, Germany
tween 80	-	Mallinkrodt Baker B.v., Deventer, NL
urea	98%	Gerbu Biotechnik GmbH, Heidelberg, Germany
yeast extract	for microbiology	Merck, Darmstadt, Germany

2.1.3 Enzymes

Table 4. Overview of used enzymes

enzyme	manufacturer
calf intestinal alkaline phosphatase (CIAP)	Fermentas GmbH, St. Leon-Rot, Germany
FastDigest Agel	Fermentas GmbH, St. Leon-Rot, Germany
FastDigest BamHI	Fermentas GmbH, St. Leon-Rot, Germany
FastDigest BspHI	Fermentas GmbH, St. Leon-Rot, Germany
FastDigest EcoRV	Fermentas GmbH, St. Leon-Rot, Germany

FastDigest HindIII	Fermentas GmbH, St. Leon-Rot, Germany
FastDigest XhoI	Fermentas GmbH, St. Leon-Rot, Germany

2.1.4 Consumables

Table 5. Overview of used consumables

material	type	manufacturer
anaerocult	A	Merck, Darmstadt, Germany
cellulose nitrate filter	pore size: 0.2 μm , sterile	Satorius AG, Göttingen, Germany
cellulose nitrate filter	pore size: 0.4 μm , sterile	Satorius AG, Göttingen, Germany
cryo pure tubes	1.8 ml	Sarstedt, Nümbrecht, Germany
VISKING dialysis tubing	MWCO 12 000 - 14 000, pore diameter ca. 25 Å,	SERVA Electrophoresis GmbH, Heidelberg, Germany
electroporation cuvettes	2 mm, sterile, med. grade, polycarbonate	Biozym Biotech Trading GmbH, Wien, Austria
	0.2 cm gap sterile electroporation cuvette,	Bio-Rad Laboratories GmbH, Munich, Germany
folded filters	diameter: 185 mm, 65 g/m ² , grade 3	Munktell & Filtrak GmbH, Bärenstein, Germany
heat shrink tubing	shrink temperature: 200 °C; Ø: 3mm	DSG-Canusa, Meckenheim, Germany
petri dishes	92x16mm, with cams, sterile	Sarstedt, Nümbrecht, Germany
pipet tips	20 μl	Gilson International B.V., Limburg, Deutschland
	200 μl , 1000 μl	Socorex Isba S.A., Ecublens, Switzerland
reaction tubes	200 μl , 1.5 ml, 2 ml	Eppendorf, Hamburg, Germany
syringes	single use, 2 ml, 5 ml, 20 ml	B. Braun Melsungen AG, Melsungen, Germany
sterile filter	Filtropur S 0.2 (0.2 μm)	Sarstedt, Nümbrecht, Germany
sterile ml tubes	15 ml, 50 ml	Sarstedt, Nümbrecht, Germany
UV cuvettes	LCH 8.5 mm, from 220 mm	Sarstedt, Nümbrecht, Germany

2.1.5 Molecular biological kits

Table 6. Overview of used molecular biological kits

kit	type	manufacturer
E.Z.N.A. Bacterial DNA Kit	DNA isolation	Omega Bio-Tek Inc., Norcross, GA, USA
peqGOLD Gelextraction Kit	gel extraction	PEQLAB Biotechnologie GmbH, Erlangen, Germany
peqGOLD Plasmid Miniprep Kit II	Plasmid isolation	PEQLAB Biotechnologie GmbH, Erlangen, Germany
Phusion High-Fidelity PCR Kit	DNA polymerase	New England Biolabs GmbH, Frankfurt, Germany
Taq Core Kit	DNA polymerase	MP Biomedicals Solon, Ohio, USA

2.1.6 Primers

Table 7. Overview of used primers

primer	sequence (5' to 3')
clos_for	CAGATAGATGTCAGACGCATGG
clos_rev	CCGGAATTATATCCAGCTGCA
CLO_1237_rev	GAATAATGACATAAAAACAAATTAAG
CLO_1237_for	CTTAATATCTCCATAATTCATATTC
CLO_2913_for	TGGCTACCACCTTTATTGTTATG
CLO_2913_rev	GTGATGATCTGGATAAGTCTTTC
CLO_3013_for	ATTTAATCCTTATTTGCCTTAAC
CLO_3013_rev	GAAATAAATTAATATTTCAATACAC
CLO_3241_for	GTACCTTCCTAGTTTCACAATAC
CLO_3241_rev	AATCTTCTTGATTATATAAATATACC
EBS_universal	CGAAATTAGAACTTGCGTTCAGTAAAC
intron_for	AGCTTATAATTATCCTTAAT
intron_rev	GTACAAATGTGGTGATAAC
met_for	CACTCTCGAGCTTAAAAATTGCAACAGTT

met_rev	ACGTAAGCTTTTCTCTATCAAATGCAAC
met2_for	TATACTCGAGCTTAAAAATTGCAACAGTTTTTAGTG
met2_rev	TATAAAGCTTTTCTCTATCAAATGCAACTAG
met.middle_for	ATAGAGAACGAATATTTGTTGTA
met.test_for	GGAGCTATAGAACATGCGCTAA
met.test_rev	CAGTTACAAACGCAACACCT
R702_for	ATGCGCTCACGCAACTGGTC
R702_rev	TTATTTGCCGACTACCTTGGTGATC

2.1.7 Vectors

Table 8: Overview of used plasmids

plasmid	relevant characteristic	source
pBAD/Myc-His A	araBad promoter, C terminal His tag, Amp ^R	Invitrogen GmbH, Darmstadt, Germany
pBAD/Myc-His A-Met	araBad promoter, C terminal His tag, Amp ^R , encodes CLO_1092	this study, synthesized by DNA2.0 Inc., CA, USA
pMA-RQ-Met	Amp ^R , encodes EES48847.1 (optimized codon usage for <i>E. coli</i>)	this study, synthesized by GENEART AG, Regensburg, Germany
pMTL007C-E2:43973-Cbo-ssp3241	Clostron plasmid containing <i>catP</i> and intron containing <i>ermB</i> RAM	this study, synthesized by DNA2.0 Inc., CA, USA
pMTL007C-E2:53142-Cbo-ssp3013	Clostron plasmid containing <i>catP</i> and intron containing <i>ermB</i> RAM	this study, synthesized by DNA2.0 Inc., CA, USA
pMTL007C-E2:53143-Cbo-ssp1237	Clostron plasmid containing <i>catP</i> and intron containing <i>ermB</i> RAM	this study, synthesized by DNA2.0 Inc., CA, USA
pMTL007C-E2:53144-Cbo-gpr	Clostron plasmid containing <i>catP</i> and intron containing <i>ermB</i> RAM	this study, synthesized by DNA2.0 Inc., CA, USA
R702	Km ^R , Sm ^R , Sp ^r , Su ^R , Tc ^R , Hg ^R	reisolated from <i>E. coli</i> CA434

2.1.8 Bacterial strains

Table 9. Overview of used *C. botulinum* strains

strain	TMW No.	source/reference
<i>C. botulinum</i> type E	2.990	Kulmbach C2, putatively isolated from fermented whale flippers, involved in a botulism outbreak in Canada, NCBI accession number NZ_ACSC00000000.1 (beluga)
<i>C. botulinum</i> type E	2.991	Kulmbach C3, (S5)
<i>C. botulinum</i> type E	2.992	Kulmbach C 45, (1576, Norwegen)
<i>C. botulinum</i> type E	2.993	Kulmbach C 125, (EG, Strain Gordon)
<i>C. botulinum</i> type E	2.994	Kulmbach C 127, isolated from salt water fish (Baumgart, 1972)
<i>C. botulinum</i> type E	2.995	Kulmbach C 128, (1537/62, Johannsen)
<i>C. botulinum</i> type E	2.996	Kulmbach C 141, (1103, Terry Roberts)
<i>C. botulinum</i> type E	2.997	LGL REB 1718
<i>C. botulinum</i> type E	2.998	LGL E 2622

Table 10. Overview of used *E. coli* strains

strain	TMW no.	genotype	source/reference
<i>E. coli</i> CA434	2.1072	<i>F⁻ mcrB mrr hsdS20(rB⁻ mB⁻) recA13 leuB6 ara-14 proA2 lacY1 galK2 xyl-5 mtl-1 rpsL20(Sm^R) glnV44 λ</i> -contains the conjugativ plasmid R702 (Tc ^R , Sm ^R , Su ^R , Hg ^R , Tra ⁺ Mob ⁺)	Department of Microbiology – TUM, Germany
<i>E. coli</i> GM2163	2.1014	<i>F⁻ dam-13::Tn 9 dcm-6 hsdR2 leuB6 his-4 thi-1 ara-14 lacY1 galK2 galT22 xyl-5 mtl-1 rpsL136 tonA31 tsx-78 supE44McrA⁻ McrB⁻</i>	Fermentas GmbH, St. Leon-Rot, Germany
<i>E. coli</i> HB101	2.39	<i>F⁻ mcrB mrr hsdS20(rB⁻ mB⁻) recA13 leuB6 ara-14 proA2 lacY1 galK2 xyl-5 mtl-1 rpsL20(Sm^R) glnV44 λ</i>	unknown
<i>E. coli</i> Top10	2.580	<i>F⁻ mcrA Δ(mrr-hsdRMS-mcrBC) φ80lacZΔM15 ΔlacX74 nupG recA1 araD139 Δ(ara-leu)7697 galE15 galK16 rpsL(Str^R) endA1 λ</i>	Invitrogen GmbH, Karlsruhe, Germany

2.2 Methods

2.2.1 Media, growth conditions and strain storage

All growth media were sterilized by autoclaving at 121 °C for 20 min. To prevent maillard reactions, sugars and media were sterilized separately. Temperature instable compounds were filter-sterilized and added after temperature treatment. To prepare agar plates, 1.5% agar was added to liquid media prior to autoclaving.

2.2.1.1 Cultivation of *E. coli* strains

All strains of *E. coli* (Table 10) were grown on lysogeny broth (LB) medium (Table 11), (Bertani, 1951). Cultures were inoculated by single colonies or by addition of 2% (v/v) fresh overnight cultures. Bacteria were incubated at 37 °C under aerobic conditions. The breeding of liquid cultures was attended by shaking. For selective conditions of growth, appropriate antibiotics were added.

Table 11. Composition of LB medium

compound	concentration [g/l]
yeast extract	5
peptone from casein	10
NaCl	10

2.2.1.2 Cultivation of *C. botulinum* strains

Media, which were used for the cultivation of *C. botulinum* strains are listed in 2.2.1.2.1. Prior to inoculation, liquid media and agar plates were stored in an anaerobic chamber (WA6600, Hereus Instruments GmbH) for a minimum of 24 h, to allow equilibration with the atmosphere (95% N₂ and 5% H₂). Liquid media were inoculated with 10% (v/v) of fresh precultures. All used *C. botulinum* strains were anaerobically incubated at 28 °C by exclusion of light. For selective conditions of growth, appropriate antibiotics were added. Depending on intended purpose, *C. botulinum* strains were incubated between 24 to 336 h.

2.2.1.2.1 *C. botulinum* growth media

Growth and sporulation media, which were used for the cultivation of *C. botulinum* strains are listed below. Generally, the preparation of media was performed according to 2.2.1.

• **TPYG (Whitmer and Johnson, 1988)**

Table 12. Composition of TPYG medium

compound	concentration [g/l]
tryptone	50
proteose peptone	5
yeast extract	20
sodium thioglycolate	1
glucose	4
pH	7 ± 0.2

• **TPYC (Artin et al., 2008)**

Table 14. Composition of TPYC medium

compound	concentration [g/l]
tryptone	50
proteose peptone	5
yeast extract	20
sodium thioglycolate	1
glucose	4
maltose	1
cellobiose	1
soluble starch	1
pH	7 ± 0.2

• **SFE (sediment fish extract)**

SFE was modified from the proteolytic *C. botulinum* sporulation medium WSH (Margosh et al., 2006). A special component of SFE is the fresh water sediment-fish-brew. For preparation of this brew, 400 g fresh water sediment and 100 g fresh rainbow trout were added with distilled H₂O to a final volume of 1 l. After steaming this brew for one hour, the mixture was filtered for five times (folded filters, diameter: 185 mm, 65 g/m², grade 3, Munktell & Filtrak GmbH). Finally, 20 g meat extract, 0.5 g proteose peptone, 5 g tryptone, 1 g sodium thioglycolate, 0.5 g cysteine hydrochloride, 2 g CaCO₃ and 250 ml fresh water sediment-fish-brew were added with H₂O, to a total volume of 950 ml. After autoclaving, 50 ml of a sterile sugar solution, containing 4 g

• **AEY (Hobbs et al., 1967)**

Table 13. Composition of AEY medium

compound	concentration [g/l]
tryptone	5
proteose peptone	20
yeast extract	5
NaCl	5
pH	7 ± 0.2

• **M140 (BAM Media Index)**

Table 15. Composition of M140 medium

compound	concentration [g/l]
polypeptone	15
yeast extract	3
starch, soluble	3
sodium thioglycollate	1
Na ₂ HPO ₄	11
pH	7.8 ± 0.1

glucose, 1 g maltose, 1 g cellobiose and 1 g soluble starch, were added. In Table 16, all components of SFE are listed collectively.

Table 16. Composition of SFE

compound	concentration [g/0.75 l]
meat extract	20
proteose peptone	0.5
tryptone	5
cysteine hydrochloride	0.5
CaCO ₃	2
glucose	4
maltose	1
cellobiose	1
starch, soluble	1

in addition of 250 ml sediment-fish-brew

2.2.2 Strain storage

For long term-storage, bacterial cell stocks were prepared. Bacteria were grown in corresponding growth medium (2.2.1.1 and 2.2.1.2) until exponential phase. Subsequently, 2 ml of growing cultures were harvested and cell pellets were resuspended in 800 µl of fresh growth medium and 800 µl of 85% glycerol. The stock solutions were stored at – 80 °C.

2.2.3 Preparation and purification of endospore suspensions

To prepare pure spore suspensions, strains of *C. botulinum* type E were grown in 300 ml sporulation medium (TPYC, AEY, M140 and SFE) (2.2.1.2.1). After anaerobic incubation (2.2.1.2) for maximal 14 d at 28 °C, spore formation was proved by phase contrast microscopy. When spore suspensions yielded in a minimum of 85% phase bright spores, cultures were harvested by centrifugation (15000 x g, 4 °C and 15 min). Depending on intended purpose, two different spore purification protocols were carried out (2.2.3.1 and 2.2.3.2).

2.2.3.1 Endospore purification for spore inactivation experiments

To prepare spore suspensions for further endospore inactivation experiments according to 2.2.8.6 and 2.2.8.7, spores were purified as described subsequently. According to 2.2.3, harvested cultures were washed in 50 ml ice-cold distilled H₂O for three times. After resuspending the spore/cell pellets in 50 ml of 50% ethanol, the suspensions were incubated for 2 h at room temperature attended by vortexing every 20 min. After three additional washing cycles in distilled H₂O, spore purity was inspected by microscopic observation. When spore suspensions did not fulfil the applicable requirements of purity, purification steps were repeated up to five times. Spore suspensions containing $\leq 98\%$ phase bright spores were harvested and spores were resuspended in 50 mM imidazole phosphate buffer (IPB). Subsequently, purified endospores were used for inactivation experiments or were stored at 4 °C until further use for a maximum of 21 d. In this purification method, the use of enzymes or ultrasonic treatment were avoided to minimize spore damages, which probably influence following inactivation experiments. In Table 17, the preparation protocol for IPB is illustrated.

Table 17. Preparation of IPB

component	concentration	alternative name
Na ₂ HPO ₄	50 mM	solution A
NaH ₂ PO ₄	50 mM	solution B
Imidazole	50 mM pH 7	solution C
mixing ratio of solutions		
Solution A was titrated with solution B to pH 7 (solution AB)		
Solution AB was mixed 1:1 with solution C		

2.2.3.2 Endospore purification for spore proteome analysis

The analysis of spore proteomes according to 2.2.7 requires very high purity levels of spore suspensions. To prevent the existence of vegetative cells and cell residues, mechanical and enzymatic treatments of suspensions could not be excluded. According to Grecz *et al.* (1962), spore purification was performed in phosphate buffer containing 100 µg/ml trypsin and 200 µg/ml lysozyme. Pellets of purified spores were resolved in 10 ml of ice-cold distilled H₂O followed by dialysis. To remove enzymes,

dialysis tubings (MWCO 12 000 - 14 000, pore diameter ca. 25 Å, SERVA Electrophoresis GmbH) were incubated for 2 d at 4 °C in a volume of five liters distilled H₂O. Purified spores were stored at 4 °C for a maximum of 3 weeks.

2.2.4 Molecular biological methods

2.2.4.1 Isolation of genomic, bacterial DNA

Bacterial DNA was isolated by using the E.Z.N.A Bacterial DNA Kit (Omega Bio-Tek Inc.) (2.1.5). Initially, strains of *E. coli* and *C. botulinum* were grown in their corresponding media (*E. coli*: LB medium; *C. botulinum*: TPYC, 2.2.1.1; 2.2.1.2.1) until to log-phase and were harvested by centrifugation. DNA isolation was performed according to the “centrifugation protocol” of the user`s manual. In aberration to manufacturer`s instructions, cell wall digestion of *C. botulinum* cells were extended to 1 h. To increase the extent of cell wall disruption, glass beads were used additionally. For storage, isolated DNA samples were kept at – 20 °C.

2.2.4.2 Isolation of plasmid DNA

Bacterial plasmid DNA was isolated using the peqGOLD Plasmid Miniprep Kit II (PEQLAB Biotechnologie GmbH) (2.1.5). Initially, strains of *E. coli* and *C. botulinum* were grown in their corresponding media (*E. coli*: LB medium; *C. botulinum*: TPYC, 2.2.1.1; 2.2.1.2.1) until log-phase and were harvested by centrifugation. In aberration to the manufacturer`s instructions, the lysis of *C. botulinum* cells were optimized by adding 10 mg/ml lysozyme to the provided solution I. Prior to addition of solution II, the reaction mixture was incubated for 30 min at 37 °C. For storage, isolated plasmid DNA was kept at – 20 °C.

2.2.4.3 Agarose gel electrophoresis

Analytical analyses of DNA fragments were conducted by agarose gel electrophoresis (Sambrook, 1989). Prior to electrophoresis, DNA samples were diluted in 0.2 volumes of 6x loading dye (Fermentas GmbH). Gels of 1% agarose (v/v) were run in the Owl EasyCast electrophoresis system (13.8 x 12 cm; Thermo Fisher Scientific Inc.) at a constant voltage of 120 V for 45 min. As running buffer component, TAE (Table 18) was utilized. To visualize nucleic acids, gels were stained in dimidium bromid and were analyzed under UV light. The digitalization was performed by a gel documentation system from INTAS-science imaging instruments GmbH.

Table 18. Composition of TAE buffer

component	concentration
tris base	400 mM
acetate	4000 mM
EDTA	10 mM
pH 8	

2.2.4.4 DNA purification from agarose gels

For the reisolation of DNA fragments from agarose gels, the peqGOLD Gel Extraction Kit (PEQLAB Biotechnologie GmbH) was used. According to the manufacturer's instructions, DNA fragments were cut out of the gels and corresponding gel slices were melted in offered binding buffer. After loading and washing of provided binding columns, DNA was eluted in 50 μ l H₂O.

2.2.4.5 Enzymatic modification of plasmid DNA

To analyze plasmid DNA or to dispose plasmid fragments for cloning experiments, vector DNA was restricted by enzymatic digestion (Table 4; FastDigest enzymes, Fermentas GmbH). The composition of a common reaction mixture is listed in Table 19. According to the manufacturer's instructions, reaction temperatures and reaction times were confirmed to optimal working conditions of used restriction enzymes. The success of enzymatic cleavage was generally proved by agarose gel electrophoresis (2.2.3.1.3).

Table 19. Composition of the digest reaction mixture

component	amount
plasmid DNA	up to 1 μ g
FastDigest enzyme	1 U
10 x FastDigest Green Buffer	2 μ l
H ₂ O	add. to 20 μ l

2.2.4.6 Dephosphorylation of DNA fragments

Prior to cloning experiments, the relegation of linearized vector DNA was prevented by dephosphorylation. To remove 5'-phosphate residues, calf intestinal alkaline phosphatase (CAIP) was employed (Fermentas GmbH). According to instructions of the manufacture, the "simplified" phosphorylation protocol was carried out. After enzymatic DNA restriction (2.2.4.5), the reaction mixture (listed in Table 19) was added with 1 unit of CIAP and was finally incubated for 5 min at 50 °C. Afterwards, dephosphorylated DNA fragments were separated by agarose gel electrophoresis (2.2.4.3). For final purification of dephosphorylated fragments, the peqGOLD Gel Extraction Kit (PEQLAB Biotechnologie GmbH) was used (2.2.4.4).

2.2.4.7 Ligation of DNA fragments

For the cloning of DNA fragments into compatible, linearized, dephosphorylated vectors (2.2.4.5 and 2.2.4.6), the ATP-dependent T4 ligase (Fermentas GmbH) was employed. In addition to T4 ligase and DNA ligase buffer (Fermntas GmbH), the reaction mixture contained vector and insert DNA in a mixing ratio of 1:1 (Table 20). To ensure ligase reaction, the mixture was incubated over night at 4 °C. Afterwards, the reaction mixture was applied for genetic transformation experiments (2.2.4.9).

Table 20. Composition of the ligation reaction mixture

component	amount
vector DNA	0.5 µg
insert DNA	0.5 µg
T4 ligase	1 U
10 x T4 DNA ligase buffer	2 µl
H ₂ O	add to 20 µl

2.2.4.8 Polymerase chain reaction (PCR)

To amplify specific DNA fragments, PCR was conducted. To evidence the presence of distinct genes or for phylogenetic sequence analyses (16S-rDNA sequencing), DNA was amplified by Taq DNA polymerase (MP Biomedicals Solon). For subsequent cloning experiments according to 2.2.6.2, DNA was amplified by employing the

Phusion High-Fidelity DNA polymerase (New England Biolabs GmbH). In comparison to Taq DNA polymerase, the Phusion High-Fidelity DNA polymerase shows increased activity and reduced error rate. Depending on the used DNA polymerase, the composition of the reaction mixtures, the reaction times and temperatures were adapted to employed polymerase enzymes. Accordingly, standard compositions of PCR reaction mixtures and PCR cycles are listed in Table 21 and Table 22.

Table 21. Composition of PCR reaction mixtures

component	Final concentration in the Taq PCR reaction mixture	Final concentration in the Phusion High-Fidelity PCR reaction mixture
Taq DNA Polymerase	0.03 U/ μ l	-
Phusion High-Fidelity DNA polymerase	-	0.02 U/ μ l
Taq reaction buffer	1x	-
Phusion reaction buffer (HF or GC)*	-	1x
dNTPs	200 μ M	200 μ M
primer forward	0.6 μ M	0.5 μ M
primer reverse	0.6 μ M	0.5 μ M
DNA template	0.05 - 0.5 μ g	0.05 - 0.25 μ g

* According to manufacturer's instructions, HF buffer was used for standard reactions. For amplification of complex or GC-rich templates, GC buffer was used.

Table 22. Parameters of PCR cycles

Cycles	PCR step	Taq PCR		Phusion High-Fidelity PCR	
		time	temperature	time	temperature
1 x	initial denaturation	1 min	94 °C	1 min	98 °C
	denaturation	35 s	94 °C	10 s	98 °C
30 x	annealing	45 s	T _m - dependent	10 – 30 s	T _m - dependent
	elongation	product size - dependent (1 kb/min)	72 °C	product size - dependent (2 kb/min)	72 °C
1 x	final elongation	7 min	72 °C	7 min	72 °C

2.2.4.9 Transformation of *E. coli* by electroporation (Dower *et al.*, 1988)

To prepare electrocompetent *E. coli* cells (Table 10), bacterial precultures were used to inoculate 250 ml LB medium. Cultures of OD₅₇₈ = 0.5 - 1.0 were chilled on ice for 30 min and were harvested by centrifugation (10 min, 5000 x g, 4 °C). The corresponding cell pellets were washed in 1 volume ice cold H₂O, followed by additional washing in 10 ml ice cold glycerol solution (10%, (v/v)). Afterwards, the cells were resuspended in 5 ml of the glycerol solution and aliquots of 50 µl were prepared. In aberration to Dower *et al.* (1988), prior to storage at -70 °C, the samples were shock frosted in liquid nitrogen.

For electroporation, competent cell aliquots were defrosted on ice and were transferred to an ice cold 2 mm electroporation cuvette (Bio-Rad Laboratories GmbH). After the addition of 1 to 3 µl plasmid DNA, the mixture was chilled on ice for 15 min. Electroporation was performed at 25 µF, 200 W and 2.5 kV in the Gene Pulser II Electroporation System (Bio-Rad Laboratories GmbH). After exposing to electric pulses, cells were transferred in 5 ml LB medium and were incubated for 1 h at 37 °C (2.2.1.1). The selection of positive transformants was carried out on LB agar plates, which contained respective antibiotics.

2.2.5 ClosTron mutagenesis

In this study, gene knock outs in *C. botulinum* should be induced by ClosTron mutagenesis. The knock out system based on the selective integration of a group II intron into target DNA by retrohoming. The presence of a retransposition-activated marker (RAM), which is placed on the group II intron artificially, enables mutant selection.

2.2.5.1 Group II introns and the retrotransposition strategy of *Lactococcus lactis**

Group II introns are mobile retroelements, which catalyze their own excision of RNA transcripts and their integration into target DNA. This retrohoming process is mediated by a ribonucleoprotein complex, which contains the excised intron RNA and the intron encoded protein (IEP). The IEP is responsible for RNA splicing, target site recognition and for the insertion of intron RNA into the DNA target site.

The group II intron, which is used for ClosTron mutagenesis, is derived from the *Lactococcus lactis* intron LI.LtrB. The intron encoded protein of LI.LtrB is LtrA, which acts as RNA maturase, DNA endonuclease and reverse transcriptase. During the retrohoming process, the ribonucleoprotein complex (consisting of excised intron RNA and LtrA) mediates target site recognition. Based on the ribonucleoprotein complex-DNA-interaction, specific base pairings between DNA and RNA indicate the intron homing site. The site identification just based on three short sequence elements, where the intron-binding sites 1 and 2 (IBS1 and IBS2) and δ' interact with the complementary exon-binding sites 1 and 2 (EBS1 and EBS2) and δ . After identification of the homing sites, LtrA catalyzes the integration of the intron RNA into the target DNA by forming a lariat intermediate. Afterwards, LtrA initiates the formation of a RNA-DNA hybrid strand by reverse transcriptase activity. The process is finished by common cell enzymes. The RNA component of the hybrid strand is degraded by endonuclease and is converted to a DNA double-strand by polymerase activity. Final gaps are bridged by ligase (Coros *et al.*, 2005; Kuehne and Minton, 2012)

*The process described above is valid for the LI.LtrB behavior in *E. coli* and is also conferrable to the behavior in *Clostridium* spp. In *Lactococcus lactis*, the integration of the group II intron preferentially occurs through an endonuclease independent pathway (here not refer explicitly).

2.2.5.2 Clostron mutagenesis by using derivatives of pMTL007C-E2

The Clostridia Research Group (CRG) developed a modular system, where *Clostridium-E.coli* shuttle plasmids can be generated in an easy, low time consuming way. The system enables the generation of plasmids containing different gram negative and positive replicons, markers, multiple cloning sites (MCS) and promoters (<http://clostron.com/>). For the generation of *C. botulinum* knock out mutants, the use of shuttle plasmid pMTL007C-E2 was suggested (Figure 3) (Heap *et al.*, 2009, B). Figure 4 (Kuehne and Minton, 2012) illustrates the process of gene knock out generation by Clostron mutagenesis.

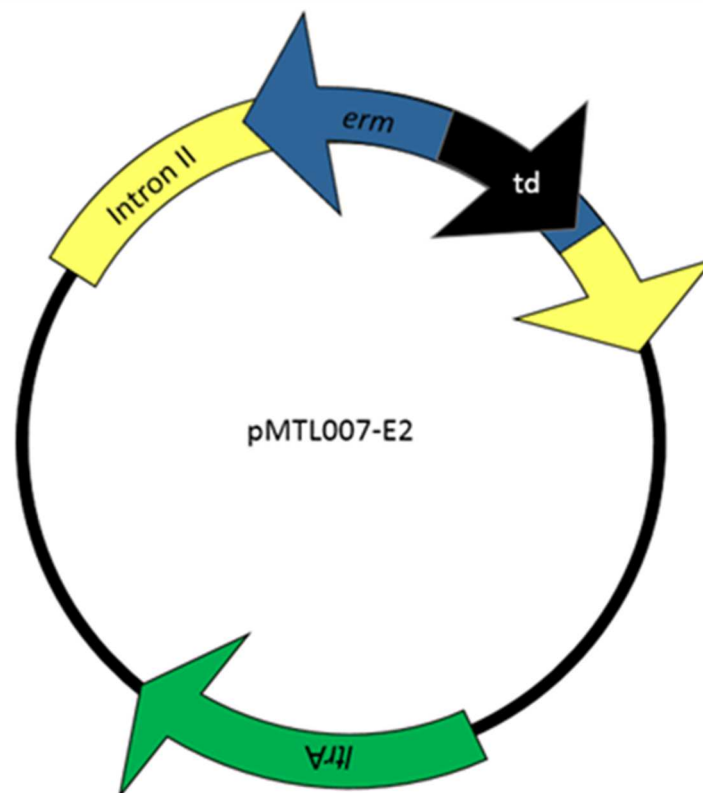


Figure 3: Plasmid map of pMTL007-E2. The figure represents a plasmid map of pMTL007-E2. The vector contains a group II intron (yellow), which is derived from LI.LtrB. Into the group II intron, the *erm* gene (blue), which permits erythromycin resistance, is inserted. The resistance gene is interrupted by the insertion of a phage *td* group I intron (black). As well the plasmid contains the *ltrA* gene, which encodes the protein LtrA. In contrast to the native LI.LtrB group II intron, *ltrA* is placed separately (Kuehne and Minton, 2012).

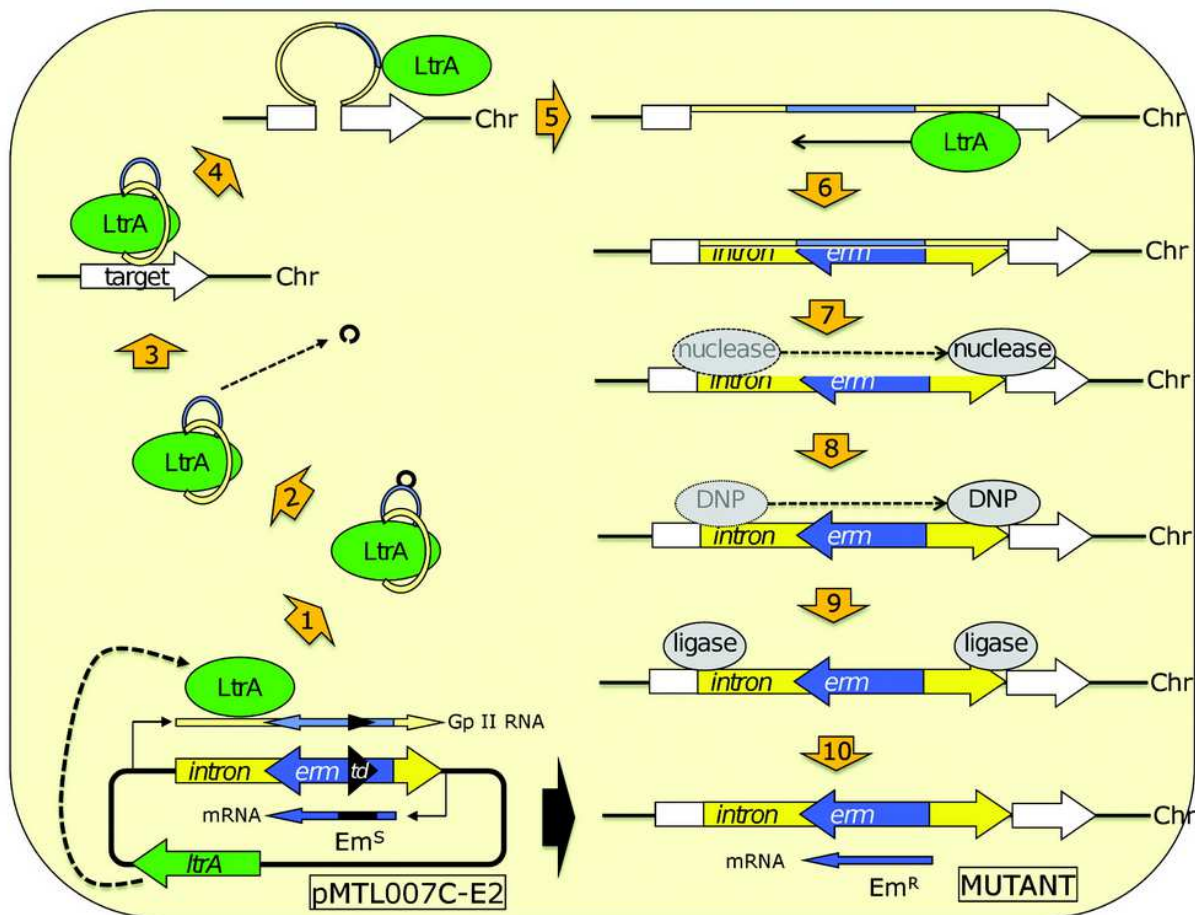


Figure 4: Clostron mutagenesis by using Clostron plasmid pMTL007C-E2. The transcription and translation of *LtrA* leads to the generation of the multifunctional LtrA. The transcription of the *erm* results in an mRNA, which contains the *td* group I intron. Generally, the *td* intron is capable to catalyze its own restriction out of RNA transcripts, but this ability depends on the direction of transcription. Inside the *erm* transcript, *td* is inactive. Consequently, the translation of the *erm* RNA does not result in erythromycin resistance. The transcription of the group II intron-construct leads to an RNA, which binds to LtrA to form the ribonucleoprotein complex (1). Based on the direction of transcription, the *td* intron gets active and is spliced out of the complex (2). LtrA mediates target site recognition (3), intron insertion (4) and the formation of a DNA-RNA hybrid strand (6). *Clostridium* host enzymes (nuclease, DNA polymerase and ligase) catalyze the formation of a DNA double strand (7, 8, 9 and 10) as described above (2.2.5.1). Based on retransposition-activated marker, knock out mutants get resistant to erythromycin (Kuehne and Minton, 2012).

As described above (2.2.5.1), target site recognition only depends on three short sequence elements. The manipulation of IBS1, IBS2 and δ' of the group II intron allows site directed intron insertion in any given DNA location. To determine the re-targeted regions of the group II intron, an online intron design tool is provided (<http://clostron.com/>), which employs the Pertuka algorithm (Pertuka *et al.*, 2004).

Clostron plasmids, which contain individual designed re-targeted regions, can be ordered at DNA2.0 Inc. (CA, USA).

2.2.5.3 Transformation of *C. botulinum*

To transfer the *Clostridium-E.coli* shuttle plasmids (derivatives of pMTL007C-E2) into *C. botulinum*, following transformation strategies were tested.

2.2.5.3.1 Plasmid transfer by conjugation

The following method was used to transform *Clostridium* spp. by conjugation, based on Heap *et al.* (2009, A). To transfer derivatives of pMTL007C-E2 vectors into *C. botulinum* type E strains, the donor strain *E. coli* CA434 was used. ClosTron plasmids were transferred into the donor strain by electroporation (2.2.4.9). Positive transformants were selected on LB agar plates supplemented with 25 µg/ml chloramphenicol and 30 µg/ml kanamycin. The *C. botulinum* recipient was cultured in 1 - 10 ml of TPYC or TPYG media (2.2.1.2.1) and harvested in different culture ages (8 - 72 h). The donor strain was incubated overnight in 1 - 10 ml LB medium, containing the corresponding antibiotics. A volume of 1 – 2 ml of the *E. coli* CA434 overnight cultures were harvested and washed in PBS to remove antibiotic residues. For the conjugal mating, cell pellets of the donor strain were resuspended in 100 – 1000 µl of the recipient culture. Consequently, the mating mixture was spotted on TPYC, TPYG or DRCM agar plates. Alternatively, the mating suspension was transferred on a nitrocellulose membrane (pore size 0.45 µm, Satorius AG), which was additionally placed on the agar plates. Conjugation plates were incubated anaerobically for 8 – 48 h, at 28 or 37 °C. To select cells of *C. botulinum*, which took up derivatives of pMTL007C-E2, colonies were transferred to TPYC, TPYG or DRCM agar plates supplemented with 250 µg/ml cycloserine and 15 µg/ml thiamphenicol. Afterwards, putative transformants were transferred to agar plates containing 2.5 µg/ml erythromycin or 15 µg/ml lincomycin, to select knock out mutants. The success of plasmid transfer and knock out generation were proved by plasmid isolation (2.2.4.2) or by PCR (2.2.4.8) and agarose gel electrophoresis (2.2.4.3).

2.2.5.3.2 Plasmid transfer by electroporation

To transform derivatives of pMTL007C-E2 vectors into *C. botulinum* type E strains, different electroporation protocols, which based on Zhou and Johnson (1993), Davis *et al.*, (2000), Oultram *et al.*, (1988) and on Mermelstein and Papoutsakis (1993), were tested or were combined with each other. All working steps, excepting centrifugation and electroporation, were performed under anaerobic conditions. Cells of *C. botulinum*

were cultured in TPYG or TPYC (2.2.1.2; 2.2.1.2.1) media, supplemented with and without 1% glycine (w/v). To produce electrocompetent cells, bacteria were harvested at different culture ages ($OD_{600} = 0.2$; 0.8 and 1.2) by centrifugation (4 °C, 10 min, 4000 x g). Afterwards, cells were washed and resuspended in 0.2 - 0.8 volumes of ice cold electroporation buffer. Following electroporation buffers were employed (a: 15% glycerol; b: 10% PEG 8000; c: SMP (270 mM sucrose, 1 mM $MgCl_2$, 7 mM $Na_2HPO_4 \cdot 7 H_2O$, pH 7.4) and d: 270 mM sucrose, 5 mM sodium phosphate, pH 7.4). Plasmid DNA (up to 10 μg) and competent cells (200 - 800 μl) were combined in electroporation cuvettes (0.2 and 0.4 cm gap). The mixtures were overlaid with 200 μl paraffin oil to protect bacteria against aerobic atmosphere, during the process of electroporation. Electroporation parameters of 2.0 – 2.5 kV, 25 μF and 200, 300, 400 and $\infty \Omega$ were employed. After application of electric pulses, the cell suspensions were diluted in 10 ml of TPYC or TPYG medium, supplemented with and without 25 mM $MgCl_2$. For regeneration, cells were incubated 3 – 9 hours, prior to transfer on selective agar plates. TPYC or TPYG agar plates supplemented with 15 $\mu g/ml$ thiamphenicol were used for the selection of positive transformants. Putative transformants were transferred to agar plates containing 2.5 $\mu g/ml$ erythromycin or 15 $\mu g/ml$ lincomycin to identify potential knock out mutants. The success of plasmid transfer and knock out generation were inspected by plasmid isolation (2.2.4.2) or PCR (2.2.4.8) and agarose gel electrophoresis (2.2.4.3).

2.2.6 Circumvention of putative restriction barriers of *C. botulinum* type E

Due to difficulties in *C. botulinum* type E strains transformation, the existence of restriction barriers was supposed. To overcome putative restriction barriers, Clostron plasmids should be methylated by following methods.

2.2.6.1 Plasmid methylation by different *E. coli* strains

To diversify the methylation status of plasmids, derivatives of pMTL007C-E2 were initially transformed (2.2.4.9) and subsequently reisolated (2.2.4.2) from *E. coli* strains with different methylation patterns. Finally, premethylated plasmids should be transferred in *C. botulinum* type E strains by electroporation (2.2.5.3.2). According to Davis *et al.* (2000), the *E. coli* strains Top10, GM2163 and HB101 (Table 10) were employed as primary hosts.

For conjugation experiments, the conjugative plasmid R702 was reisolated (2.2.4.2) from *E. coli* CA434 and was transferred into *E. coli* GM2163 by electroporation (2.2.4.9). After the additional transfer of pMTL007C-E2 derivatives, the corresponding bacteria were used as donor strain for conjugation (2.2.5.3.1).

2.2.6.2 Plasmid methylation by employing the methyltransferase (CLO_1092) of *C. botulinum* (TMW 2.990)

Presumably, *C. botulinum* (TMW 2.990) encodes a type II restriction and modification (RM) system. To exploit the methylation pattern of *C. botulinum*, the corresponding gene, which encodes for the putative methyltransferase (CLO_1092), was cloned into the expression vector pBAD/Myc-His A (Invitrogen GmbH). In *in vivo* methylation of ClosTron plasmids should be subsequently performed in *E. coli* prior to plasmid transfer into *C. botulinum* (TMW 2.990).

To prepare the expression vector pBAD/Myc-His A for the cloning experiment, plasmid DNA was restricted by employing the endonucleases XhoI and HindIII (2.2.4.5), followed by dephosphorylation (2.2.4.6). The linearized DNA fragment was separated by agarose gel electrophoresis (2.2.4.3) and consequently purified from gel (2.2.4.4).

The putative methyltransferase gene from *C. botulinum* was conformed to the codon usage of *E. coli* and was provided with suitable restriction sites. The adjusted methyltransferase gene was synthesized by the GENEART AG and was provided in a pMA-RQ (ampR) vector (The DNA sequence of the adapted methyltransferase gene is attached in the appendix).

To prepare the methyltransferase gene for the cloning experiment, pMA-RQ-Met was digested by XhoI and HindIII (2.2.4.5) and the corresponding methyltransferase gene fragment (1771 bp) was purified (2.2.4.3 and 2.2.4.4). Afterwards, the linearized pBAD/Myc-His A vector and the methyltransferase gene were ligated (2.2.4.7). Consequently, the arising plasmid pBAD/Myc-His A-Met was transformed in *E. coli* Top10 and in *E. coli* CA434 (2.2.4.9). Gene expression was induced by the application of L-arabinose. In a pilot experiment, the optimal gene expression level was analyzed, according to user's manual of the expression vector.

E. coli cells which harbored the pBAD/Myc-His A-Met vector were additionally transformed (2.2.4.9) with derivatives of pMTL007C-E2 and selected on LB agar plates, supplemented with 100 µg/ml ampicillin and 25 µg/ml chloramphenicol.

After culturing of positive transformants in selective LB medium until $OD_{600} = 0.5$, methyltransferase expression was induced by adding 0.0002% (v/v) L-arabinose. Accordingly, cells were incubated for further 3 h to allow protein expression and DNA methylation.

Induced, recombinant cells of *E. coli* CA434 were subsequently used for conjugation experiments, to transform *C. botulinum* (TMW 2.990) (2.2.5.3.1).

Induced, recombinant cells of *E. coli* Top10 were harvested and plasmids (pBAD/Myc-His A-Met and pMTL007C-E2 derivatives) were purified by the peqGOLD Plasmid Miniprep Kit II (2.2.4.2). To gain methylated derivatives of pMTL007C-E2, the plasmid mixture was separated by agarose gel electrophoresis and plasmids of interest were purified directly from agarose gels (2.2.4.4). Afterwards, pMTL007C-E2 derivatives were employed for electroporation experiments, to transform *C. botulinum* (TMW 2.990) (2.2.5.3.2).

2.2.6.3 Restriction assay and plasmid methylation by cell free extracts of *C. botulinum* (TMW 2.990)

To analyze, if plasmid derivatives of pMTL007C-E2 were degraded by *C. botulinum* (TMW 2.990), restriction assays were carried out. Cell free extracts of *C. botulinum* were prepared. In aberration to Donahue *et al.* (2000), crude extracts were produced without addition of Na₂EDTA and DTT. Afterwards, 1 µg plasmid DNA was incubated in the presence of *C. botulinum* crude extracts (50 – 200 µg) for one hour at 37 °C. Prior to analyze plasmid DNA by agarose gel electrophoresis (2.2.4.3), enzymes of the crude extract were heat-inactivated (10 minutes, 70 °C).

For *in vitro* methylation of pMTL007C-E2 derivatives, plasmid DNA was treated with cell-free extracts of *C. botulinum*, according to Donahue *et al.* (2000). Therefore, cells of *C. botulinum* were grown in TPYC medium until to $OD_{600} = 0.6 - 0.9$ (2.2.1.2) and were harvested by centrifugation. Afterwards, cell-free extracts were prepared. Among other chemicals, the used extraction buffer contained EDTA, DTT and a protease

inhibitor cocktail. EDTA was employed to chelate divalent cations, which inhibited nucleases of the crude extracts but enabled methyltransferase activity.

For *in vitro* methylation, plasmid derivatives of pMTL007C-E2 were purified from *E. coli* (2.2.4.2). According to Donahue *et al.* (2000), vector DNA was added to the reaction mixture, which contained acetates, chelating agents, the methyl group donor S-(5'-adenosyl)-L-methionine (SAM) and cell-free protein extract of *C. botulinum* (TMW 2.990) (50 µg).

After incubation for 1 h at 37 °C, enzymes of the reaction mixture were inactivated by heat treatment (10 min, 70 °C). To regain putatively methylated derivatives of pMTL007C-E2, the inactivated reaction mixture was separated by agarose gel electrophoresis (2.2.4.3), followed by plasmid purification (2.2.4.4). According to 2.2.5.3.2, purified derivatives of pMTL007C-E2 were used to transform *C. botulinum* (TMW 2.990) by electroporation.

2.2.7 Methods for protein analysis

2.2.7.1 MALDI-TOF MS (Matrix-assisted Laser Desorption/Ionization Time of Flight Mass spectroscopy)

MALDI-TOF MS represents a spectrometric technique to identify proteins or peptide fragments according to their specific masses. In this technique, the co-crystallized matrix-analyte is ionized and the corresponding protein- or peptide-ions are accelerated through an electro-static field. In a field free drift region, the ions are separated. Based on their time of flight and in due consideration of the mass to charge ratio, peptide masses can be determined. To identify specific proteins, peptide masses were compared to protein databases.

To analyze the proteome of *C. botulinum* type E endospores, which were grown on different sporulation media (TPYC, AEY, M140 and SFE (2.2.1.2.1)), MALDI-TOF MS was employed. Three biological spore suspension replicates of distinct strain/sporulation media compositions were analyzed. To ensure statistical expressiveness, ten spots of each replicate were used to acquire MALDI-TOF MS spectra.

2.2.7.1.1 Target preparation for spore protein analyzes by MALDI-TOF MS

According to 1.2.2, spores of *C. botulinum* type E (TMW 2.990, TMW 2.994 and TMW2.997) were generated on TPYC, AEY, M140 and SFE medium. After endospore purification (2.2.3.2), 200 µl of pure spore suspension (10^7 spores/ml) were harvested by centrifugation (15,000 x g, 4 °C, 1 min). After removing the supernatant, the spore pellet was resolved in 50 µl of 70% TFA (trifluoroacetic acid), followed by incubation at room temperature for 30 minutes. Subsequently, 1 µl of the mixture was spotted onto a MALDI stainless polished steel target (Bruker Daltonik (Bremen Germany)) and was air-dried. Afterwards, spots were overlaid with 1 µl matrix solution (10 mg CHCA/ml (α -cano-4-hydroxy-cinnamic acid), 50% ACN (Acetonitrile) and 2.5% TFA).

2.2.7.1.2 Recording of MALDI-TOF MS spectra and data analysis

MALDI-TOF MS spectra were acquired on a Microflex LT spectrometer (Bruker Daltonik), in a mass range of 2 to 20 kDa. Measurements were arranged in the linear positive ion mode. Analyte ionization was generated by a nitrogen laser (337 nm) at a frequency of 60 Hz. FlexControl (Version 3.3) (Bruker Daltonik) and Biotyper Automation Control (Version 2.0) were used for basic administration. For protein peak detection LIMPIC (linear MALDI-TOF MS peak identification and classification) was applied (Usbeck *et al.*, 2013).

To identify specific spore proteins of *C. botulinum* (TMW 2.990), datasets were matched to known peptide masses of the corresponding strain. The protein data were provided by UniProtKB. Because trypsin was used for endospore purification (2.2.3.2), datasets were also compared to peptide masses, which putatively resulted from protease digestion. To reconstruct theoretical isoelectric points and mass values, protein sequences from UniProtKB were computed by the Peptide Mass tool, provided on the ExPASy portal.

At synchronization of measured and provided protein/peptide masses, potential events of posttranslational modifications (methylation, dimethylation, hydroxylation, dihydroxylation, acetylation, phosphorylation, glucosylation, glutathionylation and addition of water) were also considered.

For the comparison of spore proteomes from different *C. botulinum* type E strains, which were derived from different sporulation media (TPYC, AEY, M140 and SFE), MALDI-TOF MS spectra were clustered by in house software, based on MDS (multidimensional scaling).

2.2.7.1.3 Cleaning procedure of MALDI-TOF targets

The MALDI-TOF targets were cleaned according to the manufacturer's instructions. After overlying the target for 5 minutes with 70% ethanol, the target was washed with hot tap water and was wiped with 70% ethanol. Afterwards, the target was overlaid with 100 µl 80% trifluoroacetic acid and was wiped again. Finally, the target was cleaned with deionized water and was dried again.

2.2.7.2 SDS-PAGE (sodium dodecyl sulfate polyacrylamide gel electrophoresis)

SDS-PAGE was performed to separate proteins according to their masses and to their electrophoretic mobility. In this study, the discontinuous Laemmli-system was employed (Laemmli, 1970). The acrylamide concentration of the separation gel varied from 8 up to 15%. Protein separation was operated in the Mini-PROTEAN Tetra System (Bio-Rad Laboratories GmbH), according to the manufacturer's instructions. To increase the resolution of protein separation, gels of 25 x 20 cm were prepared, additionally. Hence, the SE900 Large Format Vertical Gel Electrophoresis equipment (Hoefer Inc.), which is usually used for 2D gel electrophoresis, was utilized. The separation gels were poured in the Large Format PAGE Multiple Gel Caster. After polymerization, the glass cassettes were removed from the gel caster equipment and were fixed on the bottom and on the sides, to allow the preparation of the stacking gel. Combs were self-made, by trimming a thick plastic film. Based on vertical protein separation, samples were diluted with melted agarose prior to sample application. After polymerization of the fixed samples, wells were also filled with agarose. Proteins were separated at 65 V, 80 mA and 5 W, in running buffer according to Laemmli (1970).

2.2.7.2.1 Preparation of *E. coli* samples for SDS-PAGE

Cell pellets, which were derived from 1 ml of *E. coli* growing cultures were resuspended in 100 µl 1 x SDS-PAGE sample buffer (Table 23). Prior to application on SDS gels, samples were boiled for 5 minutes.

Table 23. Compounds of 1 x SDS-PAGE sample buffer

component	amount
Tris-HCl pH 6.8	50 mM
SDS	2%
glycerol	10%
β -mercaptoethanol	1%
EDTA	12.5 mM
bromophenol blue	0.02%

2.2.7.2.2 Preparation of endospore sample for SDS-PAGE

Volumes of 1 - 3 ml purified endospore suspensions (2.2.3.2) were harvested by centrifugation (10.000 x g, 2 min). In aberration to Harder (2001), the spore pellets were resuspended in 200 μ l SDS buffer (0.9% SDS, 0.1% Pefabloc, 100 mM Tris base, pH 8.6) followed by ultrasound treatment (HD-70/Bandelin, three cycles of 30 s, power 90%, cycle 70%, on ice). The mixtures were diluted with 700 μ l thiourea lysis buffer (6.10 M urea, 1.79 M thiourea, 65.06 mM Chaps, 1% (w/v) DTT, 0.5% (v/v) Pharmalyte 3-10). For protein solubilization the suspensions were vortexed for 20 min at 4 °C. To remove insoluble spore residues, the suspensions were centrifuged (17.500 x g at 4 °C, 30 min). Afterwards, the clear supernatants were diluted in 1 volume of 1 x SDS-PAGE sample buffer (Table 23), prior to sample application on gels. Alternatively, the samples were stored at – 80 °C until further use.

2.2.7.2.3 Staining of SDS gels

For the visualization of proteins, SDS gels were silver stained according to Blum *et al.* (1987). Alternatively, gels were stained by colloidal Coomassie, according to the manufacturer`s instructions (Roti-Blue; Carl Roth GMBH & Co.).

2.2.7.3 Protein identification by high resolution LC-MS/MS

For protein identification, SDS gels were stained by colloidal Coomassie (Roti-Blue; Carl Roth GMBH & Co.) and were destained in sterile deionized H₂O. Bands of interest were cut out under laminar flow and were analyzed by high resolution LC-MS/MS in the Zentrallabor für Proteinanalytik (Ludwig-Maximilians-Universität München, Germany). To identify distinct spore proteins of *C. botulinum* (TMW 2.990), sequences

of identified peptide fragments were matched to protein databases (UniProt KB and NCBI).

2.2.8 Characterization of soybean oil emulsions and high pressure-induced endospore inactivation in emulsion matrices

Prior to high pressure-induced inactivation of *C. botulinum* type E endospores in soybean oil emulsions, matrices of different fat contents were characterized. The effect of pressure and heat application on droplet size and emulsion stability were estimated. Additionally, the effect of non-bounded emulsifier on endospore inactivation was tested. Furthermore, the distribution of endospores in oil-water (O/W) emulsions was also analyzed, prior, during and after HPT treatment.

2.2.8.1 Preparation of (O/W) soybean oil emulsions

Soybean oil (O/W) emulsions with fat contents of 10 – 70% (v/v) were prepared. Prior to emulsification, IPB (Table 17) was added with 2% (w/v) of soybean lecithin. Afterwards, commercially available soybean oil (Sojola, Germany) was added to the buffer solution and continuously dispersed (2 min, Ultra-Turrax). Subsequently, emulsion samples were treated one minute by ultrasound (HD-70/Bandelin, 60 s, power 1000%, cycle 70%). To ensure sterility, the used equipment, buffers and oils were autoclaved.

2.2.8.2 Characterization of emulsion stability by multisample analytical centrifugation

Stabilities of soybean oil emulsions were determined by multisample analytical centrifugation (LUM GmbH, Germany). In this technique, emulsion samples are centrifuged in addition to photometric observation. In contrast to “real time” stability tests, the process of phase separation is accelerated. During centrifugation, the intensity of transmitted light is recorded as a function of phase separation position and time. The corresponding SepView software was employed to record transmission profiles and creaming kinetics. The separation behavior of emulsion samples were analyzed by comparing slopes of mathematical integrated creaming kinetic datasets (Badolato *et al.*, 2008). Emulsion samples of 1 ml were applied to LUMiFuge cuvettes and were fixed in the particle separation analyzer. During centrifugation (2000 rpm, 20 °C, 42 min), the emulsions were creamed and corresponding kinetics were acquired.

2.2.8.3 Droplet size characterization of soybean oil emulsions

2.2.8.3.1 Droplet size characterization of soybean oil emulsions prior and after heat and pressure treatment

The laser particle analyzer Mastersizer 2000 (Malvern Instruments GmbH, Germany) was employed to determine the droplet sizes of emulsions. Particles of the sample dispersed through a focused laser beam and scatter the light in defined angles, which are inversely proportional to their specific sizes. Based on light intensity and diffraction angles, particle sizes were calculated. The software of the Mastersizer 2000 converts the datasets into particle-size distributions. Furthermore, the volume mean diameters ($D [4,3]$) and the statistical parameters of particle-size distributions ($D (v, 0.1)$; $D (v, 0.5)$ and $D (v, 0.9)$) were calculated.

For droplet size characterization, soybean oil emulsions with fat contents of 10, 30, 50 and 70% were prepared (2.2.8.1). Prior to measurements, samples were treated by heat (75 °C, 10 min), pressure (750 MPa, 10 min) or by combined parameters (75 °C, 750 MPa, 10 min). Additionally, untreated emulsions were also analyzed.

2.2.8.3.2 Microscopic droplet size characterization of soybean oil emulsions during pressurization

To determine the droplet sizes of 10% soybean oil emulsions during pressurization, the HPDS-high pressure cell (Hartmann *et al.*, 2003) was used. Pressure up to 250 MPa was generated. During pressure generation and reduction, microscopic images were recorded at 200 folds of magnification.

For evaluation, diameters of characteristic soybean oil droplets were calculated by employing the graphic software GIMP 2.8.

2.2.8.4 Influence of unbounded emulsifier on high pressure- and heat-induced inactivation of *C. botulinum* type E endospores

Endospore inactivation should be performed in emulsions containing different fat contents. According to 2.2.8.1, the continuous phase of the emulsion was still enriched with 2% soybean lecithin (w/v). Accordingly, the total emulsifier concentration decreased with increasing fat content of the emulsion. Consequently, the amount of unbounded emulsifier differed as a function of variable fat contents. Due to this fact, the influence of unbounded emulsifier on endospore (TMW 2.992) inactivation was

tested. Purified endospores (2.2.3.1) were harvested by centrifugation (15000 x g, 4 °C, 15 min). Accordingly, spore pellets were resuspended in IPB (Table 17), while spore concentration was setted to approximately 1×10^7 spores/ml. Afterwards, soybean lecithin was added (0 - 5% (w/v)). Prior to spore inactivation experiments, samples were filled in to cryo tubes (1.8 ml) by avoiding air bubbles. Adjacent, samples were treated for 10 min by different pressure/temperature combinations (a: 75 °C, 0.1 MPa; b: RT, 750 MPa; c: 75 °C, 750 MPa). Subsequently, treated and untreated samples were diluted in TS+ (0.85% NaCl and 0.1% (w/v)) followed by plate count determination on TPYG agar (2.2.1.2). Finally, log reduction of endospores were calculated as a function of inactivation parameters.

Pressure treatments were arranged in a dual vessel high pressure unit (V: 2 x 7 ml; p_{\max} : 800 MPa; T_{\max} : 80 °C; Knam Schneidetechnik GmbH, Germany). As pressure transferring liquid (PTL) a mixture of PEG 400 and water (60:40) was used. Vessel temperature was regulated by using thermostating vessel jackets and an external refrigerated/heating circulator (FC 600, JULABO Labortechnik GmbH, Germany). Thermal-induced inactivation was performed in a water bath (LAUDA Dr. D. Wobser GmbH & Co., Germany).

2.2.8.5 Determination of endospore distribution in oily systems

2.2.8.5.1 Determination of endospore distribution in heterogenic oil/buffer mixtures

To analyze the distribution of *C. botulinum* type E endospores in oil/buffer mixtures “phase separation experiments” were carried out. IPB (Table 17) and soybean oil (30, 50 and 70% (v/v)) were merged to a total volume of 10 ml. Afterwards, the mixtures were homogenized for 2 minutes by employing the Ultra-Turrax. Purified endospores of TMW 2.992 (2.2.3.1) were added (5×10^6 - 2×10^7 spores/ml), followed by vortexing for one minute. To enable phase separation, the heterogenic mixtures were incubated in glass test tubes for a minimum of three weeks.

When phase separation was completed, oil-, inter- and buffer-phase were graded by pipetting. To determine the endospore distribution, collected phases were vortexed and diluted separately, prior to plate count determination on TPYG agar plates. According to Molin and Snygg (1967), the first dilution steps were performed in 55% (v/v) ethanol. For continuous dilution series, TS+ (2.2.4.4) was used.

To clarify the definition of the three different phases, the experimental setup is illustrated in Figure 5.

For more detailed determination of spore distribution, mixtures were inoculated with 1×10^6 spores/ml, as already mentioned. After phase separation, the interface and the upper line of the unmixed buffer phase ($v = 1$ ml) were additionally employed for plate count determination.

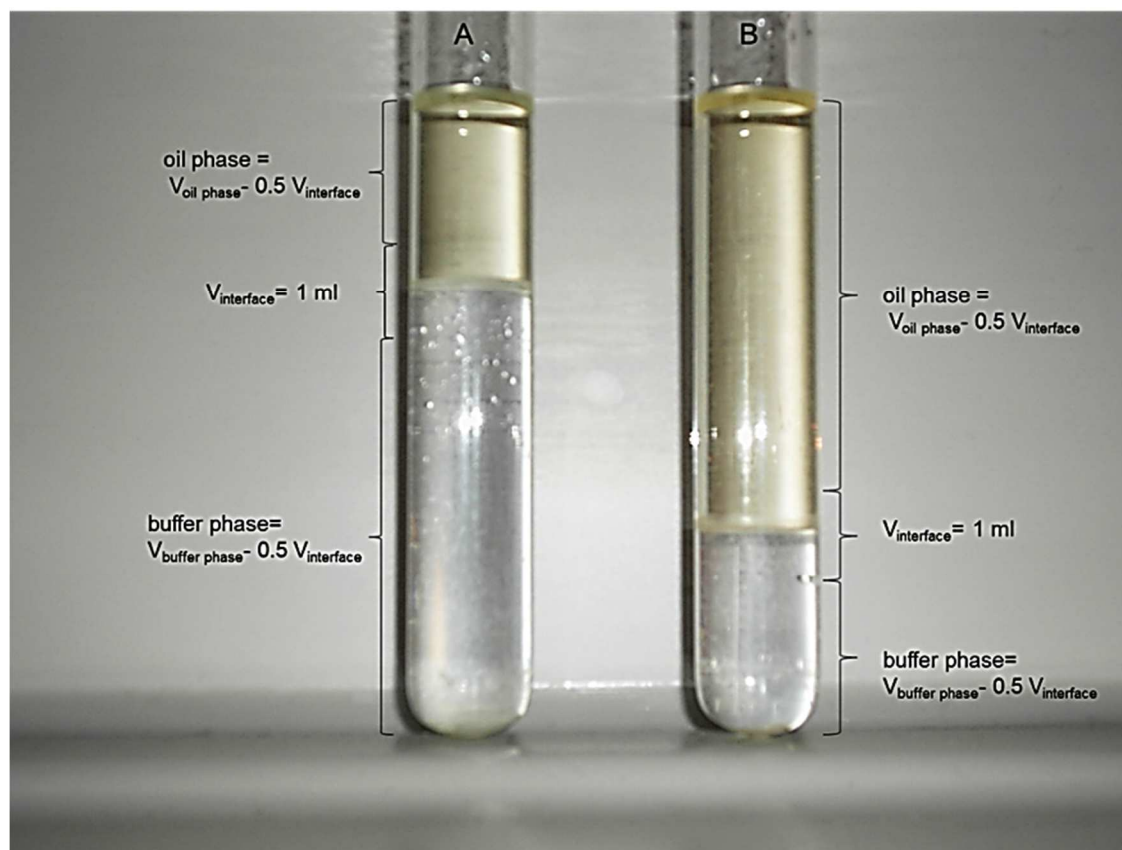


Figure 5: Definition of oil-, inter- and buffer-phase. A and B illustrate separated mixtures, which contained 30 and 70% soybean oil. The interface was defined to a total volume of 1 ml, which contained 500 µl of the oil bottom line and 500 µl of the upper buffer line. Oil- and buffer-phase were specified by subtraction of the corresponding volume of the interface.

2.2.8.5.2 Determination of endospore distribution in heterogenic oil/buffer mixtures by microscopic observation

To determine the endospore distribution in 50% soybean oil/ IPB mixtures, microscopic observations were done. According to 2.2.8.5.1, heterogenic mixtures were prepared, followed by inoculation with 5×10^5 spores/ml (2.2.3.1). Finally, percental endospore distribution was calculated by observation of 10 fields of view at 1000 fold of magnification.

2.2.8.5.3 Determination of endospore distribution in emulsion matrices by fluorescence microscopic observation

To analyze the distribution of *C. botulinum* type E endospores (TMW 2.992) in emulsion matrices, endospores were stained with the fluorescent dye SYTO 9, prior to microscopic observation. In aberration to Laflamme *et al.* (2004), pellets of approximately 10^6 purified endospores (2.2.3.1) were resuspended in 100 μ l of 0.3% DMSO (v/v) and 5 - 10 μ M SYTO 9. After incubation for 15 minutes by avoiding light, stained spores were washed in 500 μ l of 0.3% DMSO (v/v), followed by washing in IPB (Table 17). Afterwards, spore pellets were resuspended in 100 μ l IPB, containing 2% soybean lecithin (w/v). Prior to microscopic observations, model emulsions with fat contents of 30, 50 and 70% were inoculated (5×10^5 spores/ml). For fluorescence microscopic observations, the BX51WI (Olympus GmbH) and the Axiostar plus (Carl Zeiss Micro Imaging GmbH) were employed and the filter sets U-MNIBA2 and FilterSet09 were used. For statistical survey of endospore distribution in model emulsions, 10 fields of view were analyzed at 1000 fold of magnification.

2.2.8.6 Inactivation of *C. botulinum* type E endospores in emulsion matrices by heat treatment

Prior to heat-induced inactivation experiments, TPYC-derived endospores of *C. botulinum* type E (TMW 2.992) were purified according to 2.2.3.1. Subsequently, spores were diluted in IPB (Table 17) or in soybean oil emulsions (2.2.8.1) with fat contents of 30, 50 and 70% (1×10^7 spores/ml). For sample preparation, 200 μ l of the spore inoculated matrices were filled in to heat shrink tubings (DSG-Canusa, Germany). The tubes were heat sealed by avoiding air bubbles. Prior to heat treatment, the tubes were inserted into thin walled glass capillaries, which included 1 ml of the corresponding matrix. To monitor the sample-temperature profile, a thin wire thermocouple was employed. For heat-mediated inactivation at 45 – 75 °C, samples were heated in a water bath (LAUDA Dr. D. Wobser GmbH & Co., Germany). After reaching the corresponding inactivation temperature, samples were treated for a total of 10 minutes. Finally, to calculate the log reductions, treated and untreated samples were diluted according to 2.2.8.5.1, followed by plate count determination on TPYC agar.

2.2.8.7 Inactivation of *C. botulinum* type E endospores in emulsion matrices by HPT treatment

For HPT-induced inactivation of endospores, samples were prepared according to 2.2.8.6. The prepared shrink tubings were packed in to 1.8 ml cryovials and covered either with IPB or emulsions. Experiments were carried out using two different high pressure units, to explore the differences in inactivation results that can be due to adiabatic heating effects [U4000 (V = 750 ml, p_{max} = 1000 MPa, T_{max} = 100 °C, PTL (pressure transferring liquid) = PEG 400 and water (1:1)) and U111 (V = 6 ml, p_{max} = 1000 MPa, T_{max} = 100 °C, PTL = pentane hexane and extraction naphtaa silicone oil (1:1); both units constructed by Unipress, Warsaw, Poland)].

In unit U4000, temperature profiles were monitored in the PTL, whereas in U111, temperatures were measured directly in the corresponding sample matrices. In unit U4000 average compression and decompression rates of 9.45 and 85.59 MPa/s were obtained, respectively. According to experiments conducted in unit U111, average compression and decompression rates of 27.67 and 200.06 MPa/s were generated, respectively. As a function of emulsion fat content and target pressure/temperature, initial starting temperatures were adjusted individually, to ensure almost optimal isothermal holding times, in pressure unit U111. However in pressure unit U4000, as a function of target pressure and temperature, initial starting temperatures of the PTL were also adjusted individually. Consequently, target temperatures according to experiments obtained in unit U111 were equal to matrix temperatures, while in experiments conducted in unit U4000, target temperatures were equal to temperatures in the PTL. To comprehend the influence of differing locus of temperature monitoring on endospore inactivation, adiabatic heating effects in emulsion samples of different fat contents were determined. Corresponding pressure-temperature-profiles are attached (Figure AV – AXV). Cryovials treated in unit U4000 contained heat shrink tubings with inoculated sample (IPB or emulsions of different fat contents) and were filled up with IPB. Vials treated in unit U111 contained tubings with samples (only with one fat content at a time) and were filled up with emulsions of the same fat content. In unit U4000, temperature profile was monitored in the PTL, whereas in U111, temperature was measured directly in the corresponding sample matrix.

To calculate the log reductions, treated and untreated samples were diluted according to 2.2.4.5.1, followed by CFU (colony forming units) determination in TPYC pour plates.

3 RESULTS

3.1 Transformation of *C. botulinum* type E strains

In order to probe transformation and gene knock out strategies for *C. botulinum* type E strains, genes which encode SASPs (CLO_1237, CLO_3013 and CLO_3241) or the germination-specific protease (CLO_2913) were used as targets for gene knock outs with individually designed ClosTron plasmids.

Anticipatory, it should be mentioned none of the developed transformation strategies was successful to generate *C. botulinum* type E strain transformants. Consequently, the construction of *C. botulinum* mutant spores failed. Still the obtained findings of these approaches can be useful to develop further strategies for genetic modification of these wild type strains.

3.1.1 Selection of *C. botulinum* type E strains for knock out and transformation experiments

For knock out generation and for transformation experiments, a collection of nine *C. botulinum* type E strains (TMW 2.990 – TMW 2.998) were screened for the existence of SASP genes (CLO_1237 (270 bp), CLO_3013 (198 bp), CLO_3241 (186 bp) and CLO_2913 (972 bp)), by PCR (2.2.4.8). For gene amplification, the following primers, which flanked the genes of interested were designed (CLO_1237_rev, CLO_1237_for, CLO_2913_for, CLO_2913_rev, CLO_3013_for, CLO_3013_rev, CLO_3241_for and CLO_3241_rev (2.1.6)). The results of corresponding PCR screenings are displayed by the agarose gel, depicted in Figure 6. Obviously, the amplification of specific DNA fragments (435, 331, 297 and 1286 bp) in TMW 2.990, TMW 2.991, TMW 2.995 and TMW 2.997 established the existence of analogous genes. In strain TMW 2.993, only the gene analogue to CLO_1237 could be amplified. Based on these results, the strains TMW 2.990, TMW 2.991, TMW 2.995, TMW 2.997 and TMW 2.993 were selected for further knock out and transformation experiments.

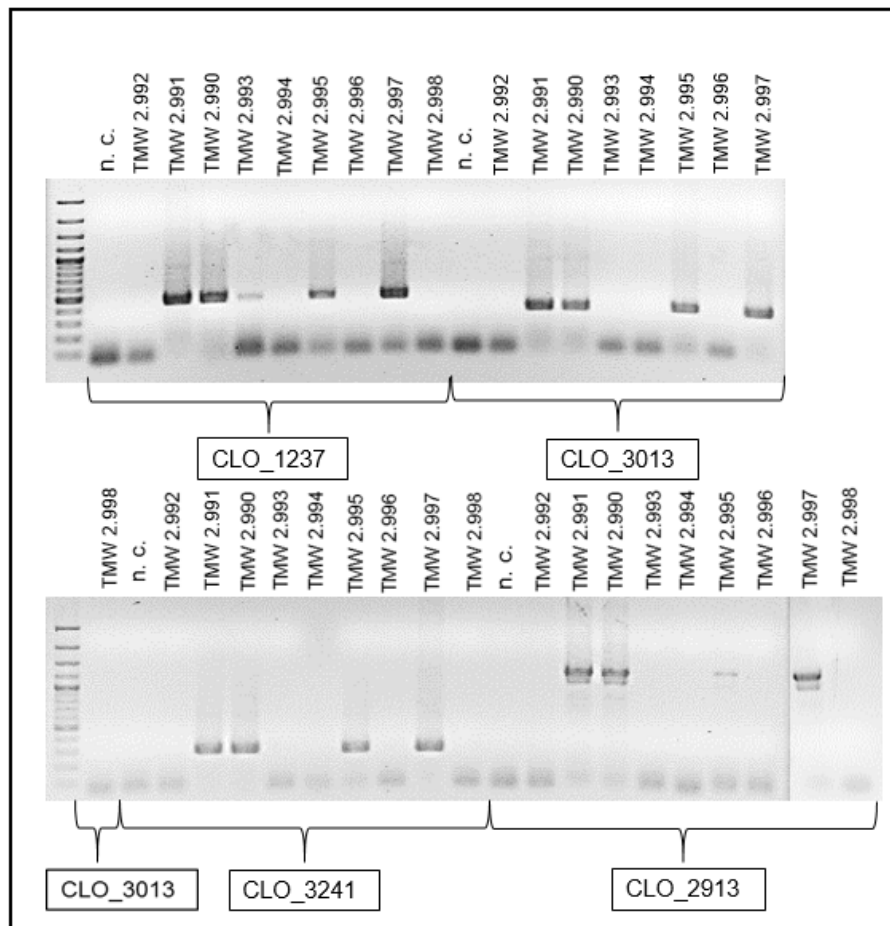


Figure 6: Gene detection in *C. botulinum* type E strains by PCR amplification. To prove the existence of gene analogues to CLO_1237, CLO_3013, CLO_3241 and CLO_2913, a total of nine *C. botulinum* type E strains (TMW 2.990 – TMW 2.998) were screened by PCR. For PCR, specific primer sets were used ((CLO_1237_rev, CLO_1237_for); (CLO_2913_for, CLO_2913_rev); (CLO_3013_for, CLO_3013_rev); (CLO_3241_for, CLO_3241_rev)). The different *C. botulinum* type E strains are indicated by TMW numbers. Reaction mixtures without DNA template were used as negative controls (n. c.). The GeneRuler 100 bp Plus was employed as marker (Fermentas GmbH).

3.1.2 Transformation of *C. botulinum* type E strains by *E. coli*-mediated conjugation

For the transformation of *C. botulinum* type E (TMW 2.990, TMW 2.991, TMW 2.995, TMW 2.997 and TMW 2.993), Clostron plasmids (pMTL007C-E2:43973-Cbo-ssp3241, pMTL007C-E2:53142-Cbo-ssp3013, pMTL007C-E2:53143-Cbo-ssp1237 and pMTL007C-E2:53144-Cbo-gpr) were tested. Prior to plasmid transfer into *C. botulinum*, Clostron plasmids were initially transformed into the donor strain *E. coli* CA434 by electroporation (2.2.4.9). Consequently, the success of *E. coli* transformation was proven by electrophoretic separation (2.2.4.3) of reisolated (2.2.4.2), BspHI digested (2.2.4.5) plasmid DNA. In Figure 7, the results of these experiments are depicted. The specific band pattern (DNA fragments of 1461, 1624, 2386 and 3562 bp) indicated, that *E. coli* CA434 strains were effectively transformed

with derivatives of pMTL007C-E2 (9033 bp). The conjugative transfer of ClosTron plasmids from *E. coli* CA434 into recipient *C. botulinum* type E strains was not successful. Neither the use of different *C. botulinum* culture media (TPYC, TPYG or DRCM), nor the application of different *C. botulinum* type E culture ages (8 - 72 h) led to positive conjugation results. The use of different mating plates and the additional use of underlayments (TPYC, TPYG, DRCM agar plates ± nitrocellulose membrane), as well variations in mating times (8 – 48 h) did not enable conjugation, respectively.

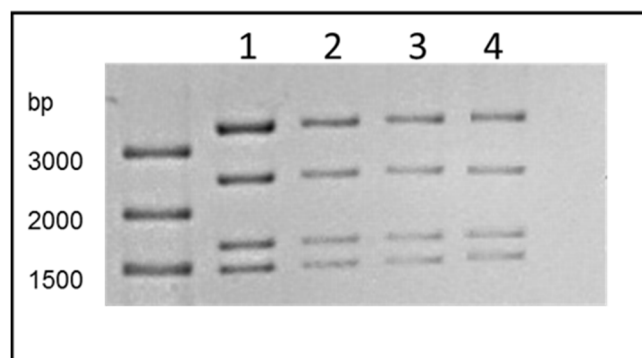


Figure 7: BspHI-mediated digestion of *E. coli* CA434-derived ClosTron plasmids. The agarose gel shows the BspHI digested ClosTron plasmids 1) pMTL007C-E2:43973-Cbo-ssp3241, 2) pMTL007C-E2:53142-Cbo-ssp3013, 3) pMTL007C-E2:53143-Cbo-ssp1237 and 4) pMTL007C-E2:53144-Cbo-gpr) after reisolation from *E. coli* CA434. DNA fragments of 1461, 1624, 2386 and 3562 bp were established. As DNA ladder, the GeneRuler 100 bp Plus (Fermentas GmbH) was used.

3.1.3 Transformation of *C. botulinum* type E strains by electroporation

According to 2.2.5.3.2, strains of *C. botulinum* type E (TMW 2.990, TMW 2.991, TMW 2.995, TMW 2.997 and TMW 2.993) should be transformed with ClosTron plasmids (pMTL007C-E2:43973-Cbo-ssp3241, pMTL007C-E2:53142-Cbo-ssp3013, pMTL007C-E2:53143-Cbo-ssp1237 and pMTL007C-E2:53144-Cbo-gpr) by electroporation.

The transfer of ClosTron plasmids into *C. botulinum* type E strains by standard electroporation protocols did not yielded in transformants. Consequently, a set of experimental parameters was diversified (2.2.5.3.2). Neither the application of glycerin to growth media (TPYC and TPYG), nor the use of cells with different culture ages ($OD_{600} = 0.2 - 1.2$) influenced the effectivity of plasmid transfer. Both the use of four different electroporation buffers (2.2.5.3.2) and the application of different cell to DNA ratios (200 – 800 μ l *C. botulinum* type E cells were supplemented with plasmid DNA up to 10 μ g) did not support plasmid transfer. Neither the use of different electroporation cuvettes (gap of 0.2 and 0.4 cm), nor diversified electroporation

parameters (2.0 – 2.5 kV; 200, 300, 400 and $\infty \Omega$) resulted in positive transformation events. Neither the application of $MgCl_2$ to the regeneration media (TPYC and TPYG), nor variations in regeneration times (3 – 9 h) did influenced the effectivity of *C. botulinum* type E transformation.

3.1.4 Circumvention of putative restriction barriers of *C. botulinum* type E

Based on difficulties in transforming *C. botulinum* type E strains, the existence of restriction barriers were supposed. To circumvent putative events of plasmid degradation by restriction endonucleases of *C. botulinum*, different plasmid methylation strategies were tested (2.2.6.1 - 2.2.6.3).

3.1.4.1 *E. coli*-mediated plasmid methylation

Prior to transformation *C. botulinum* (TMW 2.990) by electroporation, different methylation pattern of several *E. coli* strains (Top10, GM2163 and HB101) should be exploited, to premethylate derivatives of pMTL007C-E2 (2.2.6.1).

After transforming *E. coli* strains with corresponding ClosTron plasmids (2.2.1.1), the success of plasmid transfer was proven by agarose gel electrophoresis (2.2.3.1.3) of reisolated (2.2.3.1.2), BspHI digested (2.2.3.1.5) plasmid DNA. In Figure 8, the results of these experiments are depicted by the corresponding agarose gel. The evidence of specific band pattern (DNA fragments of 1461, 1624, 2386 and 3562 bp) indicated that *E. coli* strains Top10, GM2163 and HB101 were effectively transformed with derivatives of pMTL007C-E2 (9033 bp).

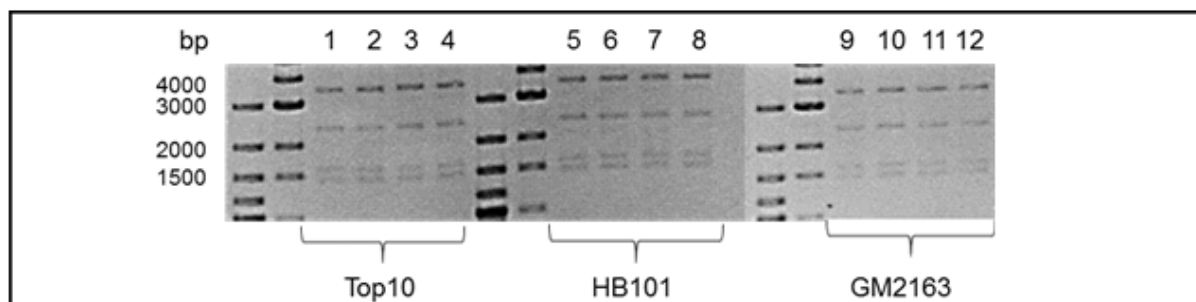


Figure 8: Digestion of ClosTron plasmids, reisolated from different *E. coli* strains. The agarose gel shows the BspHI-mediated digestion of the ClosTron plasmids (pMTL007C-E2:43973-Cbo-ssp3241 (lane: 1, 5 and 9), pMTL007C-E2:53142-Cbo-ssp3013 (lane: 2, 6 and 10), pMTL007C-E2:53143-Cbo-ssp1237 (lane: 3, 7 and 11) and pMTL007C-E2:53144-Cbo-gpr (lane: 4, 8 and 12)), which were reisolated from *E. coli* strains Top10, HB101 and GM2163. Restriction of ClosTron plasmids resulted in DNA fragments of 1461, 1624, 2386 and 3562 bp. As DNA size markers, the GeneRuler 100 bp Plus and the 1 kb plus DNA ladder (Fermentas GmbH) were used.

After reisolation of premethylated ClosTron plasmids, *C. botulinum* (TMW 2.990) should be transformed by electroporation, according to 3.1.3. Generally, neither the use of premethylated ClosTron plasmids, nor different electroporation parameters (according to 3.1.3) led to effective transformation of *C. botulinum*.

To conjugate ClosTron plasmids into *C. botulinum*, a donor strain, which differed in methylation pattern to CA434 (and also HB101) was also tested.

To generate a suitable donor strain, the conjugative plasmid R702 (69 kb) was reisolated (2.2.3.1.2) from *E. coli* CA434, followed by transformation into *E. coli* GM2163 (2.2.3.1.9). To prove the success of *E. coli* GM2163 transformation, R702 was reisolated (2.2.4.2) and analytical PCR was performed. In mentioned reaction, R702_for and R702_rev primers (2.1.6) were employed, to amplify defined DNA fragments of 1009 bp. Accordingly, transgenic strains of *E. coli* GM2163 were again prepared to become competent. Consequently, the strains were additionally transformed with specific ClosTron plasmids (pMTL007C-E2:43973-Cbo-ssp3241, pMTL007C-E2:53142-Cbo-ssp3013, pMTL007C-E2:53143-Cbo-ssp1237 and pMTL007C-E2:53144-Cbo-gpr), (2.2.4.9).

To inspect, if “double transformation” of *E. coli* GM2163 was successful, plasmids were reisolated (2.2.4.2). To prove the presence of ClosTron plasmids, reisolated plasmid DNA was digested by employing BspHI (2.2.4.5). Additionally, to evidence the presence of R702, the reisolated plasmid DNA was amplified by employing R702_for and R702_rev primers.

The agarose gel in Figure 9 confirms the success of double plasmid transfer into *E. coli* GM2163. The presence of R702 was proven by the amplified DNA fragments of 1009 bp, while the availability of ClosTron plasmids was indicated by detection of DNA fragments of 1461, 1624, 2386 and 3562 bp.

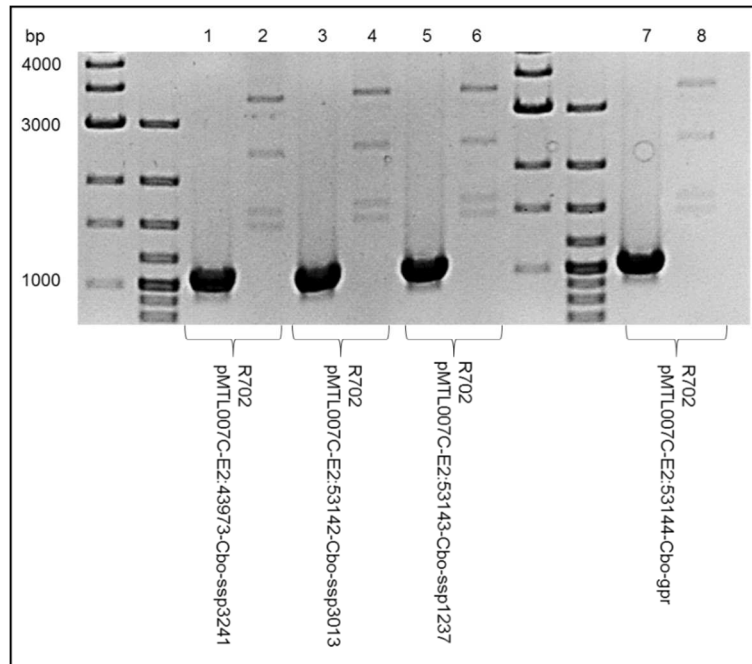


Figure 9: Evidence of double *E. coli* GM2163 transformation. Curly brackets symbolize the collective origin of reisolated plasmid DNA from a specific *E. coli* GM2163 host. In lanes 1, 3, 5 and 7, PCR amplificats according to R702_for and R702_rev primers are visualized. In lanes 2, 4, 6 and 8, results of BspHI-mediated Clostron plasmid restriction are illustrated. As DNA size markers, the GeneRuler 100 bp Plus and the 1 kb plus DNA ladder (Fermentas GmbH) were used.

“Double transformants” of *E. coli* GM2163 should be employed, to transfer Clostron plasmids into *C. botulinum* (TMW 2.990) by conjugation (2.2.5.3.1). However, the use of conjugative *E. coli* GM2163 strains, which differ in methylation pattern to *E. coli* CA434, did not lead to transformation events of *C. botulinum* TMW 2.990.

3.1.5 Plasmid methylation by employing the methyltransferase (CLO_1092) of *C. botulinum* (TMW 2.990)

The putative methyltransferase-encoding gene (CLO_1092) of *C. botulinum* (TMW 2.990) is supposed to be part of a strain-specific restriction-modification (RM) type II system (4.1.6.1). To protect foreign Clostron plasmids against endonuclease activity, the associated methyltransferase (CLO_1092) should be exploited to premethylate plasmid DNA.

According to 2.2.6.2, the corresponding methyltransferase gene was adapted to the codon usage of *E. coli*, through gene synthesis by the GENEART AG. After cloning the modified methyltransferase gene (1760 bp) into the expression vector pBAD/Myc-His A (4.1 Kb), the derived plasmid pBAD/Myc-His A-Met (5824 bp) was transferred into *E. coli* Top10 and *E. coli* CA434 (2.2.6.2 and 2.2.4.9).

The success of the cloning experiment and the attempt of plasmid transfer were confirmed by pBAD/Myc-His A-Met reisolation (2.2.4.2), followed by BspHI -mediated DNA digestion (2.2.4.5). The results are depicted in the agarose gel in Figure 10. Obviously, lane 1 presents the reisolated pBAD/Myc-His A-Met vector (5824 bp), while lane 2 presents the corresponding digestion pattern (DNA fragments of 1002 and 4822 bp).

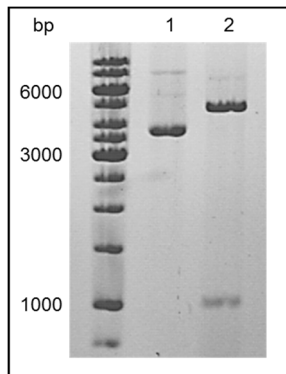


Figure 10: Confirmation of pBAD/Myc-His A-Met. The agarose gel shows the pBAD/Myc-His A-Met vector (5824 bp), which was created according to 2.2.6.2. Lane 1 represents the plasmid after reisolation from *E. coli* Top10 (2.2.4.2). In lane 2, DNA fragments of 1002 and 4822 bp are visible, which resulted from pBAD/Myc-His A-Met-mediated BspHI digestion (2.2.4.5). As DNA ladder, the 1 kb GeneRuler (Fermentas GmbH) was employed.

To analyze the gene expression level of the corresponding methyltransferase (68.25 kDa) in recombinant *E. coli* strains, liquid growing cultures were induced by applying the inducer L-arabinose (2.2.6.2). Based on crude extract analysis by SDS-PAGE, the expression of a protein with equivalent mass to CLO_1092 was confirmed, when 2×10^{-5} and 2×10^{-4} % arabinose were added, respectively (Figure 11). Finally, successful expression of the modified methyltransferase (CLO_1092) is indicated.

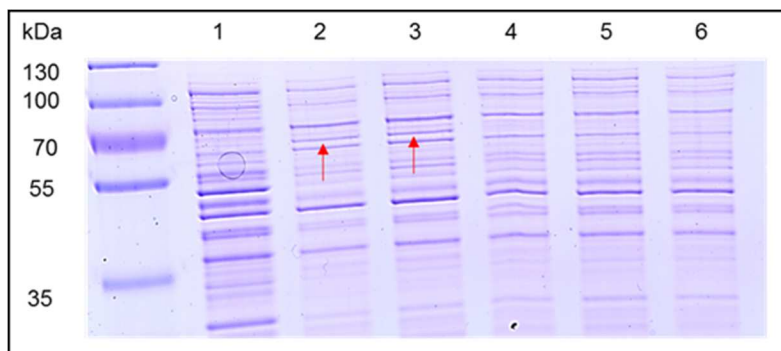


Figure 11: Methyltransferase expression in *E. coli* Top10. Depicted are crude extracts of *E. coli* Top10 transformants, which harbored pBAD/Myc-His A-Met. Expression of the corresponding methyltransferase gene (CLO_1092) was induced by 0 (lane 1), 2×10^{-5} (lane 2), 2×10^{-4} (lane 3), 2×10^{-3} (lane 4), 0.02 (lane 5) and 0.2% L-arabinose (lane 6). The red arrows in lane 2 and 3 signify the expression of a 68.25 kDa protein, which is associated to CLO_1092. As protein standard, the prestained ladder SM 0671 (Fermentas GmbH) was employed.

After the pilot protein expression, transformants of *E. coli* Top10 and *E. coli* CA434, which harbored pBAD/Myc-His A-Met were additionally transformed with a pMTL007C-E2 derivative (2.2.4.9).

To inspect, if “double transformation” of *E. coli* Top10 and CA434 was successful, plasmids were reisolated (2.2.4.2). To prove the presence of pMTL007C-E2 (9033 bp) derivatives and pBAD/Myc-His A-Met (5824 bp), reisolated plasmid DNA was digested by BspHI (2.2.4.5).

The agarose gel in Figure 12 confirmed the double plasmid transfer into *E. coli* Top10 and CA434. The presence of pMTL007C-E2:43973-Cbo-ssp3241, pMTL007C-E2:53142-Cbo-ssp3013, pMTL007C-E2:53143-Cbo-ssp1237 and pMTL007C-E2:53144-Cbo-gpr were indicated by proving DNA fragments of 1461, 1624, 2386 and 3562 bp, while the presence of pBAD/Myc-His A-Met was evidenced by indicating fragments of 1002 and 4822 bp.

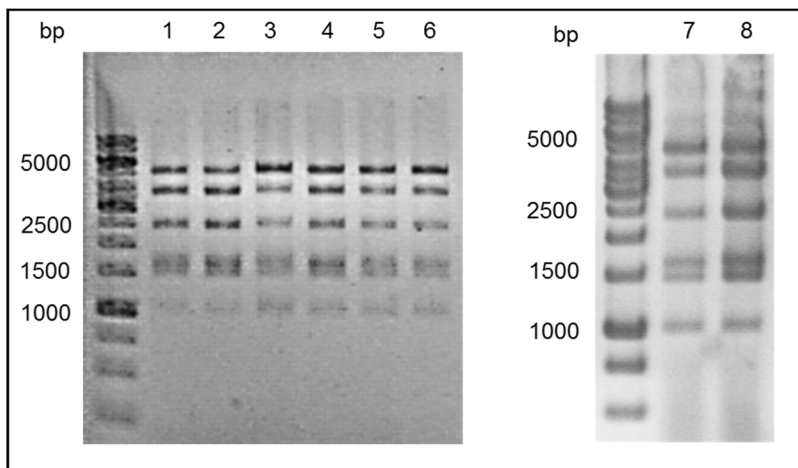


Figure 12: BspHI-mediated digestion of pBAD/Myc-His A-Met and ClosTron plasmids. The agarose gel illustrates DNA fragments of 4822, 3562, 2386, 1624, 1461 and 1008 bp, which resulted from combined BspHI digestion of pBAD/Myc-His A-Met and one specific ClosTron plasmid (pMTL007C-E2:43973-Cbo-ssp3241 (lane 1 and 5), pMTL007C-E2:53142-Cbo-ssp3013 (lane 2 and 6), pMTL007C-E2:53143-Cbo-ssp1237 (lane 3 and 7), pMTL007C-E2:53144-Cbo-gpr (lane 4 and 8). Prior to enzymatic digestion, plasmids were reisolated (2.2.4.2) from double transformants of *E. coli* Top10 (lane 1 - 4) or *E. coli* CA434 (lane 5 - 8). As DNA size marker, the 1 kb DNA ladder (Fermentas GmbH) was used.

After inducing the methyltransferase-gene expression in corresponding double transformants of *E. coli* CA434 (2.2.5.3.2), the hosts were employed for conjugation experiments. To transfer putatively premethylated ClosTron plasmids into *C. botulinum* (TMW 2.990), conjugal mating was performed according to 2.2.5.3.1.

After inducing the methyltransferase-gene expression in double transformants of *E. coli* Top10 (2.2.5.3.2), putatively premethylated ClosTron plasmids were reisolated (2.2.4.2), purified (2.2.4.4) and subsequently, *C. botulinum* (TMW 2.990) was transformed by electroporation (2.2.5.3.2).

Finally, the expression of the adapted methyltransferase-encoding gene of *C. botulinum* (CLO_1092) was induced in *E. coli*, in coexistence to one of the specific ClosTron plasmid (pMTL007C-E2:43973-Cbo-ssp3241, pMTL007C-E2:53142-Cbo-ssp3013, pMTL007C-E2:53143-Cbo-ssp1237 or pMTL007C-E2:53144-Cbo-gpr). Generally, the coexistence of the established gene product did not support the transfer of ClosTron plasmids into *C. botulinum* (TMW 2.990) neither by conjugation, nor by electroporation. This was shown by absence of transformants.

3.1.6 Restriction assay and plasmid methylation by cell free extracts of *C. botulinum* (TMW 2.990)

To demonstrate potential endonuclease activity in *C. botulinum* (TMW 2.990), ClosTron plasmids were incubated in crude extracts. To indicate putative processes of DNA degradation, corresponding reaction mixtures were incubated one hour followed by agarose gel electrophoresis. In Figure 13, plasmid DNA of pMTL007C-E2:53144-Cbo-gpr is apparent. In lane 1 of the gel, untreated plasmid DNA is visible. Obviously, the vector was present in open circular (oc) and in covalently closed (ccc) topologies. Lane 2 represents corresponding plasmid DNA, which was treated with 50 µg crude extract of *C. botulinum*. In comparison to untreated DNA, additionally linear plasmid topologies were indicated. The treatment of plasmids with 100 µg crude extract (lane 3), led to degradation of ccc plasmid variants and caused an increase of linear (l) vector DNA. Lane 4 represents plasmid DNA, which was treated with 150 µg crude extract of *C. botulinum*. Obviously, just linear vector forms were detectable. The treatment of plasmids with 200 µg crude extract led to high levels of DNA degradation (lane 5).

Finally, these observations lead to the suggestion that pMTL007C-E2:53144-Cbo-gpr was degraded by unspecific and by a site-specific endonuclease, which cuts plasmid DNA at one specific cleavage site.

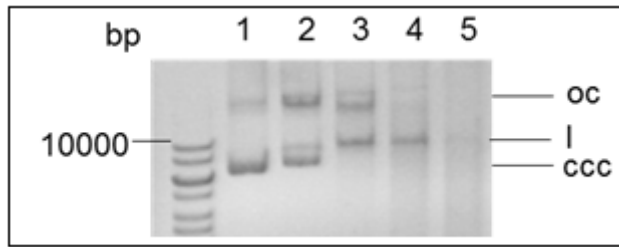


Figure 13: Crude extract-mediated digestion of pMTL007C-E2:53144-Cbo-gpr. The agarose gel illustrates plasmid DNA of pMTL007C-E2:53144-Cbo-gpr, after concentration-dependent treatment with crude extract of *C. botulinum* (TMW 2.990). In lane 1, untreated vector DNA is apparent. In lane 2 - 5, plasmid DNA is depicted, which were treated with different amounts of *C. botulinum* crude extracts (lane 2: 50 µg; lane 3: 100 µg; lane 4: 150 µg; lane 5: 200 µg), for one h at 37 °C. The different topology variants of vector DNA (oc: open circular plasmids, l: linear plasmid DNA, ccc: covalently closed circular plasmids) are marked. As DNA size marker, the 1 kb DNA ladder (Fermentas GmbH) was employed.

To circumvent predicted restriction modification systems of *C. botulinum* (TMW 2.990), plasmid DNA should be protected for endonuclease-mediated restriction by *in vitro* methylation, prior to transformation. According to 2.2.6.3, derivatives of pMTL007C-E2 were incubated in the reaction mixture for 1 h at 37 °C. The corresponding reaction mixture contained among others, crude extract of *C. botulinum*, protease inhibitors, SAM and EDTA, which reduces the activity of endonucleases. Prior to electroporation of *C. botulinum*, putatively methylated ClosTron plasmids were analyzed by agarose gel electrophoresis (2.2.4.4). The agarose gel in Figure 14 represents plasmid DNA of pMTL007C-E2:43973-Cbo-ssp3241, pMTL007C-E2:53142-Cbo-ssp3013, pMTL007C-E2:53143-Cbo-ssp1237 and pMTL007C-E2:53144-Cbo-gpr after *in vitro* methylation. Obviously, oc and ccc variants of ClosTron plasmids were existent. To transfer putatively methylated ClosTron plasmids into *C. botulinum*, vector DNA was purified from agarose gels (2.2.4.4), followed by electroporation (2.2.5.3.2).

In summary, the pre-incubation of ClosTron plasmids in mixtures of *C. botulinum* crude extracts, chelating agents, SAM and protease inhibitors did not lead to successful transformation of *C. botulinum* (TMW 2.990).

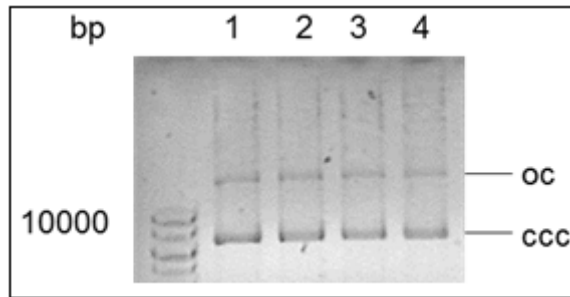


Figure 14: Clostron plasmids after *in vitro* methylation. The agarose gel represents the oc and ccc variants of Clostron plasmids (lane 1: pMTL007C-E2:43973-Cbo-ssp3241, lane 2: pMTL007C-E2:53142-Cbo-ssp3013, lane 3: pMTL007C-E2:53143-Cbo-ssp1237 and lane 4: pMTL007C-E2:53144-Cbo-gpr) after *in vitro* methylation.

3.2 Influence of sporulation medium on spore proteomes of *C. botulinum* type E

According to Lenz and Vogel (2014), the HPT resistance of *C. botulinum* type E endospores is influenced by the type of sporulation medium (TPYC, AEY, M140 and SFE) (2.2.1.2.1). Especially SFE-derived spores are more robust (Lenz and Vogel, 2014). To elucidate whether the HPT resistance of spores is mediated by media induced differences in spore proteomes, corresponding spore proteins were analyzed by MALDI-TOF MS and high resolution LC-MS/MS (2.2.7.1 - 2.2.7.3).

3.2.1 Strain- and medium- dependent character of *C. botulinum* type E spore proteomes

To analyze the strain- and sporulation medium-dependent influences on endospore proteomes, MALDI-TOF MS was conducted. For experimental setup, *C. botulinum* type E strains (TMW 2.990, TMW 2.994 and TMW 2.997) were sporulated in TPYC, AEY, M140 and SFE media (2.2.1.2.1), followed by endospore purification (2.2.3.2). After recording MALDI-TOF MS spectra, datasets were clustered by MDS (2.2.7.1.2).

The Voronoi diagram in Figure 15 represents the clustering of MALDI-TOF MS spore spectra, as a function of strain specificity (TMW 2.990, TMW 2.994 and TMW 2.997) and sporulation media (SFE, TPYC, AEY and M140). MDS was performed in due consideration to the presence and intensity of measured signals. Figure 15 illustrates that the homology of MALDI-TOF MS spore spectra were mainly influenced by the type of sporulation medium than by strain specificity. Spore spectra, which were associated to sporulation in M140 (blue circles) were predominantly grouped in region I. Spectra related to sporulation in TPYC (turquoise crosses) were preferential clustered in region II and partly showed high similarities to spectra of AEY-derived TMW 2.990 spores (red

crosses). Region III largely reflects spectra of TMW 2.994 and TMW 2.997 endospores, which were sporulated in AEY. The broad variance of data, according to AEY-derived spores, indicated that endospores exhibited highest variations in media-dependent spore proteome pattern. The tight clustered area of green crosses in region I indicated, that especially SFE-derived endospores of TMW 2.990, TMW 2.994 and TMW 2.997 showed high analogies in their MALDI-TOF MS peak pattern.

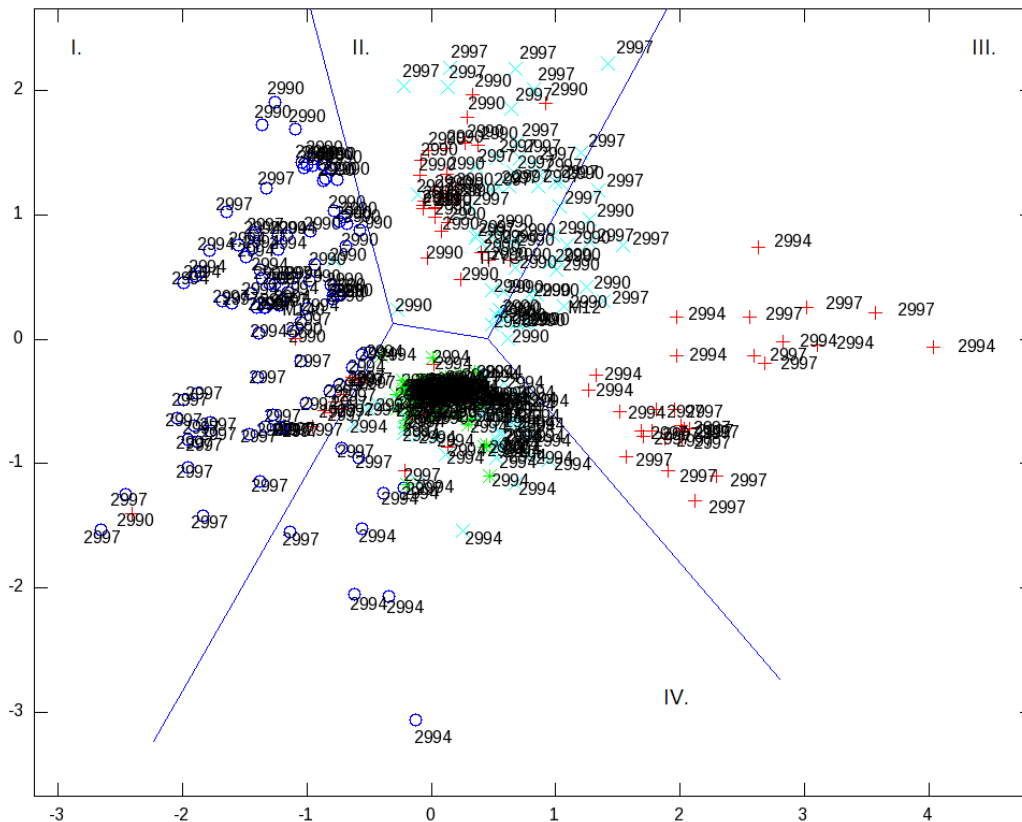


Figure 15: Cluster of MALDI-TOF MS endospore spectra. As a function of strain and sporulation medium specificity, the Voronoi diagram illustrates the analogies and differences between MALDI-TOF MS endospore spectra. Different *C. botulinum* type E strains are indicated by corresponding TMW numbers (TMW 2.990, TMW 2.994, TMW 2.997), while corresponding sporulation media are indicated by colored symbols (green crosses: SFE, red crosses: AEY, turquoise crosses: TPYC, blue circles: M140).

3.2.2 Identification of predominant proteins in SFE-derived endospores by MALDI-TOF MS

To identify proteins, which are predominantly present in SFE-derived *C. botulinum* type E spores, MALDI-TOF MS was carried out. For proteome analyses, TPYC-, M140-, AEY- and SFE-derived spores of TMW 2.990 were used. According to 2.2.3.2, endospores were purified, MALDI-TOF MS spectra were acquired (2.2.7.1.2) and datasets were clustered by MDS (Figure 16). Due to MALDI-TOF MS analysis, masses of potential proteins were calculated and datasets were compared to entries of protein

databases (UniProtKB and NCBI). Furthermore, datasets were also matched to peptide masses, which putatively resulted from trypsin digestion (2.2.7.1.2). For synchronization of measured and provided protein/peptide masses, potential events of posttranslational modifications (PTM) were also considered (2.2.7.1.2). Peak lists and results of protein identification are attached in the Table AI - AIV.

The Venn diagram in Figure 16 symbolizes the numbers and congruency of peaks, which were detected by MALDI-TOF MS, when *C. botulinum* (TMW 2.990) sporulated in SFE (blue), TPYC (light green), M140 (dark green) and in AEY (violet), respectively. According to endospores which were formed in SFE, a total of 79 significant peaks were acquired. Based on protein/peptide mass synchronization to database entries, a number of 39 different proteins could be identified (Table AI). As shown in Figure 16, TPYC- and M140-derived spores leads to similar MALDI-TOF MS peak patterns. According to MALDI-TOF MS analyses of TPYC- and M140-derived endospores, a total of 90 and 83 peaks were monitored, respectively. The evaluation of corresponding spectra led to the identification of 49 and 47 different spore proteins (Table AII and AIII), respectively. A total number of 81 peaks were detected, when AEY-derived spores were investigated by MALDI-TOF MS. Database synchronization led to the identification of 46 different spore proteins (Table AIV). The intersection of Venn diagram sectors visualizes, that a total of 40 peaks tended to be unaffected by sporulation medium. Generally, all spore proteins of *C. botulinum* (TMW 2.990), which were identified by MALDI-TOF MS (Table AI - AIV) represent structural spore proteins or seem to be involved in regulatory processes during sporulation, spore maturation or germination.

Based on increased high pressure resistance of SFE-derived spores (Lenz and Vogel, 2014), the interest was focused on proteins, which were only present in SFE endospores. Consequently, MALDI-TOF MS analysis led to the identification of 5 proteins. According to Table AI, the spore coat protein S (C5UZG3), the spore photoproduct lyase (C5UUE9), the RNA polymerase sigma factor (C5UXY2), the sporulation protein YunB (C5UZC5) and the putative uncharacterized protein (C5UTT9) were identified (highlighted in red, Table AI).

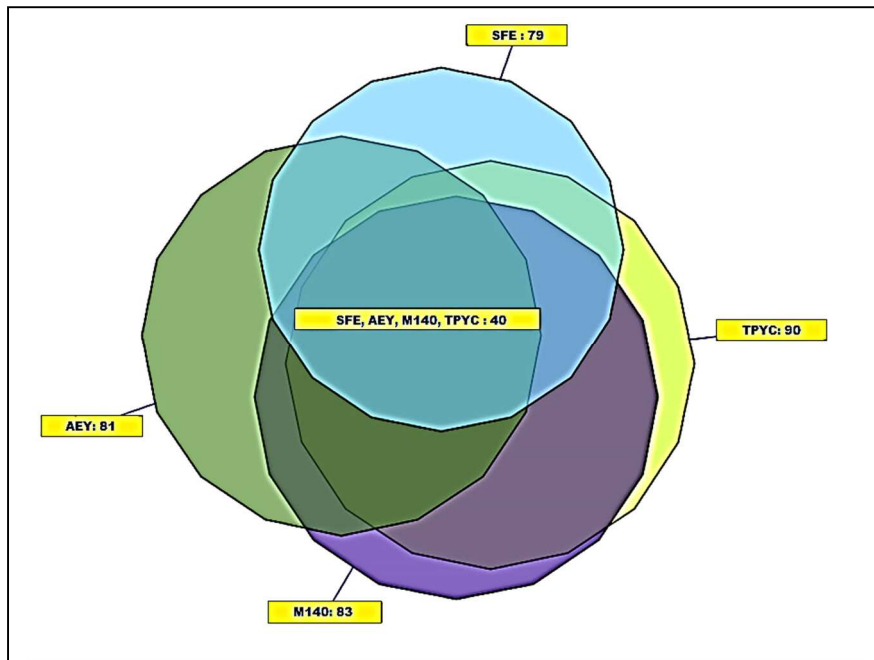


Figure 16: Venn diagram. The figure illustrates the number and congruency of peaks, which were detected by MALDI-TOF MS, when endospores of TMW 2.990 sporulated in SFE (blue), TPYC (light green), M140 (dark green) and AEY (violet).

3.2.3 Identification of predominant proteins in SFE-derived endospores by high resolution LC-MS/MS

To identify proteins which were only present in SFE-derived endospores of TMW 2.990, TMW 2.994 and TMW 2.997, SDS-PAGE and high resolution LC-MS/MS were carried out (2.2.7.2). In Figure 17 a silver stained SDS gel is illustrated, which display separated proteins of SFE-, TPYC-, AEY- and M140-derived spores. Obviously, a strong protein band of approximately 225 kDa was singly detectable in SFE-derived spores (marked in red).

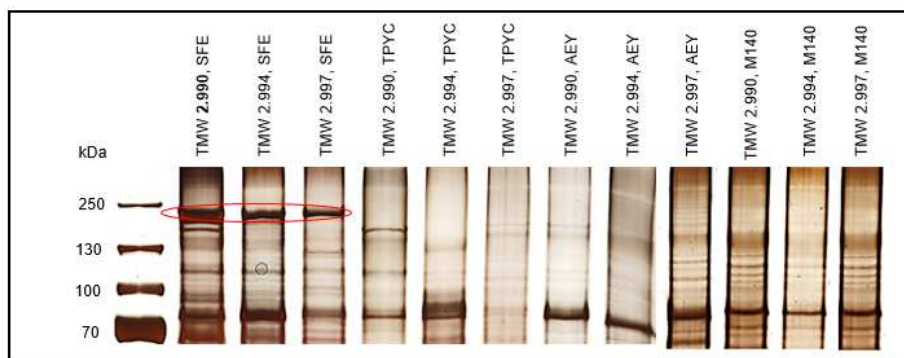


Figure 17: SDS-PAGE of endospore proteins. Visualized are silver stained spore proteins of TMW 2.990, TMW 2.994 and TMW 2.997 as a function of sporulation media (SFE, TPYC, AEY and M140). Proteins, which were singly detected in SFE-derived spores are marked in red.

Consequently, the protein band of TMW 2.990 was analyzed by high resolution LC-MS/MS. Mass spectrometric results led to the identification of 14 putative peptide fragments, containing chain length of 4 - 12 amino acids (Table AV). Database synchronization led to the suggestion, that the protein of interest represents a putative surface/cell-adhesion protein/N-acetylmuramoyl-L-alanine amidase. The alignment in Figure 18 depicts sequence analogies between identified peptide fragments and the putative surface/cell-adhesion protein/N-acetylmuramoyl-L-alanine amidase (WP_004461520.1) of *C. sporogenes*. From a total of 14 identified peptide fragments, a number of 6 were also detectable in the amino acid sequence of the *C. sporogenes* protein. The inclusion of extant peptide data (remaining 8 peptide fragments) into evaluation did not lead to protein identification results of higher significance. Also the matching of all identified peptide fragments against protein data of *C. botulinum* did not result in reliable protein identification.

```

MKKTSKALASTAALCLVLSTSSVFAAENTAVAPERLAGANRVDTAVKIAEKS FNEAWKQGONAILSAAAADANLVDSLAVAPLSYQLK
-----
APILLNDAKDSINADTLKALKANNVKTVYIATGEGVISNKAKAQLEKEGFKVERLGGKNRYETAKNILDITFKKNGGDTKNVALVSGS
APILLNDAK -----
*****

GLADALSVAPEAARKGMPILLTDGKDAVAANLAEVAKAADKVYAI GGNGII SDALVQQLKADRVSGHSRYETNAAVIKKFAGDKEFS
-----RYETNAAVIKK-----
*****

KIYLGNGQDGHVLVDSL TGSVLAAQSGSPIVLADGSLVDATKDTLKGKVS DKTGIVALGGEAVVSNDLVKEVTDIAKPEVNVKVAE SV
-----

VSLNETSVQVKGLAKDTKEADLKDKKIELKAGDITLTAKYVQSSLTEDGKANFVLENGKKLVDITTEYTVESDWAEFVVNKFVAKVVM
-----VVN
***

PYVKTINVTTKAIQAKANNVYFEAKNQYGE EIAVNGNVKDVKVTATINGVPVKE TEITKTNINDGYIITINELKEGDDVVFV FINK
NFVK-----NNVYFEAK-----
-X**          *****

IGDEDVKVGTATFKVVKAE DAVATEI SNMKAEY TSEANGHKTNEEAKVLPDDQIKLSAKISDQFGNMPAGTKARVWVEAGKDLVT
IGDEDV-----
*****

KIDASAIDEVSDSVDFTFKAIKAGDLKVSAYLANGKKVTYEVKIGAKKLEVVVKEGESGINIANVAGINHEEKIVGVVNPNGAILT
-----

PDMIKFDIKATKTSEEVKPSDVEVVAKLRGGEKDNKNDIVISVKSTKVGKYVITPYVGESVEKGIKGDIIITVTTTIDQKVASIDDIS
-----

FDAAELKTGTEIKKDIVFRNKHKEVLVLDNKAIVTVTPEIADAANNAKVTKDADKNKNILTLKADGAKTYNVVVRVKDEDVIKAFN
-----

LTFKAPFTTAVELGNDVNGVVAGDPADKAKYQEVKFLDQDGKTMIVNKEDIKVSATKPDGQPLTDISKLITLGKTYTVDKDGKVTFD
-----

VVANEKDHVVMAMKVAPAEDVVPGTYYVKVEDKDGKISDTLNI TVGSKRIAKTVEIKPAATKV VFGGKVKVNIVPKDQYGEFIVVGKE
-----DQYGEFIVVGK-----
*****

KVEVLPGTNFEASAITEINKDGGAVDAEHPLAGYQVELTGKTKGTNDVVVNIKEADKVLSTNKVSM TVDSAAGLIDSVAVDTKDIKS
-----

LYSTKAGAAEVDLNAIVKDADGTVIPVSDSDLDWKVVSQKDAEGKDVSSKTVTVDSKTGKVTATKDTVGTAVIEVTTANMKGANITL
-----

KFDNKESVAQKGTVEVINTVKTEDGKTLPLDADDKKEGIQISLDNDAKDGKDGAVKVV LNAKDQYGNLLGDQDAEIKADQITLRV
-----

GDSSVVKAEVDTKDPKGVITITAKGEGDSKVYVEYAGQTI ALDVTANKAAVDAAKSGELKEEA EKSVGALETA AAKDLTIEANLKEA
-----ITITAK-----
*****

EEATKTAKDALDKLPAGTEGLAELNRFNAADNKVKAAKEGFSVKQELEAAKTAIEGATYTLDKVNHNEVAKAKTAVGDVVNNLPEV
-----

KDKGFTVTVKDGDFVAAQDGASDGSYKFTVKLEKAGQEITSSEKTVVIPQ
-----

```

Figure 18: Alignment of identified peptide fragments against the amino acid sequence of the putative surface/cell-adhesion protein/N-acetylmuramoyl-L-alanine amidase (WP_004461520.1) of *C. sporogenes*. Sequence analogies are marked by stars. Divergences between amino acids are indicated by horizontal lines. Aberrations between amino acids, which could not be distinguished by mass spectrometric measurements are indicated by crosses.

3.3 Characterization of soybean oil emulsions and HPT-induced endospore inactivation in emulsion matrices

3.3.1 Characterization of soybean oil emulsions

3.3.1.1 Characterization of soybean oil emulsion stability

The stability of soybean oil emulsions was characterized by multisample analytical centrifugation (2.2.8.2). Integral creaming kinetics (Figure AI) of soybean oil emulsions with fat contents of 10 - 70% were recorded during centrifugation (2000 rpm, 42 min and 20 °C). Additionally, integral creaming kinetics (Figure AII - AIV) of soybean oil emulsions with fat contents of 10, 30, 50 and 70% were monitored after heat-, pressure- and HPT-treatment (75 °C/0.1 MPa; RT/750 MPa; 75 °C/750 MPa).

Generally, it should be proved that model emulsions are stable enough, to serve as matrices for subsequent high pressure and heat inactivation experiments (2.2.8.6 and 2.2.8.7).

In Figure 19, the slopes of integral creaming kinetics of model emulsions (10 – 70% fat) are depicted (corresponding raw data are attached in Figure AI). According to Figure 19, the stabilities of soybean oil emulsions were significantly influenced by the fat contents. The correlation between fat content and emulsion stability was not directly proportional. Emulsions containing 30% soybean oil appeared most stable. An increase of the fat content up to 60% led to low reduced stabilities (from $m_{30\%} = 0.002$ to $m_{60\%} = 0.0027$). The decrease of emulsion stability is more distinct, when soybean oil emulsions were prepared with 20, 70 and 10% soybean oil ($m_{20\%} = 0.0035$; $m_{70\%} = 0.0043$ and $m_{10\%} = 0.0047$).

The multisample analytical centrifugation enables the accelerated shelf life characterization of emulsions. Calculative, at standard force of gravity ($g = 1$), 0.1% of the most instable emulsion, containing 10% fat, would be creamed after 3.15 h.

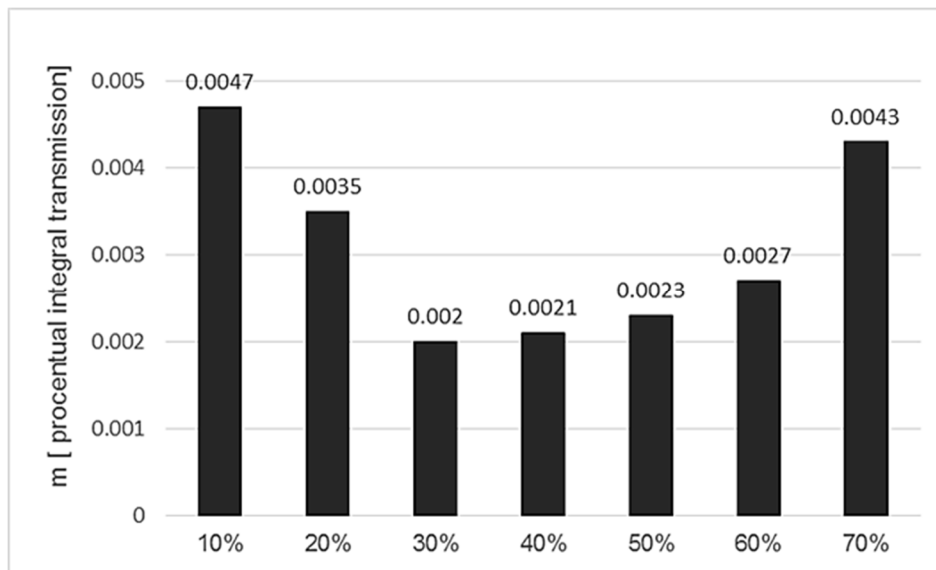


Figure 19: Slopes of integral creaming kinetics of untreated soybean oil emulsions. Depicted are slopes of the integral creaming kinetics, according to multisample analytical centrifugation (2000 rpm, 20 °C, 42 min) of soybean oil emulsions, containing 10 – 70% fat. Slope intensity is inversely proportional to emulsion stability.

In Figure 20, the slopes of integral creaming kinetics, according to heat-, pressure- and HPT-treated model emulsions (10, 30, 50 and 70% fat) are depicted (raw data are attached in Figure AII - AIV). Obviously, emulsion stability was not significantly influenced neither by heat treatment at 75 °C, pressure application of 750 MPa nor by HPT treatment (75 °C/750 MPa). When emulsions of identical fat content were exposed to mentioned parameters, the values of stability varied in a maximum range of $\Delta m = 2 \times 10^{-4}$. Soybean oil emulsions containing 10% fat tended to be most stable after treatment at 75 °C ($m_{75\text{ °C}} = 0.0038$). Sample application to 750 MPa and 75 °C/750 MPa, respectively, led to slight decrease in stability ($m_{750\text{ MPa}} = 0.0039$; $m_{75\text{ °C}/750\text{ MPa}} = 0.004$). The stabilities of soybean oil emulsions with 30% fat tended to be similar, when samples were exposed to 75 °C and 75 °C/750 MPa ($m = 0.0019$), respectively. Sole pressure treatment tended to induce a low reduction in stability ($m = 0.0021$). Similar findings were observed, when emulsions of 70% fat were exposed to heat and pressure ($m_{80\text{ °C}} = 0.0038$, $m_{750\text{ MPa}} = 0.0039$ and $m_{80\text{ °C}, 750\text{ MPa}} = 0.0038$). In emulsions with a fat content of 50%, the stability tended to decrease from temperature-treated ($m_{75\text{ °C}} = 0.0021$) via HPT-treated ($m_{75\text{ °C}/750\text{ MPa}} = 0.0022$) to high pressure-treated samples ($m_{750\text{ MPa}} = 0.0023$).

The data presented in Figure 19 and Figure 20 demonstrate, that the impact of soybean oil emulsion stability was more affected by the fat content than by pressure-, heat- and HPT-treatment. Due to the fact that pressure and heat application tended to

induce just liminal changes in stabilities, model emulsions were considered suitable for further experiments according to 2.2.8.6 and 2.2.8.7.

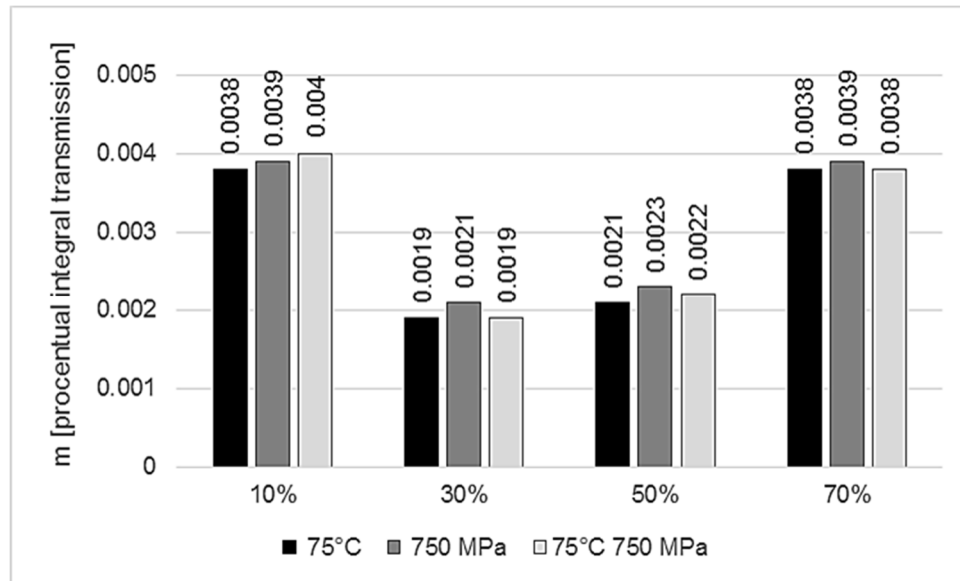


Figure 20: Slopes of integral creaming kinetics of heat-, pressure- and HPT-treated soybean oil emulsions. Depicted are slopes of the integral creaming kinetics of soybean oil emulsions, containing 10, 30, 50 and 70% fat, determined by multisample analytical centrifugation (2000 rpm, 20 °C, 42 min). Previously, samples were treated for 10 min at 75 °C/0.1 MPa (black bars); RT/750 MPa (grey bars) or 75 °C/750 MPa (light grey bars). Slope intensity is inversely proportional to emulsion stability.

3.3.1.2 Droplet size characterization of soybean oil emulsions

3.3.1.2.1 Droplet size characterization of soybean oil emulsions prior to and after heat-, pressure- and HPT-treatment

To determine the particle-size distribution of soybean oil emulsions containing 30, 50 and 70% fat, the Mastersizer 2000 (Malvern Instruments GmbH, Germany) was employed. According to 2.2.8.3.1, measurements were performed prior to and after heat-, pressure- and HPT-treatment (10 minutes at 75 °C/0.1 MPa; RT/750 MPa; 75 °C/750 MPa).

In Figure 21, the particle-size distributions of emulsion samples are depicted. Furthermore, the corresponding volume mean diameters ($D [4,3]$) and the statistical parameters of particle-size distributions ($D (v, 0.1)$; $D (v, 0.5)$ and $D (v, 0.9)$) are listed in Table 24. The statistical values reflect, that 10, 50 and 90% of the particles are smaller, than the given diameters.

These results indicate, that a bimodal behavior in droplet size distribution exists in all tested samples (with exception of 70% soybean oil emulsion, after 10 min treatment at 750 MPa). Obviously, in untreated soybean oil emulsions, the amount of small fat particles (0.42 – 3.80 μm) tended to decrease and the quantity of bigger oil droplets (3.8 – 181.97 μm) tended to increase, in correlation with increasing fat contents.

In Figure 21 A, the droplet size distributions of treated and untreated soybean oil emulsions containing 10% fat, are displayed. Untreated emulsions contained particles in the range of 0.48 to 181.97 μm . In the range of smaller particles, a modal diameter of 0.95 μm was quantified. A second maximum was monitored at a particle size of 15.14 μm . According to untreated emulsions of 10% soybean oil, an average particle diameter of 10.18 μm was measured. The statistical D-values indicate that 10% of the particles were smaller than 0.72 μm ; 50% of the fat droplets were punier than 4.26 μm and 90% of existing particles were tinier than 27.25 μm (Table 24).

Similar to untreated emulsions of 10% fat, heat-treated samples also contained particles in the range of 0.48 to 181.97 μm . In comparison to untreated emulsions of equal fat content, the average particle diameter was slightly reduced (10.14 μm). The values of D (v, 0.1) and D (v, 0.5) decreased from 0.72 to 0.69 μm and from 4.26 to 2.06 μm , respectively. Accordingly, the value of D (v, 0.9) increased from 27.25 to 30.94. In comparison to untreated emulsions of 10% fat, the amount of particles with sizes of 0.47 to 4.37 μm decreased and the quantity of droplets with sizes of 5.75 to 158.49 μm increased, in heat-treated samples.

Pressure-treated emulsions of 10% fat, included particles in the range of 0.48 - 52.48 μm . In comparison to untreated and heat-treated emulsions, the amount of bigger droplets was reduced significantly. Accordingly, the average particle diameter was also declined (5.98 μm). Droplet size distributions and statistical D-values of (D (v, 0.1 = 0.71 μm); D (v, 0.5 = 1.86 μm) and (D (v, 0.9 = 16.73 μm) exemplified, that the amount of smaller particles (0.63 - 8.71 μm) raised and the amount of bigger droplets (10 - 52.48 μm) dwindled down.

HPT-treated emulsions containing 10% soybean oil included particles in the range of 0.48 to 79.43 μm . Generally, the shape of this particle-size distribution curve is most similar to the curve of untreated emulsion. The calculated average particle diameter of 7.99 μm was reduced, when compared to untreated emulsions of equal fat content. This effect was caused by an increase of smaller droplets (0.55 - 10 μm) and a reduction of bigger particles (10 to 79.43 μm).

In untreated emulsions, containing 30% fat, particles in the range of 0.48 to 45.71 μm were monitored (Figure 21 B). Due to particle distribution, an average particle diameter of 8.03 μm was quantified (Table 24). In the range of 0.48 to 2.88 μm , the shape of droplet size distribution curves of untreated samples containing 10 and 30% fat were quite similar. On the other hand, in the range of 7.55 to 22.91 μm , the amount of particles in emulsions containing 30% fat was quite higher than in untreated emulsions containing 10% oil. In comparison to untreated emulsions of 10% fat, the amount of droplets bigger than 26.3 μm was much reduced.

In comparison to untreated soybean oil emulsions of 30% fat, heat-treated samples of equal fat content contained less particles in the range of 0.48 - 10 μm but quite more droplets with diameters of 11.48 – 52.48 μm . Therefore, in heat-treated samples containing 30% fat, an increased average particle diameter (10.37 μm) and elevated D-values ($D(v, 0.1 = 0.75)$; $D(v, 0.5 = 8.31)$ and $(D(v, 0.9 = 24.82))$ were quantified (Table 24).

In comparison to untreated samples of 30% fat, in high pressure-treated emulsions of equal fat content, slight changes in droplet size distribution were observed (Figure 21 B). In contrast to untreated samples, the amount of small particles (0.63 - 5.01 μm) was increased and the portion of big droplets (5.75 – 45.71 μm) was decreased. Therefore, a lower average particle diameter of 4.19 μm and reduced D-values ($D(v, 0.1 = 0.66 \mu\text{m})$; $D(v, 0.5 = 1.51 \mu\text{m})$ and $(D(v, 0.9 = 11.76 \mu\text{m})$ were determined.

Particle sizes from 0.48 to 39.81 μm were identified, when emulsions of 30% fat were treated by HPT. In comparison to untreated samples of 30% fat, in HPT-treated emulsions, the amount of droplets with sizes of 0.63 to 5.75 μm were higher and the number of particles in the range of 6.60 to 39.81 μm were decreased. The average particle diameter and the D-values of HPT-treated samples containing 30% fat were quite similar to data obtained from pressure-treated emulsions of 30% fat ($(D[4,3] = 4.72 \mu\text{m})$; $(D(v, 0.1 = 0.69 \mu\text{m})$; $D(v, 0.5 = 1.65 \mu\text{m})$ and $(D(v, 0.9 = 13.51 \mu\text{m}))$).

In 50% soybean oil emulsions, fat droplets in the range of 0.48 to 45.71 μm were quantified (Figure 21 C). In comparison to untreated samples of 10 and 30% soybean oil, untreated samples of 50% fat contained less particles with diameters of 0.63 to 5.75 μm and more droplets with sizes of 6.61 to 30.20 μm . Due to untreated soybean oil emulsions containing 50% fat, an average particle diameter of 9.78 μm was identified. Additionally, statistical D-values of ($D(v, 0.1 = 0.73 \mu\text{m})$; $D(v, 0.5 = 7.95$

μm) and $(D(v, 0.9 = 23.19 \mu\text{m}))$ were calculated. When emulsions of 50% soybean oil were exposed to $75 \text{ }^\circ\text{C}$, similar particle-sizes distribution than in untreated samples were observed, in the range of 0.63 to $5.01 \mu\text{m}$.

In comparison to untreated samples, heat-treated emulsions of 50% fat contained an increased amount of droplets, in the range of 5.75 to $17.38 \mu\text{m}$ and a reduced quantity of particles with diameters of 19.5 to $39.81 \mu\text{m}$. Therefore, a low reduced average particle diameter ($9.10 \mu\text{m}$) and a less reduced $D(v, 0.9)$ value of $20.17 \mu\text{m}$ were measured. On the contrary, other D -values were increased ($(D(v, 0.1 = 0.77 \mu\text{m})$ and $D(v, 0.5 = 8.21 \mu\text{m}))$), in contrast to untreated emulsions of 50% fat.

As Figure 21 C illustrates, the behavior of particle-size distribution of untreated and pressure-treated emulsions containing 50% fat were quite similar. However, in pressure-treated emulsions, the amount of particles in the range of $0.83 - 10 \mu\text{m}$ was slightly increased, whereas the quantity of droplets with sizes of $11.48 - 45.71 \mu\text{m}$ was marginally reduced. Consequently, due to equal particle-size distributions of untreated and pressure-treated samples of 50% fat, quite similar D -values were monitored. For pressure-treated emulsions, D -values of $(D(v, 0.1 = 0.73 \mu\text{m}); D(v, 0.5 = 6.73 \mu\text{m})$ and $(D(v, 0.9 = 21.62 \mu\text{m}))$ were calculated.

In contrast to particle-size distribution in untreated emulsions containing 50% soybean oil, HPT-treated samples of equal fat content contained an increased amount of smaller droplets ($0.63 - 3.80 \mu\text{m}$) and a reduced amount of bigger particles ($5.75 - 45.71 \mu\text{m}$). This effect was also traceable by a clearly reduced $D(v, 0.5)$ value ($2.52 \mu\text{m}$).

Generally, the behavior of droplet size distribution in untreated-, heat- and HPT-treated emulsions of 70% fat were quite similar (Figure 21 D). In these samples, particles of 0.48 to $69.18 \mu\text{m}$ were quantified and led to average particle diameters in the range of 15.5 to $17.95 \mu\text{m}$. Pressure treatment of 70% soybean oil emulsions resulted in a trimodal particle distribution. In other respects, the particle-size distribution in HPT-treated emulsions of 70% fat was very similar to residually samples of equal fat content. Additionally, in pressure-treated samples, particles in the range of $91.20 - 316.22 \mu\text{m}$ were measured.

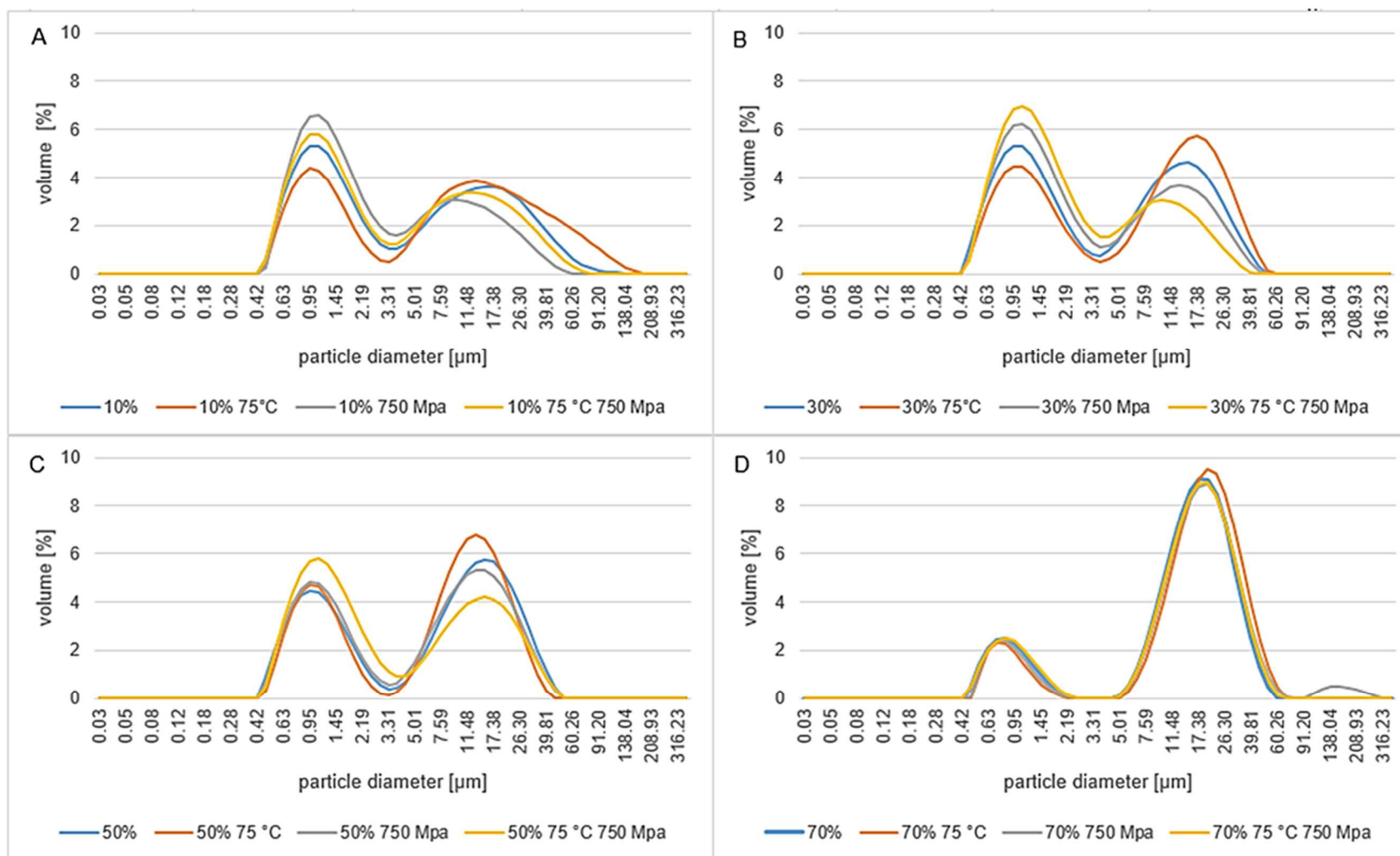


Figure 21: Particle-size distribution of soybean oil emulsions prior to and after heat-, pressure- and HPT-treatment. The figure illustrates the percentage amount of particles as a function of particle diameter. The particle distributions in soybean oil emulsions with fat contents of 10% (A), 30% (B), 50% (C) and 70% (D) are displayed. Treatment parameters are indicated by different colors (blue: untreated, orange: 75 °C/0.1MPa; grey: RT/750 MPa; yellow: 75 °C/750 MPa).

Table 24: Statistical parameters of particle-size distribution in soybean oil emulsions.

parameters	D [4,3] – volume weighted mean [μm]	D (v, 0.1) [μm]	D (v, 0.5) [μm]	D (v, 0.9) [μm]
10%	10.18	0.72	4.26	27.25
10%, 75 °C	10.14	0.69	2.06	30.94
10%, 750 MPa	5.89	0.71	1.86	16.73
10%, 75 °C, 750 MPa	7.99	0.71	2.57	22.34
30%	8.03	0.70	4.36	20.87
30%, 75 °C	10.37	0.75	8.31	24.82
30%, 750 MPa	4.19	0.66	1.51	11.76
30%, 75 °C, 750 MPa	4.72	0.69	1.65	13.51
50%	9.78	0.73	7.95	23.19
50%, 75 °C	9.10	0.77	8.21	20.17
50%, 750 MPa	8.88	0.73	6.73	21.62
50%, 75 °C, 750 MPa	7.67	0.72	2.52	20.83
70%	15.50	0.90	14.71	29.03
70%, 75 °C	17.95	1.00	16.89	32.81
70%, 750 MPa	20.50	0.94	15.82	33.23
70%, 75 °C, 750 MPa	15.77	0.89	14.91	29.85

3.3.1.2.2 Droplet size characterization of soybean oil emulsions during pressurization

Droplet sizes of 10% soybean oil emulsions were analyzed by microscopic observation, during pressure generation up to 250 MPa and during pressure reduction. For experimental setup, the HPDS-high pressure cell was used. For particle size determination, micrographs were recorded and droplet diameters were measured by employing GIMP 2.8 (2.2.8.3.2).

In Figure 22 - Figure 26, the diameters of 30 oil droplets (a - ad) are illustrated as a function of pressure application. For evaluation, micrographs were recorded in intervals of 50 MPa. Exemplarily, Figure 27 depicts microscopic images of soybean oil emulsions during pressure generation and pressure reduction. Fat droplets of identical size are indicated by equivalent numbers (1-14).

In Figure 22, the pressure-dependent changes in fat droplet diameters with initial sizes of 84.69 and 47.07 μm (a and b) are depicted. Obviously, the diameters of droplets were marginally influenced by pressure application. During the processes of pressuring and repressuring, diameters differed in a maximal range of 2.0 and 2.21 μm , respectively. Figure 23 illustrates the influence of pressure on fat droplets (c - i) with initial diameters of 36.06 – 24.76 μm . During pressure generation and release, the diameters of the droplets fluctuated between 1.9 – 3.98 μm . In Figure 24, the influence of pressure treatment to fat droplets with initial sizes of 22.64 – 16.93 μm (j - q) are displayed. For the minimal and maximal changes in diameters, variations of 1.7 and 2.96 μm were estimated. Figure 25 reflects the diameter changes of soybean oil droplets with initial sizes of 15.57 – 9.56 μm (r - x). In average, the diameters of droplets variegated in the ranges of 1.48 to 3.55 μm . The pressure-induced changes in droplet diameters with initial sizes of 15.57 - 9.56 μm (y -ad) are depicted in Figure 26. During treatment, the diameters of droplets fluctuated between 0.64 – 2.97 μm .

Generally, in the range of 0.1 to 205 MPa, droplet sizes of soybean oil emulsions containing 10% fat, were little influenced by pressure application.

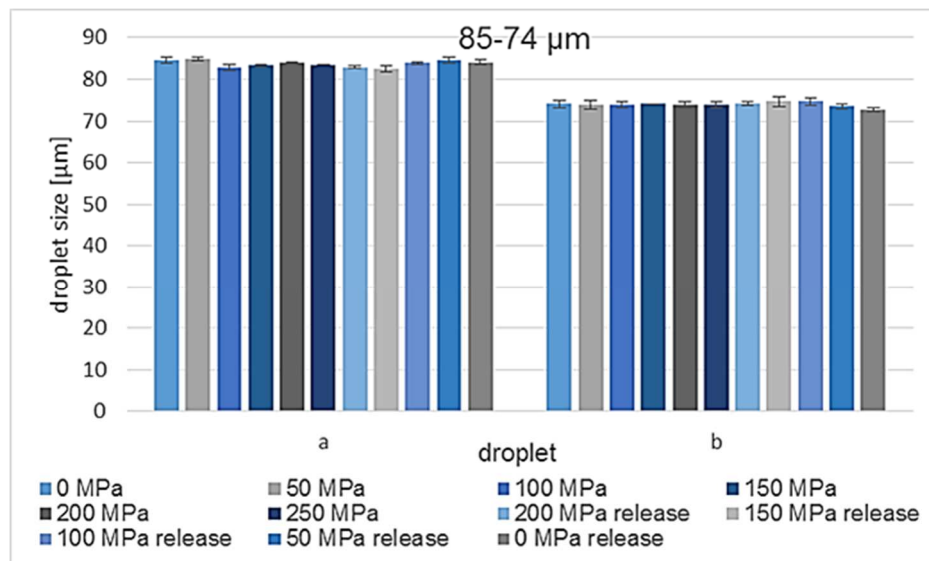


Figure 22: Diameters of soybean oil droplets during compression and decompression. The figure shows diameters of the soybean oil droplets (a and b) during pressure generation up to 250 MPa and during pressure reduction until 0.1 MPa. Different pressure levels are indicated by different bar colors.

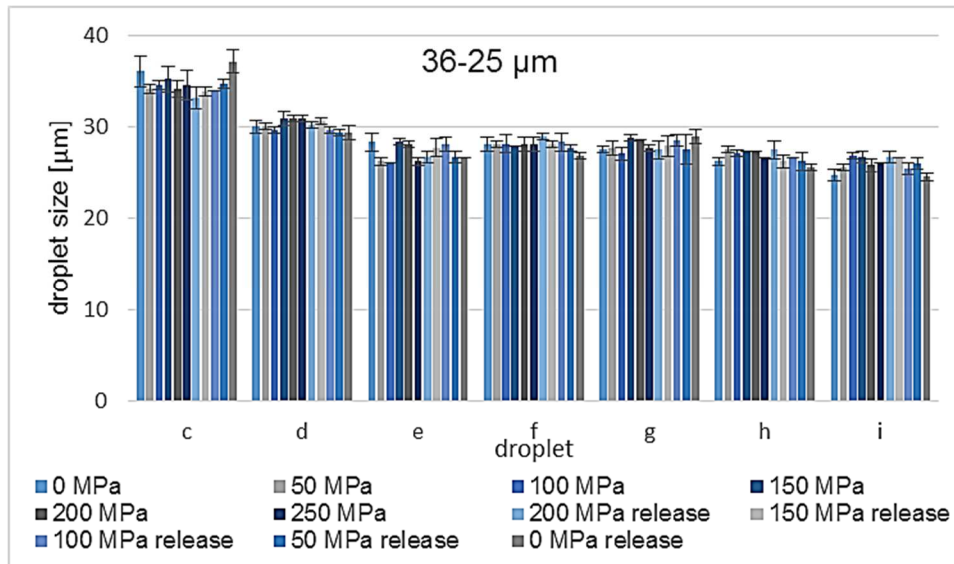


Figure 23: Diameters of soybean oil droplets during compression and decompression. The figure shows diameters of the soybean oil droplets (c - i) during pressure generation up to 250 MPa and during pressure reduction until 0.1 MPa. Different pressure levels are indicated by different bar colors.

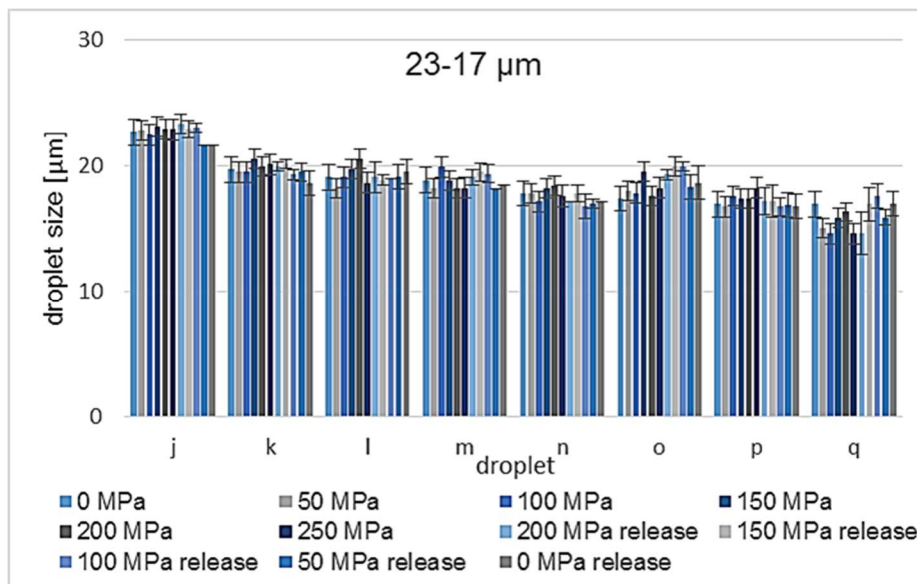


Figure 24: Diameters of soybean oil droplets during compression and decompression. The figure shows diameters of the soybean oil droplets (j - q) during pressure generation up to 250 MPa and during pressure reduction until 0.1 MPa. Different pressure levels are indicated by different bar colors.

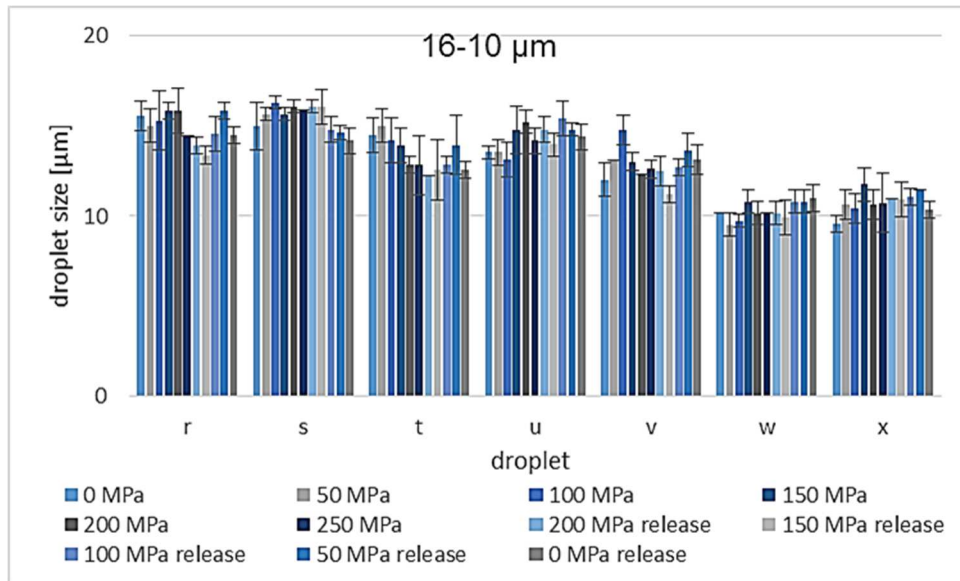


Figure 25: Diameters of soybean oil droplets during compression and decompression. The figure shows diameters of the soybean oil droplets (r - x) during pressure generation up to 250 MPa and during pressure reduction until 0.1 MPa. Different pressure levels are indicated by different bar colors

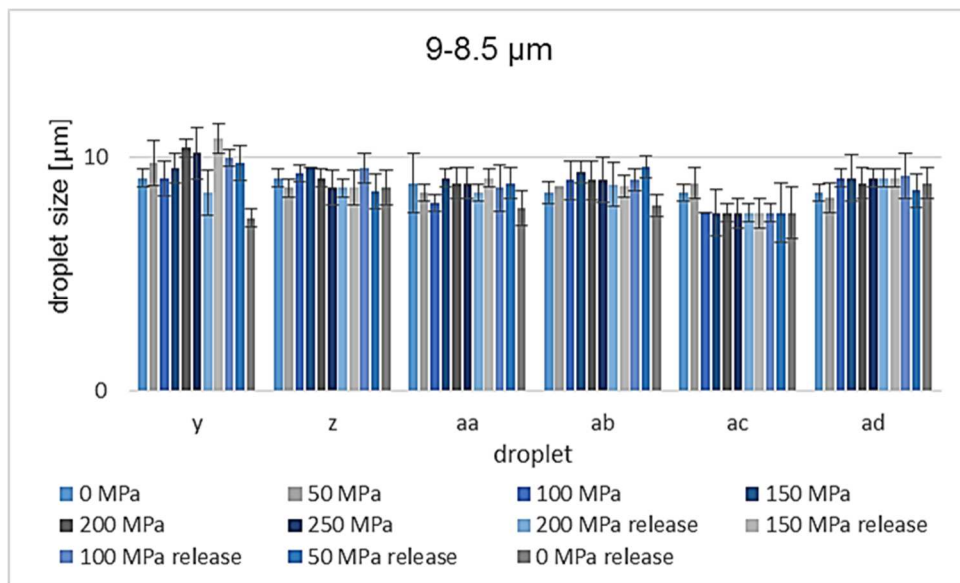


Figure 26: Diameters of soybean oil droplets during compression and decompression. The figure shows diameters of the soybean oil droplets (y - ad) during pressure generation up to 250 MPa and during pressure reduction until 0.1 MPa. Different pressure levels are indicated by different bar colors.

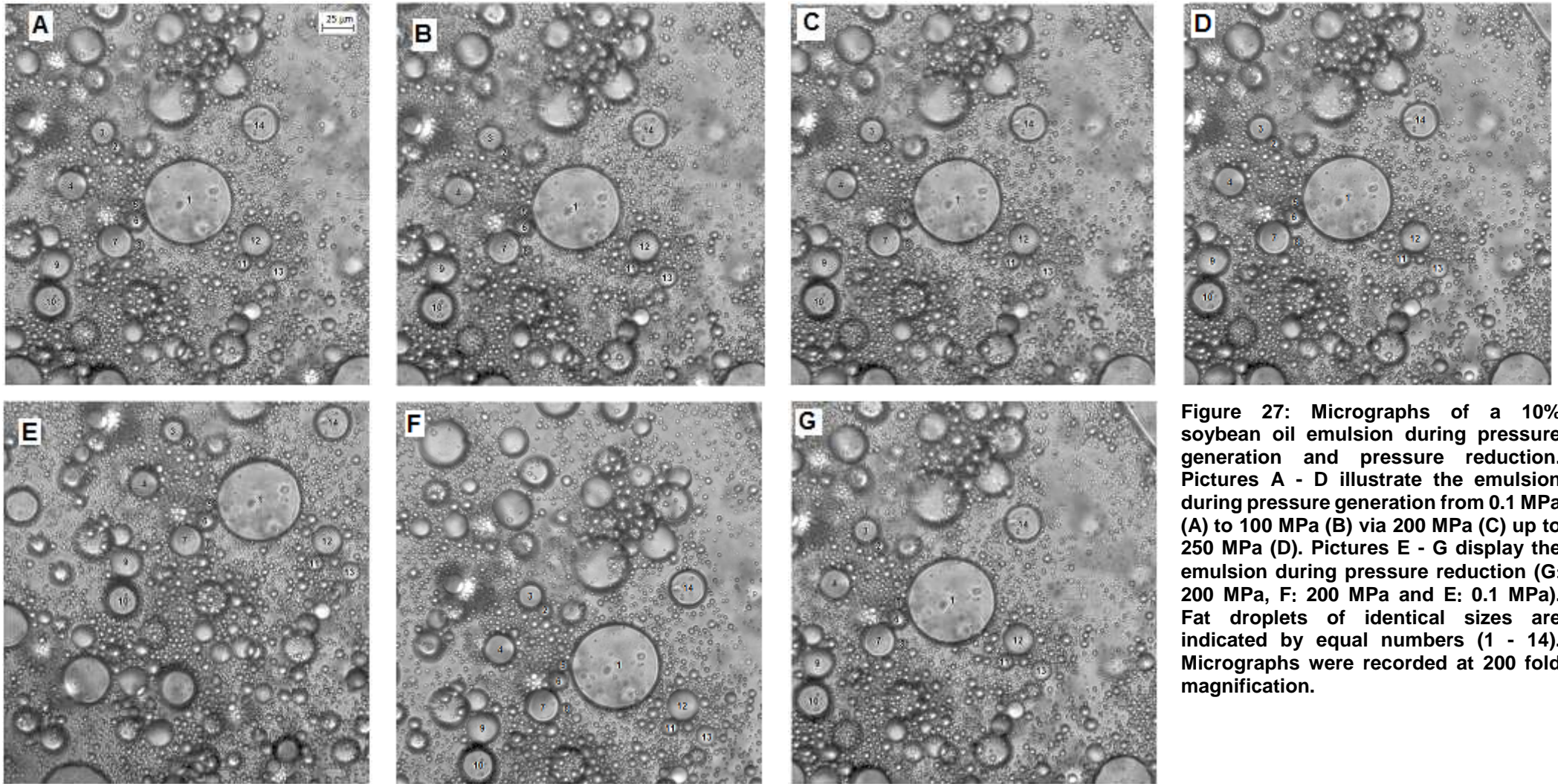


Figure 27: Micrographs of a 10% soybean oil emulsion during pressure generation and pressure reduction. Pictures A - D illustrate the emulsion during pressure generation from 0.1 MPa (A) to 100 MPa (B) via 200 MPa (C) up to 250 MPa (D). Pictures E - G display the emulsion during pressure reduction (G: 200 MPa, F: 200 MPa and E: 0.1 MPa). Fat droplets of identical sizes are indicated by equal numbers (1 - 14). Micrographs were recorded at 200 fold magnification.

3.3.1.3 Influence of unbound emulsifier on heat-, pressure- and HPT-induced inactivation of *C. botulinum* type E endospores

Further endospore inactivation experiments should be performed in emulsions with different fat contents (2.2.8.6, 2.2.8.7). According to 2.2.8.1, the continuous emulsion phase was enriched with 2% soybean lecithin (w/v). Subsequently, the emulsifier concentration decreased with increasing emulsion fat content. Due to this fact, the influence of unbound emulsifier on heat-, pressure- and HPT-induced endospore inactivation was tested.

For emulsifier-dependent spore inactivation experiments, IPB (Table 17) was added with 0 – 5% (w/v) of soybean lecithin prior to inoculation (1×10^7 TMW 2.992 spores/ml). Consequently, samples were treated for 10 min at 75 °C/0.1 MPa; RT/750 MPa and at 75 °C/750 MPa, respectively. Finally, plate count determinations of treated and untreated samples were investigated (2.2.8.4).

As a function of treatment parameters and emulsifier concentrations, results of logarithmic cell counts are depicted in Figure 28.

For untreated endospores which were stored in pure buffer, logarithmic cell counts of 6.25 were calculated. Untreated spores kept in buffer containing 1, 2 and 5% emulsifier led to equal cell counts (6.31, 6.34 and 6.32). In correlation to untreated samples, logarithmic cell counts were quite analogue, when inoculated samples of variable emulsifier concentrations were exposed to 75 °C (0% = 6.30; 1% = 6.32; 2% = 6.37 and 5% = 6.27).

Reduced germination rates were observed, when inoculated samples were exposed to pressure of 750 MPa. Due to pressure-mediated endospore inactivation, logarithmic cell counts of 5.17; 5.44; 5.50 and 5.40 were quantified, when 0, 1, 2 and 5% emulsifier were applied.

Samples, which were exposed to HPT (75 °C/750 MPa) showed similar inactivation behavior, when different amounts of soybean lecithin were used. Logarithmic cell counts of 2.55; 2.66; 2.88 and 2.26 were monitored, when samples were prepared with 0, 1, 2 and 5% emulsifier.

Finally, Figure 28 indicates that variable soybean lecithin concentrations of the matrix did not affect the heat-, pressure and HPT-induced inactivation behavior of *C.*

botulinum type E spores. Consequently, for further inactivation experiments in soybean oil emulsions with different fat contents, the effect of variable emulsifier concentrations does not have to be considered explicitly.

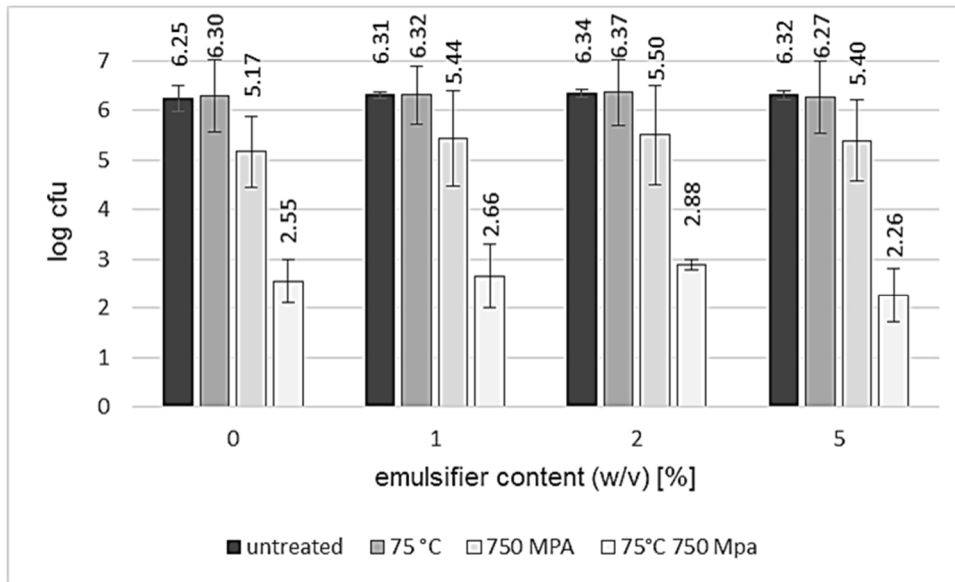


Figure 28: Influence of the emulsifier concentration on heat-, pressure- and HPT-induced inactivation behavior of *C. botulinum* type E endospores (TMW 2.992). As a function of soybean lecithin concentration (0 - 5%) and of obtained treatment parameters (untreated: black bars; 75 °C/RT: dark grey bars; RT/750 MPa: light grey bars; 75 °C/750 MPa: white bars), logarithmic cell counts are depicted.

3.3.2 Determination of endospore localization in heterogenic oil/buffer mixtures

To determine the percental endospore distribution in soybean oil/IPB mixtures, three different phases (buffer phase, oil phase and interface) were used for plate count determination (2.2.8.5.1). Therefore, mixtures of different fat contents (30, 50 and 70%) were inoculated with variable endospore (TMW 2.992) concentrations (2×10^6 , 1×10^6 and 5×10^5 spores/ml).

As a function of spore concentration, percentage spore distributions in heterogenic soybean oil/IPB mixtures (30, 50 and 70% fat) are illustrated in Figure 29.

Obviously, independent of the fat content and endospore concentration, an average of 98.18% spores were detected in the buffer phase. In interfaces, an average of 1.71% endospores were confirmed, while a tiny amount of approximately 0.1% spores were quantified in the oil phases.

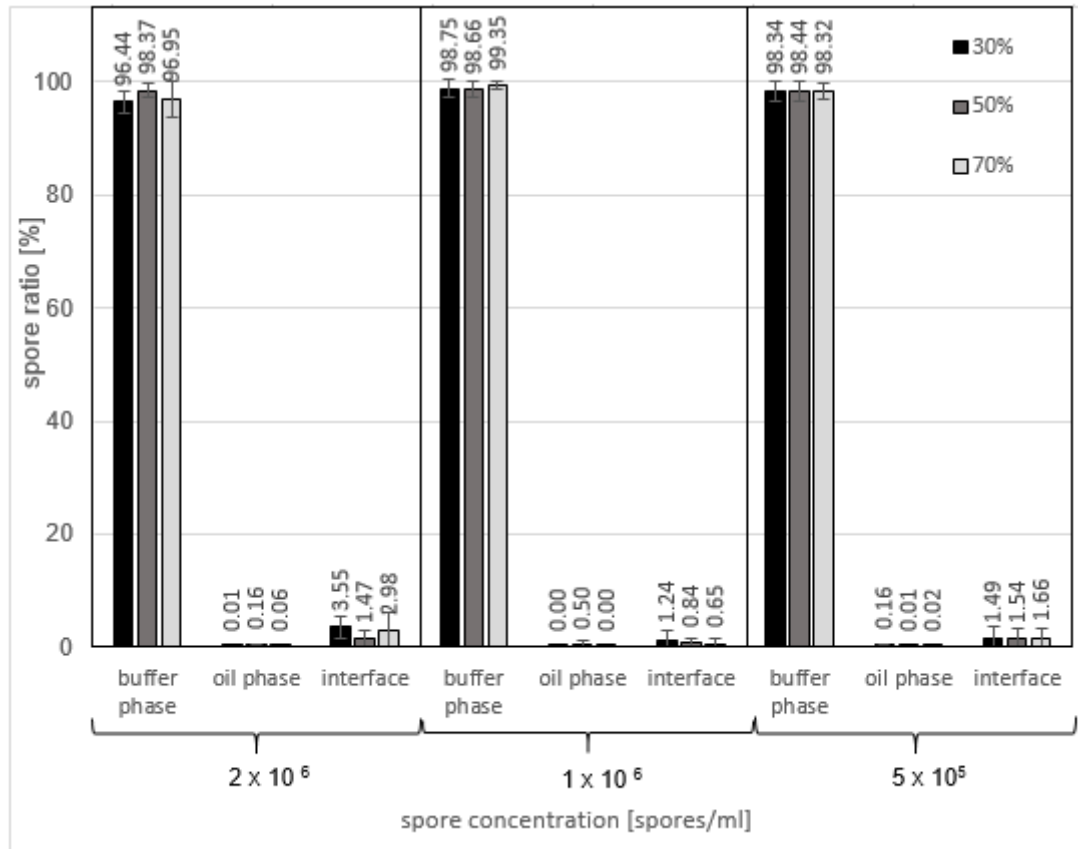


Figure 29: Percentage distribution of endospores in heterogenic soybean oil/IPB mixtures. The figure reflects the percentage distribution of TMW 2.992 endospores in the buffer phase, the oil phase and the interface of heterogenic oil/IPB mixtures of different fat contents (30%: black bars; 50%: dark grey bars; 70%: light grey bars). The mixtures were inoculated with different spore concentrations (2×10^6 , 1×10^6 and 5×10^5 spores/ml).

For detailed information of endospore distribution in soybean oil/IPB mixtures, the interface and the upper layer of the buffer phase ($v = 1$ ml) were used for additional plate count determination experiments (2.2.8.5.1). Depending on the soybean oil content (30, 50 and 70%), endospore concentrations of defined phases are displayed in Figure 30.

The highest concentration of endospores (195,833 spores/ml) was detected in the interface of mixtures containing 30% oil. In the interfaces of mixtures with fat contents of 50 and 70%, spore concentrations of 123,333 and 182,833 spores/ml were quantified, respectively. In contrast to the measured spore levels in the interfaces, the amount of endospores in the top of the surphase layer was reduced drastically. In correlation with increasing fat contents (from 30 via 50 to 70%), the endospore concentration in the upper layer of the buffer phase increased from 4010 via 4827 through to 10667 spores/ml.

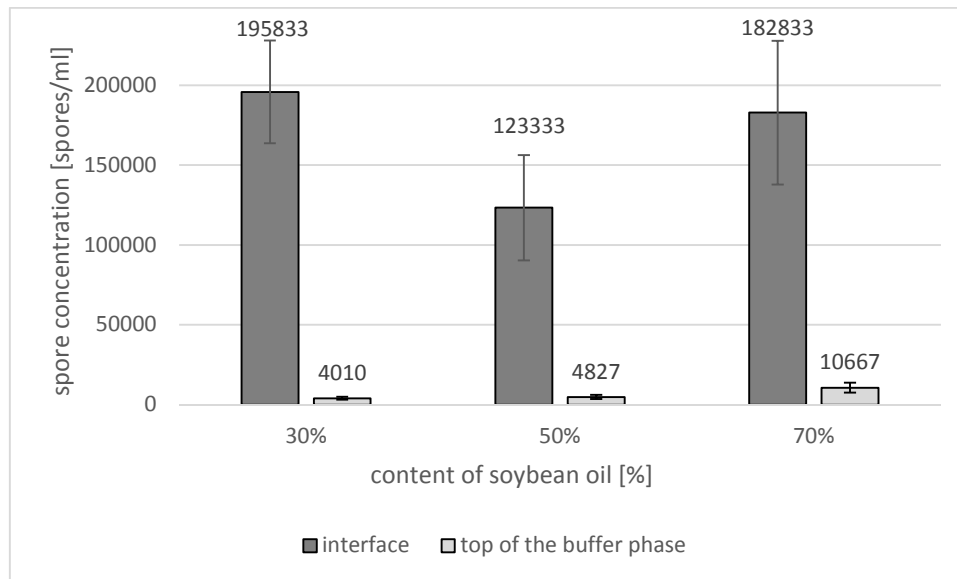


Figure 30: Endospore distribution in the interface and in surface layer of the buffer phase of heterogenic soybean oil/IPB mixtures containing different fat contents (30, 50 and 70%). Prior to plate count determination, mixtures were inoculated with 1×10^6 TMW 2.992 spores/ml.

3.3.2.1 Determination of endospore distribution in heterogenic oil/buffer mixtures by microscopic observation

To determine the percental endospore distribution in 50% soybean oil/IPB mixtures, samples were inoculated with purified endospores of TMW 2.992. Accordingly, in microscopic observations 10 fields of view were evaluated at 1000 fold of magnification. In Figure 31, results of percentage endospore arrangements in heterogenic mixtures are illustrated.

Figure 31 indicates that an average of 97.09% endospores were detected in the buffer phase, while 2.91% of spores were identified at the boundary surface of soybean oil droplets. Endospores completely imbedded in oil droplets were not observed in any case.

Figure 32 depicts a microscopic image of an inoculated mixture containing 50% soybean oil. The centered, circular structure displays a soybean oil droplet, which is surrounded by IPB. Obviously, the small refractive endospores were mainly present in the buffer phase (indicated by grey arrows), while a low number of endospores were associated to the surface of the fat droplet (indicated by black arrows).

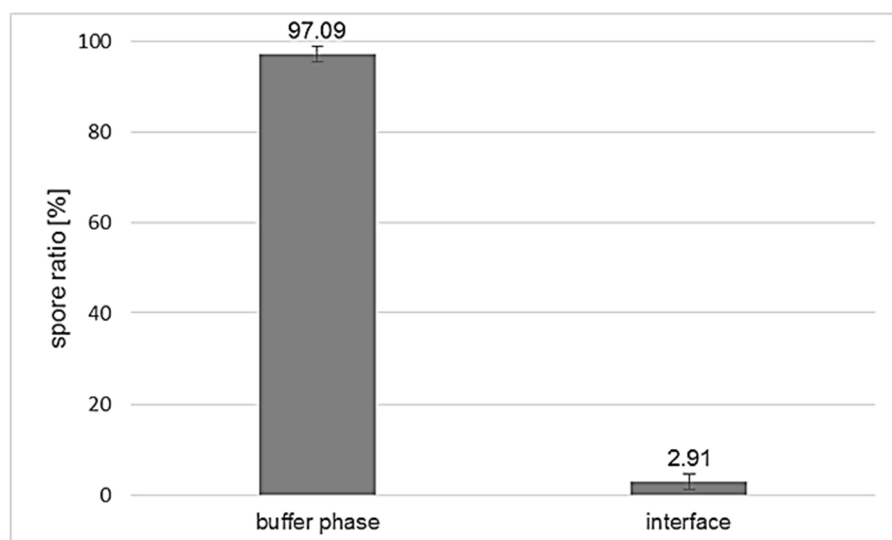


Figure 31: Percental endospore arrangement (TMW. 2.992) in 50% soybean oil/IPB mixtures. Percental endospore arrangement in oil/IPB mixtures are displayed, after evaluation of 10 fields of view.



Figure 32: Micrograph of a 50% soybean oil/IPB mixture, which was inoculated with 5×10^5 spores/ml (TMW 2.992) at 1000 fold of magnification. Endospores, which are marked by black arrows are associated to the oil droplet. Grey arrows indicate endospores, which are located in the surrounding IPB.

3.3.2.2 Determination of endospore distribution in emulsion matrices by fluorescence microscopic observation

To calculate the percental endospore arrangement in model matrices (2.2.8.5.3), SYTO 9 stained endospores and soybean oil emulsions were observed by

fluorescence microscopy. Initially, emulsions containing 30, 50 and 70% soybean oil were inoculated with 5×10^5 stained spores (TMW 2.992). To determine the localization of endospores, 10 fields of view were analyzed at 400 fold of magnification.

Figure 33 displays the percentage endospore arrangement in soybean oil emulsions of different fat contents (10, 50 and 70%). Apparently, without considering the emulsion fat content, the majority of the endospores was detected in the buffer phase (68.6 – 79%), while at the boundary surface of droplets 21 - 31.3% endospores were established. The total enclosing of endospores by fat droplets were not observed anyway. In correlation with increasing fat contents (from 30 via 50 up to 70%), the amount of endospores in the buffer phase increased from 68.6 to 73 up to 79%. Consequently, due to increasing fat content, the amount of boundary surface associated endospores decreased.

Exemplary, fluorescent micrographs of emulsions, which were inoculated with SYTO 9 stained endospores are displayed in Figure 34. The pictures A1 - A3 illustrate the association of fluorescent spores to the boundary surfaces. Spores dissolved in the buffer phase are apparent in pictures B1 - B3.

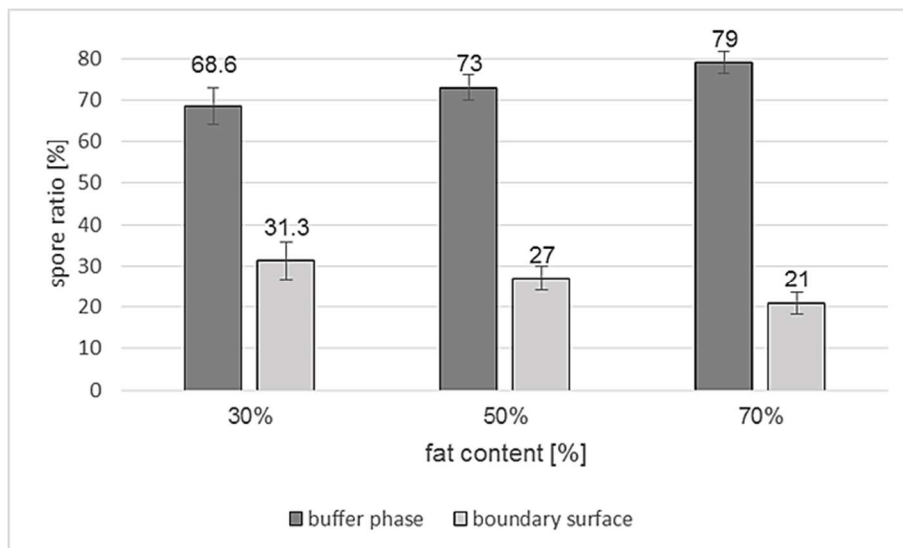


Figure 33: Percental endospore arrangement (TMW. 2.992) in 30, 50 and 70% soybean oil emulsions. The figure presents the percental arrangement of SYTO 9 stained endospores in soybean oil emulsions. To ensure statistical expressiveness, 10 fields of view were evaluated at 400 folds of magnification.

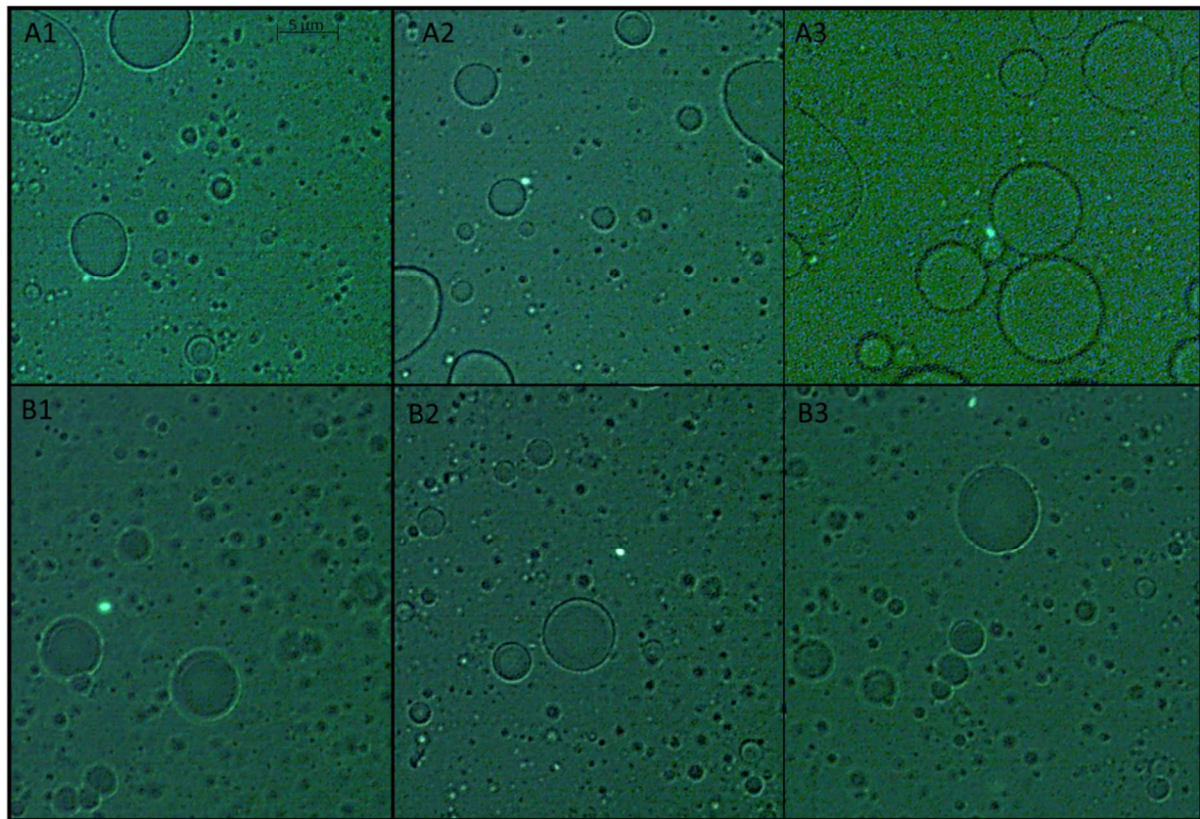


Figure 34: Localization of SYTO 9 stained endospores in soybean oil emulsions. The figure shows SYTO 9 stained endospores of TMW 2.992, which are associated to the boundary surface of soybean oil droplets (A1 - A3) and spores which are dissolved in the buffer phase (B1 - B3). Micrographs were acquired at 1000 fold of magnification.

3.3.3 Inactivation of *C. botulinum* type E endospores in emulsion matrices

3.3.3.1 Inactivation of *C. botulinum* type E endospores in emulsion matrices by heat treatment

To determine the temperature-dependent inactivation of *C. botulinum* type E endospores (TMW 2.992) in soybean oil matrices of different fat contents (0, 30, 50 and 70%), experiments according to (2.2.8.6) were conducted. Prior to plate count determination, samples were exposed for 10 minutes to 45, 60 or 75 °C.

Depending on matrix parameters and as a function of temperature intensity, corresponding log reduction values are depicted in Figure 35.

Obviously, the log reduction in pure buffer increased from 0.05 via 0.16 up to 0.30, as a function of increasing temperature (45, 60, 75 °C).

In comparison to spore reduction rates in pure buffer, the extent of spore inactivation in soybean oil emulsion of 30% fat was low reduced, when temperatures of 45 and 60

°C were applied (0.01; 0.005). However, in samples exposed to 75 °C, log reduction was increased (0.38).

Obviously, when samples of 50% fat were treated at 45 °C, the process of germination was promoted (indicated by a negative log reduction value of - 0.06). Endospores of TMW 2.992 were largely unaffected by heat treatment at 60 °C, when emulsion matrices of 50% fat were employed (log reduction of 0.003). A log reduction cycle of 0.23 was generated, when samples containing 50% fat were exposed to 75 °C.

Generally, temperature-induced endospore germination was observed, when matrices of 70% soybean oil were employed. The application of heat (45, 60 and 75 °C) led to log reduction values of -0.10; -0.25 and -0.18, respectively.

Finally, Figure 35 indicates that the extent of endospore inactivation depends on a coupled effect of temperature application and matrix constitution. By tendency, the inactivation of endospores increased by increasing temperature. Additionally, the inactivation of endospores tended to decrease as a function of increasing emulsion fat content.

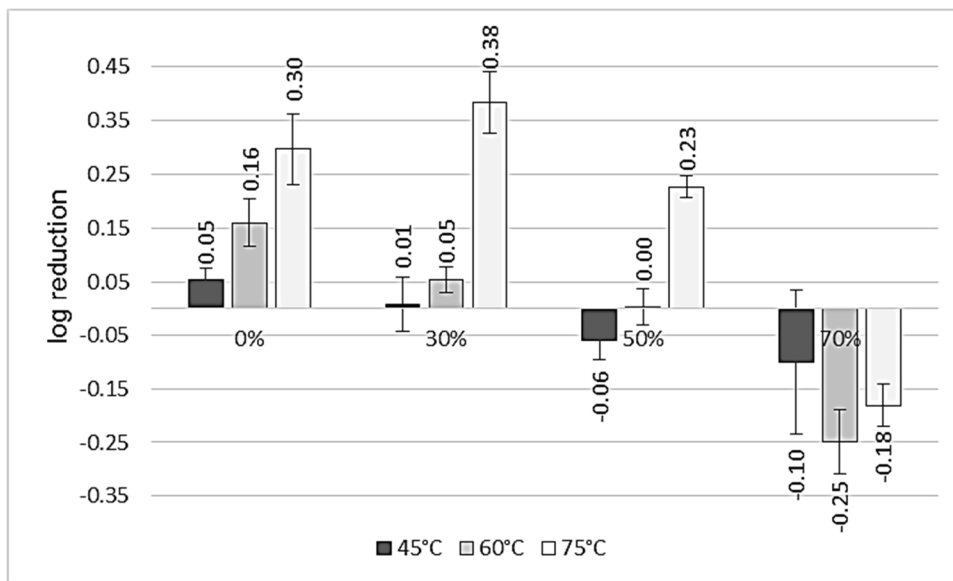


Figure 35: Temperature-dependent log reduction of TMW 2.992 endospores in soybean oil emulsions of different fat contents. The figure represents the log reduction values of TMW 2.992 spores, depending on emulsion fat contents (0,30, 50, 70%) and as a function of heat application (45 °C/10 min: black bars; 60°/10 min: dark grey bars; 75 °C/10 min: light grey bars).

3.3.3.2 Inactivation of *C. botulinum* type E endospores in emulsion matrices by HPT treatment

For HPT-induced endospore inactivation in model emulsions of different fat contents (0, 30, 50, 70%), samples were prepared according to 2.2.8.6. Consequently, samples were exposed for 10 minutes to variable HPT parameters (temperatures of: 45, 60, 75 °C; pressures of: 300, 450, 600, 750 MPa). Finally, log reductions were calculated by plate count determination. HPT-induced endospore inactivation experiments were operated in two different pressure units (single vessel apparatus U4000 and the low temperature vessel U111). Basically, the units differ in volume, in pressure transferring liquid and in the locus of pressure and temperature monitoring (2.2.8.7). Consequently, target temperatures according to experiments obtained in unit U111 were equal to matrix temperatures, while in experiments conducted in unit U4000, target temperatures were equal to temperatures in the PTL. To comprehend the influence of differing locus of temperature monitoring on endospore inactivation, adiabatic heating effects were determined as a function of different fat contents.

According to experiments obtained in single vessel apparatus U4000, log reduction values are depicted in Figure 36. As matrices, IPB or soybean oil emulsions with fat contents of 30, 50 and 70% were used. As inactivation parameters, pressures of 300, 450, 600 and 750 MPa and temperatures of 45, 60 and 75 °C were generated.

Obviously, depending on high pressure, temperature and matrix parameters, trends in endospore inactivation behavior were apparent.

The lowest endospore inactivation value was monitored (log reduction of 0.77), when samples of 70% fat were exposed to mildest pressure/temperatures conditions (300 MPa/45 °C). The maximal log reduction (3.32) was realized in soybean oil emulsions of 50% fat, at most harsh conditions (750 MPa/75 °C).

At constant pressure and matrix parameters, the log reduction of TMW 2.992 endospores tended to increase by increasing temperature.

By comparing datasets of equal pressure and matrix levels, the highest effect on endospore inactivation was observed, when emulsions of 50% soybean oil were pressured at 300 MPa, while temperature was increased from 45 to 60 °C (Δ log reduction = 1,3). Similar effects were monitored, when samples of IPB and 30%

soybean oil emulsions were treated under equal conditions (Δ log reduction = 1.09 and 1.04). Similar changes in inactivation rates were noticed, when emulsions of 70% fat were exposed to pressure of 300 or 450 MPa, respectively, while temperature was increased from 60 to 75 °C (Δ log reduction = 1.13 and 1.12).

At constant temperature and matrix parameters, the endospore mortality tended to increase by increasing pressure.

At 45 °C, the mentioned effect was clearly observable, when emulsions of 70% soybean oil were employed. When pressure was increased from 300 to 750 MPa, the log reduction raised from 0.77 to 1.28, continuously. Equal behavior of endospore inactivation was observed, when samples of 50% fat were used. When pressure was increased from 300 to 600 MPa, the log reduction increased from 1.02 to 1.41. Pressure intensification to 750 MPa led to similar spore inactivation rates, compared to pressuring at 600 MPa (log reduction = 1.40). When matrices of 0 and 30% fat were exposed to heat of 45 °C, the pressure-mediated effect can be reenacted by considering of standard deviation. When temperatures of 45 °C were exposed to emulsions containing 50 and 70% fat, the most impact of pressure-induced endospore inactivation was observed, when pressure was increased from 450 to 600 MPa (Δ log reduction = 0.31 and 0.34).

At temperatures of 60 °C and constant matrix parameters, log reductions tended to decrease, when pressure was increased from 300 to 450 MPa (with exception of values according to 50% soybean oil emulsions, treated at 450 MPa). On the contrary, the increase of pressure from 450 to 750 MPa led to an increase of log reduction values (also with exception of values according to 50% soybean oil emulsions, which were treated at 450 MPa). Independent of matrix parameters, the highest pressure-mediated killing effect at 60 °C was obtained, when pressure was increased from 600 to 750 MPa. Under referred conditions, log reduction values differed between 0.71 and 1.24. The highest endospore inactivation was established, when soybean oil emulsions of 70% fat were employed (log reduction = 1.24).

At 75 °C and constant matrix parameters, the endospore mortality also tended to increase by increasing pressure. Log reduction values between 2.29 and 3.19 were quantified in buffer matrices, when pressures of 350 to 750 MPa were generated. In soybean oil matrices with fat contents of 30, 50 and 70%, log reductions of 2.31 to

3.14; 2.15 to 3.23 and 2.41 to 2.94 were monitored as a function of pressure boost. When matrices of 0 and 30% fat were exposed to 75 °C, the highest pressure-mediated spore inactivation effect was monitored, when pressure was increased from 450 to 600 MPa (Δ log reduction = 0.42 and 0.40). In contrast, the most impact of endospore mortality in emulsions with 50 and 70% soybean oil were reached, when pressure of 600 MPa was scaled up to 750 MPa (Δ log reduction = 0.71).

At constant pressure/temperature parameters, log reductions tended to decrease by increasing fat content.

At constant pressure/temperature parameters, the endospore inactivation in IPB and 30% soybean oil emulsions was quite similar. At these conditions, log reductions differed in values of 0 to maximal 0.08. Generally, the increase of the fat content from 30 to 50% tended to affect the inactivation of endospores with more impact, than the increase from 0 to 30% (with exception of data, according to treatments at 750 MPa). At defined pressure/temperature parameters, differences in log reductions of 0.09 to 0.43 were measured, when the emulsion fat content raised from 30 to 50%. The smallest effect of increasing the fat content from 30 to 50% was quantified at parameters of 45 °C/600 MPa (Δ log reduction of 0.09). The most impact was obtained at parameters of 300 MPa/60 °C and 600 MPa/75 °C (Δ log reduction of 0.43). When samples were treated at 750 MPa, no clear correlations between fat content and endospore inactivation behavior were observed. When samples were exposed to 750MPa/45 °C, most endospores were inactivated in pure buffer (log reduction = 1.46). The log reduction decreased to 1.40 via 1.36 down to 1.28, when emulsions of 50, 30 and 70% fat were used. At inactivation parameters of 750 MPa/60 °C, the highest spore mortality was reached, when soybean oil emulsions of 70% fat were used (log reduction = 2.97). Low reduced inactivation levels were quantified, by applying emulsions containing 30 and 50% fat or by using imidazole phosphate buffer (log reductions = 2.92; 2.87 and 2.84). At parameters of 750 MPa/75 °C, the inactivation of endospores were most effective, when emulsions of 50% oil were used (log reduction = 3.23). Similar log reductions of 3.19 and 3.14 were estimated, when pure buffer and emulsions of 30% fat were employed. Most endospores survived, when matrices of 70% fat were used (log reduction = 2.94).

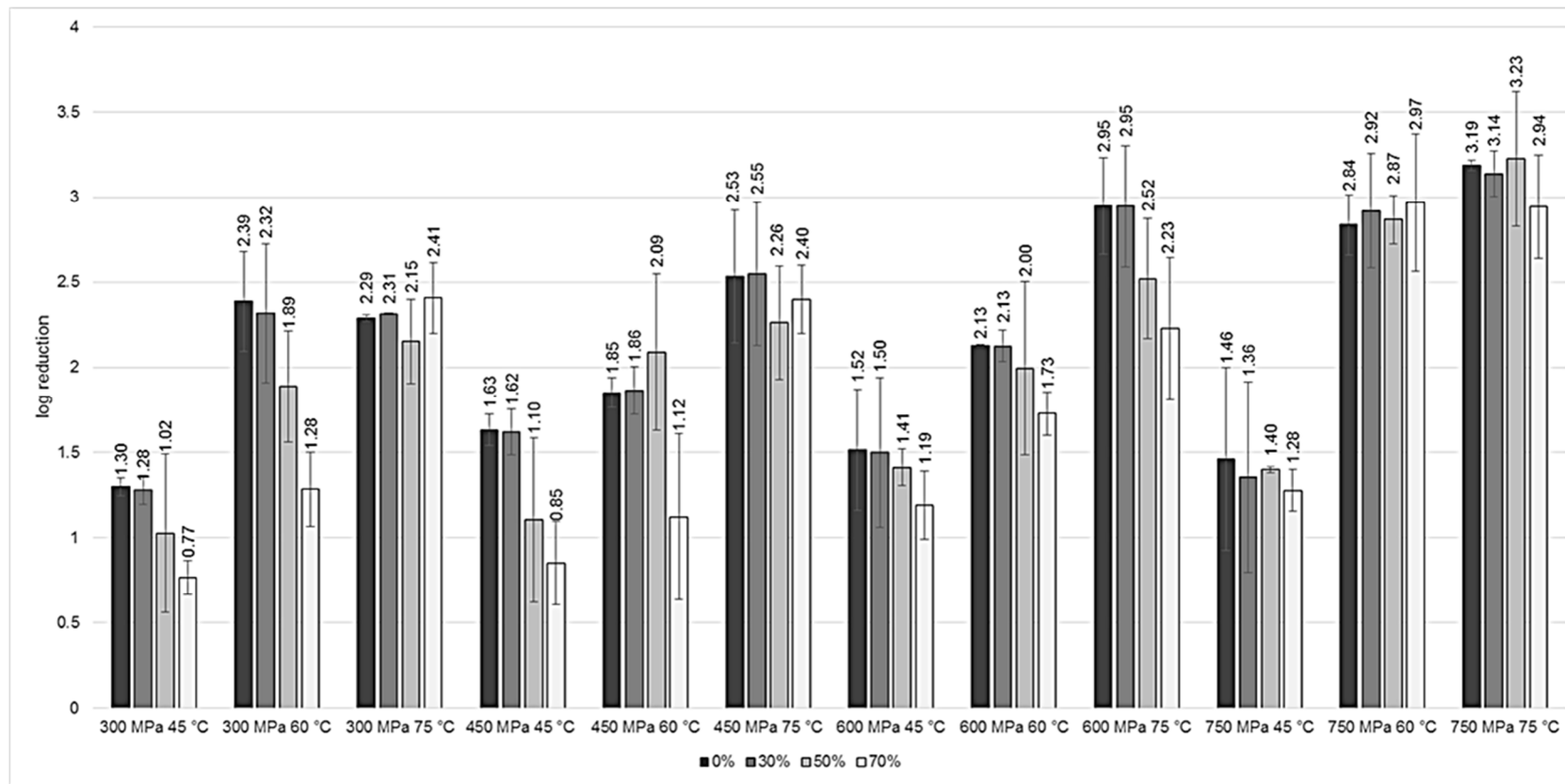


Figure 36: HPT-dependent log reductions of *C. botulinum* type E endospores (TMW 2.992) in emulsion matrices with different fat contents. Corresponding experiments were obtained in the high pressure unit U4000. Bar grouping indicate different HPT treatment intensities, i.e. 300, 450, 600 and 750 MPa combined with 45, 60 and 75 °C applied for a constant dwell of 10 min. Bar colors indicate fat contents (black = 0%, dark gray = 30%, light gray = 50%, white = 70% oil). Error bar indicate standard deviation calculated from three independent experiments.

According to experiments, which were performed in the low temperature vessel U111, log reduction values are depicted in Figure 37. As matrices, soybean oil emulsions with fat contents of 30, 50 and 70% were used. As inactivation parameters, pressures of 300, 450, 600 and 750 MPa and temperatures of 60 and 75 °C were generated.

Lowest endospore inactivation was observed at 450 MPa/60 °C, when emulsions of 70% fat were employed (log reduction = 0.59). Most endospores were killed at conditions of 600 MPa/75 °C, when emulsions of 30% fat were used (log reduction = 2.73).

At constant pressure and matrix parameters, endospore inactivation tended to increase by increasing temperatures. At equal pressure and matrix levels, the highest effect on endospore inactivation was observed, when emulsions of 70% soybean oil were pressured at 600 MPa, while temperature was increased from 60 to 75 °C (Δ log reduction = 1,42). Generally, the impact of increasing temperature (from 60 to 75 °C) was more effective at pressures of 450 and 600 MPa, than at pressure levels of 300 and 750 MPa.

At constant matrix and temperature parameters, the extent of spore inactivation tended to increase by increasing pressure levels. When emulsion samples of 30, 50 and 70 % fat were treated at 60 °C, log reduction values increased from 0.93 to 2.26; from 0.73 to 1.85 and from 0.82 to 1.73 respectively, while pressure was increased from 300 to 750 MPa. When pressure was increased from 300 to 750 MPa at constant temperature of 75 °C, log reduction values increased from 1.25 to 2.57; from 1.45 to 2.67 and from 1.47 to 2.46 respectively, when emulsions of 30, 50 and 70% fat were used. At 60 °C, the most impact on endospore inactivation was observed, when pressure was increased from 600 to 750 MPa. However, at 75 °C, pressure increase from 450 to 600 MPa was most effective to induce endospore inactivation.

At constant HPT parameters, log reductions tended to decrease by increasing fat contents. Clear protective effects exerted by the fat were determined at treatment parameters of 450 MPa, 60 °C; 450 MPa, 75 °C; 600 MPa, 60 °C and 750 MPa, 60 °C. At equal HPT levels, the highest effect on endospore inactivation was observed, when samples were treated at 60 °C/750 MPa, while the fat content of the emulsion was increased from 30 to 70%. (Δ log reduction = 0.53).

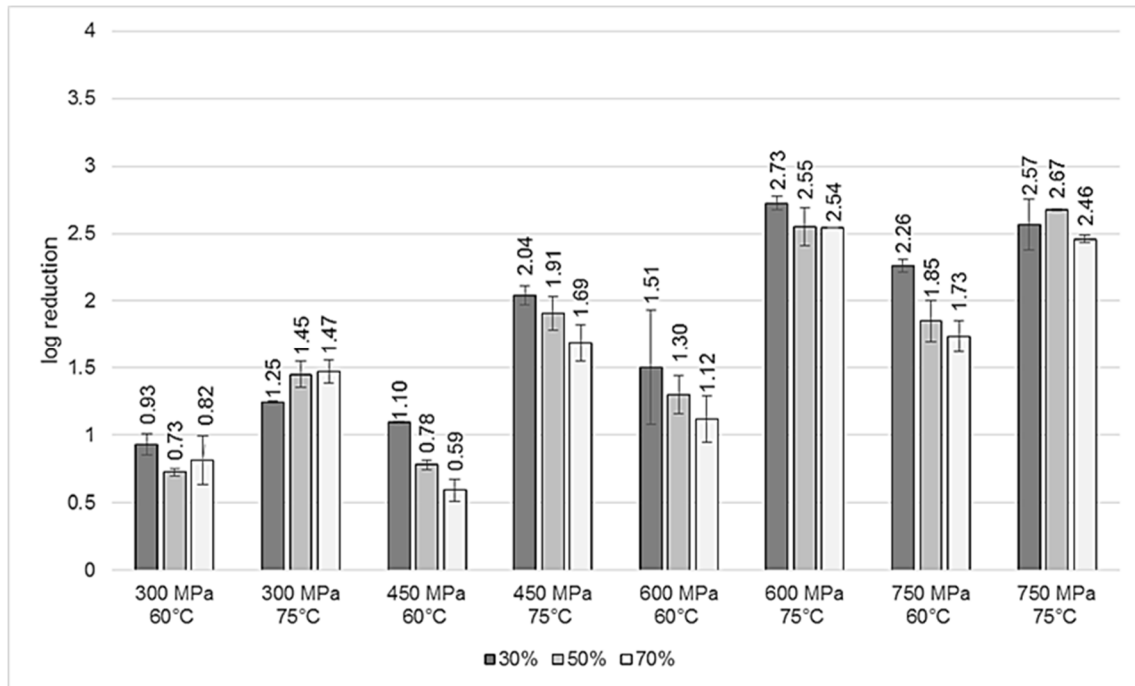


Figure 37: HPT-dependent log reductions of *C. botulinum* type E endospores (TMW 2.992) in emulsion matrices with different fat contents. Corresponding experiments were obtained in the high pressure unit U111. Bar grouping indicate different HPT treatment intensities, i.e. 300, 450, 600 and 750 MPa combined with 60 and 75 °C applied for a constant dwell of 10 min. Bar colors indicate fat contents (black = 0%, dark gray = 30%, light gray = 50%, white = 70% oil). Error bar indicate standard deviation calculated from three independent experiments.

According to pressure/temperature profiles obtained in the low temperature vessel U111, matrix-dependent effects of adiabatic heating were calculated. Soybean oil emulsions containing 30, 50 and 70% fat showed mean values for ideal adiabatic heat of compression of 4.13; 5.16 and 5.84 °C/100 MPa, respectively. Expectably, as a function of increasing emulsion fat content, adiabatic heating effects increased.

4 DISCUSSION

4.1 Knock out generation of *C. botulinum* type E strains

The genus *Clostridium* includes a large number of strains, which are of industrial and also of clinical interest. Especially the solvent producers *C. acetobutylicum*, *C. beijerinckii* (Montoyaa *et al.*, 2000) and *C. thermocellum* (Lynd *et al.* 2005) play a major role in biotec industry. On the other hand, pathogens such as *C. botulinum*, *C. tetani*, *C. perfringens* and *C. difficile* (Brüggemann, 2005) can present serious health threats. Based on the importance of such organisms, the investigation of metabolic processes is of great interest. In this context, the generation of knock out mutants presents a powerful tool for basic research. In this study, the primary interest focused on *C. botulinum* type E strains, which belong to the non-proteolytic group II. Members of this group are phylogenetically distinct from group I, III and IV strains, which are closer related to each other (Collins and East, 1998). Based on their potential to grow at temperatures low as around 3 °C, *C. botulinum* type E strains constitute a threat for REPFEDs (refrigerated processed foods of extended durability) and consequently for food industry and consumers (ACMSF report, 1992).

One aim of this study was to establish transformation and gene knock out strategies for *C. botulinum* type E strains. However, all developed transformation strategies were not suitable to generate *C. botulinum* type E transformants. Consequently, the construction of *C. botulinum* type E mutant spores was not successful. Although, *C. botulinum* type E transformants could not be generated, the developed transformation strategies will probably be helpful for other bacterial transformation studies.

Among others, the success of ClosTron mutagenesis can be influenced by:

- character of ClosTron plasmids (4.1.2)
 - type of replicon for gram positive bacteria
 - type of replicon for gram negative bacteria
 - compatible plasmid marker genes
 - suitable promoters
 - design of the side-specific group II introns

- conjugation parameters (4.1.4)

- ingredients of culture media
- density of cell cultures
- donor to recipient ratios
- ingredients and surface character of mating plates
- mating times
- mating temperatures

- electroporation parameters (4.1.5)

- time constant (which depends on capacitance and resistance and in turn on ionic strength of electroporation buffer and sample volume)
- field strength (which depends on instrumental adjustment and gap size of electroporation cuvettes)
- ingredients of culture and recovery media
- culture age
- character and quantity of DNA

- existence of restriction modification (RM) systems (4.1.6)

- host-dependent recognition sites of restriction endonucleases (REase)
- methylation pattern of foreign plasmid DNA

To indicate differences in transformation approaches and to indicate potential factors, which can influence the success of bacterial transformation processes (listed above), tested strategies are discussed in detail.

4.1.1 Strain selection for ClosTron mutagenesis

Prior to knock out and transformation experiments, nine *C. botulinum* type E strains (TMW 2.990 – TMW 2.998) were screened for the existence of target genes (CLO_1237, CLO_3013, CLO_3241, CLO_2913), by PCR (2.2.4.8; 3.1.1). Based on the published genome sequence of *C. botulinum* (TMW 2.990), primers, which flank the genes of interests, were designed. As expected, the existence of these genes was confirmed in *C. botulinum* (TMW 2.990) by amplification of specific DNA fragments (435, 331, 297 and 1286 bp). Amplicons of equal size were detected, when genomic

DNA of TMW 2.991, TMW 2.995 and TMW 2.997 was used for PCR screening. For strain TMW 2.993, only a DNA fragment of 435 bp was detectable, when CLO_1237_for/ CLO_1237_rev primers were used. For strains TMW 2.992, TMW 2.994, TMW 2.996 and TMW 2.998, genes of interest could not be amplified.

Based on the results of PCR screening, it is likely that TMW 2.991, TMW 2.995 and TMW 2.997 harbor equivalent genes to CLO_1237, CLO_3013, CLO_3241 and CLO_2913, while TMW 2.993 only contains a homolog gene to CLO_1237. Consequently, for knock out and transformation experiments, the strains TMW 2.992, TMW 2.994, TMW 2.996, TMW 2.998 and TMW 2.993 were selected, while the strains TMW 2.992, TMW 2.994, TMW 2.996 and TMW 2.998 were excluded.

4.1.2 Choice of Clostron plasmids for *C. botulinum* type E mutagenesis

The Clostridia Research Group (CRG) developed a promising approach, which enables the generation of stable and selectable knock out mutants, in the genus *Clostridium* (2.2.3.2, Heap *et al.*, 2009, B). For Clostron mutagenesis, a modular plasmid system is available, which enables the combination of four variable plasmid modules. Each typical Clostron plasmid contains a replicon for gram-positive bacteria, a replicon for gram-negative bacteria, a selective plasmid marker and the specific group II intron, which also contains a group I interrupted selective marker gene (Figure 3, Heap *et al.*, 2009, A). For knock out generation in *C. botulinum*, Heap *et al.* (2009, B) recommended the use of retargeted pMTL007C-E2 vectors. Other publications referred to pMTL007C-E2 and pMTL007-mediated *C. botulinum* type A mutagenesis (Bradshaw *et al.*, 2010; Cooksley *et al.*, 2010; Selby *et al.*, 2011; Söderholm *et al.*, 2011 and Kirk *et al.*, 2012). The vectors pMTL007 and pMTL007-E2 just differ in their promoter region, which regulates the group II intron expression. The plasmid pMTL007 contains the isopropyl β -D-1-thiogalactopyranoside (IPTG) inducible *fac* promoter, while pMTL007C-E2 carries the constitutive *fdx* promoter. In this study, the Clostron plasmids pMTL007C-E2:43973-Cbo-ssp3241, pMTL007C-E2:53142-Cbo-ssp3013, pMTL007C-E2:53143-Cbo-ssp1237 and pMTL007C-E2:53144-Cbo-gpr were generated, which were all derived from the backbone of pMTL007C-E2. The pMTL007C-E2 plasmid includes the replicon of the *C. butyricum* plasmid pCB102, the *ColE1+tra* module (which enables plasmid replication in *E. coli* and conjugative transfer), the chloramphenicol/thiamphenicol resistance permitting *catP* gene, and the *ermB* RAM intron marker (Heap *et al.*, 2009, B).

As mentioned above, mutants of *C. botulinum* type A have successfully been generated, by employing retargeting pMTL007 and pMTL007C-E2 vectors, respectively (Heap *et al.*, 2009 B; Bradshaw *et al.*, 2010; Cooksley *et al.*, 2010; Selby *et al.*, 2011; Söderholm *et al.*, 2011 and Kirk *et al.*, 2012). However, according to their phylogenetic positions, these strains are highly related to *C. sporogenes* and obviously exhibit quite a few metabolic and structural differences to *C. botulinum* type E strains (Collins and East). Potentially, the pMTL007C-E2 plasmid was not suitable for knock out generation in *C. botulinum* type E strains.

Possibly, the *C. butyricum*-derived replicon was not compatible for plasmid replication in *C. botulinum* type E. Transformation experiments with *C. botulinum* ATCC 3502 have shown that the character of gram positive replicons influenced the frequency of plasmid transfer. When *C. botulinum* ATCC 3502 was transformed with ClosTron plasmids containing the replicons pBP1 and pCB102 respectively, the transformation efficiency was much higher than by employing plasmids, which harbor pCD6 or pIM13 replicons (Heap *et al.*, 2009 A).

Furthermore, it cannot be ruled out that the constitutive expression of the group II intron (mediated by the *fdx* promoter) led to toxic concentrations of translation or transcription products. Experiments in *C. sporogenes* and *C. acetobutylicum* indicated that constitutive group II intron expression permits increased insertion frequencies. However, information concerning life-threatening effects, which are caused by constitutive intron expression, are not available (Heap *et al.*, 2007).

Further reasons for insufficient pMTL007C-E2 transfer into *C. botulinum* type E strains could be attributed to the incompatibility of the *catP* gen. The plasmid marker permits chloramphenicol/thiamphenicol resistance by encoding an acetyltransferase. Enzymatic activity permits the acetylation of chloramphenicol/thiamphenicol molecules and consequently prevents the association of antibiotics to bacterial ribosomes (Huggins *et al.*, 1992). Finally, if *catP* gene expression does not result in an active chloramphenicol/thiamphenicol acetyltransferase, positive transformants would not become resistant against antibiotic application.

During this study, no efficient transfer of pMTL007C-E2 derivatives into *C. botulinum* type E strains could be evidenced. Since successful plasmid transfer represents the basis for effective ClosTron mutagenesis, sources of error, which may have resulted

from incompatible group II elements (defective designed group II elements; intron insertion into non-target sites), are not discussed.

4.1.3 Transformation of *C. botulinum* type E strains

To transform plasmid derivatives of pMTL007C-E2 into *C. botulinum* type E strains, different conjugation and electroporation strategies were tested. In the following section, parameters, which conceivably exert influences on transformation efficiency, are discussed.

4.1.4 Transformation of *C. botulinum* type E strains by conjugation

In this study, the *C. botulinum* type E strains TMW 2.990, TMW 2.991, TMW 2.995, TMW 2.997 and TMW 2.993 were tested for transformation with pMTL007C-E2-derived ClosTron plasmids by conjugation.

In previous publications, efficient conjugative plasmid transfer of retargeted pMTL007C-E2 / pMTL007 vectors into *C. botulinum* were reported (Bradshaw *et al.*, 2010; Cooksley *et al.*, 2010; Selby *et al.*, 2011; Söderholm *et al.*, 2011 and Kirk *et al.*, 2012). In all mentioned studies, conjugation was mediated by the donor strain *E. coli* CA434. This strain is isogenic with *E. coli* HB101, but additionally carries the conjugative IncPb plasmid R702, which harbors *tra* and *mob* genes (Purdy *et al.*, 2002; Hedges and Jacob, 1974). For effective mating, donor to recipient ratios of 10:1 or 10:2 were suggested. In the mentioned studies, successful transformation of *C. botulinum* was obtained, when mating plates (TPYG/TYG) were anaerobically incubated for 7h at 37 °C (Selby *et al.*, 2011; Cooksley *et al.*, 2010 and Bradshaw *et al.*, 2010).

Bacterial conjugation frequency can be affected by several parameters. Transformation efficiency can be increased when optimal conditions of cell density and donor to recipient ratio are selected (Sasaki *et al.*, 1988; Al-Masaudi *et al.*, 1991 and Fernandez-Astoraga *et al.*, 1992).

In this study, the donor strain *E. coli* Ca434 was used. For conjugation experiments, cell densities of 1×10^7 up to 3×10^9 CFU/ml were used and donor to recipient ratios of 10:0.5 up to 10:10 were tested. Nevertheless, variation in cell densities and donor to recipient ratios did not promote successful conjugation of *C. botulinum* type E strains (3.1.2).

According to Sasaki *et al.* (1988), the ages of cell cultures can also influence the conjugation frequency. Depending on strain specificity, cells in exponential phase can be more appropriate for conjugation compared to stationary phase cells. In this study, *C. botulinum* type E cells of different growth phases (8 - 72 h) were tested. Nevertheless, the use of different recipient culture ages did not support the process of conjugation.

Both medium ingredients and surface character of mating plates can also influence the conjugal transformation efficiency. Specific medium ingredients can induce bacterial aggregation leading to a decrease in plasmid transfer frequency (Al-Masaudi *et al.*, 1991). Furthermore, mating plates containing elevated concentration of TOC (total organic carbon) can contribute to increased plasmid transfer rates in *E. coli*- mediated conjugation events (Fernandez-Astoraga *et al.*, 1992). Depending on specificities of donor and recipient strains, transformation frequency can be increased, when mating is performed on nitrocellulose membrane surfaces (Lampkowska *et al.*, 2008). Sasaki *et al.* (1988) suggested, that the surface of filtermembranes facilitates plasmid transfer frequencies, because denser cell contact between donor and recipient were offered.

In this study, neither the use of different mating plates (TPYG, TPYC and DRCM), nor the additional application of nitrocellulose membranes (pore size 0.45 µm, Satorius AG) led to positive conjugation results. Therefore, a limited contact of cells in the experimental setting should not be the reason for failed transformation.

According to Heap *et al.* (2009), the required mating time primarily depends on recipient and plasmid characteristics and properties. For plasmid transfer from *E. coli* CA434 into *Clostridium* ssp., an incubation period of 8 - 24 h is recommended. In studies, where retargeted pMTL007 respectively pMTL007C-E2 vectors were transmitted by *E. coli* CA434 into *C. botulinum* type A strains, mating plates were commonly incubated anaerobically at 37 °C for 7 h (Selby *et al.*, 2011; Cooksley *et al.*, 2010 and Bradshaw *et al.*, 2010). *E. coli*-mediated conjugation experiments indicated that mating temperature can also influence the process of plasmid transfer. According to Fernandez-Astoraga *et al.* (1992), temperature variations in the range of 7.7 °C led to changes in approximately 10-folds transconjugant quantities of.

According to this study, mating plates were anaerobically incubated between 7 and 48 h, at 28 and 37 °C, respectively. Obviously, variations in mating time and temperature

did not contribute to transformation of *C. botulinum* type E strains. Since the mating temperature needs to match the requirements of both genera employed, it remains speculative whether higher or lower temperatures may enable conjugation.

4.1.5 Transformation of *C. botulinum* type E strains by electroporation

In this study, strains of the *C. botulinum* type E (TMW 2.990, TMW 2.991, TMW 2.995, TMW 2.997 and TMW 2.993) were tested for their transformation with pMTL007C-E2-derived ClosTron plasmids by electroporation. However, plasmid transfer into *C. botulinum* type E strains by electroporation was not successful.

Generally, during the processes of electroporation, competent cells and exogenous DNA are exposed to high-voltage pulses. The electric pulse induces the transient permeabilisation of cellular membranes, which enables the invasion of foreign DNA into cells. For successful transformation, different cell types require different electroporation conditions, which have to be determined (Jordan *et al.*, 2008). Additionally, transformation efficiencies can be optimized by variations in influence factors such as culture medium, culture age, composition of recover medium, and the character and quantities of used DNA (Dürre, 2005).

Furthermore, the time constant (T) and the electric field strength (E) are important parameters, which can affect transformation efficiency. The time constant is given by the product of resistance (R) and capacitance (C) of the electroporation apparatus. Resistance and capacitance can be regulated by instrument adjustment. Resistance can also be modified by ionic strength and sample volume. The electric field strength is given by the quotient of voltage (V) and the distance between the electrodes (cm). Consequently, field strength can be regulated by instrument adjustment and by the gap size of electroporation cuvettes (User manual of Gene Pulser II Electroporation System, Bio-Rad Laboratories GmbH).

According to Zhou and Johnson (1993) and Davis *et al.* (2000), efficient electroporation of *C. botulinum* group I and II strains were reported. In studies of Zhou and Johnson (1993) and Davis *et al.* (2000), cells of *C. botulinum* were cultivated in TPYG or glycine supplemented TPYG media. Transformation experiments with gram positive bacteria indicated that strong cell wall structures represent a barrier for incoming DNA. It has been shown that transformation efficiency of gram-positive bacteria can be increased, when cell wall impairing additives like glycine are added to growth media (Powell *et al.*,

1987; Holo and Nes, 1989; Cruz-Rodz and Gilmore, 1990). In this study, *C. botulinum* type E strains were cultured in TPYG/TPYC media supplemented with and without 1% glycine (w/v). However, the transformation of *C. botulinum* type E strains remained unsuccessful and no positive effects of media and additives used were observed.

Transformation efficiency also depends on bacterial culture ages. Transformation experiments with *C. botulinum* Hall A indicated that highest numbers of transformants were obtained, when middle log phase cells ($OD_{600} = 0.8$) were employed (Zhou and Johnson, 1993). Additionally, successful transformation of *C. botulinum* ATCC 25765 has been reported in studies of Cruz-Rodz and Gilmore (1990), in which cultures of $OD_{600} = 0.8$ were applied. In contrast, for successful transformation of *C. acetobutylicum*, cell cultures of $OD_{600} = 1.1$ were recommended (Mermelstein and Papoutsakis, 1993). In this studies, *C. botulinum* type E cultures of different growth phases ($OD_{600} = 0.2, 0.8$ and 1.2) were introduced for electroporation experiments. Consequently, the application of different *C. botulinum* aged cultures did not support transformation efficiency.

According to publications by Zhou and Johnson (1993) and by Davis *et al.* (2000), 0.8 ml and 0.3 ml of competent *C. botulinum* cells were applied, respectively. Since sample volume affects sample resistance, this parameter also influence the process of transformation.

To optimize transformation efficiencies, Zhou and Johnson (1993) used plasmid DNA in the range of 0 - 10 μg . The highest transformation rates of *C. botulinum* Hall A were accomplished, when 1 μg DNA was applied. Davis *et al.* (2000) reported about successful transformation of *C. botulinum* ATCC 25765 by employing plasmid DNA of 0.1 - 2 mg/ml. According to this study, transformation efficiencies of *C. botulinum* type E strains were tested for their improvement by employing volumes of 0.2 – 0.8 ml competent cells and plasmid DNA up to 10 μg . Finally, no positive influence on plasmid transfer was induced when different ratios of cell volumes and quantities of DNA were applied in electroporation experiments.

The use of suitable electroporation buffers play a major role in efficient plasmid transfer as well. For transformation of prokaryotic cells, high resistance buffers (>3000 ohms) are required. Generally, the ionic strength of buffers can influence sample resistance and finally transformation efficiency (Jordan *et al.*, 2008). Experiments according to

Zhou and Johnson (1993) demonstrated that highest numbers of *C. botulinum* transformants (2960 transformants/ μg DNA) were generated, when 10% PEG 8000 was used. When 15% glycerol and SMP (2.2.5.3.2) were used, the amount of transformants was 37.5 and 97.98% lower. According to Davis *et al.* (2000), adequate transformation results were obtained (10^3 - 10^4 transformants/ μg DNA), when 10% PEG 6000 or SMP buffers were used.

According to this work, mentioned electroporation buffers were used to transform *C. botulinum* type E strains (2.2.3.2.3.2). Although used buffers differed in ingredients and in ionic strength, no transformants of *C. botulinum* type E strains were generated.

As already mentioned, field strength and time constant represent important factors in electroporation processes. According to Davis *et al.* (2000), field strengths between 6.25 and 10 kV/cm were required to transform *C. botulinum* ATCC 25765. In experiments according to Zhou and Johnson (1993), highest numbers of *C. botulinum* Hall A transformants were generated ($\sim 4 \times 10^8$ transformants/ μg DNA), when a field strength of 6.25 kV/cm was employed. According to this work, field strengths of 5, 6.25, 10 and 12.5 kV/cm were generated to transform *C. botulinum* type E strains.

In addition to variations in ionic strength and sample volumes, the time constant can be regulated by instrumental adjustment of resistance and capacitance. In publications, which described positive transformation events of clostridia, capacitances of 25 μF were setted. For transformation of *C. beijerinckii*, *C. botulinum* and *C. acetobutylicum*, resistance parameters of 200, 400 and $\infty \Omega$ were recommended (Dürre, 2005; Davis *et al.* 2000; Mermelstein and Papoutsakis, 1993). According to transformation experiments of this study, capacitances of 25 μF and resistance parameters of 200, 300, 400 and $\infty \Omega$ were applied. Finally, neither the variation of field strengths (5, 6.25, 10 and 12.5 kV/cm), nor the variations in resistance parameters (200, 300, 400 and $\infty \Omega$) contributed to a successful transformation of *C. botulinum* type E strains.

According to Zhou and Johnson (1993) and to Davis *et al.* (2000), electroporated *C. botulinum* cells were recovered in TPYG medium and supplemented with 25 mM MgCl_2 . Electroporation experiments according to Berthier *et al.* (1996) indicated that the number of transformants increased up to 600-fold, when 80 mM MgCl_2 were added to the recover medium. Berthier *et al.* (1996) supposed that the positive effect of MgCl_2

was not induced by enhanced post-pulse survival but rather by a better maintenance of plasmids in recipient cells. In this study, *C. botulinum* type E strains were recovered in TPYG/TPYC medium supplemented with and without 25 mM MgCl₂. Neither the use of two different recover media, nor the addition of MgCl₂ led to the successful transformation of *C. botulinum* type E strains.

4.1.6 Restriction modification systems

The difficulties in *C. botulinum* type E strain transformation (3.1.2, 3.1.3) could be related to the presence of RM systems. The occurrence of prokaryotic RM systems constitute a common hindrance in bacterial transformation (Elhai *et al.*, 1997; Berndt *et al.*, 2003). RM systems represent prokaryotic protection mechanisms, which prevent the invasion of foreign DNA. The most RM systems consist of a restriction endonuclease (REase) and a methyltransferase (MTase). The REase is able to sense specific DNA recognition sequences. Depending on the methylation status of the recognition site, cleaving sites are attacked or spared by REase activity. Consequently, the methylation status of the recognition site depends on the activity of corresponding MTase. Based on specific DNA methylation pattern, the REase is able to distinguish between inherent and foreign DNA. The identification of external DNA, which lacks the strain-specific methylation pattern, leads to endonucleolytic cleavage by REase activity (Bayliss *et al.*, 2006; Pingoud and Jeltsch, 2001).

Based on enzyme composition, cofactor requirements and the mode of action, RM systems are classified in four different groups (types I, II, III and IV), (Roberts *et al.*, 2003). Type I RM enzymes typically consist of two REase subunits (catalyze DNA cleavage), one specificity subunit (required for DNA sequence recognition) and two MTase subunits (catalyze the methylation reaction). For the cleaving reaction, the cofactors ATP, SAM and Mg²⁺ are required, whereas methyltransferase activity only depends on SAM. In type I RM systems, DNA cleavage occurs in a considerable distance from the recognition side. After complex binding to unmodified recognition sites, ATP-mediated bidirectional DNA translocation is performed. DNA is cleaved, when two enzyme complexes converge. Depending on the methylation status of the target DNA, the enzymatic action mode of the complex is regulated. When the recognition side is completely unmethylated, the DNA is assessed to be foreign. Consequently REase gets active. When the recognition side is hemi-methylated (just at one strand of the duplex), the molecule is recognized as newly replicated bacterial

DNA. Accordingly, MTase catalyzes the modification of the unmethylated strand. If the recognition site is fully methylated, the DNA is recognized to be part of the bacterial genome (Studier and Bandyopadhyay, 1988; Tock and Dryden, 2005).

Type II RM systems commonly consist of two separate REase and MTase enzymes, which recognize the same palindromic DNA sequence. Generally, type II MTases act as SAM-dependent monomers. Based on the diversity in amino acid sequences and different behavior, type II REase are divided into eleven Mg²⁺-dependent overlapping subclasses (Pingoud and Jeltsch, 2001, Roberts *et al.*, 2003). Generally, the cleaving site of all type II REase is present inside or adjacent to the recognition site. Typically, type II REases act as homodimers. However, monomers or tetramers are also known (Tock and Dryden, 2005).

Predominantly, type III RM systems are present in phages and gram-negative bacteria (Bickle and Krüger, 1993). These systems consist of two homolog REase (catalyze DNA cleavage) and two equal MTase subunits (asymmetric target site recognition and modification). The cofactors ATP and Mg²⁺ are required for endonuclease activity, while methylation reaction depends on SAM. DNA cleavage by type III RM systems occur at fixed locations, 25 - 27 bp from the recognition site, and require the formation of a hetero-oligomeric complex (REase₂MTase₂). Similar to type I RM systems, after complex binding to unmodified recognition sites, ATP-mediated DNA translocation is performed. DNA is cleaved, when two inversely oriented enzyme complexes converge. In contrast, subunits of MTases are able to act independently (Tock and Dryden, 2005; Srikhanta *et al.*, 2010).

Type IV systems consist of one or two proteins that exclusively cleave DNA when the recognition site is modified by methylation, hydroxymethylation or glycosyl-hydroxymethylation (Roberts *et al.*, 2003). Since this prokaryotic defense strategy is based on restriction of "false methylated" foreign DNA, type IV systems do not contain MTases. The most famous member of this group is the Mg²⁺- and GTP-dependent McrBC system of *E. coli* K12 (Tock and Dryden, 2005). Group-wide classification parameters of type IV systems (cofactor requirements, recognition and cleaving sites) are not known.

In the genus *Clostridium*, a multitude of RM systems were proven to exist. Transformation experiments with *C. acetobutylicum* ATCC 824, *C. cellulolyticum*

ATCC 353, *C. botulinum* ATCC25765, *C. difficile* CD3 and *C. difficile* CD6 indicated that the transfer of extra chromosomal elements were hindered by REase activity (Mermelstein and Papoutsakis, 1993; Jennert *et al.*, 2000; Davis *et al.*, 2000 and Purdy *et al.*, 2002).

4.1.6.1 Putative restriction modification systems of *C. botulinum* (TMW 2.990)

The database “REBASE” (<http://rebase.neb.com/rebase/rebase.html>) includes published and unpublished information of restriction enzymes, DNA methyltransferases and related proteins, which likely are involved in restriction and modification processes. Based on conserved DNA sequence motives, the database also provides information on predicted RM systems (Roberts *et al.*, 2005). According to REBASE, in *C. botulinum* beluga (TMW 2.990) the presence of a type II (CboE1ORF1092P, M.CboE1ORF1092P) and a type IV RM system (CboE1ORFAP) is predicted. Based on REBASE information, the putative type II REase recognizes sequence motives of 5′ GCNGC 3′, whereas the corresponding cleaving site is unknown. Supposedly, the putative type II MTase generates modified 5-methylcytosin bases. Corresponding recognition and cleaving sites of the putative type IV REase are unknown. In Figure 38, the gen organization of *C. botulinum* (TMW 2.990), according to RM encoding and surrounding genes, are depicted. The MTase (M.CboE1ORF1092P; locus-tag: CLO_1092) and the REase (CboE1ORF1092P; locus-tag: CLO_1093) of the putative type II RM system are encoded by genes of 1760 bp (Figure 38, A). These genes are interrupted by a non-encoding region of 94 bp. CLO_1091, which is arranged downstream of the putative MTase gene and encodes for a protein of unknown function. Upstream of CLO_1093, an additional putative restriction endonuclease gene is encoded (CLO_1094). According to REBASE, CLO_1091 and CLO_1094 seem not to be involved in the mentioned RM system. The CLO_1966 gen (2969 bp), which encodes for the putative REase CboE1ORFAP of the predicted type IV RM system, is depicted in Figure 38 B. The putative REase gene is flanked by genes of opposite reading direction (CLO_1965 and CLO_1967). According to NCBI, mentioned genes encode a sugar transport protein and a MutT/NUDIX family protein. Consequently, CLO_1965 and CLO_1967 seem not to be involved in the putative RM type IV system. Assuming that REBASE information of putative *C. botulinum* (TMW 2.990) RM systems are confidential, foreign DNA have to comply specific requirements to overcome these restriction barriers. Based on the existence

of the putative type II RM system, 5' GCNGC 3'-motives have to be protected by C5 methylation at one specific cytosine. The existence of the predicted type IV REase implies that specific but unknown sequence motives of foreign DNA have to be unmethylated.

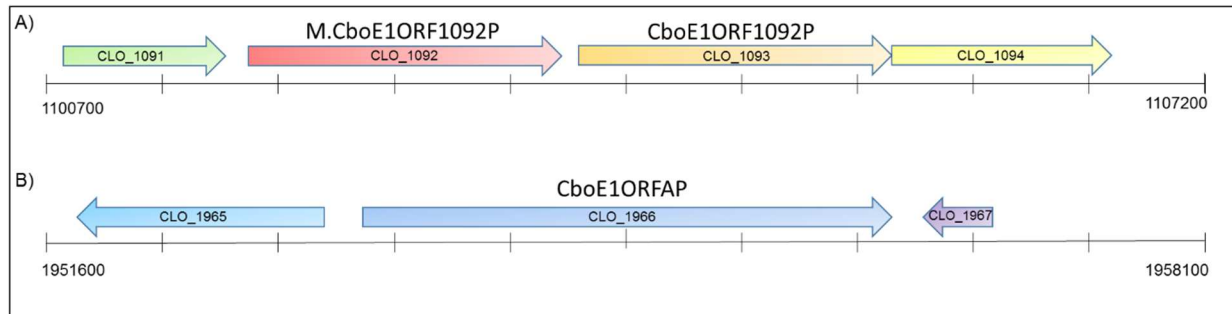


Figure 38: Organization of RM systems encoding and flanking genes. Depicted are the DNA fragments 1100700 - 1107200 bp (A) and 1951600 - 1958100 bp (B) of the *C. botulinum* (TMW 2.990) genome. Genes are illustrated as arrows, which contain the corresponding NCBI locus-tags. According to REBASE information, genes which encode MTase and REase of the putative type II RM system (A) are labeled M.CboE1ORF1092P and CboE1ORF1092P. The REase gene according to the predicted type IV RM system (B), is also indicated and labeled CboE1ORFAP.

4.1.6.2 Strategies to circumvent putative restriction barriers of *C. botulinum* type E

The occurrence of bacterial RM systems often prevents the process of genetic transformation. These barriers can be overcome when foreign DNA is methylated in the strain-specific pattern. In this study, pMTL007C-E2-derived ClosTron plasmids were methylated by different strategies prior to *C. botulinum* (TMW 2.990) transformation (2.2.6.1 - 2.2.6.3).

4.1.6.2.1 Methylation of plasmid DNA, by different *E. coli* strains

To increase the number of *C. botulinum* ATCC transformants, Davis *et al.* (2000) premethylated plasmid DNA by different *E. coli* strains (Top10, GM2163 and HB101) with different methylation patterns, prior to electroporation. Transformation efficiency of *C. botulinum* ATCC was increased by a factor of two, when vector DNA was premethylated in *E. coli* GM2163.

According to Davis *et al.* (2000), the different methylation patterns of the *E. coli* strains Top10, GM2163 and HB101 should be exploited to optimize transformation of *C. botulinum* (TMW 2.990). In Figure 39, transformation experiments conducted in this study are depicted.

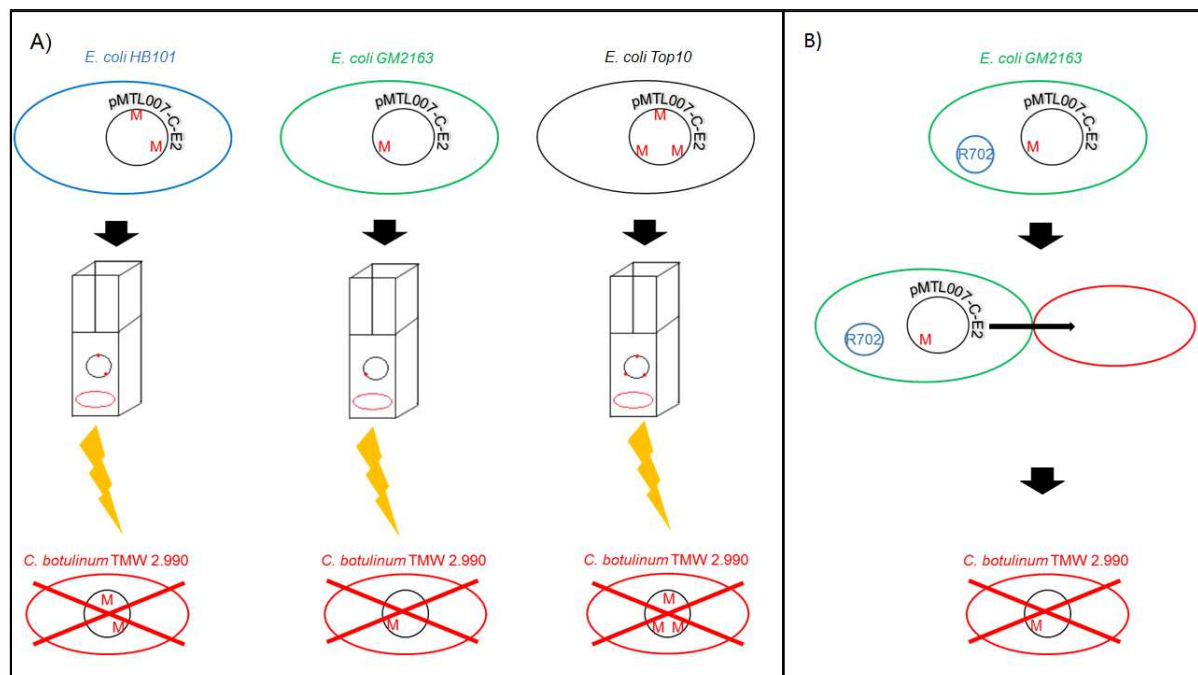


Figure 39: Transformation strategies of *C. botulinum* (TMW 2.990) by exploiting methylation patterns of different *E. coli* strains. Transformation assays of *C. botulinum* are depicted after premethylation of pMTL007C-E2 derivatives by different *E. coli* strains (Top10, GM2163, HB101) are depicted. Figure A illustrates plasmid transfer by electroporation, while figure B reflects plasmid transfer by conjugation. The arrangement of plasmid associated methyl groups (red marked M) indicate different methylation patterns of *E. coli* strains.

Unfortunately, the premethylation of Clostron plasmids (pMTL007C-E2:43973-Cbo-ssp3241, pMTL007C-E2:53142-Cbo-ssp3013, pMTL007C-E2:53143-Cbo-ssp1237, pMTL007C-E2:53144-Cbo-gpr) by *E. coli* strains with different methylation patterns (HB101, GM2163, Top 10) did not increase transformation efficiency of *C. botulinum* (TMW 2.990), when electroporation was carried out (Figure 39A).

Several members of the genus *Clostridium* produce high amounts of extracellular nucleases, which can affect transformation frequencies (Hielm *et al.*, 1998; Swiatek *et al.*, 1987; Blascheck and Klacik, 1984). Davis *et al.* (2000) supposed that transformation of *C. botulinum* BL151 was prevented by nuclease secretion, when electroporation was performed. During electroporation processes, the presence of extracellular nucleases can inhibit the uptake of foreign DNA, whereas in conjugative processes, the activity of extracellular nucleases does not present a problem (Wu *et al.*, 2000).

Conjugation experiments in this work indicated that transformation of *C. botulinum* type E strains was insufficient when *E. coli* Ca434 was employed as donor strain. Consequently, an additional conjugative *E. coli* host (*E. coli* GM2163, which harbors

plasmid R702) was constructed (2.2.6.1). Nevertheless, further experiments indicated that the conjugative *E. coli* strain GM2163 was also not suitable to transfer derivatives of pMTL007C-E2 into *C. botulinum* (3.1.4.1).

Generally, most laboratory strains of *E. coli* contain a collection of three different site-specific DNA methyltransferases, which are encoded by *dam*, *dcm* and *hsdM/S* genes (May and Hattaman, 1975; Hattman *et al.*, 1978; Lautenberger *et al.*, 1978; Kan *et al.*, 1979; Wyszynski *et al.*, 1993 and Suzuki, 2012). In Table 25, the genotype-dependent methylation patterns of *E. coli* Top10, GM2163, Ca434 and HB101 are listed. Additionally, this table contains information concerning frequencies of sequence motives corresponding to pMTL007C-E2-derived Clostron plasmids.

Table 25: Genotype-dependent methylation patterns of *E. coli* strains and corresponding sequence frequency in pMTL007C-E2-derived Clostron plasmids. Residues, which can be modified by methyltransferases are marked by stars. Red colored stars indicate that corresponding residues are methylated, while blue colored stars indicate that corresponding residues are unmethylated.

<i>E. coli</i> strain	Relevant sequence motives	frequencies of relevant sequence motives in pMTL007C-E2 derivatives [quantity/ pMTL007C-E2 derivative]
Ca434/HB101	TGA*[N ₈]TGCT	0
	AGCA*[N ₈]TCA	1
	GA*TC	14
	CC*AGG	5
	CC*TGG	5
GM2163	AA*[N ₆]GTGC	0
	GCA*[N ₆]GTT	1
	GA*TC	14
	CC*AGG	5
	CC*TGG	5
TOP10	AA*[N ₆]GTGC	0
	GCA*[N ₆]GTT	1
	GA*TC	14
	CC*AGG	5
	CC*TGG	5

(May and Hattaman, 1975; Hattman *et al.*, 1978; Lautenberger *et al.*, 1978; Kan *et al.*, 1979; Wyszynski *et al.*, 1993 and Suzuki, 2012; 2.1.8)

Considering that predicted type II and type IV RM systems of *C. botulinum* (TMW 2.990) are actually existent, the ineffective transfer of premethylated plasmid DNA into *C. botulinum*, is explainable. As shown in Table 25, the methyltransferases of the mentioned *E. coli* strains do not synthesize methylated sequence motives (GCNGC), which correspond to the recognition site of the putative CboE1ORF1092P restriction endonuclease of *C. botulinum* (TMW 2.990). Derivatives of pMTL007C-E2 contain a

total of 24 GCNGC-motives, which were consequently not protected for endonuclease activity according to CboE1ORF1092P. Considering that also the type IV RM system is existent, additional plasmid methylation contributes to the risk of DNA restriction events. The use of a bacterial strain, which expresses a 5' GCNGC 3' substrate affine methyltransferase would be promising for effective plasmid premethylation. Ideally, this desirable strain should be poor in other additional methyltransferases.

4.1.6.2.2 Methylation of plasmid DNA by methyltransferases of *C. botulinum* (TMW 2.990)

According to transformation experiments with *C. acetobutylicum* ATCC 824 and *C. botulinum* ATCC 25765, strain-specific restriction barriers can be overcome, when plasmid DNA is premethylated in genetically modified *E. coli* hosts, which encode methyltransferases of corresponding *Clostridium* strains (Mermelstein and Papoutsakis, 1993 and Davis *et al.*, 2000). Effective transformation of *C. cellulolyticum* ATCC 35319 was also reported when plasmid DNA was *in vitro* methylated by purchasable methyltransferases (Tardif *et al.*, 2001).

In this study, the expression vector pBAD/Myc-His A-Met was developed, which encodes the predicted methyltransferase M.CboE1ORF1092P of *C. botulinum* (TMW 2.990). After transforming *E. coli* Top 10 and Ca434 with pBAD/Myc-His A-Met, the expression of a 68.25 kDa protein was proved (protein mass is equivalent to the mass of M.CboE1ORF1092P), (3.1.5). Consequently, transgenic *E. coli* host cells were additionally transformed with pMTL007C-E2-derived ClosTron plasmids (3.1.5, Figure 12) while methyltransferase expression was induced. Accordingly, putative premethylated ClosTron vectors were tested for their insertion into *C. botulinum* (TMW 2.990) by conjugation or electroporation as depicted in Figure 40 A and B.

Nevertheless, the expression of the methyltransferase M.CboE1ORF1092P in coexistence to ClosTron plasmids did not contribute to effective plasmid transfer of pMTL007C-E2 derivatives into *C. botulinum* (TMW 2.990) (neither by conjugation, nor by electroporation (3.1.5)).

The inefficiency of *C. botulinum* transformation could be related to several factors:

- Indeed, in recombinant *E. coli* hosts (Top 10 and Ca434) the expression of a 68.25 kDa protein was confirmed (equivalent mass to M.CboE1ORF1092P). Nevertheless, it was not proved that this protein actually catalyzed methyltransferase reactions. The

recombinant expression of inactive proteins perhaps can be explained by instability of mRNA, by differences in codon usage, by protein missfoldings and by cytoplasmatic degradation processes.

- Assuming that ClosTron plasmids would be correctly premethylated at 5' GCNGC 3' motives by M.CboE1ORF1092P activity, the corresponding vector would be protected for CboE1ORF1092P-mediated endonuclease cleavage. However, the activity of the putative type IV REase CboE1ORFAP of *C. botulinum* (TMW 2.990) would lead to DNA restriction, when corresponding recognition sites were methylated by *E. coli* hosts. This obstacle could potentially be overcome, when host strains of poor methylase activity are used (Baneyx, 1999).

To identify potential endonuclease activity in *C. botulinum* (TMW 2.990), crude extract restriction assays were performed (2.2.6.3). Consequently, pMTL007C-E2-derived plasmid DNA was incubated in the presence of 0 - 200 µg crude extracts of *C. botulinum*. Electrophoretic analyses of treated and untreated plasmids indicated that DNA degradation increased as a function of increasing crude extract concentration (3.1.6). Treatment with 200 µg crude extract led to strong plasmid DNA degradation near to the detection limit. Based on these results, the presence of unspecific nucleases in *C. botulinum* (TMW 2.990) is a likely explanation for the failure of transformation. Electrophoretic analysis also indicated that untreated plasmids were present in oc and ccc topologies, while the formation of linear plasmid DNA was stimulated when the crude extract concentration was increased. Consequently, the increase of linear plasmid DNA was caused by a reduction of oc and ccc forms. Based on mentioned observations, the existence of a REase is possible, which cleaves derivatives of pMTL007C-E2 at one specific cleaving site. Possibly, this REase is equivalent to the putative type IV REase CboE1ORFAP. In this *in vitro* restriction assay, the activity of the putative type II REase CboE1ORF1092P could not be established. Based on the fact that type II REases cleave near or inside their recognition sites, CboE1ORF1092P activity would lead to the generation of 24 DNA fragments of approximate sizes between 6 and 1641 bp. However, parameters according to *in vitro* restriction assays were not suitable for CboE1ORF1092P activity. Additionally, it might be possible that the genes CLO_1092 and CLO_1093 do not encode for an active type II RM system.

Donahue *et al.* (2000) developed an *in vitro* methylation assay, which enables to overcome *Helicobacter pilori* restriction barriers. This assay is based on the premethylation of plasmid DNA by reaction mixtures containing crude extract of the corresponding *Helicobacter pilori* strain, chelators of divalent cations, SAM and protease inhibitors.

According to Donahue *et al.* (2000), slightly modified *in vitro* methylation experiments were conducted (2.2.6.3). In Figure 40 C, *in vitro* methylation experiments, which were done in this work, are illustrated. Finally, *in vitro* methylation of pMTL007C-E2-derived plasmid DNA did not contribute to effective plasmid transfer into *C. botulinum* (TMW 2.990) (3.1.5). The electrophoretic analysis of plasmid DNA after treatment with the reaction mixture indicated, that oc and ccc plasmid topologies were still existent (3.1.6, Figure 14). The absence of linearized vector DNA leads to the conclusion that REase activity could be inhibited by chelation of divalent cations. The inefficient transformation of *C. botulinum* (TMW 2.990) could be accounted to several parameters:

- Potentially, *in vitro* parameters were inadequate for catalytic activity of putative methyltransferases. Consequently, pMTL007C-E2-derived plasmid DNA would not be protected for *C. botulinum* (TMW 2.990) REases.
- Assuming that nucleolytic cleavage would be attributed to type IV REase activity, *in vitro* methylation of pMTL007C-E2-derived plasmid DNA would be impossible. This potential barrier could be overcome, when vectors without corresponding type IV REase recognition sites would be used. Otherwise, the utilization of primordial host strains, which differ in the methylation pattern compared to *E. coli* Top10, would be promising.

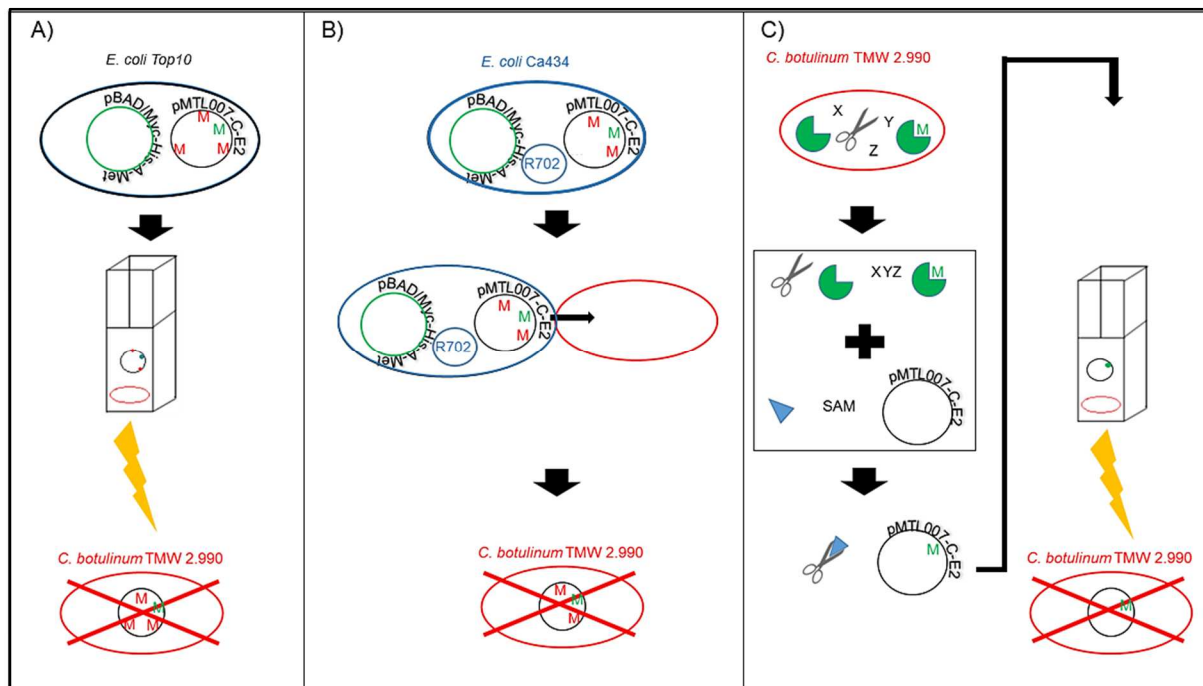


Figure 40: Transformation strategies of *C. botulinum* (TMW 2.990) by taking advantages of the methyltransferase CLO_1092 and by cell free extracts. In figure A and B, experiments according to 2.2.6.2 and 3.1.5 are depicted. In experiment A, the electrotransformation-mediated transformation of *C. botulinum* (TMW 2.990) after methylation of ClosTron plasmids in *E. coli* Top10, which additionally harbored the vector pBAD/Myc-His A-Met, was tested. In experiment B, the conjugation-mediated transformation of *C. botulinum* (TMW 2.990) after methylation of ClosTron plasmids in *E. coli* Ca434, which also contained the vector pBAD/Myc-His A-Met, was tested. Methyl groups are depicted by red and green marked “M”. The arrangement of plasmid associated red marked methyl groups symbolize the different methylation pattern of the *E. coli* strains Top10 and Ca434. The green labeled methyl groups indicate methylation pattern, which were associated with methyltransferase activity of CLO_1092 (encoded by pBAD/Myc-His A-Met). In figure C, experiments according to 2.2.6.3 and 3.1.6 are illustrated. In the mentioned experiment, electrotransformation-mediated transformation of *C. botulinum* employing ClosTron plasmid methylation in *C. botulinum* (TMW 2.990) derived crude extract reaction mixture was tested. Among methyltransferases (green tree-quarter circle) and restriction endonucleases (scissors), the crude extract contained other soluble cell components (X, Y, Z). Additional to the *C. botulinum* crude extract, the reaction mixture (content of the black square) implied chelating agents (blue triangle), SAM and pMTL007-C-E2-derived plasmid DNA. Crude extract-derived methylation pattern are marked by green labeled M.

4.1.7 Conclusion: Knock out generation of *C. botulinum* type E strains

In this study, neither the generation of knock out mutants nor the establishment of *C. botulinum* type E transformants was successful. Although several physiological and experimental parameters of conjugation and electrotransformation processes were modified, no successful transformation results were obtained. Considering that the experiments did not contribute to the generation of *C. botulinum* type E transformants, it was speculated that the existence of RM systems could be a major reason impeding successful transformation. Restriction assays revealed specific REase activity in *C. botulinum* (TMW 2.990) crude extract. The corresponding REase seems to restrict pMTL007C-E2 derivatives at one specific cleaving site. Possibly, the REase activity

can be assigned to the existence of a putative type IV REase (CboE1ORFAP) according to REBASE. In *in vitro* assays, no enzymatic activity was detected, which confirmed the existence of the predicted type II REase CboE1ORF1092P. Plasmid methylation in the *E. coli* strains Top10, GM2163, HB101 and Ca434 did not contribute to overcoming *C. botulinum* (TMW 2.990) restriction barriers. Premethylation of plasmids through recombinant protein expression of the putative MTase M.CboE1ORF1092P in *E. coli* Top10 and Ca434 also resulted in ineffective *C. botulinum* (TMW 2.990) transformation.

Although no *C. botulinum* type E transformants could be generated, the developed transformation strategies will probably be helpful in other bacterial transformation processes.

Recently, Mascher *et al.* (2013) published that they successfully generated knock out mutants of *C. botulinum* beluga (TMW 2.990) by ClosTron mutagenesis. Similar to the transformation attempts according to this study, they transformed derivatives of pMTL007C-E2 vectors by *E. coli* Ca434-mediated conjugation. Problems in overcoming restriction barriers were not reported. By comparing experimental setups, no differences between the used protocols can be detected. Nevertheless, the authors did not provide information about transformation efficiencies. The wild-type strain of *C. botulinum* beluga was initially isolated from a food-borne botulism outbreak in 1950 (Dolman and Chang, 1953). Consequently, it cannot be ruled out that genetically different cell lines evolved in the course of time.

4.2 Influence of the sporulation medium on *C. botulinum* type E spore proteomes

Several studies indicated that the type of sporulation medium can affect the sporulation behavior and the heat resistance of *Clostridium* endospores (Tsuji and Perkins, 1962; Roberts, 1965; Peck *et al.*, 1992; Dixit *et al.*, 2005). Lenz and Vogel (2014) investigated the sporulation medium-dependent heat, high pressure and HPT resistance of *C. botulinum* type E spores. Accordingly, the highest resistances was observed when spores were formed in SFE medium, whereas spore resistance was lower when other sporulation media were used (TPYC > AEY > M140). This study also indicated that the type and concentration of medium dissolved divalent cations play a major role in medium-dependent spore resistance. Lenz and Vogel (2014) discussed that the Ca²⁺

content of the sporulation medium can affect the level of spore-specific Ca-DPA and influence the gene expression profile of spore formers, which in turn can influence endospore resistance (Sugiyama, 1951; Stewart *et al.*, 1980; Kihm *et al.*, 1990; Oomes *et al.*, 2009). The heat and high pressure resistance of *C. botulinum* type E spores was not remarkably affected by Mg^{2+} -levels, whereas the absence of Mg^{2+} led to decreased spore resistance against HPT treatment. The presence of Mn^{2+} in the sporulation medium led to increased heat resistance of *C. botulinum* type E spores. The availability of Mn^{2+} might increase the activity of repair mechanisms, could lead to increased concentrations of heat protective Mn-DPA complexes, and influence the structure of cortex peptidoglycan (Kihm *et al.*, 1990; Atrih and Forster, 2001). Additionally, high pressure and HPT resistance of endospores were increased when Mn^{2+} was present in the sporulation medium. This fact could be explained by an increased activity of Mn^{2+} -dependent enzymes, which are involved in endospore maturation. Among the mineral content, other sporulation media compounds like amino acids, peptones, sugars, organic and fatty acids are known to influence the sporulation behavior and in turn, the spore structure and resistance properties (Sugiyama, 1951; Perkins and Tsuji, 1962; Roberts *et al.*, 1965; Decaudin and Tholozan, 1996; De Jong *et al.*, 2002). However, it is not known in detail, how sporulation in different media influences the resistance properties of spores.

Therefore, strain-specific and sporulation medium-dependent differences in *C. botulinum* type E endospore proteomes were analyzed in this study. Spores of the strains TMW 2.990, TMW 2.994 and TMW 2.997 were grown on TPYC, AEY, M140 and SFE and analyzed by MALDI-TOF MS and high resolution LC-MS/MS (2.2.7 - 2.2.7.3; 3.2 - 3.2.3). Both methods were used to identify proteins only present in SFE-derived endospores, which might be involved in increased HPT spore resistance.

4.2.1 MALDI-TOF MS analyses of medium-dependent spore proteomes

During sporulation, the gene expression profile is likely to be influenced by sporulation conditions. This can result in specific spore properties, which are at least partially reflected by changes in the protein composition of mature spores. Among others, MALDI-TOF MS presents a mass spectrometry based proteomic approach, which ensure the large-scale analysis of protein expression profiles, as a function of variable environmental conditions (Aebersold and Mann, 2003).

In this study, MALDI-TOF MS spore spectra were acquired as a function of strain specificity and sporulation medium composition. The clustering of obtained spectra indicated that the homologies of peak patterns were mainly influenced by the type of sporulation medium, whereas the strain character tended to play a secondary role (3.2.1). This mentioned results confirm the fact that sporulation velocity and spore resistances are more influenced by medium composition than by strain specificity (Lenz and Vogel, 2014). Especially the HPT-tolerant SFE-derived endospores showed higher similarities in MALDI-TOF MS spore spectra than spores, which were obtained from other media (TPYC, AEY, M140). Seemingly, SFE induced a typical strain-independent proteome pattern, which might be connected to increased spore resistance. However, due to the high diversity of medium compounds (nitrogen- and carbon-sources, vitamins, reducing agents, buffering and growth affecting substances, 2.2.1.1.2.1), it is difficult to spot single components which are responsible for distinct alterations in the protein composition of spores.

However, the analysis of spectra obtained for strain TMW 2.990 spores indicated that the occurrence of 40 peaks were unaffected by the type of sporulation media (3.2.2). Corresponding protein/peptide mass synchronization led to the identification of 17 proteins, which probably represent essential spore proteins. Putative functions of mentioned proteins were predicted by identifying conserved protein domains by using the protein BLAST tool provided by NCBI. Consequently, the functions according to the 17 proteins can be associated to different sporulation stages. The conserved domain protein C5UY96 represents a phosphatase of a regulatory two-component system. The stage II proteins C5UTB, C5UP91 and C5UU70 are involved in septum formation and in engulfment of the forespore. The function of the stage III protein C5US13 is unknown, while C5URS8 apparently represents a protein, which regulates gene expression. The stage IV proteins C5UXW8 and C5UU4 are likely involved in spore coat morphogenesis, whereas the stage V proteins C5UY42, C5UPN2 and C5UU73 play a role in cortex synthesis. The function of C5RA3 is unknown, but this protein contains a peptidoglycan-binding domain. The transcription factor w^k (C5UXY8RNA) was also existent in the majority of all *C. botulinum* (TMW 2.990) spores. The proteins C5UUt3 and C5UUT2 are presumably involved in spore maturation. The spore cortex lytic enzymes C5UT36 and C5UUG2 are responsible for spore germination. In summary, the proteins, which could be identified in the majority of TPYC-, SFE-, AEY- and M140-derived TMW 2.992 spores are apparently involved

in regulatory processes and in endospore morphogenesis. The analysis of MALDI-TOF MS spore spectra indicated that the number and congruency of TPYC- and M140-derived *C. botulinum* (TMW 2.990) spores showed higher similarities in comparison to spores, which grew on other media (AEY, SFE) (Figure 16). Nevertheless, the HPT tolerance of M140- and AEY-derived endospores tended to be quite similar. However, in comparison to TPYC-derived spores, the HPT resistance of M140- and AEY-derived spores were reduced (Lenz and Vogel, 2014). The mentioned results indicated that a high congruence in MALDI-TOF MS peak pattern does not necessarily correlate with HPT resistance. Presumably, the proteins, which were present in both TPYC- and M140-derived *C. botulinum* spores, are not decisive for their HPT resistance. The increased HPT resistance of TPYC-derived endospores compared to M140 spores could result from proteins, which were only expressed, when spores were formed in TPYC medium or by proteins present in both TPYC and SFE-derived spores (Figure 17). Two unique proteins were identified in TPYC-derived endospores (C5UXH7 and C5URQ3), whereas proteins, which were present only in TPYC- and SFE-derived spores, were not detected. The protein GerA (C5UXH7) represents a germinant receptor. In *Bacillus* spores, it is commonly known that relatively low high pressure levels (50 - 300 MPa) trigger germination via the activation of germinant receptors. According to *B. subtilis* spores, an increased level of germinant receptors (GerA) leads to increased rates of high pressure-induced germination (Setlow, 2007). Therefore, it is more likely to assume that the presence of additional germination receptors promote increased sensitivity against high pressure treatments. The application of higher pressure levels (300 – 800 MPa) promote the release of DPA, which in turn trigger later events in the process of spore germination (Setlow, 2007). Wild type and mutant spores of *B. subtilis*, which lack all functional nutrient receptors, showed equal germination characteristics when pressures of 500 - 600 MPa were applied (Wuytack *et al.*, 2000; Black *et al.*, 2007, A). According to findings by Lenz and Vogel (2014), TPYC-derived *C. botulinum* (TMW 2.990) spores are more resistant to high pressure (20 °C/ 800MPa) and HPT treatments (80 °C/800 MPa) than M140- and AEY-derived spores. Together with the findings reported here, this indicates that, like in *Bacillus* spores, high pressure/HPT inactivation of *C. botulinum* type E spores is likely to occur independently from the presence of nutrient germinant receptors. Generally, the involvement of germinant receptors in the response of *Clostridium* spores to high pressure treatments even at low pressure levels is questionable and might be

significantly different from those in *Bacillus* spores. The protein C5URQ3 represents one of three small acid-soluble proteins (SASP), which are encoded in the genome of *C. botulinum* (TMW 2.990) (according to NCBI). In clostridia, predominantly α/β -types of the spore-specific proteins are present, whereas spores of other species can also contain SASPs of the γ -type. SASPs of the α/β -type are known to be associated to spore DNA, which in turn permits protection against heat, UV radiation and a variety of DNA-damaging toxic compounds. SASPs also serve as amino acid sources during spore germination (Fairhead *et al.*, 1993; Setlow 1995; Raju *et al.*, 2006). Contradictory to observations of this study, Setlow (1985) and Johnson (1981) reported that in *B. subtilis* the expression levels of SASPs were not significantly influenced by the sporulation medium. In comparison to wild type spores, knock out mutants of *C. perfringens* spores showed reduced heat resistance, when just one of three SASPs encoding genes were interrupted (Raju *et al.*, 2006). In comparison to wild type spores, knock out mutants of *B. subtilis*, which had defects in α/β -type SASP encoding genes, showed reduced resistance against HPT treatment when pressures above 300 MPa and temperatures of 65 °C were applied (Lee *et al.*, 2007). In comparison to M140- and AEY-derived spores of *C. botulinum*, the increased HPT resistance of TPYC-derived spores might be mediated by an increased level of SASPs. To confirm the mentioned assumption further research is required.

According to Lenz and Vogel (2014), *C. botulinum* type E spores showed the highest resistance against HPT treatments, when spores were formed in SFE. Based on MALDI-TOF MS analyses, a total of 5 proteins was identified solely in SFE-derived spores (C5UZG3, C5UTT9, C5UZC5, C5UXY2, C5UUE9).

Possibly, the occurrence of mentioned proteins are involved in increased HPT resistance (3.2.2). C5UZG3 represents a spore coat protein of the CotS family. C5UTT9 represents a protein of unknown function but contains a conserved Cot F domain (identified by the protein BLAST tool of NCBI) and thus, might also serve as spore coat protein in *C. botulinum* (TMW 2.990).

The cortex of endospores is surrounded by a complex, mechanically flexible protein coat, which also contributes to spore resistance. The spore coat ensures the exclusion of large toxic molecules but enables the invasion of smaller nutrients, which are required for spore germination. The complex process of spore coat assembly is regulated by a high number of transcriptional and regulatory factors. Additionally, the

high diversity of coat proteins impedes a detailed understanding of the spore coat structure (Takamatsu *et al.*, 1999; Dirks, 2002; Kim *et al.*, 2006). Most research focused on the structures of *B. subtilis* coats. Although the information is not directly transferrable to *Clostridium*, it might help to classify potential functions of the coat proteins identified here.

Five hours after initiation of the sporulation process, CotS expression is observable in spores of *B. subtilis*. After coat assembly, the corresponding polypeptide is located in the inner coat and/or on the outside of mature *B. subtilis* spores. Knock out mutants, which contained disrupted *cotS* genes, did not show abnormal behavior in growth, sporulation, germination, and in resistance against organic solvents (Takamatsu *et al.*, 1999; Abe *et al.*, 1998). Potentially, the CotS family protein (C5UZG3), which was identified in SFE-derived *C. botulinum* (TMW 2.990) spores, has equal tasks as CotS proteins of *B. subtilis*. CotF proteins of *B. subtilis* are small structural polypeptides, which are also present in the inner spore coat (Cutting *et al.*, 1991; Imamura *et al.*, 2009). Perhaps, C5UTT9 also represents a structural protein in the coat of *C. botulinum* (TMW 2.990) spores. It is known that the expression profile of spore coat genes can be significantly influenced by the type of sporulation media (Zheng *et al.*, 1988). Information about the correlation between spore coat composition and HPT resistance are rare. According to Paidhungat *et al.* (2002), coat defective spores of *B. subtilis* showed equal inactivation behavior in response to high pressure treatments (550 MPa) compared to undamaged spores.

A third protein, which was only found in SFE-derived endospores, represents a spore photoproduct lyase (C5UUE9). During spore germination, this kind of enzymes are involved in repair mechanisms of UV-mediated DNA damages (Kneuttinger *et al.*, 2013). Because it is not suspected that HPT treatment induces such kind of DNA mutations, the interconnection between increased HPT resistance and the occurrence of photoproduct lyases is questionable.

Another protein, which could be identified only in SFE-derived spores represents the sporulation protein YunB (C5UZC5). According to Eichenberger *et al.* (2003), *yunB* genes are largely conserved in bacilli and clostridia. *YunB* mutant spores of *B. subtilis* showed reduced heat resistance and delayed activation of the late sporulation transcription factor σ^E . Because YunB seems to play a major role in sporulation efficiency (Eichenberger *et al.*, 2003), it is not obvious that this protein could not be

identified in TPYC-, M140- and AEY-derived spores of TMW 2.990. Presumably, the identification of YunB in SFE-derived spores was caused by elevated concentrations, in comparison to spores, which were obtained from other media. Generally, MALDI-TOF MS constitutes a highly sensitive mass spectrometry proteomic approach. However, it cannot be ruled out statistically, that specific proteins were ionized by lower frequencies than others. Consequently, signals of low reproducibility were excluded from final evaluation. Because no detailed information about the function of C5UZC5 is available, it cannot be excluded that the presence or rather the increased amount of YunB permits increased HPT resistance of endospores.

Additionally, the protein C5UXY2, which represents the RNA polymerase factor σ^G was also solely identified in SFE-derived spores of *C. botulinum* (TMW 2.990). Generally, sporulation constitutes a complex process, which is highly regulated by a number of transcription factors. Both in bacilli and clostridia the key regulators include the essential master regulator Spo0A and the alternative sigma factors σ^F , σ^E , σ^G , σ^H and σ^K . (Losick and Pero, 1981; Sauer *et al.*, 1995; Paget and Helmann, 2003; Kirk *et al.*, 2014). Currently, most research focus on the sporulation cascade in *B. subtilis*, while corresponding mechanism in clostridia are widely unknown. Although the general sporulation cascade and many regulatory proteins involved are conserved among *Bacillus* and *Clostridium* species, the time required for proceeding through this cascade and sigma factor regulons are considerably different. The importance of the sporulation sigma factors in *C. botulinum* has been demonstrated by Kirk *et al.* (2014), since knock out mutants of *C. botulinum*, which lack in σ^G , σ^F , σ^E or σ^K were unable to form viable heat resistant spores. Thus, it can be concluded that σ^G is also involved in the effect of sporulation medium composition, when spores of *C. botulinum* were formed on TPYC, M140 and AEY. Probably the amounts of σ^G in TPYC-, M140- and AEY-derived spores were below the detection limit. However, it is not completely clear whether an increased σ^G level contributes to increased HPT resistance of endospores.

Finally, to confirm or exclude if the proteins C5UZG3, C5UTT9, C5UZC5, C5UXY2 or C5UUE9 permit increased HPT resistance of *C. botulinum* (TMW 2.990) spores, additional research will be required.

4.2.2 Identification of predominant proteins in SFE-derived endospores by high resolution LC-MS/MS

To identify further potential proteins, which mediate increased HPT tolerance of SFE-derived spores, SDS-PAGE patterns of TPYC-, M140-, AEY- and SFE-derived *C. botulinum* type E spores (TMW 2.990, TMW 2.994 and TMW 2.997) were compared to each other (3.2.3). Consequently, in SFE-derived spores of all tested strains, a protein of approximately 225 kDa was identified, while the mentioned protein was absent in other spore samples. For specific protein identification, the protein band according to TMW 2.990 was analyzed by high resolution LC-MS/MS. From a total of 14 identified peptide fragments, a number of 6 showed sequence similarities to a putative surface/cell-adhesion protein/N-acetylmuramoyl-L-alanine amidase (WP_004461520.1) of *C. sporogenes* (Figure 18). Surprisingly, no convincing sequence similarities to proteins of *C. botulinum* beluga (TMW 2.990) could be established. Evidently, the proteins of interest were not derived from protein residues of SFE medium (data not shown). The disagreement in sequence similarity to *C. botulinum* could be explainable, because the published genome is an unfinished draft sequence. According to the database of NCBI, the genome of *C. botulinum* beluga (TMW 2.990) is provided on 6 contigs. To date, gapless genome data of this *C. botulinum* strain is not available. Optionally the corresponding gene, which encodes the identified protein is currently not annotated. Sequence similarities between the six identified peptide fragments and the amidase of *C. sporogenes* lead to the suggestion that the protein of interest have similar tasks compared to the amidase. The fact that these two proteins differ in masses (161.92 and ca. 225 kDa) and disagree in eight peptide fragments, do not reinforce the mentioned theory, but this is also explainable. The high mass difference between these two proteins could be explain by abnormal migration in SDS-PAGE. The disagreement in peptide fragments could either be explained by common divergences in sequence similarities or by protein contaminations or rather were derived from proteins, which showed equal migration in SDS-PAGE.

N-acetylmuramoyl-L-alanine amidases are involved in the process of cortex peptidoglycan formation. In comparison to conventional peptidoglycan of vegetative cells and primordial cell walls of endospores, the structure of cortex peptidoglycan differs slightly. In cortex peptidoglycan, the majority of muramic acid side chains are removed and approximately 50% of muramic acids are convert to muramic lactam.

Consequently, the cortex peptidoglycan is less cross-linked and more flexible than conventional one. The conversion of muramic acids into muramic δ -lactam requires the cleavage of mucopeptide side chains, which is catalyzed by N-acetylmuramoyl-L-alanine amidases, followed by acetylation and transpeptidation. Accordingly, N-acetylmuramoyl-L-alanine amidases represent fundamental enzymes, which are involved in cortex maturation (Popham *et al.*, 1996 a; Kukushima *et al.*, 2002). The cortex is known to maintain dormancy, core dehydration and heat resistance. *B. subtilis* spores, which contain cortex peptidoglycan of elevated cross-linking levels, showed defects in core hydration and in turn in heat resistance (Popham *et al.*, 1995 and 1996 b; Atrih *et al.*, 1996). According to Alderton, Snell (1963) and Warth (1978), the reduction of crosslinks during cortex peptidoglycan synthesis promote the dehydration of the spore core by a mechanical action (Alderton and Snell, 1963; Warth, 1978). Nevertheless, mutant spores of *B. subtilis*, which fail in the assembly of muramic lactam structures are unable to germinate, but show similar heat resistance than wild type spores. Popham *et al.* (1996) suggested that the level of muramic lactam do not influence the magnitude of core dehydration and heat resistance. Popham concluded that muramic lactams serve as specific determinants for cortex lytic enzymes (CLEs). Generally, the cortex structure of spore formers is largely conserved. Atrih and Foster (2001) indicated that the sporulation media composition has dramatic effects on the cortex structure. For example, the cortex of Nutrient Broth (NB)-derived *B. subtilis* spores contained a reduced level of δ -lactam and L-alanine side chains, while the amount of tetrapeptide side chains was increased (in comparison to CCY-derived *B. subtilis* spores). Additionally, NB-derived spores showed reduced heat resistance, contained low levels of Mn^{2+} , had low protoplast wet density and sporulated underwent spontaneous. When $MnCl_2$ was added to NB medium, corresponding spores showed equal heat resistance, germination-behavior and peptidoglycan structures than CCY-derived spores. On the one hand, Atrih and Foster (2001) suggested that the reduced availability of Mn^{2+} is responsible for the low protoplast wet density and in turn for reduced heat resistance. On the other hand, they assumed that Mn^{2+} influence the expression level of genes and/or enzymatic activities, which are involved in cortex synthesis and maturation. Atrih and Foster (2001) mentioned that the presence of muramic δ -lactam admittedly are required for CLE activation but speculated that conformations of CLEs are probably stabilized by specific cortex *architecture*.

The results of this study leads to the suggestion that SFE-derived *C. botulinum* type E spores contain a higher level of N-acetylmuramoyl-L-alanine amidases than spores which were formed on other media. Consequently, the cortex of SFE-derived spores is probably less cross-linked and more flexible than in other spores, which may led to increased HPT resistance. To date, no information is available, which gives lectures about correlations between the crosslinking levels of the cortex and HPT resistance. Potentially, the declining level of crosslinkings during δ -lactam formation induce increased core dehydration and in turn increased dormancy and HPT resistance in clostridia. According to assumptions of Atrih and Foster (2001), the specific cortex structure of SFE-derived spores conceivably permits increased stability on CLEs and finally increased finally HPT resistance. Finally, further research will be necessary to evidence that the cortex structure, especially the δ -lactam level, influences the HPT resistance of endospores.

4.2.3 Conclusion: Influence of the sporulation medium on *C. botulinum* type E spore proteomes

MALDI-TOF MS analyses of spores of three different *C. botulinum* type E strains indicated that the spore proteome can be influenced by the kind of sporulation media. Spores, which were obtained in SFE, showed higher similarities in their protein pattern than spores, which were formed in TPYC, AEY and M140 media. This high similarity among SFE-derived spores of different *C. botulinum* type E strains exceeded that the similarity of one strain grown on different media, which indicates that the protein composition of spores is more dependent on sporulation conditions than on inherent strain-specific differences. This typical medium-specific, largely strain-independent protein composition might be involved in conferring increased HPT resistance. Based on MALDI-TOF MS analyses, a total of 5 proteins were identified only in SFE-derived spores. These proteins might serve as structural spore coat proteins, are involved in repairing of UV-mediated DNA damages, serves as transcription regulator, and are involved in regulating spore development and sporulation efficiency. To evidence that these proteins are actually involved in increased HPT resistance of *C. botulinum* type E endospores, further research will be required. The identification of the essential forespore-specific, late sporulation transcription factor σ^G only in SFE-derived spores indicates, that even the highly sensitive MALDI-TOF MS approach has certain limitations for the detection of proteins in low amounts.

Spore protein analysis by SDS-PAGE and high resolution LC-MS/MS indicated that SFE-derived endospores probably contain an elevated level of N-acetylmuramoyl-L-alanine amidases. Accordingly, it is assumed that the cortex peptidoglycan of SFE-derived spores contains an elevated level of muramic δ -lactam and consequently a decreased degree of crosslinking. Potentially, the mentioned effect leads to increased core dehydration, which in turn permits increased spore dormancy and increased HPT resistance. Further research is necessary to evidence these theories

Finally it has to be mentioned that HPT resistance of endospores are unlikely to be mediated by the presence of single factors. It is rather assumed that the increased HPT resistance of SFE-derived *C. botulinum* type E spores were mediated by the sum of several proteomic factors.

4.3 HPT-induced inactivation of *C. botulinum* type E spores in model emulsion matrices

Food products are highly diverse in their composition and various food components are known to influence spore resistance to physical treatments. To ensure adequate food safety for innovative HPT-treated food products, a detailed understanding of protective effects exerted by the food matrix is important. Previously, most studies of high pressure-induced inactivation of microorganism and bacterial endospores focused on model suspensions or complex food products such as juices, vegetables and meat. However, data on the effect of the important food constituent fat, in the absence of other food components, is scarce. In this study, model soybean oil emulsions (O/W) of different fat contents were produced and characterized. Basic information on stability and droplet size distribution (prior, during and after heat-, high pressure- and HPT-treatment) was gathered. Spore localization in heterogenic oil/buffer systems and emulsions was determined by phase-dependent CFU determination and microscopic observation. Additionally, the heat-, pressure- and HPT-induced inactivation behavior of *C. botulinum* type E spores in emulsion matrices was investigated.

4.3.1 Characterization of model emulsions

4.3.1.1 Emulsion stability and droplet size distribution

Emulsions are metastable dispersions of two or more unmixable liquids or liquid crystals, which are stabilized by surfactants (Bengoechea *et al.*, 2010). In this study,

(O/W) soybean oil emulsions with fat contents of 10 to 70% were prepared, which served as model matrices for further temperature-/pressure-dependent inactivation studies. To ensure that model emulsions are stable during high pressure processing, stability tests were carried out. Emulsion stability can be defined as the resistance against changes in physicochemical properties depending on time. Creaming, sedimentation, flocculation, coalescence and phase inversion are processes, which influence droplet sizes parameters and finally emulsion stability (McClements, 2004; Bengoechea *et al.*, 2010). Among a variety of factors, especially the type of emulsion components, mixture ratio, pH, energy input, viscosity and temperature can influence emulsion stability (Sjöblom, 2006). Currently, information concerning the influence of pressure on emulsion stability is limited. Previous studies indicated that the average droplet size of O/W emulsions was slightly increased, when high pressure was applied. Nevertheless, the influence on emulsion stability was less affected by high pressure treatment than by mild heat application (Dickinson and James, 1998; Antona *et al.*, 2001 and Zhu *et al.*, 2014). Olive oil/water emulsions (30% v/v) were found to remain stable after treatment at 900 MPa for 30 min (Simpson and Gilmore, 1997). Soybean oil/water emulsions (20% v/v) persist treatments at 600 MPa/40 °C, when the pH was higher than 4 (Karbstein *et al.*, 1992).

In this study, the stability of soybean oil emulsions was analyzed by multisample analytical centrifugation and by analyzing droplet size distributions (2.2.8.2; 2.2.8.3.1). Creaming kinetics indicated that the stability of soybean oil emulsions primarily depended on the fat content. Emulsion containing 30% soybean oil, exhibited the highest stability (decay rate: 0.1%/6.73 h). The continuous increase of the emulsion fat content up to 60% led to a low decrease in emulsion stability. No proportional correlation between fat content and emulsion stability was determined, e.g. stability decreased consecutively, when emulsions were prepared with 20, 70 and 10% soybean oil. According to the most instable emulsion containing 10% fat, a decay rate of 0.1%/3.15 h was calculated.

Thus, emulsion stability depends on the corresponding fat content. Because the continuous phase of the emulsions was enriched with 2% soybean lecithin (w/v), the total concentration of emulsifier decreased with increasing fat content. Evidently, a nearly optimal ratio of fat to emulsifier was given in emulsions containing 30% soybean oil. The decrease of emulsion stability, as a function of increasing fat content (up to

70%), was potentially caused by a deficit in emulsifier availability. An underdose of emulsifier could have resulted in insufficient coating of fat droplets, which in turn leads to decreased emulsion stability (Shinoda and Arai, 1964; Pan *et al.*, 2004). Nevertheless, an excess of soybean lecithin can also induce decreasing emulsion stability. Overdoses of emulsifier can promote the generation of oil-free lecithin vesicles, which in turn reduce the emulsifying capacity (Krafft *et al.*, 1991). This mentioned effect could be responsible for the comparatively low stability of soybean oil emulsions with fat contents of 10 and 20%.

To investigate the influence of heat (75 °C), high pressure (750 MPa) and HPT (75 °C/750 MPa) application on emulsion stability, treated samples containing 10, 30, 50 and 70% fat were analyzed by multisample analytical centrifugation. (2.2.8.3.1). The corresponding results indicated (3.3.1) that neither heat and pressure treatment, nor application of HPT, significantly influenced the emulsion stability. When emulsions of equal fat content were treated at mentioned parameters, the values of stability varied in a maximum range of $\Delta m = 2 \times 10^{-4}$.

Additionally, droplet size distribution of treated model emulsions (10, 30, 50, 70% fat) was investigated by laser particle analyzer. Corresponding results indicated that a bimodal behavior in droplet size distribution exists in all tested samples (with exception of 70% soybean oil emulsion, after 10 min treatment at 750 MPa) (Figure 21). Since the energy input during emulsification influences the droplet size distribution of emulsions (Salager *et. al*, 2002), the bimodal distribution is likely to be a result of the two different modes of energy input used (by Ultra-Turrax and by ultrasonic homogenizer).

Emulsions containing smaller droplets are generally more stable, than those containing bigger ones. Based on bimodal droplet size distributions, no clear correlation between statistical parameters of droplet diameters (Table 24) and emulsion stability, was evidenced. In comparison to untreated soybean oil emulsions of 10, 30 and 50% fat, heat-treated samples contained an increased amount of large particles and a reduced quantity of small droplets. This mentioned effect is commonly known. As a function of increasing temperature, the emulsion viscosity decreases. Additionally, an increase of Brownian motion leads to an increase of droplet collision frequency. Both effects support the process of coalescence (Sjöblom, 2006).

In contrast to untreated and heat-treated emulsions of 10 and 30% fat, pressure-treated samples contained an increased amount of small particles and a decreased number of big droplets. This phenomenon differs from observations according to Dickinson and James (1998). They demonstrated that pressure treatment of monomodal O/W emulsions led to a small increase in the average droplet size. In emulsions with fat contents of 50 and 70%, the droplet size distribution was equal to untreated samples of the same fat level.

The effect of pressure-induced changes in droplet size distributions in emulsions of 10 and 30% fat might be explained by following theories. Suppositionally, an overdose or slight overdose of emulsifier induces the formation of emulsifier micelles, the emulsifying capacity would be reduced. Potentially, micelle structures were destroyed by high pressure application. Consequently, the emulsifying capacity would be increased again. The energy changes, during the process of decompression, can lead to shearing effects. Thus, newly generated fat droplets could be covered by free phospholipids and the formation of small droplets would be promoted.

Equal effects were observed when α -lactalbumin containing emulsions were treated at 600 MPa. Pressure treatment induces an increased emulsifying capacity of α -lactalbumin. The authors supposed that this effect was caused by pressure-induced generation of molten α -lactalbumin globules (Rodiles-López *et al.*, 2007). However, pressure-induced changes in protein and lecithin conformation cannot be compared. Information concerning high pressure effects on non-protein surfactants is rare. Studies according to ionic and non-ionic surfactants indicated that pressurization exert an influence on the critical micelle concentration (CMC). Pressure application in the range of 100 – 400 MPa induced the dissociation of micelles, while continuous increasing of led to aggregation of monomers to micelles again (Kaneshina *et al.*, 1974; Offen and Turley, 1982; Lesemann *et al.*, 1998 and Winter 2001).

In comparison to untreated and heat-treated emulsion samples of 10% fat, the application of HPT (75 °C, 750 MPa, 10 min) led to an increased amount of small droplets and a decreased amount of big particles. Nevertheless, in relation to pressure-treated emulsions, reduced amounts of small droplets and increased numbers of big particles were found. Apparently, the effect of HPT application on droplet size distribution was caused by the sum of temperature and pressure effects (Figure 21).

In comparison to untreated, heat- and pressure-treated emulsions containing 30 and 50% fat, HPT-treated emulsions contained increased amounts of small and decreased amounts of big particles. The droplet size distribution of HPT-treated soybean oil emulsions containing 70% fat was similar to untreated, heat- and high pressure-treated samples, of equal fat content.

In summary, emulsions and their behavior at elevated pressure and/or temperature levels are very complex influenced by numerous factors. Thus, it can only be speculated on changes on the molecular level involved in the slight alterations after the physical treatments applied here. In this study, the temperature-, high pressure- and HPT-induced changes in emulsion stability and droplet size distribution were shown to be relatively low. These results indicate that the emulsions prepared in this study are stable at least during the time frame required to conduct pressure- and temperature- induced endospore inactivation experiments.

4.3.1.2 Microscopic droplet size characterization of soybean oil emulsions during pressurization

Various previous studies that focused on pressure-induced changes in emulsion droplet sizes solely relied on droplet size determination after processing. In this study, high pressure microscopy was conducted to monitor changes in emulsion droplets during pressurization. Soybean oil emulsions containing 10% fat were used to study the behavior of fat droplets during pressure generation up to 250 MPa and also during pressure reduction (2.2.8.3.2). The corresponding results indicated that sizes of soybean oil droplets (initial diameters of 5 - 85 μm) were largely unaffected by pressure application, in the range of 0.1 to 250 MPa (3.3.1.2.2). Generally, droplet sizes of 10% soybean oil emulsions were influenced by pressure generation and pressure reduction in a range of maximal 0.64 – 3.98 μm . In consideration of standard deviations, the actual effects seem to be much lower. Correlations between defined changes in pressure levels and defined changes in droplet sizes could not be determined. Additionally, no correlations between initial diameters and pressure- induced volume changes were observable.

4.3.1.3 Influence of unbounded emulsifier on heat-, pressure- and HPT-induced inactivation of *C. botulinum* type E endospores

Endospore inactivation was performed in emulsions with different fat contents. For emulsion preparation, the continuous phase was enriched with 2% soybean lecithin (w/v), consequently the total concentration of emulsifier decreased with increasing fat content. Experiments according to 2.2.8.4 were conducted to exclude the effect of different lecithin concentrations on the inactivation behavior of *C. botulinum* type E endospores. Corresponding results indicated that after an application of constant pressure and temperature parameters (75 °C/0.1 MPa; RT/750 MPa; 75 °C/750 MPa), the number of inactivated endospores was not significantly affected by soybean lecithin concentrations (0, 1, 2 and 5% (w/v)), (3.3.1.3). Obviously, variable lecithin concentrations do not affect the high pressure- and temperature-induced behavior of endospore inactivation. Consequently, for matrix-dependent inactivation experiments, the variable lecithin concentrations in emulsions of different fat contents have not been considered explicitly.

4.3.2 Determination of endospore distribution in oily systems

To gain a better understanding for heat and pressure-mediated endospore inactivation in emulsion matrices, endospore distribution in oily systems was analyzed. Information about the distribution of microorganisms in emulsions or in liquid immiscible systems is rare. According to Zuccaro *et al.* (1951), yeast cells in oil/water systems were both presented in the oily phase and also in the water phase. Nevertheless, the majority of cells were associated to the boundary surface. Also in hexadecane/water mixtures, cells of *Listeria monocytogenes* and *Yersinia enterocolitica* were predominantly present at the surface of hexadecane droplets. Based on the definition that an organism is hydrophilic when more than 50% of the cells or spores can be found in the aqueous phase, Miller categorized *E. coli*, *Listeria innocua*, *Paeonia anomala*, *Saccharomyces cerevisiae* and endospores of *Alicyclobacillus acidoterrestris* to be hydrophilic. Conidia of *Aspergillus niger*, *Penicillium glabrum* and endospores of *Bacillus subtilis* were described as being hydrophobic.

To determine the endospore distribution in oily systems, inoculated oil/IPB mixtures of variable mixing ratios were analyzed by phase-dependent plate count determinations and by microscopic observations (2.2.8.5.1 and 2.2.8.5.2). Endospore distributions in soybean oil emulsions were determined by fluorescent microscopy. The phase-

dependent CFU determination indicated that the endospore distribution in heterogenic soybean oil/IPB mixtures was neither affected by the fat content of the mixture (30, 50 and 70% oil) nor by the amount of inoculated endospores (2×10^6 spores/ml; 1×10^6 spores/ml and 5×10^5 spores/ml). Without considering the fat content and the spore concentration of corresponding mixtures, an average of 98.18% endospores were found in the buffer phase, while 1.72% of endospores were associated to the interfaces. A low amount of 0.1% spores were detected in the oily phase (3.3.2).

According to the definition of Miller (2006), endospores of *C. botulinum* type E are predominantly hydrophilic.

In experiments obtained in this study, interfaces consisted of an oil/buffer phase mixture. To ensure that endospores, which were located at the interface, did not primarily resulted from endospores which were in fact dissolved in the buffer phase, more detailed plate count experiments were conducted. Consequently, spore concentrations in the interface and in the upper buffer phase were compared to each other (2.2.8.5.1). The corresponding results indicated that independent on the fat content of the mixture (30, 50 and 70%), the endospore concentration in the interface was much higher, than in the upper buffer phase (3.3.2). In heterogenic soybean oil/buffer mixtures with fat contents of 30%, the concentration of endospores in the interface was about 49 times higher, than in the upper buffer phase. In mixtures of 50 and 70% soybean oil, the ratio of endospores in the upper buffer phase to spores in the interface was about 1:25 and 1:17 (3.3.2), respectively. These results lead to the suggestion that a small number of endospores was actually associated to the boundary surface. If the interface-derived endospores would actually be attributed to the buffer phase volume-fraction, the endospore concentration in the upper buffer phase should be nearly two times higher, than in the interface. In Figure 41 A and B, two model conceptions of endospore distributions in heterogenic oil/buffer mixtures are depicted. The mentioned result leads to the suggestion that model conception B seems to be more realistic than conception A.

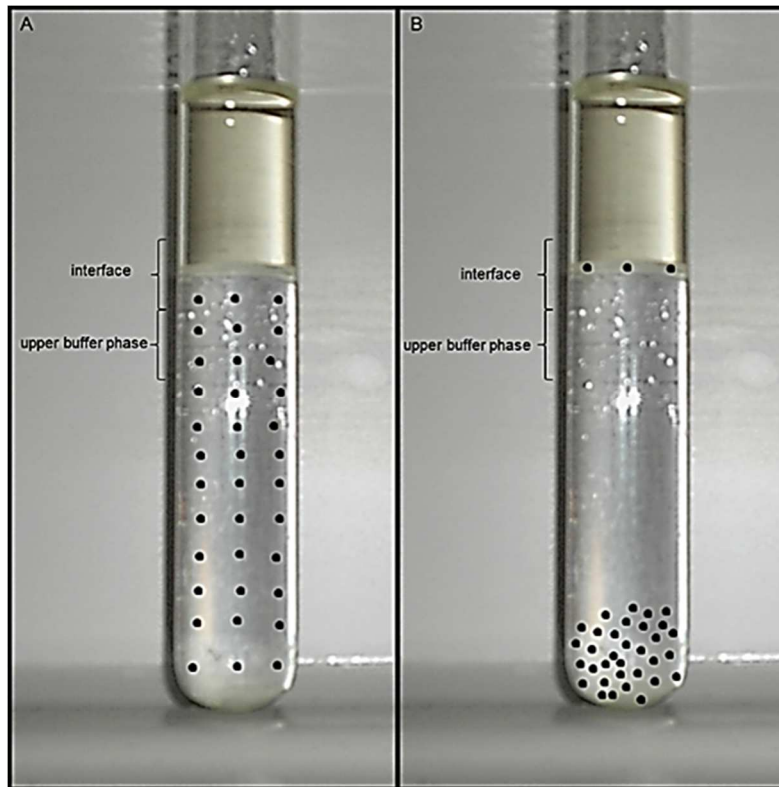


Figure 41: Model conceptions of endospore distributions in heterogenic oil/buffer mixtures. Black points represent endospores. Curly brackets display the interface and the upper buffer phase.

Microscopic analyzes of inoculated soybean oil/buffer mixtures led to equal results as the plate count experiments. In mixtures of 50% soybean oil, about 97.09% of the endospores were dissolved in the buffer phase, while about 2.91% endospores tended to be associated to the surface of soybean oil droplets. Events that endospores were completely embedded in oil droplets, were not observed in any case (3.3.2.1).

Generally, endospores show increased hydrophobicity, in comparison to their corresponding vegetative cells. This might be related to the relative abundance of proteins in the outer coat and in the exosporium (Matz *et al.*, 1970; Takumi *et al.*, 1979; Doyle *et al.*, 1984 and Wiencek *et al.*, 1990). Obviously, buffer phase dissolved and boundary surface associated endospores differed in their surface character, i.e. in comparison to buffer-dissolved endospores, the surface of interface associated endospores tends to be more hydrophobic. This observation is likely to reflect the common heterogeneity in bacterial spore populations. Generally, environmental conditions like sporulation medium, pH, aeration, etc. can lead to significant variations in endospore properties. Because members of populations do not sporulate synchronously, time-dependent changes in environmental conditions are likely to be responsible for the heterogeneity of endospore population. The heterogeneity of spore

populations can also be explained by stochastically variations in spore protein levels (Gerhardt and Marquis, 1989; Elowitz *et al.*, Melly *et al.*, 2002; Margosch *et al.*, 2004; Hornstra *et al.*, 2009; Stecchini *et al.*, 2009; Abel-Santos, 2012). Accordingly, spore populations can contain variable spore coat and exosporium protein compositions. Consequently, surface hydrophobicity of spore populations can be variable and could finally be responsible for heterogenic endospore localization in biphasic oil/buffer mixtures.

The microscopic observations of spore inoculated soybean oil emulsions also indicated that the majority of endospores was dissolved in the continuous phase (3.3.2.2). As a function of increasing fat content (30 > 50 > 70%), the percental amount of buffer phase dissolved endospores increased (68.6 > 73 > 79%). In comparison to spore distribution in heterogenic oil/buffer mixtures the amount of oil-surface associated endospores in emulsions was increased by approximately ten fold. The mentioned result leads to the suggestion that the availability of emulsifier influences the number of boundary surface-associated endospores.

Contradictory in sunflower oil/water systems, the availability of emulsifier (SDS) did not influence the distribution of embedded microorganisms (Miller, 2006). On the other hand, Hansen and Rieman (1963) proposed that microbial transition into oily environments would be supported, in the presence of surfactants.

According to this study, the concentration of emulsifier also tended to influence the quantity of surface associated endospores. As already mentioned above, the total concentration of emulsifier decreased, with increasing emulsion fat content. Optionally, the thickness of emulsifier coats, which surrounded the soybean oil droplets, affected the quantity of surface associated endospores.

It have been generally reported that, endospores tend to show hydrophobic surface character. This, however, can vary between species and strains, and can be influenced by sporulation conditions (Koshikawa *et al.*, 1989; Anderson and Rönner, 1998; Wiencek *et al.*, 1990; Husmark and Rönner 1992 and Husmark 1993). In this study, analysis of spore distribution in soybean oil/buffer systems showed that hydrophobicity of *C. botulinum* type E endospores (TMW 2.992) is relatively low. In comparison to experiments also performed in oil/water systems, endospores of *A. acidoterrestris* showed equal distribution behavior (Miller, 2006) as compared to the *C. botulinum* type

E spore used here. Koshikawa *et al.* (1989) referred that *Bacillus* endospores equipped with an exosporium are more hydrophobic than those which lack one. Electron microscopic analyses indicated that endospores of *C. botulinum* type E contain a thick exosporium and have an unusual spore coat morphology, containing extraordinary appendages (Hodgkiss and Ordal, 1996). In Figure 42 electro micrographs of *C. botulinum* beluga (TMW 2.990) endospores are depicted (Hodgkiss and Ordal, 1996). Consequently, the relatively low affinity of *C. botulinum* type E spores to fatty surfaces potentially resulted from loss of exosporia during spore purification processes. Additionally, the unusual morphology of *C. botulinum* type E spore coats might be involved in the low affinity to fat droplets.

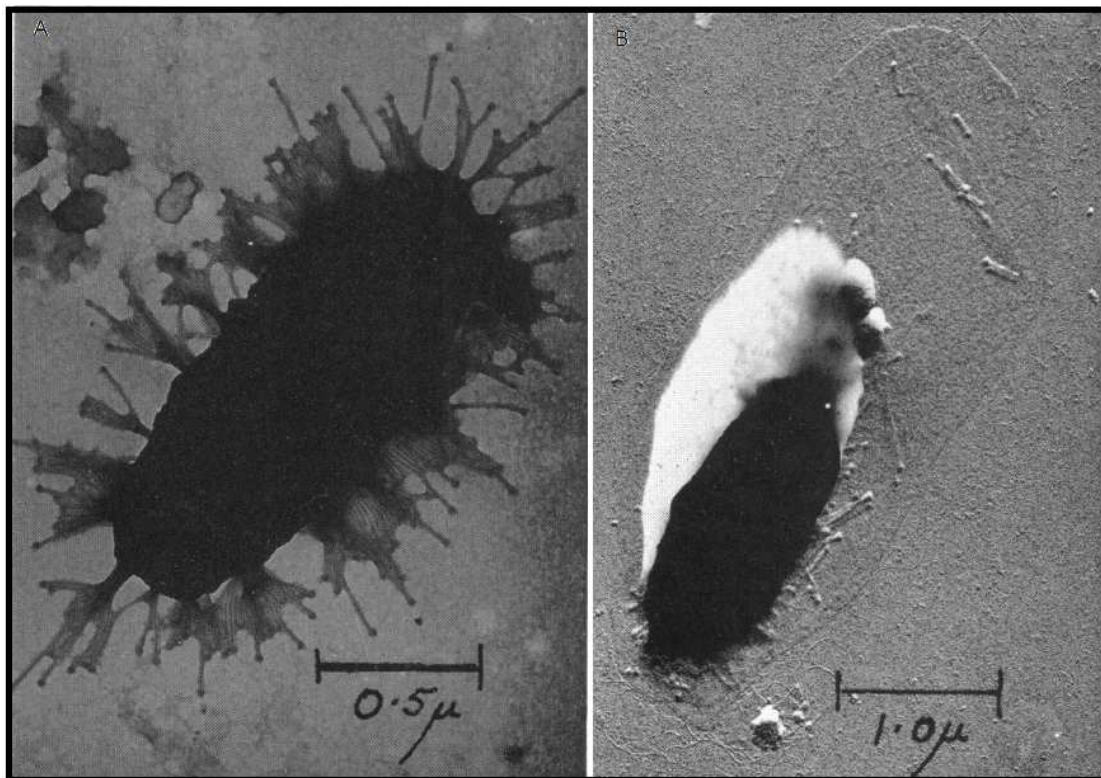


Figure 42: Electro micrographs of *C. botulinum* beluga endospores (Hodgkiss and Ordal, 1996). In picture A, a trypsin-treated and ammonium molybdate prepared endospore is displayed. The unusual appendages of the spore coat is apparent. In picture B, an endospore with intact exosporium (slightly transparent structure) is visualized. The bright white structure resulted from gold-palladium preparation.

4.3.3 Inactivation of *C. botulinum* type E endospores in emulsion matrices by heat treatment

Microorganisms are generally more resistant to heat inactivation, when they are dissolved in oil, than in water or buffer systems (Molin and Snygg, 1967; Senhaji and Loncin, 1977; Ababouche *et al.*, 1995 and Senhaji, 1997). Especially endospores, which are suspended in lipid phases are partially able to survive temperatures, which

are applied in conventionally food sterilization processes (Jensen, 1954; Gervasini, 1963; Hersom and Hulland, 1963). Until now, the protective effect of fat is not completely understood and several authors suggest different mechanisms. According to Lang (1935), the thermal protective effect of fat is based on the low heat conductivity of lipids. Whereas, Slesarewski (1931) supposed that the reduced water availability in oily environments is responsible for reduced thermal inactivation of microorganisms. Molin and Snygg (1967) observed that the extent of heat-induced inactivation of *B. cereus* endospores in soybean oil and triolein were increased, when low amounts of water were added. Albeit, they also recognized that the protective effect of fat varied, when different lipids of equal water content were used as matrices. Consequently Molin and Snygg concluded, that primarily the kind of lipids exert specific effects on heat resistance. They supposed, that the presence of free fatty acids leads to endospore stabilizing effects. Zuccaro *et al.* (1951) did not recognized variations in thermal inactivation behavior of bacteria and yeasts, when the treatments were performed in different type of oils. Contradictory, Miller (2006) observed that thermal inactivation behavior of microorganisms differed in the presence of different oils. Nevertheless, no clear correlations between oil specificity and extent of heat-induced inactivation were indicated. Miller concluded that the extent of heat protective effects were influenced by the synergy of microbial strains and type of oil matrices. In comparison to thermal inactivation studies in pure oil, studies on microbial inactivation behavior in emulsion matrices are rare. Senhaji and Loncin (1977) investigated the heat resistance of *Bacillus subtilis* spores in several liquid systems (pure phosphate buffer, pure soybean oil, a two phase system containing separated layers of oil and buffer, and two emulsions with widely different fat contents). Corresponding results indicated that the temperature-dependent decimal reduction time was extensively higher, when spores were heated in pure oil, than in other systems. When inactivation was performed in pure buffer or in emulsion systems, corresponding heat survival curves of *B. subtilis* spores showed quite similar progression, when temperatures of 85, 95 and 105 °C were applied. When experiments were conducted in the system, containing separated layers, the extent of endospore reduction at 85 °C resembled the inactivation behavior in buffer and emulsions. Whereas at higher temperatures, the survival curves were more equal to them, which were obtained in pure oil. Finally, Senhaji and Loncin also supposed that the protective effect of fat were caused by the low availability of water. They also alluded that solubility of water in oil increases with increasing temperature.

Further studies of Senhaji (1977) lead to the suggestion that the protective effect of oil/water systems only applies, when define circumstances are given. According to that, the majority of microorganisms were situated in the oil phase. Additionally, the system have to present a specific volume to surface ratio. Only if the temperature-dependent diffusion of water into oil presents a limiting factor, a sufficient water saturation of the oil phase is ensured. Finally, Senhaji supposed that emulsions containing small fat droplets, do not permit heat protective effects on embedded microorganisms.

In this study, the thermal-induced inactivation behavior of *C. botulinum* type E spores was analyzed in pure buffer and in soybean oil emulsions of different fat contents (30, 50, 70% fat). Inoculated samples were exposed for 10 minutes to 45, 60 or 75 °C (2.2.8.6; 3.3.3.1). Consequently, the corresponding log reductions were calculated by plate count determinations. Generally, the corresponding results indicated that the extent of endospore inactivation clearly depended on temperature and matrix parameters. Expectably, in pure buffer, the number of inactivated endospores increased, as a function of increasing temperature. At constant temperature parameters, the log reduction cycles, which were obtained in emulsion samples, were quite lower than in those, which were obtained in pure buffer (with exception of values according to inactivation at 75 °C; in 30% soybean oil emulsion). The mentioned results lead to the suggestion that endospores were heat protected by dispersed oil droplets. Furthermore, the protective effect of emulsions tended to increase with increasing fat contents. When emulsion samples of 50 and 70% soybean oil were treated at 45 °C or 45, 60 and 75 °C, even negative log reduction values were obtained. These effects were probably mediated by common heat-induced endospore activation (Keynan *et al.*, 1964). The mentioned results disagree with observations and theories according to Senhaji (1977). In this study, the assumption that emulsions just mediate heat protective effects, when endospores are embedded in fat droplets of low dispersed systems, was not confirmed. In consideration of results obtained in this study, the heat protective effect of emulsions is not trivial explainable. For instance, on the one hand the application of equal temperatures to samples containing 30 and 70% fat led to endospore inactivation, on the other hand the application promotes endospore activation.

The finding, that the number of spores attached to the oil/buffer interface tend to decrease with increasing fat content, seems to be contradictory to the general assumption that oil droplets have to be in contact or at least in close proximity to spores, to exert a protective effect on them. However, it is not known whether the endospore distribution in emulsions changes as a function of temperature and/or pressure. Decreased viscosity of the oil at high temperatures or increased Brownian motion could facilitate the association of endospores to the interface or even penetration of endospores into the oil droplets. Accordingly, an increased number of oil droplets in emulsions with high fat contents might lead to an increase in the number of collision events compared to low fat emulsions.

Finally, the mechanisms accounting for heat protective effects of fat on endospores and microorganisms are not completely understood. This study indicates that heat inactivation of *C. botulinum* type E endospores is more retarded in soybean oil emulsion compared to buffer systems. Contradictorily to Senhaji (1977), this study indicated that emulsions of highly dispersed levels can exert heat protective effects on endospores. According to Senhaji (1977), conventional heat sterilized food emulsions do not present a microbial risk for consumers, when emulsion stability is ensured and the process of coalescence is avoided. Admittedly, in thermal endospore inactivation experiments according to this study, applied temperatures were much lower than in common industrial sterilization processes. Considering the obtained results, the statements according to Senhaji (1977) need to be interpreted carefully. Among others, thermal inactivation of microorganisms strongly depends on species and strain specificities, on morphological status of corresponding organism and character of the surrounding matrix (Müller and Weber, 1996). Based on the complexness of emulsion systems and on conflicting results in thermal-induced inactivation experiments, further research is required.

4.3.4 Inactivation of *C. botulinum* type E endospores in emulsion matrices by HPT treatment

The high pressure-induced inactivation of vegetative bacteria is evidently caused by alterations in multiple molecular targets. The high pressure-induced reduction of cytoplasmic membrane fluidity and consequently, the decreased level of membrane transport activities seems to play a major role in mentioned processes. Additionally, protein denaturation, reduced enzymatic activities, effects on DNA replication,

transcription and translation are evidently responsible for high pressure-induced inactivation of microorganisms (Cheftel, 1995; Knorr, 1995; Chilton *et al.*, 1997; Gänzle and Vogel, 2001).

Several studies indicated that the success of high HPT-induced conservation processes strongly depends on the food matrix character and on the kind of target organisms. Evidently, the embedment of microorganisms in fat containing matrices permit increased resistance against pressure and temperature treatments (Simpson and Gilmour, 1997; Miller 2006; Morales *et al.* 2006; Ananta *et al.* 2001). In comparison to studies on HPT-induced inactivation of microorganisms in aqueous systems and common food matrices (juices, vegetables, meet, etc.), the knowledge concerning inactivation in fatty foods and emulsions is limited. In this field, the majority of research focus on milk and dairy products (Hite, 1899; Shibauchi, 1992 and Orlie, 2010). Miller (2006) analyzed the pressure-dependent inactivation of *Lactococcus lactis* and *Listeria innocua* (350 – 800 MPa) in the presence of different matrices with variable fat contents. The highest pressure tolerance was obtained, when bacteria were embedded in sunflower oil. Accordingly, pressure tolerance decreased, when mayonnaise and buffer matrices were used. Simpson and Gilmour (1997) indicated that the pressure-induced inactivation mode of *Listeria monocytogenes* was more reduced in olive oil/water emulsions than in pure buffer. Simpson and Gilmour (1997) assumed that bacteria, which were associated to fat droplets, supposedly are protected by reduced levels of water availability.

High pressure/HPT is known to induce germination of endospores, which consequently leads to spore rehydration, loss of resistance properties and promote finally spore inactivation (Setlow, 2007). Studies that focused on the pressure-induced inactivation of bacterial endospores in fatty matrices or emulsions are seldom. According to Ananta *et al.* (2001), the extent of HPT-induced inactivation of *Geobacillus stearothermophilus* spores in cocoa mass increased remarkably, when the matrix moisture content was increased.

Generally, the mechanism according to protective effects of fat on HPT-treated endospores are still unknown. Accordingly, the reduced availability of water apparently play an important role in this process.

In this work, the HPT-induced inactivation behavior of *C. botulinum* type E spores (TMW 2.992) was analyzed in pure IPB and in soybean oil emulsions of different fat contents (30, 50, 70%). Inoculated samples were exposed for 10 minutes to variable HPT parameters (temperatures of: 45, 60, 75 °C; pressures of: 300, 450, 600, 750 MPa). For the experimental setup, two different pressure units were employed (single vessel apparatus U4000 and the low temperature vessel U111), which differ in volume, in the use of pressure transferring liquid and in the location of pressure and temperature monitoring.

The inactivation of *C. botulinum* type E endospores tend to depend on both, HPT intensity and matrix parameters. Experiments, which were obtained in the single vessel apparatus U4000 indicated, that endospore mortality tended to increase as a function of increasing pressure and temperature. As a function of increasing emulsion fat content, the extent of endospore inactivation tended to decrease, i.e. the protective effect of fat appeared to diminish as a function of increasing HPT intensity (Figure 36).

A similar effect was observed, when inactivation experiments were conducted in the pressure unit U111 (Figure 37). Generally, HPT-induced endospore inactivation was lower, when experiments were conducted in unit U111. Exemplarily, when HPT parameters of 60 °C and 300 MPa were applied to emulsion samples containing 30% fat, the corresponding log reductions differed by 1.39 cycles, when different pressure units were used (Figure 36 and Figure 37).

Different HPT units were used to explore the differences in inactivation results that can occur due to adiabatic heating effects. Treatments in unit U111 ensured isothermal holding times at the target pressure, i.e. target processing temperatures were not exceeded (Figure 37). In contrast, the experimental setup using unit U4000 did not consider matrix-dependent effects on adiabatic heating (Figure 36). Consequently, the sample temperature of emulsions treated in pressure unit U4000 were much higher than target temperatures in the corresponding PTL. As a function of increasing pressure intensity and emulsion fat content, the mentioned effect is more pronounced. In turn, at equal target parameters and emulsion fat contents, sample temperature of emulsions treated in pressure unit U4000 were also much higher, than in corresponding emulsions treated in unit U111. The great differences in inactivation levels observed, impressively demonstrates the huge impact, adiabatic heating effects can exert on the final outcome of inactivation studies. Since the compression-mediated

temperature increase in fatty food can be up to three-fold higher compared to water (Ting *et al.* 2002), this should especially be considered, whenever experiments are carried out in matrices/food with varying fat contents.

The mentioned results suggest that the fat content of food plays an important and, to date, probably underestimated role in the protection of *C. botulinum* type E or other bacterial endospores against high pressure treatments. As fat is a common constituent of the majority of food, this represents an important finding for future food safety considerations. To clarify the role of the fat content in aqueous systems containing fat and to gain further insight into underlying mechanisms, emulsion model systems with more precisely defined parameters could be used.

Contradictions between endospore localization and fat content-dependent endospore inactivation, are discussed in 4.3.3. Theories, which focused on heat-dependent changes in endospore localization were also assumed to be transferable to effects caused by HPT treatments.

4.3.5 Conclusion: HPT-induced inactivation of *C. botulinum* type E spores in model emulsion systems

Primarily, the stability of soybean oil emulsions tended to depend on the fat content and seemingly on the emulsifier to oil ratio. Generally, soybean oil emulsions containing 10, 30, 50 and 70% fat remain stable after treatments for 10 min at 75 °C/0.1 MPa; RT/750 MPa and 75 °C/750 MPa. After sample treatments at mentioned conditions, slight changes in droplet size distributions were observed. However, no clear correlations between treatment parameters and changes in distribution can be established. This effect might be related to heat-, pressure- and concentration-dependent changes in physical emulsifier configuration. The majority of *C. botulinum* type E spores (TMW 2.992) tended to show hydrophilic surface character, while a minority tended to be more hydrophobic, which reflects the heterogeneity of spore populations. Heat- and high pressure-induced spore inactivation in emulsion systems clearly tended to decrease with increasing oil contents. To date, the mechanism of heat- and pressure- protective effects of oil are known. However the reduced availability of water seems to play a major role in this processes. The compression of fat containing samples led to increased adiabatic heating effects and in turn permitted increased endospore inactivation in non-isothermal processes.

SUMMARY

High pressure processing represents an innovative method for the generation of high quality food. For the inactivation of bacterial endospores, the combined application of high pressure and elevated temperatures are required. Until now, the molecular mechanism of HPT-induced inactivation of endospores, namely that one of clostridia, is not understood in detail. Fundamentally, HPT tolerance of spores depends on strain specificity, sporulation conditions and matrix properties. Accordingly, process parameters, which are required for the generation of safe food products, are not predictable readily and requires fundamental research. This study focused on factors affecting the high pressure tolerance of *C. botulinum* type E spores, which belong to the non-proteolytic group II. Members of this group are phylogenetically far removed from group I, III and IV strains, which are phylogenetically more related to each other (Collins and East, 1998). Based on the ability to grow and to produce toxins at temperatures as low as 3.3 °C, *C. botulinum* type E strains have a special position in the group of food spoiling pathogens.

In this work several independent approaches were taken to provide insight in factors determining high pressure resistance of *C. botulinum* type E endospores.

- Probing transformation and knock out strategies for detailed mechanistic analysis of spore resistance.
- Analyses of sporulation media induced spore proteomes and identification of proteins, which mediate increased high pressure resistance.
- Investigation of matrix-dependent effects on HPT-induced inactivation behavior of endospores, in model emulsions of different fat contents.

Until now, most research focused on the HPT-induced spore inactivation mechanism in *B. subtilis*, while the knowledge concerning on inactivation of *Clostridium* spores is relatively rare. To investigate the role of SASPs and of the germination-specific protease (CLO_2913) in HPT-induced inactivation mechanisms, transformation strategies were probed for their suitability in *C. botulinum* type E strains by employing the ClosTron system. It was apparent that the transfer of plasmid DNA into *C. botulinum* type E strains was not possible by conventional transformation techniques. Because efficient transformation represent a requirement for site-specific

mutagenesis, the aim of this study subsequently focused on the development of effective transformation techniques of *C. botulinum* type E strains. Generally, knock out generation represents an instrumental technic for the investigation of physiological and mechanistical processes. Based on the high variability in experimental setups, it can be widely excluded that physiological and experimental factors of conventional electroporation and conjugation processes were responsible for difficulties in *C. botulinum* type E strain transformation. Both, results of *in vitro* crude extract restriction assays and the presence of conserved gene motives (provided on REBASE), leads to the suggestion that the success of *C. botulinum* (TMW 2.990) transformation was prevented by the existence of RE systems. According to information on REBASE, the occurrence of a type II and a type IV RM system was predicted. Results of the crude extract restriction assay leads to the suggestion that *C. botulinum* (TMW 2.990) encodes a site-specific endonuclease, which is not conform to the endonuclease of the predicted type II RM system. The RM system could neither be overcome through the premethylation of plasmid DNA by different *E. coli* strains (Top10, GM2163, HB101, CA434), nor by the premethylation through the recombinant methyltransferase of the predicted type II RM system. Transformation was also unsuccessful when plasmids were *in vitro* methylated by modified *C. botulinum* (TMW 2.990) crude extracts. Finally transformants of *C. botulinum* could not be generated in this study. Presumably, the uptake of foreign DNA was prevented by the presence of a type IV RM system. Optionally, the transformation of *C. botulinum* (TMW 2.990) will be possible when vectors without corresponding type IV REase recognition sites will be used.

Although no *C. botulinum* type E transformants could be generated, the insights provided in *C. botulinum* restriction modification systems may be helpful in developing transformation strategies.

Among others, the HPT tolerance of endospores can be influenced by sporulation conditions. For instance, the HPT resistance of *C. botulinum* type E spores were significantly higher in SFE-derived spores than in spores, which were formed on TPYC, AEY and M140 (Lenz and Vogel, 2014). Accordingly, MALDI-TOF MS derived spore proteomes of three different *C. botulinum* type E strains, which were obtained from mentioned sporulation media, were compared to each other. Additionally, spore proteins, which are potentially involved in increased HPT resistance, were identified by MALDI-TOF MS and high resolution LC-MS/MS. The corresponding results indicated

that SFE-derived spores showed higher similarities in protein pattern than spores, which were formed on other used media. The similarity of spore protein spectra obtained from different strains on SFE were higher than those obtained from the same strain sporulated on different media. Finally, SFE medium tended to induce a typical, strain-independent proteome pattern, which promoted increased HPT resistance of type E spores.

Based on MALDI-TOF MS analysis, a total of 5 proteins was solely identified in SFE-derived *C. botulinum* (TMW 2.990) spores, while proteins were not detectable in TPYC-, AEY- and M140-derived spores. Consequently, indicated proteins are potentially involved in increased HPT resistance. In SFE-derived endospores, the spore photoproduct lyase (C5UUE9), the sporulation protein YunB (C5UZC5), the RNA polymerase factor δ^G (C5UXY2) and the putative spore coat proteins (C5UZG3 and C5UTT9) were identified. Spore photoproduct lyases are known to be involved in repairing mechanism of UV-mediated DNA damages. Since HPT treatment is not suspected to induce suchlike DNA mutations, the correlation between HPT resistance and the presence of photoproduct lyases is questionable. YunB (C5UZC5) and the RNA polymerase factor δ^G (C5UXY2) represent essential proteins, which are required for the generation of functional endospores. Finally, it is not obvious that these proteins couldn't be identified in TPYC-, M140- and AEY-derived spores. It is possible that the identification of YunB and δ^G in SFE-derived spores were caused by higher concentrations in comparison to spores which were obtained from other media. In SFE-derived spores, two potential spore coat proteins (C5UZG3, C5UTT9) of the CotS and CotF family were identified. Until now, experimental data, which attest correlations between spore coat character and HPT tolerance, are not available.

Spore protein analysis by SDS-PAGE and high resolution LC-MS/MS leads to the suggestion that SFE-derived spores contained an elevated level of N-acetylmuramoyl-L-alanine amidases. Consequently, the cortex peptidoglycan of SFE-derived spores optionally contained an elevated level of muramic δ -lactam and was finally less cross-linked than in spores derived from other sporulation media. Supposable, this effect led to increased core dehydration and/or to increased stability of CLEs, which in turn resulted in increased spore dormancy and in increased HPT resistance.

To evidence that the proteins (C5UZG3, C5UTT9) or finally elevated levels of N-acetylmuramoyl-L-alanine amidases are actually responsible for increased HPT resistance of *C. botulinum* type E spores, further research will be required.

Finally, it is unlikely that HPT resistance of endospores is mediated by the presence of single factors. Rather, the increased HPT resistance of SFE-derived *C. botulinum* type E spores is mediated by the sum of several proteomic factors.

Generally, in HPT-induced food preservation processes, the microbial inactivation behavior strongly depends on matrix character. Evidently, microorganisms are more resistant to heat and pressure inactivation, when they are embedded in fat or emulsion matrices. Until now, these effects are widely unknown. Several theories try to explain these effects by the low heat conductivity of lipids, a reduced water availability in oily environments or by endospore stabilizing effects in the presence of free fatty acids (Slesarewski, 1931; Lang, 1935; Molin & Snygg, 1967; Senhaji, 1977; Senhaji & Loncin, 1977). Nevertheless, the understanding of HPT-induced inactivation behavior of microorganisms in fatty environments would probably support the commercial launch of such novel, high quality food products. This work indicated that soybean oil emulsions of 10 – 70% fat are widely stable enough to endure HPT processing parameters (10 min, 75 °C/750 MPa). Heating (75 °C), pressuring (750 MPa) or the application of combined parameters, led to slight changes in droplet size distributions. Nevertheless, no clear correlations between treatment parameters and changes in droplet sizes could be established. Conceivably, these effects could be explained by heat-, pressure- and concentration-dependent changes in the emulsifying properties of soybean lecithin. Microscopic analysis of emulsions and plate count determinations according to spore inoculated biphasic oil/buffer systems indicated that the majority of *C. botulinum* spores were suspended in the buffer phase, while the minority of spores were associated to fat surfaces. Apparently, differences in spore surface hydrophobicity were caused by heterogeneity in spore populations.

Heat- and HPT-dependent inactivation experiments in emulsion systems evidenced that the extent of endospore inactivation decreased as a function of increasing oil content.

To estimate the matrix-dependent effects of adiabatic heating and finally the influence of the mentioned effect to the extent of endospore reduction, inactivation experiments

were conducted in two different high pressure units (U111 and U4000). Treatments in unit U111 ensured isothermal holding times at the target pressure, while treatments in U4000 did not consider matrix-dependent effects on adiabatic heating. These experiments indicated that great differences in inactivation levels were observed when equal process parameters were operated in the two different pressure units. Consequently, the pressuring of fatty matrices led to high adiabatic heating effects, which in turn strongly influenced the inactivation behavior of endospores. Finally, these results lead to the suggestion that the fat content of matrices play an important and, to date, underestimated role in the protection of *C. botulinum* type E and probably other bacterial endospores against high pressure treatments. Because fat represents a common constituent of most food products, mentioned findings are important for future food safety considerations.

ZUSAMMENFASSUNG

Die Hochdruckbehandlung stellt eine vielversprechende Technik zur Erzeugung von innovativen, hoch qualitativen Lebensmitteln dar. Um die mikrobiologische Unbedenklichkeit von Lebensmitteln zu gewährleisten, muss vor allem eine umfangreiche Inaktivierung von pathogenen Endosporen erzielt werden. Dieses kann durch die kombinierte Anwendung von hohen Drücken und Temperaturen bewerkstelligt werden. Derzeit sind die molekularen Mechanismen, welche die HPT-induzierte Inaktivierung von Endosporen regulieren, noch nicht komplett aufgeklärt. Bekanntlich sind Stamm Spezifitäten und Sporulationsbedingungen maßgeblich an der Ausprägung von HPT-Toleranzen beteiligt. Des Weiteren hängt das Maß der Inaktivierbarkeit stark von der Beschaffenheit der Lebensmittelmatrix ab. Daher müssen die benötigten Prozessparameter an die Beschaffenheit der Lebensmittelmatrix und an die HPT-Toleranzen von Leitkeimen angepasst werden, um eine umfangreiche mikrobiologische Sicherheit von Hochdruck behandelten Produkten zu gewährleisten.

Der thematische Schwerpunkt dieser Arbeit lag in der Analyse von Faktoren, welche die HPT-Toleranzen von *Clostridium botulinum* Typ E Sporen beeinflussen. *Clostridium botulinum* Typ E Stämme sind der Gruppe II zuzuordnen, welche die nicht proteolytischen Stämme zusammenfasst. Phylogenetisch grenzen sich Vertreter der Gruppe II stark von den näher verwandten Gruppen I, III und IV ab (Collins und East, 1998). Die besondere Fähigkeit bereits ab Temperaturen von 3 °C zu wachsen und Toxine produzieren zu können, begründet das erhöhte Interesse gegenüber Typ E Stämmen. Beispielsweise bieten vakuumverpackte, kühlgelagerte Lebensmittel eine mögliche Lebensgrundlage für derartige Keime und stellen somit eine potentielle Gefahrenquelle für Konsumenten dar.

In dieser Arbeit wurden unabhängige Ansätze zur Identifizierung von Faktoren verfolgt, welche die Ausprägung von HPT-Toleranzen in *C. botulinum* Typ E Sporen beeinflussen können.

- Erforschung von Transformations- und Knock-out-Strategien, zur mechanistischen Analyse der Sporenresistenz.

- Identifizierung von relevanten Sporenproteinen, welche an der Ausprägung von erhöhten HPT-Resistenzen beteiligt sind.
- Untersuchung des Matrix abhängigen Inaktivierungsverhalten von Endosporen, in Emulsionen mit variablen Fettgehalten.

Wissenschaftliche Schwerpunkte im Bereich der HPT-induzierten Inaktivierung von Endosporen konzentrieren sich derzeit vorrangig auf Untersuchungen von *B. subtilis* Sporen. Im Vergleich dazu ist das Wissen über HPT-induzierte Mechanismen in *Clostridien* Sporen eher begrenzt.

Um die Funktionen von SASPs und der keimungsspezifischen Protease (CLO_2913) im HPT-induzierten Inaktivierungsmechanismus von *C. botulinum* Typ E zu untersuchen, wurden verschiedenste Transformations-Strategien getestet, um Knock-out Mutanten generieren zu können. Es stellte sich heraus, dass *C. botulinum* Typ E Stämme nicht nach konventionellen Methoden transformiert werden konnten. Sowohl Rohextrakt-Restriktionsanalysen, als auch die Existenz von konservierten Gen-Sequenzmotiven deuteten darauf hin (REBASE), dass *C. botulinum* beluga (TMW 2.990) spezielle RM-Systeme besitzen könnte, welche die Aufnahme von fremder DNA verhindern. REBASE Datenbankeinträge suggerieren, dass *C. botulinum* (TMW 2.990) sowohl über ein Typ II, als auch über ein Typ IV RM-System verfügen könnte. Demzufolge codiert das potentielle Typ II System für die Methyltransferase M.CboE1OPF1092P und die Restrictionsendonuklease CboE1OPF1092P, wohingegen das potentielle Typ IV System ausschließlich für eine Restrictionsendonuklease (CboEORFAP) codiert.

Die Ergebnisse der Rohextrakt-Restriktionsanalysen zeigen, dass *C. botulinum* (TMW 2.990) eine Restrictionsendonuklease synthetisiert, die jedoch nicht Teil des erwähnten Typ II Systems zu sein scheint.

Um dem Abbau von fremder DNA durch stammspezifische Restriktionsnukleasen in *C. botulinum* typ E Stämmen entgegen zu wirken, wurden die zu transferierenden Plasmide durch verschiedene Methyltransferasen methyliert, welche sich im Ursprungs und der Spezifität unterschieden.

Die *in vivo* Methylierungen von pMTL007C-E2-Derivaten, durch die *E. coli* Stämme Top10, GM2163, HB101, CA434 konnten jedoch nicht dazu beitragen, dass genannte

Vektoren in *C. botulinum* Typ E Stämme transferiert werden konnten. Auch die rekombinante Expression der Methyltransferase (M.CboE1ORF1092P) in *E. coli* (Top 10 und CA434) führte nicht dazu, dass Koexistente pMTL007C-E2-Derivate nachfolgend in *C. botulinum* transformiert werden konnten. Auch die Methylierung der Plasmide durch modifizierten Rohextrakt von *C. botulinum* (TMW 2.990), hatte keinen positiven Einfluss auf die Transformationseffizienz.

Es ist nicht auszuschließen, dass es sich bei dem im Rohextrakt nachgewiesenen Enzym, um die bereits erwähnte Type IV Restriktionsendonuklease (CboEORFAP) handeln könnte. Demzufolge könnte *C. botulinum* (TMW 2.990) eventuell mit Vektoren transformiert werden, welche keine entsprechenden Erkennungssequenzen tragen, beziehungsweise welche in der Erkennungssequenz nicht methyliert sind.

Wie bereits erwähnt, wird die Ausprägung der HPT-Toleranz von Endosporen stark von den vorherrschenden Sporulationsbedingungen beeinflusst. Beispielsweise zeigten *C. botulinum* Typ E Sporen eine weitaus höhere Toleranz gegenüber HPT, wenn diese in SFE Medium angezogen wurden, als welche, die in herkömmlichen Medien (TPYC, AEY, M140) angewachsen sind (Lenz und Vogel, 2014). Aufgrund dessen wurden die Proteome von verschiedenen *C. botulinum* Typ E Sporen (TMW 2.990; TMW 2.994; TMW 2.997) in Abhängigkeit der erwähnten Sporulationsmedien analysiert. Der Vergleich von MALDI-TOF MS Spektren zeigte, dass die Analogie der Sporen-Proteome von verschiedenen Typ E Stämmen höher war, wenn diese in SFE Medium gewachsen sind, als bei Stamm-identischen Sporen, welche in unterschiedlichen Medien angezogen wurden (SFE, TPYC, AEY, M140). Augenscheinlich führte die Sporulation in SFE Medium zur Ausprägung eines charakteristischen Sporen-Proteoms, welches nicht primär durch die Stammspezifität geprägt wurde und zur erhöhten HPT-Resistenz der Sporen beitrug.

Mittels MALDI-TOF MS Analysen wurden in *C. botulinum* (TMW 2.990) fünf Proteine detektiert, welche sich nur in SFE-Sporen nachweisen ließen und welche somit an der Ausprägung der erhöhten HPT-Toleranz beteiligt sein könnten. Demzufolge wurde die Sporen-spezifische Photolyase (C5UUE9), das Sporulationsprotein YunB (C5UZC5), der RNA-Polymerase spezifische Faktor δ^G (C5UXY2) und potenzielle Sporen-Mantelproteine (C5UZG3 und C5UTT9) identifiziert.

Während der Keimung katalysieren Sporen-spezifische Photolyasen die Regenerierung von UV-induzierten DNA Schäden. Es gibt jedoch keinerlei Hinweise darauf, dass derartige DNA Schäden durch die Anwendung von Hochdruck und Hitze induziert werden. Daher ist es fragwürdig, ob ein direkter Zusammenhang zwischen der gesteigerten HPT-Resistenz von *C. botulinum* (TMW 2.990) Sporen und der Existenz der Photolyase (C5UUE9) besteht.

Sowohl das Sporulationsprotein YunB als auch der Faktor δ^G scheinen essentielle Sporenproteine zu sein. Daher ist es unklar, weshalb diese Proteine nicht in *C. botulinum* Sporen nachgewiesen werden konnten, welche in konventionellen Medien sporuliert sind (TPYC, AEY und M140). Es ist jedoch nicht auszuschließen, dass die Konzentrationen von YunB und δ^G in den HPT-sensitiveren Sporen weitaus geringer waren und somit unter der Nachweisgrenze lagen. Ob sich erhöhte HPT-Resistenzen von Sporen auf erhöhte YunB und δ^G Konzentrationen zurückführen lassen, bleibt jedoch unklar.

Bekanntlich übt die Zusammensetzung des Sporulationsmediums einen starken Einfluss auf den komplexen Aufbau des Sporenmantels aus. Derzeit existieren jedoch keine wissenschaftlichen Studien, die den Einfluss von Mantelproteinen auf die HPT-Resistenz von Endosporen, geltend machen. Um zu verifizieren, ob die Existenzen von C5UZG3 und C5UTT9 tatsächlich zur erhöhten HPT-Resistenz von *C. botulinum* (TMW 2.990) Sporen beiträgt, sind weiterführende Untersuchungen von Nöten.

Mittels SDS-PAGE wurde in SFE-Sporen verschiedener *C. botulinum* Typ E Stämme (TMW 2.990; TMW 2.994; TMW 2.997) ein Protein nachgewiesen, welches nach Sporulation in TPYC, AEY und M140 nicht detektiert werden konnte. Weiterführende Untersuchungen mittels High-Resolution LC-MS/MS ergaben, dass es sich hierbei wahrscheinlich um eine N-Acetylmuramoyl-L-Alanin Amidase handelte. Daher ist davon auszugehen, dass das Rinden-Peptidoglycan von SFE-Sporen ein erhöhtes Maß an Muramin δ -Lactamen aufweist und somit weniger quervernetzt ist, als bei herkömmlichen Sporen. Vermutlich trägt der herabgesetzte Vernetzungsgrad dazu bei, dass der Sporenkern von SFE-Sporen in einem höheren Maß dehydratisiert werden kann. Des Weiteren besteht die Vermutung, dass der reduzierte Vernetzungsgrad des Peptidoglycans zur Stabilisierung von Keimungs-spezifischen-lytischen-Enzymen (CLEs) führen kann. Diese Effekte könnten theoretisch zu

verstärkten Dormanz und somit auch zu einer erhöhten HPT-Resistenz von Endosporen führen.

Abschließend wird davon ausgegangen, dass die HPT-Toleranz von Endosporen nicht durch einzelne Faktoren bestimmt wird. Es ist somit wahrscheinlicher, dass die Gesamtheit und der Charakter des Sporenproteoms zur Ausprägung von Resistenzen führen.

Bekanntlich ist die Inaktivierbarkeit von Mikroorganismen, in HPT-induzierten Konservierungsprozessen, stark vom Charakter der verwendeten Lebensmittelmatrix abhängig. Nachweislich lassen sich Mikroorganismen schlechter abtöten, wenn diese in eine Matrix mit erhöhtem Fettgehalt eingebettet sind. Einige Theorien stützen sich darauf, dass die geringe Wärmeleitfähigkeit von Lipiden, die reduzierte Verfügbarkeit von Wasser oder stabilisierende Effekte von freien Fettsäuren, einen schützenden Effekt auf Endosporen ausüben können (Slesarewski, 1931; Lang, 1935; Molin & Snygg, 1967; Senhaji, 1977; Senhaji & Loncin, 1977).

Weiterführende Kenntnisse, die sich auf die HPT-induzierte Inaktivierung von Endosporen in fetthaltigen Matrices stützen, können beispielsweise zur Entwicklung von innovativen Lebensmitteln, mit verbesserter Qualität beitragen.

Rheologische Messungen konnten belegen, dass die thermodynamischen Stabilitäten von Sojaöl Emulsionen (10 - 70% Öl (v/v)), hoch ausgeprägt waren. Es wurde bewiesen, dass die Lagerstabilitäten der Modell-Emulsionen sogar weitestgehend erhalten blieben, nachdem diese mit hohen Drücken und Temperaturen behandelt wurden (10 min bei 75 °C/0,1 MPa; RT/750 MPa; 75 °C/750 MPa). Die Tröpfchengrößenverteilungen in Sojaöl Emulsionen wurden nur geringfügig von den genannten Hitze- und Temperaturparametern beeinflusst. Es konnte jedoch kein allgemeingültiger Zusammenhang zwischen dem Ausmaß der Veränderung der Tröpfchengrößenverteilung und den Einflussgrößen von Druck, Temperatur und Fettgehalt hergestellt werden. Eventuell kann die emulgierende Wirkung des Sojalecithins durch die Summe der genannten Einflussgrößen in unterschiedlicher Art und Weise beeinflusst werden, was somit zu unkalkulierbaren Veränderungen der Tröpfchengrößenverteilung führen kann.

Die lokalen Verteilungen von Endosporen in Emulsionen und heterogenen Öl/Puffer-Gemischen wurden durch mikroskopische als auch angewandte Methoden analysiert.

Allgemein konnte gezeigt werden, dass sich die Mehrheit der angeimpften Sporen, in den wässrigen Phasen befanden. Hingegen waren die Anzahlen der Sporen, welche sich an die Grenzflächen der Fettphasen anlagerten, stark reduziert. Aufgrund der heterogenen Verteilung von Sporen wird angenommen, dass sich die Hydrophobizitäten einzelner Sporen voneinander unterscheiden. Dieses Phänomen lässt sich beispielsweise durch die Heterogenität von Sporenpopulationen begründen.

Experimente in denen *C. botulinum* Typ E Sporen in Emulsionen mit unterschiedlichen Fettgehalten durch die Einwirkung von Hitze bzw. HPT abgetötet wurden zeigten, dass die Abtötungsraten mit Anstieg des Fettgehalts abnahmen.

Um Zusammenhänge zwischen dem Fettgehalt der Matrix, dem Effekt der adiabatischen Erwärmung und der Inaktivierungseffizienz von Endosporen zu erkennen, wurden Inaktivierungsstudien in zwei verschiedenen Hochdruckanlagen durchgeführt (U111 und U4000). Die Verwendung der Hochdruckeinheit U111 ermöglichte es Versuche unter annähernd isothermen/isobaren Bedingungen durchzuführen. Hingegen wurden während der HPT-Generierung in der Hochdruckeinheit U4000, keine adiabatischen Effekte berücksichtigt. Ein Vergleich der Ergebnisse zeigte, dass sich die Inaktivierungseffizienzen in den beiden Anlagen stark voneinander unterscheiden, wenn gleiche Prozessparameter gewählt wurden. Folglich führte die Hochdruckbehandlung der fetthaltigen Proben zu starken adiabatischen Effekten.

Schlussendlich wurde gezeigt, dass der Fettgehalt von Lebensmittel-Matrices einen erheblichen Einfluss auf die hochdruckinduzierte Inaktivierungseffizienz von *C. botulinum* Type E Sporen ausübt. Da Fett ein allgegenwärtiger, variabler Bestandteil von vielen Lebensmitteln ist, muss diesem Faktor bei der Entwicklung von Hochdruckbehandelten Lebensmitteln, ein erhöhtes Maß an Aufmerksamkeit gewidmet werden.

REFERENCES

- Ababouch, L. H., Gritit, L., Eddafry, R. and Busta, F. F.** (1995) Thermal inactivation kinetics of *Bacillus subtilis* spores suspended in buffer and in oils. *Journal of Applied Bacteriology*, 78, 6, 669-676
- Abe, A., Koide, H., Kohno, T. and Watabe K.** (1995) A *Bacillus subtilis* spore coat polypeptide gene, cotS. *Microbiology*, 141, 6, 1433-1442
- Abel-Santos, E.** (2012) Bacterial spores: Current Research and Applications, *Caister Academic Press*, chapter 12, 199-212
- Aebersold, R. and Mann, M.** (2003) Mass spectrometry-based proteomics. *Nature*, 422, 198-207
- Ahvenainen, R.** (1996) New approaches in improving the shelf life of minimally processed fruit and vegetables. *Trends in Food Science & Technology*, 7, 6, 179-187
- Alderton, G. and Snell, N.** (1963) Base exchange and heat resistance in bacterial spores. *Biochemical and Biophysical Research Communications*, 31, 10, 139-143
- Al-Masaudi, S. B., Russell, A. D. and Day, M. J.** (1991) Factors affecting conjugative transfer of plasmid pWG6 13, determining gentamicin resistance, in *Staphylococcus aureus*, *Journal of Medical Microbiology*, 34, 103-107
- Andersson, A. and Rönnner, U.** (1998) Adhesion and removal of dormant, heat-activated, and germinated spores of three strains of *Bacillus cereus*. *Biofouling*, 13, 1, 51-67
- Ananta, E., Heinz, V., Schlüter, O. and Knorr, D.** (2001) Kinetic studies on high-pressure inactivation of *Bacillus stearothermophilus* spores suspended in food matrices. *Innovative Food Science & Emerging Technologies*, 2, 4, 261-272
- Antona, M., Chapleaub, N., Beaumala, V., Delépineb, S., de Lamballerie-Antonb, M.** (2001) Effect of high-pressure treatment on rheology of oil-in-water emulsions prepared with hen egg yolk. *Innovative Food Science & Emerging Technologies*, 2, 1, 9-21
- Atrih, A., Zöllner, P., Allmaier, G. and Foster, S. J.** (1996) Structural analysis of *Bacillus subtilis* 168 endospore peptidoglycan and its role during differentiation. *Journal of Bacteriology*, 178, 21, 6173-6183
- Arnon, S. S., Schechter, R., Inglesby, T. V., Henderson, D. A., Bartlett, J. G., Ascher, M.S., Eitzen, E., Fine, A. D., Hauer, J., Layton, M., Lillibridge, S., Osterholm, M. T., O'Toole, T., Parker, G., Perl, T. M., Russell, P. K., Swerdlow, D. L., Tonat, K.,** (2001). Botulinum toxin as a biological weapon. *The Journal of American Medical Association*, 285, 8, 1059-1070
- Artin, I., Carter, A. T., Holst, E., Löwenklev, M., Mason, D. R., Peck, M. W., and Radström, P.** (2008) Effects of Carbon Dioxide on Neurotoxin Gene Expression in Nonproteolytic *Clostridium botulinum* Type E. *Applied and environmental microbiology*, 74, 8, 2391-2397

- Atrih, A. and Foster, S. J.** (2001) Analysis of the role of bacterial endospore cortex structure in resistance properties and demonstration of its conservation amongst species. *Journal of Applied Microbiology*, 91, 2, 364-372
- Badolato, B. B., Aguilar, F., Schuchmann, H. P., Sobisch, T. and Lerche, D.** (2008) Evaluation of long term stability of model emulsions by multisample analytical centrifugation. *Colloid and Polymer Science*, 134, 66-73
- Baumgart, J** (1972) Occurrence and demonstration of *Clostridium botulinum* in salt water fish. *Archiv für Lebensmittelhygiene*, 23, 34-39
- Baneyx, F.** (1999) Recombinant protein expression in *Escherichia coli*. *Current Opinion in Biotechnology*, 10, 5, 411-421
- Bayliss, C. D., Callaghan, M. J. and Moxon, E. R.** (2006) High allelic diversity in the methyltransferase gene of a phase variable type III restriction-modification system has implications for the fitness of *Haemophilus influenzae*. *Nucleic Acids Research*, 34, 14, 4046-4059
- Bengoechea, C., Romero, A., Aguilar, J. M., Cordobés, F. and Guerrero A.** (2010) Temperature and pH as factors influencing droplet size distribution and linear viscoelasticity of O/W emulsions stabilised by soy and gluten proteins. *Food Hydrocolloids*, 24, 8, 783-791
- Berndt, C., Meier, P and Wackernagel, M.** (2003) DNA restriction is a barrier to natural transformation in *Pseudomonas stutzeri* JM300. *Microbiology*, 149, 4, 895-901
- Bertani, G.** (1951) Studies on lysogenesis. I. The mode of phage liberation by lysogenic *Escherichia coli*. *Journal of Bacteriology*, 62, 3, 293-300
- Berthier, F., Zagorec, M., Champomier-Vergès, M., Ehrlich, S. D. and Morel-Deville, F.** (1996) Efficient transformation of *Lactobacillus sake* by electroporation. *Microbiology* 142, 5, 1273-1279
- Bickle, T. A. and Krüger. D. H.** (1993) Biology of DNA restriction. *Microbiological Reviews*, 57, 2, 434-450
- Black, E. P., Koziol-Dube, K., Guan, D., Wie, J., Setlow, B., Cortezzo, D. E., Hoover, D. G. and Setlow, P.** (2005) Factors Influencing Germination of *Bacillus subtilis* Spores via Activation of Nutrient Receptors by High Pressure. *Applied and environmental microbiology*, 71, 10, 5879-5887
- Black, E. P., Wei, J., Atluri, S., Cortezzo, D. E., Koziol-Dube, K., Hoover, D. G. and Setlow P.** (2007, A) Analysis of factors influencing the rate of germination of spores of *Bacillus subtilis* by very high pressure. *Journal of Applied Microbiology*, 102, 1, 65-76
- Black, E. P., Setlow, P., Hocking, A. D., Stewart, C. M., Kelly, A. L. and Hoover, D. G.** (2007, B) Response of Spores to High-Pressure Processing. *Comprehensive Reviews in Food Science and Food Safety*, 6, 4, 103-119
- Blaschek, H. P. and Klacik, M. A.** (1984) Role of DNase in recovery of plasmid DNA from *Clostridium perfringens*. *Applied and environmental microbiology*, 48, 1, 178-181
- Blum, H., Beier, H. and Gross, H.J.** (1987). Improved silver staining of plant proteins, RNA and DNA in polyacrylamide gels. *Electrophoresis*, 8, 93-99.

- Bradshaw, M., Marshall, K. M., Heap, J. T., Tepp, W. H., Minton, N. P. and Johnson, E. A.** (2010) Construction of a Nontoxigenic *Clostridium botulinum* Strain for Food Challenge Studies. *Applied and environmental microbiology*, 76, 2, 387-393
- Brüggemann, H.** (2005) Genomics of clostridial pathogens: implication of extrachromosomal elements in pathogenicity. *Current Opinion in Microbiology*, 8, 5, 601-605
- Bridgman, P. W.** (1914) The coagulation of albumen by pressure. *Journal of Biological Chemistry*, 19, 511-512.
- Cano, R. J and Borucki, M. K.** (1995) Revival and identification of bacterial spores in 25- to 40-million-year-old Dominican amber. *Science*, 268, 5213, 1060-1064
- Cheftel, J. C.** (1995) Review: High-pressure, microbial inactivation and food preservation. *Food Science and Technology International*, 1, 2, 75-90
- Chilto, P., Isaacs, N. S., Mackey, B. and Stenning, R.** (1997) The Effects of high hydrostatic pressure on bacteria. In Hermans, K: High Pressure Research in the Biosciences and Biotechnology. *Leuven University Press, Leuven*, 225-228
- Collins, M. D. and East, A. K.** (1998) Phylogeny and taxonomy of the food-borne pathogen *Clostridium botulinum* and its neurotoxins. *Journal of Applied Microbiology*, 84, 1, 5-17
- Cooksley, C. M., Davis, I. J., Winzer, K., Chan, W. C., Peck, M. W. and Minton, N. P.** (2010) Regulation of neurotoxin production and sporulation by a Putative agrBD signaling system in proteolytic *Clostridium botulinum*. *Applied and environmental microbiology*, 76, 13, 4448-4460
- Coros, C. J., Landthaler, M., Piazza, C. L., Beauregard, A., Esposito, D., Perutka, J., Lambowitz, A. M. and Belfort M.** (2005) Retrotransposition strategies of the *Lactococcus lactis* LI.LtrB group II intron are dictated by host identity and cellular environment. *Molecular Microbiology*, 56, 2, 509-524
- Cruz-Rodz, A. L. and Gilmore, M. S.** (1990) High efficiency introduction of plasmid DNA into glycine treated *Enterococcus faecalis* by electroporation. *Molecular Genetics and Genomics*, 224, 1, 152-154
- Cutting, S., Zheng, L. B. and Losick, R.** (1991) Gene encoding two alkali-soluble components of the spore coat from *Bacillus subtilis*. *Journal of Bacteriology*, 173, 9, 2915-2919
- Davis, T. O., Henderson, I., Brehm, J. K. and Minton, N. P.** (2000) Development of a Transformation and Gene Reporter System for Group II, Non-Proteolytic *Clostridium botulinum* Type B Strains. *Journal of Molecular Microbiology and Biotechnology*, 2, 1, 59-69
- De Jong, A. E., Beumer, R. R. and Rombouts, F. M.** (2002) Optimizing sporulation of *Clostridium perfringens*. *Journal of Food Protection*, 65, 9, 1457-1462
- Decaudin, M. and Tholozan, J. L.** (1996) A comparative study on the conditions of growth and sporulation of three strains of *Clostridium perfringens* type A. *Canadian Journal of Microbiology*, 42, 3, 298-304

- Dickinson, E. and James, J. D.** (1998) Rheology and Flocculation of High-Pressure-Treated β -Lactoglobulin-Stabilized Emulsions: Comparison with Thermal Treatment. *Journal of Agricultural and Food Chemistry*, 46, 2565-2571
- Dodds, K. L. and Austin, W. A.** (1997) *Clostridium botulinum*. In Doyle, M. P., Beuchert, L. R. and Montville, T.J., *Food Microbiology, Fundamentals and Frontiers*, ASM Press, Washington D. C., Chapter 15
- Driks A.** (2002) Maximum shields: the assembly and function of the bacterial spore coat. *Trends in Microbiology*, 10, 6, 251-254
- Dixit, A., Alam, S. I., Dhaked, R. K. and Singh, L.** (2005) Sporulation and Heat Resistance of Spores from a *Clostridium sp.* RKD. *Journal of Food Science*, 70, 7, 367-373
- Donahue, J. P., Israel, D. A., Peek, R. M., Blaser, M. J. and Miller, G. G.** (2000) Overcoming the restriction barrier to plasmid transformation of *Helicobacter pylori*. *Molecular Microbiology*, 37, 5, 1066-1074
- Dong, H., Zhang, Y., Dai, Z., Li mail, Y.** (2010) Engineering *Clostridium* Strain to Accept Unmethylated DNA, PLoS ONE, 5, 2, e9038. doi:10.1371/journal.pone.0009038
- Dower, W. J., Miller, J. F. and Ragsdale, C. W.** (1988) High efficiency transformation of *E. coli* by high voltage electroporation. *Nucleic Acids Research*, 16, 13, 6127-6145
- Doyle, R. J., Nedjat-Haiem, F. and Singh, J. S.** (1984) Hydrophobic characteristics of Bacillus spores. *Current Microbiology*, 10, 6, 329-332
- Doyle, R. J. and Rosenberg, M.** (1995). Measurement of microbial adhesion to hydrophobic substrata. *Methods in Enzymology*, 253, 542-550
- Doyle, M. P., Beuchat, L. R., Montville, T. J.** (1997) Food Microbiology. Fundamentals and Frontiers, ASM Press, 288-304
- Dürre, P.** (2005) Handbook on Clostridia, CRC Press Taylor and Francis Group, LLC, Chapter 3, 43-62
- Eichenberger, P., Jensen, S. T., Conlon, E. M., van Ooij, C., Silvaggi, J., González-Pastor, J.E., Fujita. M., Ben-Yehuda, S., Stragier, P., Liu, J. S., Losick, L.** (2003) The σ^E Regulon and the Identification of Additional Sporulation Genes in *Bacillus subtilis*. *Journal of Molecular Biology*, 327, 5, 945-972
- Eisenbrand, G.** (2005) Safety assessment of high pressure treated foods. *Molecular Nutrition & Food Research*, 49, 12, 1168-1174
- Elhai, J., Vepritskiy, A., Muro-Pastor, A. M., Flores, E. and Wolk, C. F.** (1997) Reduction of conjugal transfer efficiency by three restriction activities of *Anabaena sp.* strain PCC 7120. *Journal of Bacteriology*, 179, 6, 1998-2005
- Elowitz, R. B., Levine, A. J., Siggia, E. D. and Swain P. S.** (2002) Stochastic gene expression in a single cell. *Science*, 297, 5584, 1183-1187

- Erbguth, F. J.** (2004) Historical Notes on Botulism, *Clostridium botulinum*, Botulinum Toxin, and the Idea of the Therapeutic Use of the Toxin. *Movement Disorders*, 19, 8, 2-6
- Errington, J.** (1993) *Bacillus subtilis* sporulation: regulation of gene expression and control of morphogenesis. *Microbiological Reviews*, 57, 1, 1–33
- Errington, J.** (2003) Regulation of endospore formation in *Bacillus subtilis*. *Nature Reviews Microbiology* 1, 117-126
- Fairhead, H., Setlow, B. and Setlow, P.** (1993) Prevention of DNA damage in spores and in vitro by small, acid-soluble proteins from *Bacillus* species. *Journal of Bacteriology*, 175, 5, 1367-1374
- Farkas, J.** (1998) Irradiation as a method for decontaminating food: A review. *International Journal of Food Microbiology*, 44, 3, 189-204
- Farkas, D. F. and Hoover, D. G.** (2011) High Pressure Processing. *Journal of Food Science*, 65, 8, 47-64
- Fernandez-Astorga, A., Muela, A., Cisterna, R., Iriberry, J. and Barcina, I.** (1992) Biotic and abiotic factors affecting plasmid transfer in *Escherichia coli* strains. *Applied and environmental microbiology*, 58, 1, 392-398
- Fukushima, T., Yamamoto, H., Atrih, A., Foster, S. J. and Sekiguchi, J.** (2002) A Polysaccharide Deacetylase Gene (*pdaA*) Is Required for Germination and for Production of Muramic δ -Lactam Residues in the Spore Cortex of *Bacillus subtilis*. *Journal of Bacteriology*, 184, 21, 6007-6015
- Gänzle, M. G. and Vogel, R. F.** (2001) On-line fluorescence determination of pressure mediated outer membrane damage in *Escherichia coli*. *Systematic and Applied Microbiology*, 24, 4, 477-485
- Gänzle, M. G., Margosch, D., Buckow, R., Ehrmann, M. A., Heinz, V. and Vogel R. F.** (2007) Pressure and Heat Resistance of *Clostridium botulinum* and Other Endospores. In Doona C. J., Florence E. F., *High Pressure Processing of Food*. IFT Press, Chicago, Chapter 5
- Gerhardt, P. and Marquis, R. E.** (1989). Spore thermoresistance mechanisms. In Regulation of Prokaryotic Development. Edited by I. Smith, R. Slepecky & P. Setlow. Washington, DC: American Society for Microbiology, 43-63.
- Gervasini, C.** (1963) Wärmebehandlung von Lebensmitteln. *Dechema-Monographien Verlag Chemie GmbH.*, 263-286
- Grecz, N., Anellis, A. and Schneider, M. D.** (1962) Procedure for cleaning of *Clostridium botulinum* spores. *Journal of Bacteriology*, 84, 3, 552-558
- Gunnison, J. B., Cummings, J. R. and Meyer, K. F.** (1936) *Clostridium botulinum* type E. *Proceedings of the Society for Experimental Biology and Medicine*, 35, 278-280
- Hansen, N. H. and Riemann, H.** (1963) Factors Affecting the Heat Resistance of Nonsporing Organisms. *Journal of Applied Bacteriology*, 23, 3, 314-333

- Hartmann, P. A.** (1997) The Evolution of Food Microbiology. In *Doyle, M. P., Beuchert, L. R. and Montville, T.J., Food Microbiology, Fundamentals and Frontiers*, ASM Press, Washington D. C., Chapter 1
- Hatheway, C. L.** (1993) *Clostridium botulinum* and other clostridia that produce botulinum neurotoxin, In *Hauschild, A. H. W. and Dodds, K. L., Clostridium botulinum: Ecology and Control in Foods*. Marcel Dekker, Inc., New York
- Hattman, S. M., Brooks, J. E. and Masurekar, M.** (1978) Sequence Specificity of the PI modification methylase (*M. Eco P_i*) and the DNA methylase (*M. Eco dam*) controlled by the *Escherichia coli dam* gene. *Journal of Molecular Biology*, 126, 367-360
- Harder, A.** (2001). Wissenschaftszentrum für Ernährung, Landnutzung und Umwelt. Dissertation. FG Proteomik, Technische Universität München, Munich, Germany.
- Hartmann, M., Pfeifer, F., Dornheim, G. and Sommer, K.** (2003) HPDS-Hochdruckzelle zur Beobachtung mikroskopischer Phänomene unter Hochdruck. *Chemie Ingenieur Technik*, 75, 11, 1763-1767
- Hazen, E. L.** (1938) Incitants of human botulism. *Science*, 87, 413-414
- Heap, J. T., Pennington, O. J., Cartman, S. T. and Minton, N.P.** (2009, A) A modular system for *Clostridium* shuttle plasmids. *Journal of Microbiological Methods*, 78, 1, 79-85
- Heap, J. T., Kuehne, S. A., Ehsaan, M., Cartman, S. T., Cooksley, C. M., Scott, J. C. and Minton, N. P.** (2009, B) The ClosTron: Mutagenesis in *Clostridium* refined and streamlined. *Journal of Microbiological Methods*, 80, 1, 49-55
- Heap, J. T., Pennington, O. J., Cartman, S. T., Carter, G. P. and Minton, N.P** (2007) The ClosTron: a universal gene knock-out system for the genus *Clostridium*. *Journal of Microbiological Methods*, 70, 3, 452-464
- Hedges, R. W. and Jacob, A. E.** (1974) Transposition of Ampicillin Resistance from RP4 to Other Replicons. *Molecular Genetics and Genomics*, 132, 31—40
- Hemley, R. J.** (2000) Effects of high pressure on molecules. *Annual Review of Physical Chemistry*, 51, 763—800
- Hersom, A. C., and Hulland, E. D** (1963) Canned foods, 4th ed. J. A. Churchill Ltd., London.
- Hielm, S., Björkroth, J., Hyytiä, E. and Korkeala, K.** (1998) Genomic Analysis of *Clostridium botulinum* Group II by Pulsed-Field Gel Electrophoresis. *Applied and environmental microbiology*, 64, 2, 703-708
- Hite, B. H.** (1899) The effect of pressure in the preservation of milk. *Bulletin of West Virginia University of Agricultural Experiment Station*, 58, 15-35
- Hite, B.H., Giddings, N.J. and Weakley, C.E.** (1914) The effect of pressure on certain microorganisms encountered in the preservation of fruits and vegetables. *Bulletin of West Virginia University of Agricultural Experiment Station*, 46, 2-67

- Hobbs, G., Stiebrs, A. and Eklund, M. W.** (1967) Egg yolk reaction of *Clostridium botulinum* type E in different basal media. *Journal of Bacteriology*, 93, 1192
- Hodgkiss, M. and Ordal, Z. J.** (1996) Morphology of the Spore of Some Strains of *Clostridium botulinum* Type E. *Journal of Bacteriology*, 91, 5, 2031-2036
- Holo, H. and Nes, I. F.** (1989) High-Frequency Transformation, by Electroporation, of *Lactococcus lactis* subsp. *cremoris* Grown with Glycine in Osmotically Stabilized Media. *Applied and environmental microbiology*, 55, 12, 3119-3123
- Hornstra, L. M., Beek, A. T., Smelt, J. P., Kallemeijn, W. W. and Brul, S.** (2009) On the origin of heterogeneity in (preservation) resistance of *Bacillus* spores: Input for a 'systems' analysis approach of bacterial spore outgrowth. *International Journal of Food Microbiology*, 134, 1-2, 9-15
- Huggins, A. S., Bannam, T. L., and Rood, J. I.** (1992) Comparative Sequence Analysis of the catB Gene from *Clostridium butyricum*. *ANTIMICROBIAL AGENTS and CHEMOTHERAPY*, 36, 11, 2548–2551
- Husmark, U. and Rönner, U.** (1992) The influence of hydrophobic, electrostatic and morphologic properties on the adhesion of *Bacillus* spores. *Biofouling*, 5, 4, 335-344
- Husmark, U.** (1993) Adhesion Mechanisms of Bacterial Spores to Solid Surfaces. *Chalmers University of Technology, Göteborg, Ph.D thesis*
- Hyttiä, E., Hielm, S. and H. Korkeala** (1998) Prevalence of *Clostridium botulinum* type E in Finnish fishand and fishery products. *Epidemiology & Infection*, 120, 3, 245-250
- Imamura, D., Kuwana, R., Takamatsu, H. and Watabe, K.** (2009) Localization of Proteins to Different Layers and Regions of *Bacillus subtilis* Spore Coats. *Journal of Bacteriology*, 192, 2, 518-524
- Jennert, K. C., Tardif, C., Young, D. and Young, M.** (2000) Gene transfer to *Clostridium cellulolyticum* ATCC 35319. *Microbiology*, 146, 12, 3071-3080
- Jensen, L. B.** (1954) Microbiology of meat, 3rd ed. *Garrard Press, Champaign, Ill.*
- Johnson, W. C. and Tripper, D. J.** (1981) Acid-Soluble Spore Proteins of *Bacillus subtilis*. *Journal of Bacteriology*, 146, 3, 972-982
- Jordan, E. T., Collins, M., Terefe, J., Ugozzoli, L. and Rubio, T.** (2008) Optimizing Electroporation Conditions in Primary and Other Difficult-to-Transfect Cells. *Journal of Biomolecular Techniques*, 19, 5, 328-334
- Kan, N. C., Lautenberger, J. A., Edgell, M. H. and Hutchison, C. A.** (1979) The nucleotide sequence recognized by the Escherichia coli K12 restriction and modification enzymes. *Journal of Molecular Biology*, 130, 2, 191-209
- Kaneshina, S., Tanaka, M. and Tomida, T.** (1974) Micelle formation of sodium alkylsulfate under high pressures. *Journal of Colloid and Interface Science*, 48, 3, 450-465

- Karbstein, H., Schubert, H., Scigalla, W. and Ludwig, H.** (1992) Sterilization of emulsions by means of high pressure. *In High pressure and biotechnology, Colloques INSERM/John Libbey Eurotext Ltd.*, 224; 345-348
- Kessler, H. G.** (2002) Food and Bio Process Engineering: Dairy Technology. A. Kessler (Publishing House A. Kessler) • München
- Keynan, A., Evenchik, Z., Halvorson, H. O. and Hastings, J. W.** (1964) Activation of bacterial endospores. *Journal of Bacteriology*, 88, 2, 313-318
- Kihm, D. J., Hutton, M. T., Hanlin, J. H. and Johnson, E. A.** (1990) Influence of transition metals added during sporulation on heat resistance of *Clostridium botulinum* 113B spores. *Applied and Environmental Microbiology*, 56, 3, 681-685
- Kim, H., Hahn, M., Grabowski, P., McPherson, D. C., Otte, M. M., Wang, R., Ferguson, C. C., Eichenberger, P. and Driks. A.** (2006) The *Bacillus subtilis* spore coat protein interaction network. *Molecular Microbiology*, 59, 2, 487-502
- Kirk, D. G., Dahlsten, E., Zhang, Z., Korkeala, H. and Lindström, M.** (2012) Involvement of *Clostridium botulinum* ATCC 3502 Sigma Factor K in Early-Stage Sporulation. *Applied and environmental microbiology*, 78, 13, 4590-4596
- Kirk, D. G., Zhang, Z., Korkeala, H. and Lindström, M.** (2014) Alternative Sigma Factors SigF, SigE, and SigG Are Essential for Sporulation in *Clostridium botulinum* ATCC 3502. *Applied and Environmental Microbiology*, 80, 16, 5141-5150
- Kneuttinger, A. C., Heil, K., Kashiwazaki, G. and Carell, T.** (2013) The radical SAM enzyme spore photoproduct lyase employs a tyrosyl radical for DNA repair. *Chemical Communications*, 49, 7, 722-724
- Knorr, D.** (1995) Hydrostatic pressure treatment of food: microbiology. In: Gould, G. W.: New methods of food preservation. *Blackie Academic & Professional, an imprint of Chapman & Hall, London, Glasgow, Weinheim, New York, Tokyo, Melbourne, Madras*, 159 – 175.
- Koshikawa, T., Yamazaki, M., Yoshimi, M., Ogawa, S., Yamada, A., Watabe. K. and Torii M.** (1989) *Journal of General Microbiology*, 135, 10, 2717-2722
- Krzikalla, K. I.** (2007) Hochdruckinduzierte Veränderungen von Lebensmittelinhaltsstoffen. *Dissertation, Fakultät III – Prozesswissenschaften der Technischen Universität Berlin*
- Kuehne, S. A., Heap, J. T., Cooksley, C. M., Cartman, S. T. and Minton, N.P.** (2012) Clostron-mediated engineering of *Clostridium*. *Bioengineered*, 3,4, 247-254
- Kurochkin, B. and Emelyanchik, K.** (1973) Seal meat as a source of botulism. *Voprosy pitaniia*, 1, 141-148
- Laemmli, U. K.** (1970) Cleavage of Structural Proteins during the Assembly of the Head of Bacteriophage T4. *Nature*, 227, 680-685
- Laflamme, C., Lavigne, S., Ho, J. and Duchaine, C.** (2004) Assessment of bacterial endospore viability with fluorescent dyes. *Journal of Applied Microbiology*, 96, 684–692

- Lampkowska, J., Feld, L., Monaghan, A., Toomey, N., Schjørring, S., Jacobsen, B., van der Voet, H., Andersen, S. R., Bolton, D., Aarts, H., Krogfelt, K. A., Wilcks, A. and Bardowski, J.** (2008) A standardized conjugation protocol to assess antibiotic resistance transfer between lactococcal species. *International journal of food microbiology*, 127, 1-2, 172-175
- Lang, O. W.** (1935) Thermal processes for canned marine products. *Berkeley, Univ. of California Press, Publications in public health*, 2, 1, 1-182
- Lautenberger, J. A., Kan, N. C., D. Lackays, D., Linn, M., EDGELI, H. et al.,** (1978) Recognition site of *Escherichia coli* B restriction enzyme on 4XsB1 and simian virus 40 DNAs: an interrupted sequence. *Proceedings of the National Academy of Sciences of the USA*, 75: 2271-2275
- Lee, J. K., Movahedi, S., Harding, S. E., Mackey, B. M. and Waites, W. M.** (2007) Effect of small, acid-soluble proteins on spore resistance and germination under a combination of pressure and heat treatment. *Journal of Food Protection*, 70, 9, 2168-2171
- Lenz, C. A. and Vogel R. F.** (2014) Effect of sporulation medium and its divalent cation content on the heat and high pressure resistance of *Clostridium botulinum* type E spores. *Food Microbiology*, 44, 156-167
- Lequette, Y., Garenaux, E., Tauveron, G., Dumez, S., Perchat, S., Slomianny, C., Lereclus, D., Guerardel, Y. and Faille, C.** (2011) Role Played by Exosporium Glycoproteins in the Surface Properties of *Bacillus cereus* Spores and in Their Adhesion to Stainless Steel. *Applied and Environmental Microbiology*, 77, 14, 4905-4911
- Lesemann, M., Thirumoorthy, K., Joong Kim, Y., Jonas, J. and Paulaitis, M. E.** (1998) Pressure Dependence of the Critical Micelle Concentration of a Nonionic Surfactant in Water Studied by H-NMR. *Langmuir*, 14, 19, 5339-5341
- Lichtenberg, D., Rosenberg, M., Sharfman, N. and Ofek, I.** (1985). A kinetic approach to bacterial adherence to hydrocarbon. *Journal of Microbial Methods*, 4, 141-146
- Losick, R. and Pero, J.** (1981) Cascades of sigma factors, *Cell*, 25, 3, 582-584
- Lück, E. and Jager, M.** (1995) Chemische Lebensmittelkonservierung Stoffe, Wirkungen, Methoden. 3. Edition; Springer-Verlag: Berlin, Heidelberg, New York, Barcelona, Budapest, Hong Kong, London, Mailand, Paris, Tokyo, 1995.
- Lynd, L. R., van Zyl, W. H., McBride, J. E., Laser, M.** (2005) Consolidated bioprocessing of cellulosic biomass: an update. *Current Opinion in Biotechnology*, 16,5, 577-583.
- Macdonald, T. E., Helma, C. H., Shou, Y., Valdez, Y. E., Ticknor, L.o., Foley, B. T., Davis, S. W., Hannett, L. O., Kelly-Cirino, C. D., Barash, J. R., Arnon, S.S., Lindström, M., Korkeala, H., Smith, L.A., Smith, T. J., & Hill, K.K.** (2011). Analysis of *Clostridium botulinum* serotype E strains by using multilocus sequence typing, amplified fragment length polymorphism, variable-number tandem-repeat analysis, and botulinum neurotoxin gene sequencing. *Applied and Environmental Microbiology*, 77,24, 8625-8634

- Margosch, D., Gänzle, M. G., Ehrmann, M. A and Vogel, R. V.** (2004) Pressure Inactivation of *Bacillus* Endospores. *Applied and Environmental Microbiology*, 70, 12, 7321-7328
- Margosch, D., Ehrmann, M. A., Gänzle, M. G. and Vogel, R. F.** (2004 b) Comparison of pressure and heat resistance of *Clostridium botulinum* and other endospores in mashed carrots. *Journal of Food Protection*, 67, 11, 2530-2537
- Margosch, D.** (2004 c) Behaviour of bacterial endospores and toxins as safetydeterminants in low acid pressurized food. *Dissertation, Wissenschaftszentrum Weihenstephan für Ernährung, Landnutzung und Umwelt der Technischen Universität München/Weihenstephan*
- Margosch, D., Ehrmann, M. A., Buckow, R., Heinz, V., Vogel, R. F. and Gänzle, M. G.** (2006). High-pressure-mediated survival of *Clostridium botulinum* and *Bacillus amyloliquefaciens* endospores at high temperature. *Applied and Environmental Microbiology*, 72, 3476-3481
- Mascher, G., Derman, Y., Kirk, D. G., Palonen, E., Lindström, M. and Korkeala, H.** (2013) The two-component system CLO3403/CLO3404 of *Clostridium botulinum* E1 Beluga is important for cold-shock response and growth at low temperature. *Applied and Environmental Microbiology*, 80, 1, 399-407
- Mathys, A. and Knorr, D.** (2009) High-pressure processing. In: *Stadler, R. H. and Lineback, D. R., Process-Induced Food Toxicants: Occurrence, Formation, Mitigation, and health risks.* Wiley, Hoboken, New Jersey
- Matz, L. L., Beaman, T. C and Gerhardt, P.** (1970) Chemical Composition of Exosporium from Spores of *Bacillus cereus*. *Journal of bacteriology*, 101, 1, 196-201
- May, M. S. and Hattaman, S.** (1975) Deoxyribonucleic acid-cytosine methylation by host- and plasmid-controlled enzymes. *Journal of Bacteriology*, 122, 129-138
- McClements, D. J.** (2004) *Food Emulsions: Principles, Practices, and Techniques*, Second Edition. *CRC Press*
- Melly, E., Genest, P. C., Gilmore, M. E., Little, S., Popham, D. L., Driks, A. and Setlow P.** (2002) Analysis of the properties of spores of *Bacillus subtilis* prepared at different temperatures. *Applied and Environmental Microbiology*, 92, 6, 1105-1115
- Mermelstein, L. D. and Papoutsakis, E. T.** (1993). In Vivo methylation in *Escherichia coli* by the *Bacillus subtilis* phage -3T I methyltransferase to protect plasmids from restriction upon transformation of *Clostridium acetobutylicum* ATCC 824. *Applied and Environmental Microbiology*, 59, 4, 1077-1081
- Miller, R. J.** (2006) Verteilung und Inaktivierung von Mikroorganismen in binären Systemen (Öl-in-Wasser-Emulsionen). *Dissertation, Wissenschaftszentrum Weihenstephan für Ernährung, Landnutzung und Umwelt der Technischen Universität München/Weihenstephan, Fachgebiet: Haushalts- und Betriebshygiene*
- Molin, M. and Snygg, B. G.** (1967) Effect of Lipid Materials on Heat Resistance of Bacterial Spores. *Applied Microbiology*, 15, 6, 1422-1426

- Morales, P., Calzada, J., Rodríguez, B., de Paz, M., Gaya, P. and Nuñez, M.** (2006) Effect of cheese water activity and carbohydrate content on the barotolerance of *Listeria monocytogenes* Scott A. *Journal of Food Protection*, 69, 6, 1328-1333
- Müller, G. and Weber, H.** (1996) Mikrobiologie der Lebensmittel Grundlagen. *Behr's Verlag, Hamburg*
- Montoyaa, D., Spitiaa, S., Silvab, E. and Schwarzc, W. H.** (2000) Isolation of mesophilic solvent-producing clostridia from Colombian sources: physiological characterization, solvent production and polysaccharide hydrolysis. *Journal of Biotechnology*, 79, 2, 117-126
- Nicholson, W. L., Munakata, N., Horneck, G., Melosh, H. J. and Setlow, P.** (2000) Resistance of Bacillus Endospores to Extreme Terrestrial and Extraterrestrial Environments. *Microbiology and Molecular Biology Reviews*, 64, 3, 548-572
- Offen, H. W. and Turley, W. D.** (1982) Pressure-induced phase transition of MyTAB micelles in water. *Journal of Colloid and Interface Science*, 87, 2, 442-446
- Oomes, S. J., Jonker, M. J., Wittink, F. R., Hehenkamp, J. O., Breit, T. M., Brul, S.** (2009) The effect of calcium on the transcriptome of sporulating *B. subtilis* cells. *International Journal of Food Microbiology*, 133, 3, 234-243
- Orlien, V. L., Boserup, L. K. and Olsen, K.** (2010) Casein micelle dissociation in skim milk during high-pressure treatment: Effects of pressure, pH and temperature. *Journal of Dairy Science*, 93, 12-18
- Oultram, J. D., Loughlin, M., Swinfield, T.-J., Brehm, J. K., Thompson, D. E. and Minton, N. P.** (1988) Introduction of plasmids into whole cells of *Clostridium acetobutylicum* by electroporation. *FEMS Microbiology Letters*, 56, 1, 83-88
- Paget, M. S. and Helmann, J. D.** (2003) The sigma 70 family of sigma factors. *Genome Biology*, 4, 1, 203
- Paidhungat, M., Setlow, B., Driks, A. and Setlow, P.** (2000) Characterization of Spores of *Bacillus subtilis* Which Lack Dipicolinic Acid. *Journal of Bacteriology*, 182, 19, 5505-5512
- Paidhungat, M., Setlow, B., Daniels, W. B., Hoover, D., Papafragkou, E. and Setlow, P.** (2002) Mechanisms of Induction of Germination of *Bacillus subtilis* Spores by High Pressure. *Applied and Environmental Microbiology*, 68, 6, 3172-3175
- Pan, L. G., Tomás, M.C. and Añón, M.C.** (2004) Oil-in-Water Emulsions Formulated with Sunflower Lecithins: Vesicle Formation and Stability. *Journal of Oil & Fat Industries* 81, 3, 241-244
- Paredes, C. J., Alsaker, K. V., Papoutsakis, E. T.** (2005) *Nature Reviews Microbiology*, 3, 969-978
- Paredes-Sabja, D., Setlow, P., Sarker, M. R.** (2011) Germination of spores of *Bacillales* and *Clostridiales* species: mechanisms and proteins involved. *Trends in Microbiology*, 19, 2, 85-94
- Patterson, M. F., Linton, M. and Doona, C. J.** (2007) in *Doona C. J., Florence E. F., High Pressure Processing of Food*. IFT Press, Chicago, Chapter 1

- Peck, M. W., Fairbairn, D. A. and Lund, B. M.** (1992) The effect of recovery medium on the estimated heat-inactivation of spores of non-proteolytic *Clostridium botulinum*. *Letters in Applied Microbiology*, 15, 4, 146-151
- Perkins, W. E. and Tsuju, K.** (1962) Sporulation of *Clostridium botulinum* II. Effect of argenin and its degradation products on sporulation in a synthetic medium. *Journal of bacteriology*, 84, 86-94
- Perutka, J., Wang, W., Goerlitz, D. and Lambowitz, A. M.** (2004) Use of computer-designed group II introns to disrupt *Escherichia coli* DExH/D-box protein and DNA helicase genes. *Journal of Molecular Biology*, 336, 2, 421-439
- Pfister, M.K.-H., Butz, P., Heinz, V., Dehne, L. I., Knorr, D. and Tauscher, B.** (2000) Der Einfluss der Hochdruckbehandlung auf chemische Veränderungen in Lebensmitteln. *Bundesinstitut für gesundheitlichen Verbraucherschutz und Veterinärmedizin, Pressestelle: Berlin*
- Pingoud, A. and Jeltsch, A.** (2001) Structure and function of type II restriction endonucleases. *Nucleic Acid Research*, 29, 18, 3705-3727
- Popham, D. L., Illades-Aguiar, B. and Setlow, P.** (1995) The *Bacillus subtilis* dacB gene, encoding penicillin-binding protein 5*, is part of a three-gene operon required for proper spore cortex synthesis and spore core dehydration. *Journal of Bacteriology*, 177, 16, 4721-4729
- Popham, D. L., Helin, J., Costello, E. E. and Setlow, P.** (1996 b) Analysis of the peptidoglycan structure of *Bacillus subtilis* endospores. *Journal of Bacteriology*, 178, 22, 6451-6458
- Popham, D. L., Helin, J., Costello, C. E. and Setlow, P.** (1996 a) Muramic lactam in peptidoglycan of *Bacillus subtilis* spores is required for spore outgrowth but not for spore dehydration or heat resistance. *Proceedings of the National Academy of Sciences*, 93, 26, 15405-15410
- Powell, I. B., Achen, M. G., Hillier, A. J. and Davidson, B. E.** (1988) A Simple and Rapid Method for Genetic Transformation of Lactic Streptococci by Electroporation. *Applied and Environmental Microbiology*, 54, 3, 655-660
- Purdy, D., O’Keeffe, T. A. T., Elmore, M., Herbert, M., McLeod, A., Bokori-Brown, M., Ostrowski, A. and Minton, N. P.** (2002) Conjugative transfer of clostridial shuttle vectors from *Escherichia coli* to *Clostridium difficile* through circumvention of the restriction barrier. *Molecular Microbiology*, 46, 2, 439–452
- Qina, B-L., Pothakamurya, U. R., Barbosa-Cánovasa, G. V., Swanson, B. G. and Pelegc, M.** (2009) Nonthermal pasteurization of liquid foods using high-intensity pulsed electric fields. *Critical Reviews in Food Science and Nutrition*, 36, 6, 603-627
- Nonthermal pasteurization of liquid foods using high-intensity pulsed electric fields
- Raju, D., Waters, M., Setlow, P. and Sarker, M, R.** (2006) Investigating the role of small, acid-soluble spore proteins (SASPs) in the resistance of *Clostridium perfringens* spores to heat. *BMC Microbiology*, 6, 50

- Reineke, K., Doehner, I., Schlumbach, K., Baier, D., Mathys, A. and Knorr, D.** (2011) The different pathways of spore germination and inactivation in dependence of pressure and temperature. *Innovative Food Science and Emerging Technologies*, 13, 31-41
- Roberts, T. A.** (1965) Sporulation of *Clostridium botulinum* Type E in Different Culture Media. *Journal of Applied Bacteriology*, 28, 1, 142-146
- Roberts, T. A., Ingram, M. and Skulberg, A.** (1965) The Resistance of Spores of *Clostridium botulinum* Type E to Heat and Radiation. *Journal of Applied Bacteriology*, 28, 1, 125-141
- Roberts, J. R., Belfort, M., Bestor, T., Bhagwat, A. S., Bickle, T. A., Bitinaite, J., Blumenthal, R. M., Degtyarev, S. K. H., Dryden, D. T. F., Dybvig, K. et al.** (2003) A nomenclature for restriction enzymes, DNA methyltransferases, homing endonucleases and their genes. *Nucleic Acids Research*, 31, 7, 1805-1812
- Rodiles-López, J. O., Jaramillo-Flores, M. E., Gutiérrez-López, G. F., Hernández-Aranab, A., Fosado-Quiroz, R. E., Barbosa-Cánovas, G. V. and Hernández-Sánchez, H.** (2007) Effect of high hydrostatic pressure on bovine α -lactalbumin functional properties. *Journal of Food Engineering*, 87, 3, 363-37
- Richard, J. R., Tamas, V., Janos, P. and Macelis, D.** (2005) REBASE—restriction enzymes and DNA methyltransferases. *Nucleic Acids Research*, 33, 230-232
- Salager, J-L., Andérez, J. M., Briceño, M. I., Pérez de Sánchez, M. and Ramírez de Gouveia, M.** (2002) Emulsification yield related to formulation and composition variables as well as stirring energy. *Revista Técnica de la Facultad de Ingeniería Universidad del Zulia*, 25, 3, 129-139
- Sale, J. H., Gould, G. W. and Hamilton W. A.** (1970) Inactivation of Bacterial Spores by Hydrostatic Pressure. *Journal of General Microbiology*, 60, 3, 323-334
- Sambrook, J., Fritsch, E. F. and Maniatis, T.** (1989) *Molecular Cloning: a Laboratory Manual*. (2. edition). Cold Spring Harbor Laboratory, Cold Spring Harbor, New York, USA
- Sarker, M. R., Akhtar, S., Torres, J. A., Paredes-Sabja, D.** (2013) High hydrostatic pressure-induced inactivation of bacterial spores. *Critical Reviews in Microbiology*, Posted online
- Sasaki, Y., Taketomo, N. and Sasaki, T.** (1988) Factors affecting transfer frequency of pAM beta 1 from *Streptococcus faecalis* to *Lactobacillus plantarum*. *Journal of Bacteriology*, 170, 12, 5939-5942
- Sauer, U., Santangelo, J. D., Treuner, A., Buchholz, M. and Dürre, D.** (1995) Sigma factor and sporulation genes in *Clostridium*. *FEMS Microbiology Reviews*, 17, 3, 331-340
- Schlegel, H. G.** (1992) *Allgemeine Mikrobiologie*. Georg Thieme Verlag, Stuttgart, New York, 7. überarbeitete Auflage, p. 79-83

- Selby, K., Lindström, M., Somervuo, P., Heap, J. T., Minton, N. P. and Korkeala, H.** (2011) Important Role of Class I Heat Shock Genes *hrcA* and *dnaK* in the Heat Shock Response and the Response to pH and NaCl Stress of Group I *Clostridium botulinum* Strain ATCC 3502. *Applied and Environmental Microbiology*, 77, 9, 2823-2830
- Senhaji, A. F. and Loncin, M.** (1977) The protective effect of fat on the heat resistance of bacteria (I). *International Journal of Food Science & Technology*, 12, 3, 203-216
- Senhaji, A. F.** (1977) The protective effect of fat on the heat resistance of bacteria (II). *International Journal of Food Science & Technology*, 12, 3, 217-230
- Setlow, P.** (1985) Protein degradation during bacterial spore germination. In *Fundamental and Applied Aspects of bacterial Spores*, ed. Ellar, London Academic, 285-296
- Setlow, P.** (1995) Mechanisms for the Prevention of Damage to DNA in Spores of Bacillus Species. *Annual Review of Microbiology*, 49, 29-54
- Setlow, P.** (2003) Spore germination. *Current Opinion in Microbiology*, 6, 6, 550-556
- Setlow, P.** (2007) in Doona C. J., Florence E. F., *High Pressure Processing of Food*. IFT Press, Chicago, p. 15
- Setlow, B., Peng, L., Loshon, C. A., Li, Y.-Q., Christie, G. and Setlow, P.** (2008) Characterization of the germination of *Bacillus megaterium*. *Journal of Applied Microbiology*, 107, 1, 318-328
- Shibauchi, H., Yamamoto, Y. and Sagara, Y.** (1992) Conformational change of casein micelles by high pressure treatment. *High pressure and Biotechnology, J. Libbey Eurotext*, 239-242
- Shinoda, K. and Arai, H.** (1964) The Correlation between Phase Inversion Temperature In Emulsion and Cloud Point in Solution of Nonionic Emulsifier. *The Journal of Physical Chemistry*, 68, 12, 3485-3490
- Simpson, R. K. and Gilmour, A.** (1997) The effect of high hydrostatic pressure on *Listeria monocytogenes* in phosphate-buffered saline and model food systems. *Journal of Applied Microbiology*, 83, 2, 181-188
- Sjöblom, J.** (2006) Emulsions and Emulsion Stability: Surfactant Science Series/61. CRC Press Taylor and Francis Group, LLC
- Slesarewski, W.** (1931) Über die Widerstandsfähigkeit der Bakterien bei Erhitzen derselben in Fettstoffen. *Zeitschrift für Fleisch- und Milchhygiene*, 42, 30-32
- Söderholm, H., Lindström, M., Somervuo, P., Heap, J., Minton, N., Lindén, J. and Korkeala, H.** (2011) *cspB* encodes a major cold shock protein in *Clostridium botulinum* ATCC 3502. *International journal of food microbiology*, 146, 1, 23-30
- Srikhanta, Y. N., Fox, K. L. and Jennings, M. P.** (2010) The phasevarion: phase variation of type III DNA methyltransferases controls coordinated switching in multiple genes. *Nature*, 465, 8, 194-206

- Stecchini, M. L., Spaziani, M., Del Torre, M. and Pacor S.** (2009) *Bacillus cereus* cell and spore properties as influenced by the micro-structure of the medium. *Applied and environmental microbiology*, 106, 6, 1838-1848
- Studier, F.W. and Bandyopadhyay, P.K.** (1988) Model for how type I restriction enzymes select cleavage sites in DNA. *Proceedings of the National Academy of Sciences of the United States of America*, 88, 13, 4677-4681
- Stewart, M., Somlyo, A. P., Somlyo, A. V., Shuman, H., Lindsay, J. A., Murrell, W. G.** (1980) Distribution of calcium and other elements in cryosectioned *Bacillus cereus* T spores, determined by high-resolution scanning electron probe x-ray microanalysis. *Journal of Bacteriology*, 43, 1, 481-491
- Sugiyama, H.** (1951) studies on factors affecting the heat resistance of *Clostridium botulinum*. *Journal of Bacteriology*, 62, 1, 81-96
- Suzuki, H.** (2012) Host-Mimicking Strategies in DNA Methylation for Improved Bacterial Transformation. *Methylation - From DNA, RNA and Histones to Diseases and Treatment, InTech, Chapter 9*
- Swiatek, P. J., Allen, S. D., Siders, A. J. and Lee, H. C.** (1987) DNase production by *Clostridium septicum*. *Journal of Clinical Microbiology*. 25, 2, 437-438
- Takamatsu, H., Kodama, T. and Watabe, K.** (1999) Assembly of the CotSA coat protein into spores requires CotS in *Bacillus subtilis*. *FEMS Microbiology Letters*, 174, 1, 201-206
- Takumi K, Kinouchi T and Kawata T.** (1979) Isolation and partial characterization of exosporium from spores of a highly sporogenic mutant of *Clostridium botulinum* type A. *Microbiology and Immunology*, 23, 6, 443-454
- Tardif, C., Maamar, H., Balfin, M. and Belaich, J. P.** (2001) Electrotransformation studies in *Clostridium cellulolyticum*. *Journal of Industrial Microbiology & Biotechnology*, 27, 271-274
- Ting, E., Balasubramaniam, V.M., Raghubeer, E.** (2002) Determining thermal effects in high pressure processing. *Food Technology*, 56, 31-35
- Tock, M. R. and Dryden, D. T.** (2005) The biology of restriction and anti-restriction. *Current Opinion in Microbiology*, 8, 4, 466-472
- Tonello-Samson, C.** (2014) Industrial Applications of High Pressure Processing in Food Industries. *Book of Abstracts, 8th international Conference on High Pressure Bioscience and Biotechnology, France, p. 48*
- Tsuji, K. and Perkins, W. E.** (1962) Sporulation of *Clostridium botulinum* I. *Journal of Bacteriology*, 84, 1, 81-85
- Usbeck, J. C., Kern C. C., Vogel R. F. and Behr, J.** (2013) Optimization of experimental and modelling parameters for the differentiation of beverage spoiling yeasts by Matrix-Assisted-Laser-Desorption/Ionization–Time-of-Flight Mass Spectrometry (MALDI–TOF MS) in response to varying growth conditions. *Food Microbiology*, 36, 2, 379-387

- Warth, A. D.** (1978) Molecular structure of the bacterial spore. *Advances in Microbial Physiology*, 17, 1-47
- Whitmer, M. E. and Johnson, E. A.** (1988) Development of improved defined media for *Clostridium botulinum* serotypes A, B, and E. *Applied and environmental microbiology*, 54, 3, 753-759
- Wienczek, K. M., Klapes, N. A. and Foegeding, P. M.** (1990) Hydrophobicity of Bacillus and Clostridium spores. *Applied and environmental microbiology*, 56, 9, 2600-2605
- Wilsona, D. R., Dabrowskia, L., Stringera, S., Moezelaarb, R. and Brocklehursta, T. F.** (2008) High pressure in combination with elevated temperature as a method for the sterilisation of food. *Trends in Food Science & Technology*, 19, 6, 289-299
- Winter, R.** (2001) Effects of hydrostatic pressure on lipid and surfactant phases. *Current Opinion in Colloid & Interface Science*, 6, 3, 303-312
- WU, S., LO, S. K., SHAO, C. P., TSAI, H. W., and HOR, L. I.** (2001) Cloning and Characterization of a Periplasmic Nuclease of *Vibrio vulnificus* and Its Role in Preventing Uptake of Foreign DNA. *Applied and environmental microbiology*, 67, 1, 82-88
- Wuytack, E. Y., Boven, S. and Michiels, C. W.** (1998) Comparative study of pressure-induced germination of Bacillus subtilis spores at low and high pressures. *Applied and environmental microbiology*, 64, 9, 3220-3224
- Wuytack, E. Y., Soons, J., Poschet, F. and Michiels, C. W.** (2000) Comparative Study of Pressure- and Nutrient-Induced Germination of *Bacillus subtilis* Spores. *Applied and environmental microbiology*, 66, 1, 257-261
- Wuytack, E. Y. and Michiels, C. W.** (2001) A study on the effects of high pressure and heat on *Bacillus subtilis* spores at low pH. *International Journal of Food Microbiology*, 64, 3, 333-341
- Wyszynski, M., Gabbara, S. and Bhagwat, A. S.** (1993) Cytosine deaminations catalyzed by DNA cytosine methyltransferases are unlikely to be the major cause of mutational hot spots at sites of cytosine methylation in *Escherichia coli*. *Genetics*, 91, 4, 1574-1578
- Zhou, Y. and Johnson, E. A.** (1993) Genetic transformation of *Clostridium botulinum* hall a by electroporation. *Biotechnology Letters*, 15, 2, 121-126
- Zhou, Y., Sugiyama, H. Nakano, H. and Johnson, E. A.** (1995) The Genes for the *Clostridium botulinum* Type G Toxin Complex Are on a Plasmid. *Infection and Immunity*, 63, 5, 2087-2091
- Zhu, X., Ye, A., Teo, H. J., Lim, S. J. and Singh, S.** (2014) Oxidative stability of fish oil-in-water emulsions under high-pressure treatment. *International Journal of Food Science & Technology*, 49, 6, 1441-1448
- Zuccaro, J. B., Powers, J. J., Morse, R. E. and Mills W. C.** (1951) The thermal death times of yeast in oil and movement of the yeast between the oil and the water phases of French dressing. *Food Research*, 16, 1-6, 30-38

APPENDIX**DNA sequence of the methyltransferase gene (CLO_1092) of *C. botulinum* (TMW 2.990), which is adapted to the codon usage of *E. coli***

CTCGAGTCTGAAAATTGCAACCGTGTTTAGCGGTATTGGTGCAATTGAACATGCACTGAAAC
GCATTGGTATCGAACATGAAATTGTTTTTCGCAAGCGATAATGGCGAAGTGAACATCTTCAA
AAAAACATCGGCACCAACTTCATCGACATCAAAAATGAACTGGACCGCCTGAAAAAATCAT
CAAAGAAATCGATATCAAAGTGGAAAGCGACTATGAGTATCTGACCGATCTGGATCAGCATC
TGAATCGCATTAACTATAAAGTTGTGGAAGTGCAGAATCAGTGCAATAATACCACCCTGGAT
GTGAACTATATCCTGAACGAAATCGAAGATGAAAAAGTAAAAAAGAGATCGAGAAAATCTA
CAAAAATACGATAGCTTCACCAACATCGAGGATGTTGATAAAGTTCTGATTCTGGGCCTGA
TCGAAAAAGTAACAAAAAATGTTCAAACAGGTGAGCGTGAACACCGATATTAACACCAAA
CTGGTTCTGAAAGAGGTGAAAGAAGTTATCGTACAGCTGAACATGCTGGATGAAAAAATTGA
AACCTGCATATCCATAGCGAACTGCGCAAAATTGAAGATTATACCGAGAAAAAATAATG
TGGATAACCTGTATAAAGGCAAAGAAAAAAGCAACTTTGTGAAACAGAGCTATTTTCGCCAAC
TATGATATTACCGATGAACGCTTTCATTGGAACGTGAGCTTTATTGATGGTGCCAGTATAC
CAATAAAGTGGACCTGTTTGTGGTGGTAGCCCGTGTGAGAGCTTTAGCATGGTTGGTAAAC
AGCGTGGTCTGGGTGATACCCGTGGCACCCTGTTTTTATGAATATGCACGTCTGGTTAAAGAG
ATCCAGCCGAAAGTTTTTATCTATGAGAATGTTAAAGCCGTGCTGAGCAATGATGGTGGTAA
AACCTGGAATACCATGAGCCAGATTTTCGATGATCTGGGTTATCAGTGGAAACTGATGGTGC
TGAATAGCAAAGATTATGGTGTGTCACAGAATCGCGAACGTATTTTTGTTGTGGGTTTTTCGT
AATGATCTGGAAGTGGTTAAACCGTTTTGAAGAACCGGAAAAAGTGAACCTGAACAAAAAAT
GAAAGATTATCTGCTGGATAACGTGAGCGGCAAATATTACCTGAATAGTAAAGGTGTTGCCT
TCGTGACCGATAACAAAAACCTGCAGAAAAAATGGACCCAGATTGATGGCGATATTCAGCTG
TGTCAGAAAAAAACCAGCAGTTTTAATTGGCACGGCGATTTTTGTTTTTGTGGAAGAAAAACA
AAACATGGATAAAACCATGCACGATCTGGAAAAATACTTCCTGAGCGAGAAAGTCGAGAAAT
ATGTTCTGAGCAGCGGCACCAAAAACCTTTTATAGCAAACCGAAAATTGACCTGGAAGTTGCA
CGTCCGCTGCTGACCACCATGCATAAAATGCATCGTGCCGGTGTGATAATTATGTTACCAC
CGAAGGTCGTATTCGTAAACTGACACCGCGTGAATGTCTGCGTCTGATGGGTTTTTGTGATA
GCTTTAAAATCGTTGTGAGCGACACCCAGATTTATCAGCAGGCAGGTAATAGCATTGTTGTG
GATGTTCTGATTGCCATCGTCAACAAAATTATCGAAAGCCTGCCGAACATTATTGAGGGTAA
AGGCTATAATTACAAAAGCACCATTAACAACAATGTGAACAAAACCAACCGGAACAAACAGC
TGAA ACTGGTTGCATTTGATCGCGAATAAAAGCTT

Group II intron sequence of pMTL007C-E2:53143-Cbo-ssp1237

AGCTTATAATTATCCTTAATATTCCAAAATGTGCGCCAGATAGGGTGTAAAGTCAAGTAGT
TTAAGGTACTACTCTGTAAGATAACACAGAAAACAGCCAACCTAACCGAAAAGCGAAAGCTG
ATACGGGAACAGAGCACGTTGGAAAGCGATGAGTTACCTAAAGACAATCGGGTACGACTGA
GTCGCAATGTTAATCAGATATAAGGTATAAGTTGTGTTTACTGAACGCAAGTTTTCTAATTT
GGTTAATATCCGATAGAGGAAAAGTGTCTGAAACCTCTAGTACAAAGAAAGGTAAGTTAGCAT
TTTGGACTTATCTGTTATCACCACATTTGTAC

Group II intron sequence of pMTL007C-E2:43973-Cbo-ssp3241

AGCTTATAATTATCCTTAAATGTCGTTCCGGTGCGCCAGATAGGGTGTTAAGTCAAGTAGT
TTAAGGTACTACTCTGTAAGATAACACAGAAAACAGCCAACCTAACCGAAAAGCGAAAGCTG
ATACGGGAACAGAGCACGGTTGGAAAGCGATGAGTTACCTAAAGACAATCGGGTACGACTGA
GTCGCAATGTTAATCAGATATAAGGTATAAGTTGTGTTTACTGAACGCAAGTTTCTAATTTT
GGTTACATTCCGATAGAGGAAAGTGTCTGAAACCTCTAGTACAAAGAAAGGTAAGTTATACG
GAACGACTTATCTGTTATCACCACATTTGTAC

Group II intron sequence of pMTL007C-E2:53142-Cbo-ssp3013

AGCTTATAATTATCCTTAAATGGGCGTACCAGTGCGCCAGATAGGGTGTTAAGTCAAGTAGT
TTAAGGTACTACTCTGTAAGATAACACAGAAAACAGCCAACCTAACCGAAAAGCGAAAGCTG
ATACGGGAACAGAGCACGGTTGGAAAGCGATGAGTTACCTAAAGACAATCGGGTACGACTGA
GTCGCAATGTTAATCAGATATAAGGTATAAGTTGTGTTTACTGAACGCAAGTTTCTAATTTT
GGTTCCCATCCGATAGAGGAAAGTGTCTGAAACCTCTAGTACAAAGAAAGGTAAGTTAAATG
GTACGACTTATCTGTTATCACCACATTTGTAC

Group II intron sequence of pMTL007C-E2:53144-Cbo-gpr

AGCTTATAATTATCCTTAAAACCCGATGTAGTGCGCCAGATAGGGTGTTAAGTCAAGTAGT
TTAAGGTACTACTCTGTAAGATAACACAGAAAACAGCCAACCTAACCGAAAAGCGAAAGCTG
ATACGGGAACAGAGCACGGTTGGAAAGCGATGAGTTACCTAAAGACAATCGGGTACGACTGA
GTCGCAATGTTAATCAGATATAAGGTATAAGTTGTGTTTACTGAACGCAAGTTTCTAATTTT
GGTTGGTTTCCGATAGAGGAAAGTGTCTGAAACCTCTAGTACAAAGAAAGGTAAGTTAACTA
CATCGACTTATCTGTTATCACCACATTTGTAC

Table AI: MALDI-TOF MS based protein identification in TMW 2.990 endospores derived from SFE. The table provides measured peaks and intensities which were acquired by MALDI-TOF MS (first and second column). Based on peak detection and in due consideration of the mass to charge ratio (column three), potential protein/peptide masses were calculated (column four). In the fifth column (mass (db)), protein masses are present, which were provided by UniProtUK or resulted from trypsin digestion (calculated by the PeptideMass tool, provided on the ExPASy portal). The sixth column (mass (db) + PTM) represents the peptide masses of column five by considering of post translational modifications (column eight). Resulting isoelectric points are illustrated in column seven. In column nine, database entries of identified proteins are depicted, secondary protein names are specified in column ten. The symbols “_TPRX” behind the protein description indicates the number of peptide fragment, which resulted from trypsin digestion of the identified protein

peak (m/z)	intensity	charge	cal. mass	mass (db)	mass (db) + PTM	pI (db)	modification	UniProtKB entry	protein name_(nr. of peptide after trypsin digestion)
2044	66	1	2043	2028.1	2042.1	7.48	Methylation	C5US15	Stage III sporulation protein AE_TRP8
2044	66	1	2043	2028.3	2042.4	9.6	Methylation	C5US90	Stage II sporulation protein M_TRP6
2051.5	34	1	2050.5	2033.5	2049.5	8.91	Hydroxylation	C5UTB9	Peptidase M56, BlaR1_TRP9
2133.5	151	1	2132.5	2117.4	2133.4	6.54	Hydroxylation	C5UZM9	Putative uncharacterized protein _TRP3
2304	23	1	2303	2285.6	2303.6	5.25	Water	C5UU70	Stage II sporulation protein E_TRP10
2305.2	22	1	2304.2	2285.6	2303.6	5.25	Water	C5UU70	Stage II sporulation protein E_TRP10
2318	25	1	2317	2316.6	2316.6	4.92	unmodified	C5UP92	Germination protease_TRP4
2385.5	114	1	2384.5	2352.7	2384.7	4.93	Dihydroxylation	C5UXW8	Stage IV sporulation protein A_TRP5
2405.5	53	1	2404.5	2389.9	2403.9	7.48	Methylation	C5US15	Stage III sporulation protein AE_TRP6
2417	53	1	2416	2415.7	2415.7	5.08	unmodified	C5URW9	Spore coat protein, CotS family_TRP2
2555.8	14	1	2554.7	2541.8	2555.9	8.77	Methylation	C5UZG3	Spore coat protein S_TRP2
2555.8	14	1	2554.7	2542	2556	9.45	Methylation	C5UPN2	Stage V sporulation protein B_TRP10
2555.8	14	1	2554.7	2542	2556	9.35	Methylation	C5UPN2	Stage V sporulation protein B_TRP10
2628	19	1	2627	2608.2	2626.2	9.38	Water	C5UUT2	Spore maturation protein B_TRP3
2628	19	1	2627	2608.2	2626.2	4.57	Water	C5UUU1	CotH protein_TRP9
2739.8	493	1	2738.7	2722.4	2738.4	9.53	Hydroxylation	C5UXH6	Spore germination protein_TRP7
2836.5	23	1	2835.5	2817.5	2835.5	8.99	Water	C5UZC5	Sporulation protein YunB_TRP1

2930.5	19	1	2929.5	2928.5	2928.5	8.91	unmodified	C5UTB9	Peptidase M56, BlaR1, putative _TRP5
2930.5	19	1	2929.5	2929.2	2929.2	8.05	unmodified	C5UUE9	Spore photoproduct lyase _TRP2
2997	91	1	2996	2969.3	2997.3	4.67	Dimethylation	C5UVG2	Putative spore-cortex-lytic enzyme _TRP6
3213.2	1057	1	3212.2	3196.5	3212.5	8.91	Hydroxylation	C5UTB9	Peptidase M56, BlaR1, putative _TRP3
3309.2	48	1	3308.2	3308.1	3308.1	9.53	unmodified	C5UXH6	Spore germination protein _TRP4
3483.5	791	1	3482.5	3483.2	3483.2	9.66	unmodified	C5UU73	Spore cortex biosynthesis protein YabQ _TRP2
3581.2	1937	1	3580.2	3553.9	3581.9	5.14	Dimethylation	C5URA3	Putative uncharacterized protein _TRP1
3628.8	884	1	3627.7	3613.4	3627.5	9.45	Methylation	C5UPN2	Stage V sporulation protein _TRP5
3628.8	884	1	3627.7	3613.4	3627.5	9.35	Methylation	C5UPN2	Stage V sporulation protein B _TRP5
3673	582	1	3672	3659.1	3673.1	6.54	Methylation	C5UZM9	Putative uncharacterized protein _TRP1
3969	195	1	3968	3948.4	3966.4	5.21	Water	C5UY42	Stage V sporulation protein R _TRP1
4225.2	36	1	4224.2	4208.8	4222.8	4.67	Methylation	C5UVG2	Putative spore-cortex-lytic enzyme _TRP4
4225.2	36	1	4224.2	4211.7	4225.7	9.08	Methylation	C5UXY2	RNA polymerase sigma factor _TRP1
4614.5	139	1	4613.5	4572.9	4615	7.65	Acetylation	C5UP91	Stage II sporulation protein P _TRP1
4624	126	1	4623	4606.9	4621	4.98	Methylation	C5UV84	Spore cortex-lytic enzyme _TRP2
4639.5	136	1	4638.5	4606.9	4638.9	4.98	Dihydroxylation	C5UV84	Spore cortex-lytic enzyme _TRP2
4952.2	48	1	4951.2	4647.2	4952.5	8.93	Glutathionylation	C5UXY8	RNA polymerase sigma factor _TRP1
5098.2	48	1	5097.2	5070.3	5098.3	4.63	Dimethylation	C5UT36	Spore-cortex-lytic enzyme, sleb _TRP1
5098.2	48	1	5097.2	5070.3	5098.3	5.09	Dimethylation	C5UT36	Spore-cortex-lytic enzyme, sleb _TRP1
5189.5	7	1	5188.5	5023.9	5186.1	9.45	Glucosylation	C5UPN2	Stage V sporulation protein B _TRP1
5189.5	7	1	5188.5	5023.9	5186.1	9.35	Glucosylation	C5UPN2	Stage V sporulation protein B _TRP1
5610	7	1	5609	5574.9	5606.9	9.3	Dihydroxylation	C5UZP4	Sigma-K factor processing regulatory protein BofA _TRP1
5653.5	7	1	5652.5	5574.9	5654.9	9.3	Phosphorylation	C5UZP4	Sigma-K factor processing regulatory protein BofA _TRP1
5869	17	1	5868	5849.6	5865.6	4.67	Hydroxylation	C5UVG2	Putative spore-cortex-lytic enzyme _TRP2

6091.8	34	1	6090.7	6092.4	6092.4	8.04	unmodified	C5UY96	Conserved domain protein
6111.8	23	1	6110.7	6092.4	6108.3	8.04	Hydroxylation	C5UY96	Conserved domain protein
6342	219	1	6341	6300.1	6342.1	5.7	Acetylation	C5URF0	Stage V sporulation protein AF_TRP2
6565.8	54	1	6564.7	6483.8	6563.8	5.46	Phosphorylation	C5UTT9	Putative uncharacterized protein_TRP1
6829.8	41	1	6828.7	6817.4	6831.4	6.51	Methylation	C5US13	Stage III sporulation protein AC
9628.8	4	2	19255.5	19221.4	19249.	9.38	Dimethylation	C5UUT2	Spore maturation protein B
9791.8	3	1	9790.7	9710.4	9790.4	9.77	Phosphorylation	C5URS8	Stage III sporulation protein D
10192.8	30	2	20383.5	20387.5	20387.	8.99	unmodified	C5UUT3	Spore maturation protein A

Table All: MALDI-TOF MS based protein identification in TMW 2.990 endospores derived from TPYC. The table provides measured peaks and intensities which were acquired by MALDI-TOF MS (first and second column). Based on peak detection and in due consideration of the mass to charge ratio (column three), potential protein/peptide masses were calculated (column four). In the fifth column (mass (db), protein masses are present, which were provided by UniProtUK or resulted from trypsin digestion (calculated by the PeptideMass tool, provided on the ExPASy portal). The sixth column (mass (db) + PTM) represents the peptide masses of column five by considering of post translational modifications (column eight). Resulting isoelectric points are illustrated in column seven. In column nine, database entries of identified proteins are depicted, secondary protein names are specified in column ten. The symbols “_TPRX” behind the protein description indicates the number of peptide fragment, which resulted from trypsin digestion of the identified protein.

peak (m/z)	intensity	charge	cal. mass	mass (db)	mass (db) + PTM	pI (db)	modification	UniProtKB entry	protein name_(nr. of peptide after trypsin digestion)
2045	64	1	2044	2030.1	2044.2	7.65	Methylation	C5UP91	Stage II sporulation protein P_TRP4
2052.5	32	1	2051.5	2038.3	2052.3	6.09	Methylation	C5UVG3	Putative spore-cortex-lytic enzyme_TRP13
2134.2	30	1	2133.2	2117.4	2133.4	6.54	Hydroxylation	C5UZM9	Putative uncharacterized protein_TRP3
2208.5	15	1	2207.5	2194.3	2208.4	4.57	Methylation	C5UUU1	CotH protein_TRP14
2304.5	23	1	2303.5	2285.6	2303.6	5.25	Water	C5UU70	Stage II sporulation protein E_TRP10
2305.8	23	1	2304.7	2285.6	2303.6	5.25	Water	C5UU70	Stage II sporulation protein E_TRP10
2319.2	26	1	2318.2	2285.6	2317.6	5.25	Dihydroxylation	C5UU70	Stage II sporulation protein E_TRP10

2386.2	125	1	2385.2	2352.7	2384.7	4.93	Dihydroxylation	C5UXW8	Stage IV sporulation protein A _TRP5
2406.2	43	1	2405.2	2389.9	2405.9	7.48	Hydroxylation	C5US15	Stage III sporulation protein AE _TRP6
2418	50	1	2417	2389.9	2418	7.48	Dimethylation	C5US15	Stage III sporulation protein AE _TRP6
2524	27	1	2523	2521.8	2521.8	5.25	unmodified	C5UU70	Stage II sporulation protein E _TRP7
2689	28	1	2688	2674.9	2688.9	4.41	Methylation	C5UYG6	CotJB protein _TRP1
2740.2	77	1	2739.2	2722.4	2738.4	9.53	Hydroxylation	C5UXH6	Spore germination protein _TRP7
2790.8	31	1	2789.7	2790.2	2790.2	6.09	unmodified	C5UVG3	Putative spore-cortex-lytic enzyme _TRP3
2997.5	94	1	2996.5	2969.3	2997.3	4.67	Dimethylation	C5UVG2	Putative spore-cortex-lytic enzyme _TRP6
3214	378	1	3213	3196.5	3212.5	8.91	Hydroxylation	C5UTB9	Peptidase M56, BlaR1_TRP3
3330.5	29	1	3329.5	3286.7	3328.7	4.57	Acetylation	C5UUU1	CotH protein _TRP6
3389.5	23	1	3388.5	3308.1	3388	9.53	Phosphorylation	C5UXH6	Spore germination protein _TRP4
3484	751	1	3483	3483.2	3483.2	9.66	unmodified	C5UU73	Spore cortex biosynthesis protein YabQ _TRP2
3581.8	2039	1	3580.7	3553.9	3581.9	5.14	Dimethylation	C5URA3	Putative uncharacterized protein _TRP1
3629.2	778	1	3628.2	3613.4	3627.5	9.45	Methylation	C5UPN2	Stage V sporulation protein B _TRP5
3629.2	778	1	3628.2	3613.4	3627.5	9.35	Methylation	C5UPN2	Stage V sporulation protein B _TRP5
3787.8	23	1	3786.7	3768.3	3786.3	6.48	Water	C5UXH7	Spore germination protein GerA _TRP2
3820.8	18	1	3819.7	3659.1	3821.3	6.54	Glucosylation	C5UZM9	Putative uncharacterized protein _TRP1
3969.2	185	1	3968.2	3948.4	3966.4	5.21	Water	C5UY42	Stage V sporulation protein R _TRP1
4577.5	72	1	4576.5	4543.1	4575.1	5.6	Dihydroxylation	C5UVY6	ATP-dependent protease_TRP1
4614.8	139	1	4613.7	4572.9	4615	7.65	Acetylation	C5UP91	Stage II sporulation protein P _TRP1
4627.5	123	1	4626.5	4606.9	4624.9	4.98	Water	C5UV84	Spore cortex-lytic enzyme_TRP2
4640.5	137	1	4639.5	4606.9	4638.9	4.98	Dihydroxylation	C5UV84	Spore cortex-lytic enzyme _TRP2
4952.2	71	1	4951.2	4647.2	4952.5	8.93	Glutathionylation	C5UXY8	RNA polymerase sigma factor_TRP1
5098	70	1	5097	5070.3	5098.3	4.63	Dimethylation	C5UT36	Spore-cortex-lytic enzyme_TRP1
5098	70	1	5097	5070.3	5098.3	5.09	Dimethylation	C5UT36	Spore-cortex-lytic enzyme,_TRP1
5647.2	9	1	5646.2	5649	5649	9.66	unmodified	C5UU73	Spore cortex biosynthesis protein YabQ _TRP1

5865.5	14	1	5864.5	5849.6	5863.6	4.67	Methylation	C5UVG2	Putative spore-cortex-lytic enzyme _TRP2
6091.5	40	1	6090.5	6092.4	6092.4	8.04	unmodified	C5UY96	Conserved domain protein
6111.8	37	1	6110.7	6092.4	6108.3	8.04	Hydroxylation	C5UY96	Conserved domain protein
6711.5	17	1	6710.5	6694.5	6708.5	5.19	Methylation	C5URQ3	Small, acid-soluble spore protein beta
6829.2	52	1	6828.2	6817.4	6831.4	6.51	Methylation	C5US13	Stage III sporulation protein AC
7719	7	4	30872	30863.7	30863.	6.11	unmodified	C5US30	Sporulation transcription factor Spo0A
9629.2	30	2	19256.5	19221.4	19249.	9.38	Dimethylation	C5UUT2	Spore maturation protein B
9790.5	6	1	9789.5	9710.4	9790.4	9.77	Phosphorylation	C5URS8	Stage III sporulation protein D
10191.8	47	2	20381.5	20387.5	20387.	8.99	unmodified	C5UUT3	Spore maturation protein A
10287	8	3	30858	30863.7	30863.	6.11	unmodified	C5US30	Sporulation transcription factor Spo0A

Table AIII: MALDI-TOF MS based protein identification in TMW 2.990 endospores derived from M140. The table provides measured peaks and intensities which were acquired by MALDI-TOF MS (first and second column). Based on peak detection and in due consideration of the mass to charge ratio (column three), potential protein/peptide masses were calculated (column four). In the fifth column (mass (db), protein masses are present, which were provided by UniProtUK or resulted from trypsin digestion (calculated by the PeptideMass tool, provided on the ExPASy portal). The sixth column (mass (db) + PTM) represents the peptide masses of column five by considering of post translational modifications (column eight). Resulting isoelectric points are illustrated in column seven. In column nine, database entries of identified proteins are depicted, secondary protein names are specified in column ten. The symbols “_TPRX” behind the protein description indicates the number of peptide fragment, which resulted from trypsin digestion of the identified protein.

peak (m/z)	intensity	charge	cal. mass	mass (db)	mass (db) + PTM	pI (db)	modification	UniProtKB entry	protein name_(nr. of peptide after trypsin digestion)
2044.8	58	1	2043.7	2030.1	2044.2	7.65	Methylation	C5UP91	Stage II sporulation protein P _TRP4
2304.8	19	1	2303.7	2285.6	2303.6	5.25	Water	C5UU70	Stage II sporulation protein E_TRP10
2318.8	18	1	2317.7	2316.6	2316.6	4.92	unmodified	C5UP92	Germination protease _TRP4
2385.8	94	1	2384.7	2352.7	2384.7	4.93	Dihydroxylation	C5UXW8	Stage IV sporulation protein A _TRP5
2404.5	35	1	2403.5	2389.9	2403.9	7.48	Methylation	C5US15	Stage III sporulation protein AE _TRP6
2417.5	47	1	2416.5	2415.7	2415.7	5.08	unmodified	C5URW9	Spore coat protein, CotS family_TRP2

2475.2	12	1	2474.2	2455.7	2473.8	5.28	Water	C5UXH8	Germination protein, Ger(X)C family _TRP4
2670.2	15	1	2669.2	2669	2669	5.01	unmodified	C5URP3	Delta-lactam-biosynthetic de-N-acetylase _TRP1
2670.2	15	1	2669.2	2669	2669	5.5	unmodified	C5URP3	Delta-lactam-biosynthetic de-N-acetylase_TRP1
2689	25	1	2688	2674.9	2688.9	4.41	Methylation	C5UYG6	CotJB protein_TRP1
2735.2	29	1	2734.2	2721.2	2735.2	9.45	Methylation	C5UPN2	Stage V sporulation protein B_TRP9
2735.2	29	1	2734.2	2721.2	2735.2	9.35	Methylation	C5UPN2	Stage V sporulation protein B_TRP9
2997.2	73	1	2996.2	2969.3	2997.3	4.67	Dimethylation	C5UVG2	Putative spore-cortex-lytic enzyme_TRP6
3187.2	40	1	3186.2	3185.8	3185.8	6.51	unmodified	C5US13	Stage III sporulation protein AC_TRP1
3214	75	1	3213	3196.5	3212.5	8.91	Hydroxylation	C5UTB9	Peptidase M56, BlaR1, putative _TRP3
3238.2	46	1	3237.2	3238.7	3238.7	4.67	unmodified	C5UVG2	Putative spore-cortex-lytic enzyme_TRP5
3331	36	1	3330	3286.7	3328.7	4.57	Acetylation	C5UUU1	CotH protein _TRP6
3388.5	15	1	3387.5	3344.2	3386.3	9.6	Acetylation	C5US90	Stage II sporulation protein M_TRP3
3464	79	1	3463	3384.3	3464.3	5.7	Phosphorylation	C5URF0	Stage V sporulation protein AF_TRP4
3484.2	66	1	3483.2	3483.2	3483.2	9.66	unmodified	C5UU73	Spore cortex biosynthesis protein YabQ_TRP2
3581.8	2060	1	3580.7	3553.9	3581.9	5.14	Dimethylation	C5URA3	Putative uncharacterized protein_TRP1
3629	1163	1	3628	3613.4	3627.5	9.45	Methylation	C5UPN2	Stage V sporulation protein B_TRP5
3629	1163	1	3628	3613.4	3627.5	9.35	Methylation	C5UPN2	Stage V sporulation protein B_TRP5
3969.2	261	1	3968.2	3948.4	3966.4	5.21	Water	C5UY42	Stage V sporulation protein R_TRP1
4614.5	96	1	4613.5	4572.9	4615	7.65	Acetylation	C5UP91	Stage II sporulation protein P_TRP1
4640.2	85	1	4639.2	4606.9	4638.9	4.98	Dihydroxylation	C5UV84	Spore cortex-lytic enzyme_TRP2
4952.2	53	1	4951.2	4647.2	4952.5	8.93	Gluthationylation	C5UXY8	RNA polymerase sigma factor_TRP1
5098	66	1	5097	5070.3	5098.3	4.63	Dimethylation	C5UT36	Spore-cortex-lytic enzyme, sleb_TRP1
5098	66	1	5097	5070.3	5098.3	5.09	Dimethylation	C5UT36	Spore-cortex-lytic enzyme, sleb_TRP1
5647.8	8	1	5646.7	5649	5649	9.66	unmodified	C5UU73	Spore cortex biosynthesis protein YabQ_TRP1
6091.8	36	1	6090.7	6092.4	6092.4	8.04	unmodified	C5UY96	Conserved domain protein

6112.5	20	1	6111.5	6092.4	6110.4	8.04	Water	C5UY96	Conserved domain protein
6344.5	70	1	6343.5	6300.1	6342.1	5.7	Acetylation	C5URF0	Stage V sporulation protein AF_TRP2
6375.5	105	2	12749	12730.7	12744.	5.89	Methylation	C5UPA2	Anti-sigma F factor antagonist
6829.5	36	1	6828.5	6817.4	6831.4	6.51	Methylation	C5US13	Stage III sporulation protein AC
7949.5	5	1	7948.5	7909.7	7951.7	4.67	Acetylation	C5UUG2	Putative spore-cortex-lytic enzyme_TRP1
9629.5	14	2	19257	19221.4	19249.	9.38	Dimethylation	C5UUT2	Spore maturation protein
9792.5	5	1	9791.5	9710.4	9790.4	9.77	Phosphorylation	C5URS8	Stage III sporulation protein D
10192.2	56	2	20382.5	20387.5	20387.	8.99	unmodified	C5UUT3	Spore maturation protein A
10477.8	6	1	10476.7	10309.8	10472	4.59	Glucosylation	C5UXY1	Sporulation protein, YlmC/YmxH family

Table AIV: MALDI-TOF MS based protein identification in TMW 2.990 endospores derived from AEY. The table provides measured peaks and intensities which were acquired by MALDI-TOF MS (first and second column). Based on peak detection and in due consideration of the mass to charge ratio (column three), potential protein/peptide masses were calculated (column four). In the fifth column (mass (db), protein masses are present, which were provided by UniProtUK or resulted from trypsin digestion (calculated by the PeptideMass tool, provided on the ExPASy portal). The sixth column (mass (db) + PTM) represents the peptide masses of column five by considering of post translational modifications (column eight). Resulting isoelectric points are illustrated in column seven. In column nine, database entries of identified proteins are depicted, secondary protein names are specified in column ten. The symbols “_TPRX” behind the protein description indicates the number of peptide fragment, which resulted from trypsin digestion of the identified protein.

peak (m/z)	intensity	charge	cal. mass	mass (db)	mass (db) + PTM	pI (db)	modification	UniProtKB entry	protein name_(nr. of peptide after trypsin digestion)
2044.2	45	1	2043.2	2028.3	2042.4	9.6	Methylation	C5US90	Stage II sporulation protein M_TRP6
2044.2	45	1	2043.2	2030.1	2044.2	7.65	Methylation	C5UP91	Stage II sporulation protein P_TRP4
2130.8	36	1	2129.7	2115.3	2129.3	9.16	Methylation	C5UXU1	Sporulation integral membrane protein YibJ_TRP9
2132	35	1	2131	2117.4	2131.4	6.54	Methylation	C5UZM9	Putative uncharacterized protein_TRP3
2158	61	1	2157	2157.2	2157.2	8.52	unmodified	C5UVZ8	Putative sporulation protein YyaC_TRP2
2158	61	1	2157	2157.4	2157.4	4.57	unmodified	C5UUU1	CotH protein_TRP15

2186.2	50	1	2185.2	2168.4	2184.4	5.6	Hydroxylation	C5UVY6	ATP-dependent protease, Lon family_TRP5
2304.5	19	1	2303.5	2285.6	2303.6	5.25	Water	C5UU70	Stage II sporulation protein E_TRP10
2318	20	1	2317	2316.6	2316.6	4.92	unmodified	C5UP92	Germination protease_TRP4
2385.2	84	1	2384.2	2352.7	2384.7	4.93	Dihydroxylation	C5UXW8	Stage IV sporulation protein A_TRP5
2403	49	1	2402	2372.8	2400.9	9.38	Dimethylation	C5UUT2	Spore maturation protein B_TRP4
2403	49	1	2402	2373.8	2401.9	9.74	Dimethylation	C5UP97	Stage V sporulation protein AE_TRP2
2403	49	1	2402	2373.8	2401.9	8.82	Dimethylation	C5UP97	Stage V sporulation protein AE_TRP2
2429.8	49	1	2428.7	2427.6	2427.6	5.75	unmodified	C5UVN1	Spore coat polysaccharide biosynthesis protein SpsC_TRP3
2458	45	1	2457	2442.1	2456.1	9.16	Methylation	C5UXU1	Sporulation integral membrane protein YibJ_TRP8
2458	45	1	2457	2443.8	2457.8	6.09	Methylation	C5UVG3	Putative spore-cortex-lytic enzyme_TRP5
2627.2	29	1	2626.2	2607.1	2625.2	8.99	Water	C5UUT3	Spore maturation protein A_TRP5
2627.2	29	1	2626.2	2608.2	2626.2	9.38	Water	C5UUT2	Spore maturation protein B_TRP3
2627.2	29	1	2626.2	2608.2	2626.2	4.57	Water	C5UUU1	CotH protein_TRP9
2671	53	1	2670	2669	2669	5.01	unmodified	C5URP3	Delta-lactam-biosynthetic de-N-acetylase_TRP1
2671	53	1	2670	2669	2669	5.5	unmodified	C5URP3	Delta-lactam-biosynthetic de-N-acetylase_TRP1
2730.5	39	1	2729.5	2715.3	2729.3	5.38	Methylation	C5US12	Stage III sporulation protein AB_TRP3
2730.5	39	1	2729.5	2715.3	2729.3	9.6	Methylation	C5US90	Stage II sporulation protein M_TRP4
2739.5	32	1	2738.5	2721.2	2737.2	9.45	Hydroxylation	C5UPN2	Stage V sporulation protein _TRP9
2739.5	32	1	2738.5	2721.2	2737.2	9.35	Hydroxylation	C5UPN2	Stage V sporulation protein B_TRP9
2739.5	32	1	2738.5	2722.4	2738.4	9.53	Hydroxylation	C5UXH6	Spore germination protein _TRP7
2790	19	1	2789	2790.2	2790.2	6.09	unmodified	C5UVG3	Putative spore-cortex-lytic enzyme_TRP3
2997	122	1	2996	2969.3	2997.3	4.67	Dimethylation	C5UVG2	Putative spore-cortex-lytic enzyme_TRP6
3213.2	226	1	3212.2	3196.5	3212.5	8.91	Hydroxylation	C5UTB9	Peptidase M56, BlaR1, putative_TRP3
3330.5	43	1	3329.5	3286.7	3328.7	4.57	Acetylation	C5UUU1	CotH protein _TRP6

3483.8	291	1	3482.7	3483.2	3483.2	9.66	unmodified	C5UU73	Spore cortex biosynthesis protein YabQ_TRP2
3581.2	1806	1	3580.2	3553.9	3581.9	5.14	Dimethylation	C5URA3	Putative uncharacterized protein_TRP1
3628.8	872	1	3627.7	3613.4	3627.5	9.45	Methylation	C5UPN2	Stage V sporulation protein_TRP5
3628.8	872	1	3627.7	3613.4	3627.5	9.35	Methylation	C5UPN2	Stage V sporulation protein B_TRP5
3969	233	1	3968	3948.4	3966.4	5.21	Water	C5UY42	Stage V sporulation protein R_TRP1
4257.5	25	1	4256.5	4254.5	4254.5	4.57	unmodified	C5UUU1	CotH protein_TRP3
4952	80	1	4951	4647.2	4952.5	8.93	Glutathionylation	C5UXY8	RNA polymerase sigma factor_TRP1
5098	57	1	5097	5070.3	5098.3	4.63	Dimethylation	C5UT36	Spore-cortex-lytic enzyme, sleb_TRP1
5098	57	1	5097	5070.3	5098.3	5.09	Dimethylation	C5UT36	Spore-cortex-lytic enzyme, sleb2_TRP1
6092	25	1	6091	6092.4	6092.4	8.04	unmodified	C5UY96	Conserved domain protein
6112.8	17	1	6111.7	6092.4	6110.4	8.04	Water	C5UY96	Conserved domain protein
6829.8	55	1	6828.7	6817.4	6831.4	6.51	Methylation	C5US13	Stage III sporulation protein AC
7949	8	1	7948	7909.7	7951.7	4.67	Acetylation	C5UVG2	Putative spore-cortex-lytic enzyme_TRP1
8926.8	7	1	8925.7	8907.1	8923.1	9.3	Hydroxylation	C5UZP4	Sigma-K factor processing regulatory protein BofA
9629.8	64	2	19257.5	19221.4	19249.	9.38	Dimethylation	C5UUT2	Spore maturation protein B
9792	4	1	9791	9710.4	9790.4	9.77	Phosphorylation	C5URS8	Stage III sporulation protein D
10192.8	44	2	20383.5	20387.5	20387.	8.99	unmodified	C5UUT3	Spore maturation protein A
10766.8	3	1	10765.7	10730.3	10762.	4.53	Dihydroxylation	C5UX61	Sporulation protein, YImC/YmxH family

Peptide identification by high resolution LC-MS/MS

Table AV: Putative amino acid sequences of identified peptide fragments. The table illustrates the putative amino acid sequences of identified peptides, which were associated to high resolution LC-MS/MS analyses of the characteristic SDS gel bands (3.2.3). For sequence analyzes, the distinct protein band, which were associated to sporulation of TMW 2.990 in SFE (ca. 225 kDa) were used. Based on mass similarity of individual amino acids and on unpredictability of spatial orientations of dipeptides, potential sequence variation of defined peptides are listed.

No. of identified peptide fragment	Putative amino acid sequence
1	GTAPMPNGF
	ASAPMPNGF
	RYETNAAVIQK
	RYETNAAVIKK
	RYETNAAVLQK
2	RYETNAAVLKK
	KYETNAAVIQK
	KYETNAAVIKK
	KYETNAAVLKK
3	TSEE
4	FEATG
	GTAEF
5	FDITP
	FDLTP
	PTIDK
	PTLDK
	PTISR
	PTLSR
	KFGVVIFEGYPK
6	KFGVVLFEFYPK
	KGFVVIFEGYPK
	KGFVVLFEFYPK
	RFGVVIFEGYPK
	RFGVVLFEFYPK
	RGFVVIFEGYPK
	RGFVVLFEFYPK
7	IGDEDV
	LGDEDV
8	KNANNVYFEAK
	RNANNVYFEAK
9	VVNFVVK
	VVNNFVK

10	RITITAK RLTITAK RITLTAK RLTLTAK
11	AFNITFK AFNLTFK
12	HSPDDITE HSPDDLTE
13	APIIINDAK APIILNDK APILINDAK APILLNDK APLLLNDK APLLINDAK APLILNDK APLIINDAK
14	GWYGFIVVGK WGYGEFIVVGK DQYGEFIVVGK QDYGEFIVVGK ENYGEFIVVGK NEYGETFVVGK GWYGEFLVVGK WGYGEFLVVGK DQYGEFLVVGK QDYGEFLVVGK ENYGEFLVVGK NEYGEFLVVGK

Integral creaming kinetics

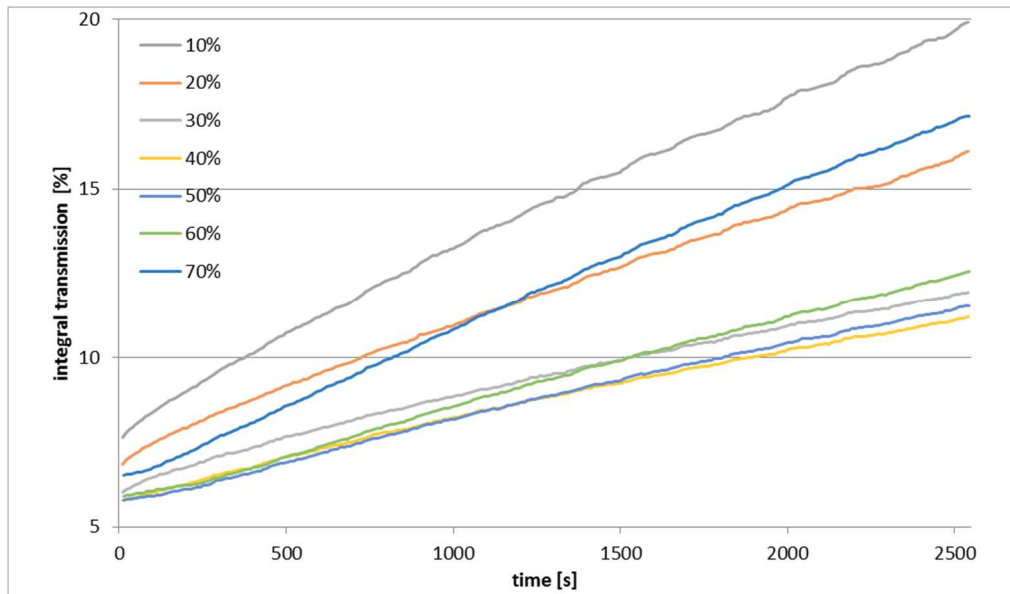


Figure AI: Integral creaming kinetics of untreated soybean oil emulsions with fat contents of 10 – 70%.

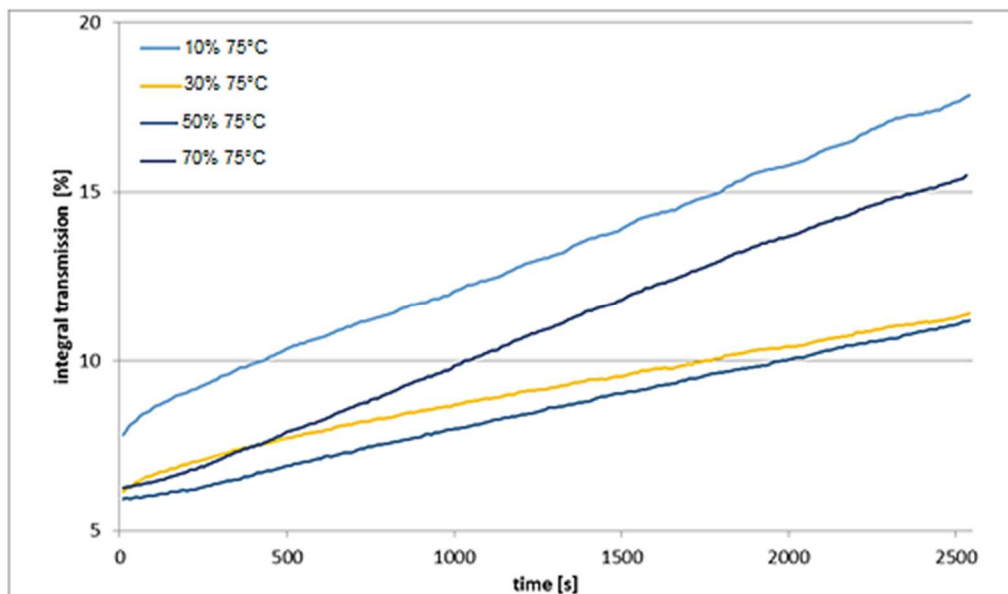


Figure AII: Integral creaming kinetics of heat-treated soybean oil emulsions with fat contents of 10, 30, 50 and 70%.

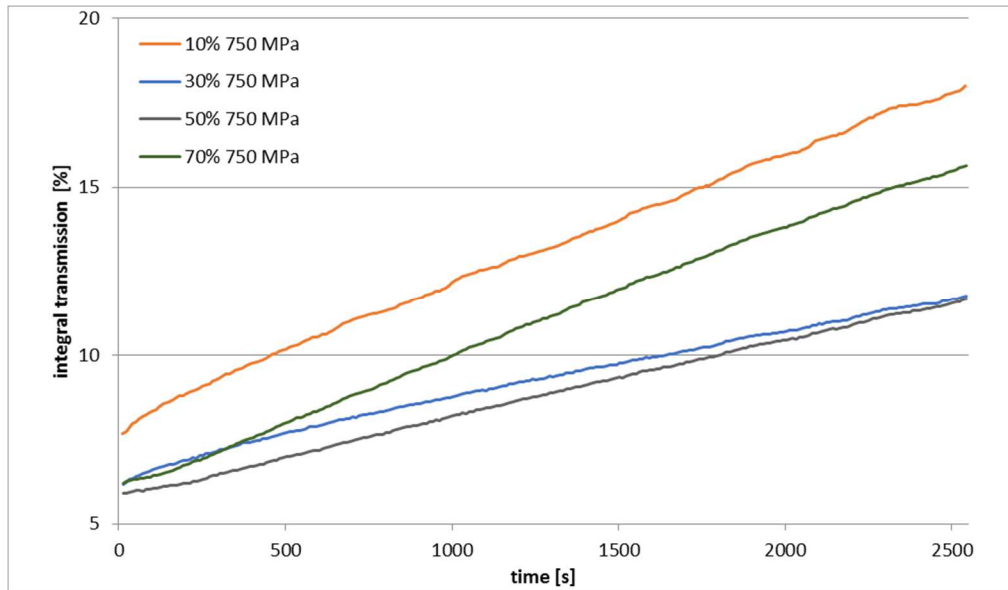


Figure AIII: Integral creaming kinetics of pressure-treated soybean oil emulsions with fat contents of 10, 30, 50 and 70%.

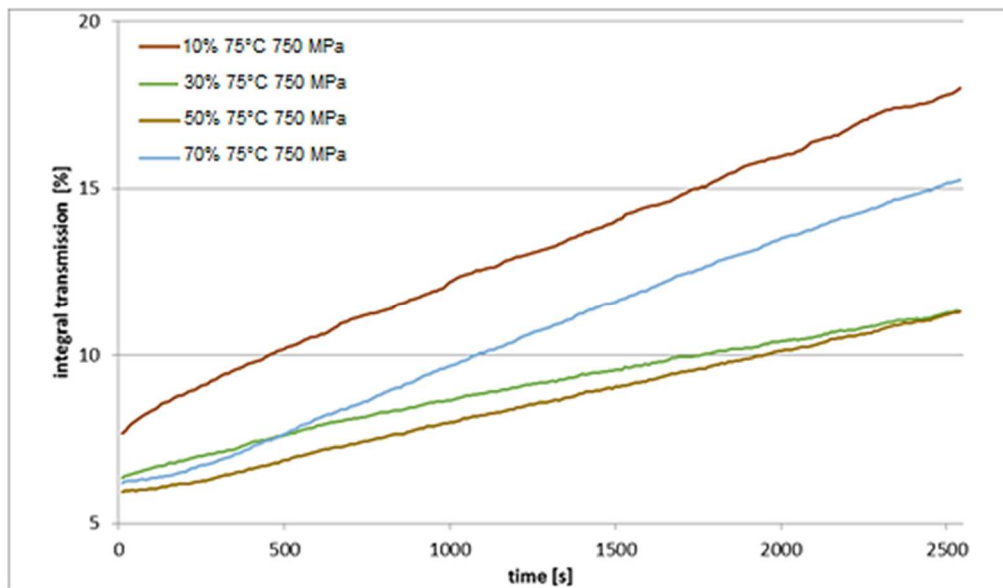


Figure AIV: Integral creaming kinetics of heat/pressure-treated soybean oil emulsions with fat contents of 10, 30, 50 and 70%.

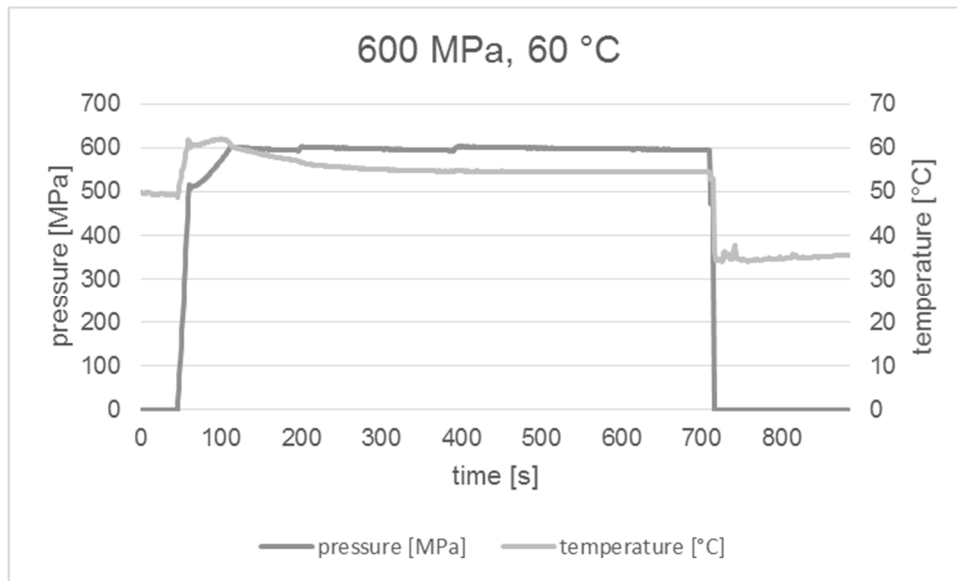


Figure AV: High pressure- temperature-time profile recorded during HPT in the single vessel apparatus U4000. The figure displays pressure and temperature profiles as a function of time, when experimental parameters of 600 MPa and 60 °C were employed. Pressure profiles are displayed in black, while temperature profiles are depicted in grey. During pressure holding, mean parameters of 55.39 °C and 598 MPa were monitored in the pressure transferring liquid. Pressure were generated and degenerated by rates of 9.64 and 99.66 MPa/s.

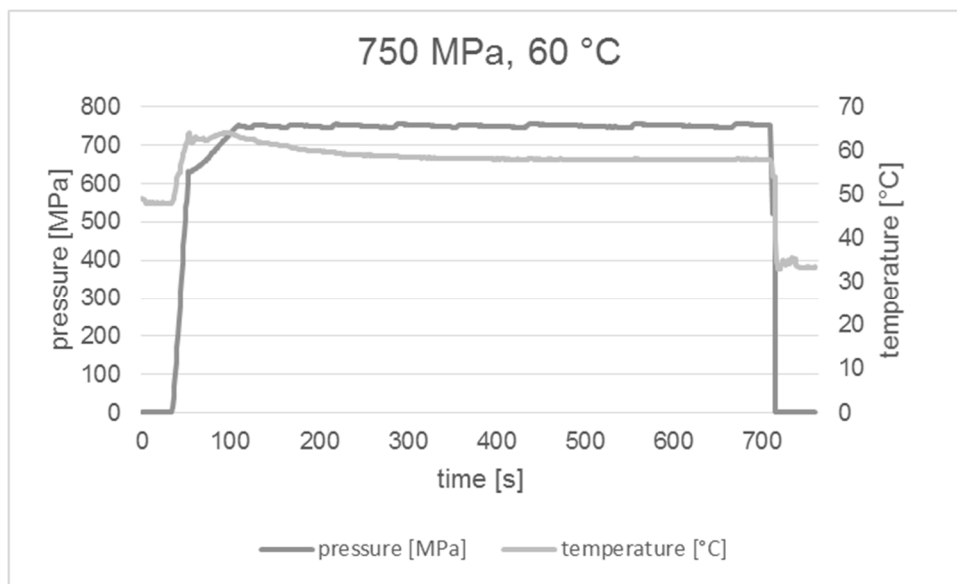


Figure AVI: High pressure- temperature-time profile monitored during HPT in the single vessel apparatus U4000. The figure illustrated pressure and temperature profiles as a function of time, when experimental parameters of 750 MPa and 60 °C were applied. Pressure profiles are displayed in black, while temperature profiles are depicted in grey. During pressure holding, mean parameters of 58.74 °C and 751 MPa were monitored in the pressure transferring liquid. Pressure were generated and degenerated by rates of 10.88 and 125.09 MPa/s.

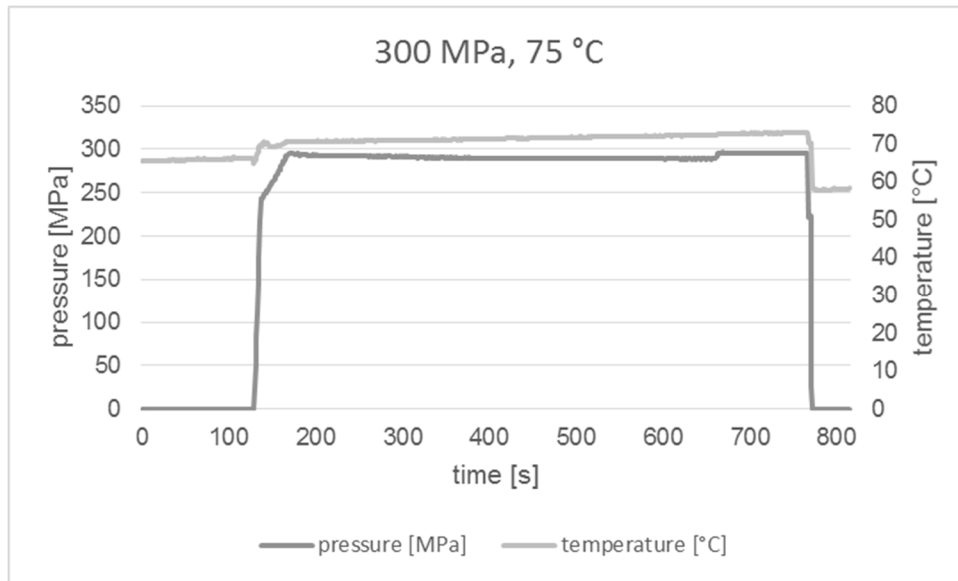


Figure AVII: High pressure- temperature-time profile recorded during HPT in the single vessel apparatus U4000. The figure displays pressure and temperature profiles as a function of time, when experimental parameters of 300 MPa and 75 °C were employed. Pressure profiles are displayed in black, while temperature profiles are depicted in grey. During pressure holding, mean parameters of 71.64 °C and 291 MPa were monitored in the pressure transferring liquid. Pressure were generated and degenerated by rates of 5.11 and 48.56 MPa/s.

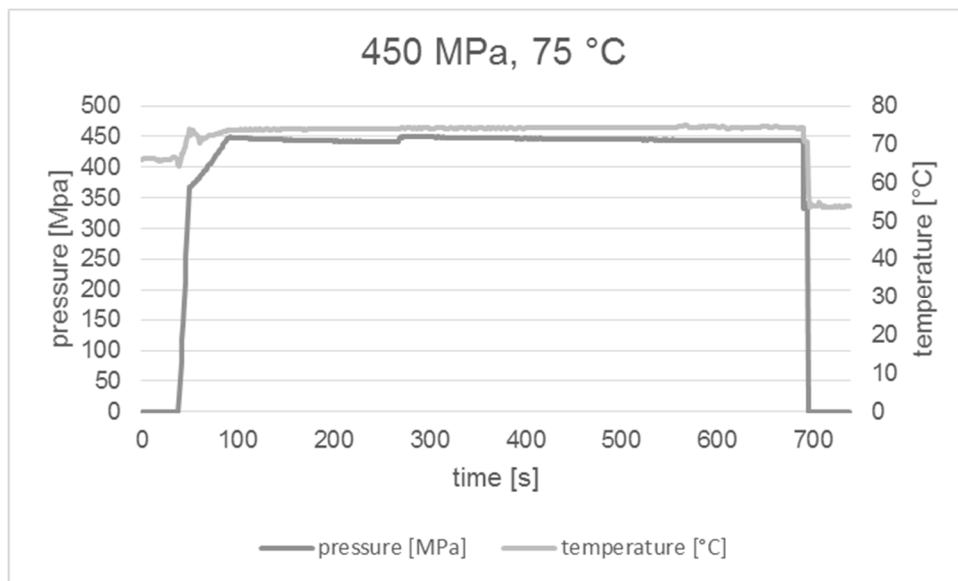


Figure AVIII: High pressure- temperature-time profile monitored during HPT in the single vessel apparatus U4000. The figure illustrated pressure and temperature profiles as a function of time, when experimental parameters of 450 MPa and 60 °C were applied. Pressure profiles are displayed in black, while temperature profiles are depicted in grey. During pressure holding, mean parameters of 74.20 °C and 445.06 MPa were monitored in the pressure transferring liquid. Pressure were generated and degenerated by rates of 8.40 and 74.17 MPa/s.

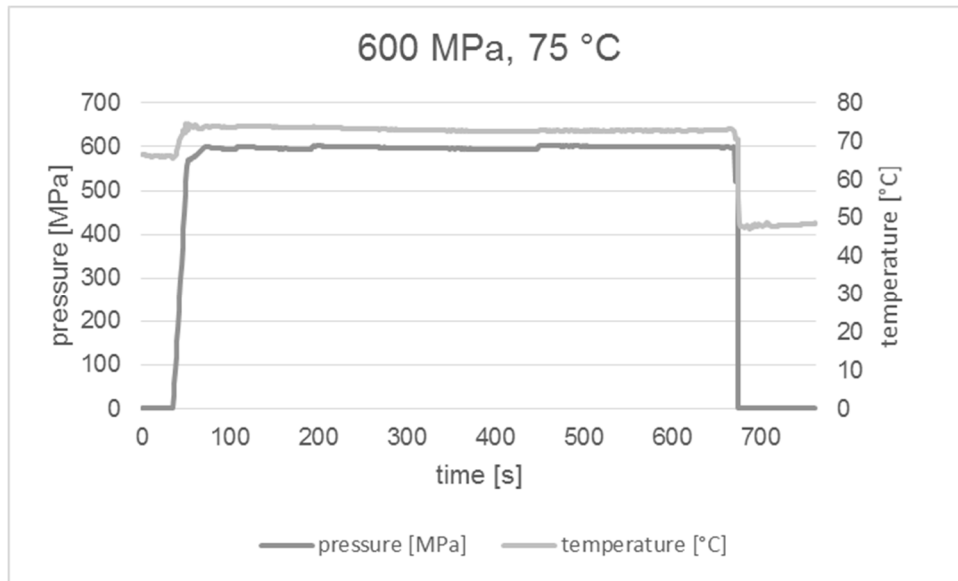


Figure AIX: High pressure- temperature-time profile recorded during HPT in the single vessel apparatus U4000. The figure displays pressure and temperature profiles as a function of time, when experimental parameters of 600 MPa and 75 °C were employed. Pressure profiles are displayed in black, while temperature profiles are depicted in grey. During pressure holding, mean parameters of 73 °C and 598.3 MPa were monitored in the pressure transferring liquid. Pressure were generated and degenerated by rates of 16.17 and 119.66 MPa/s.

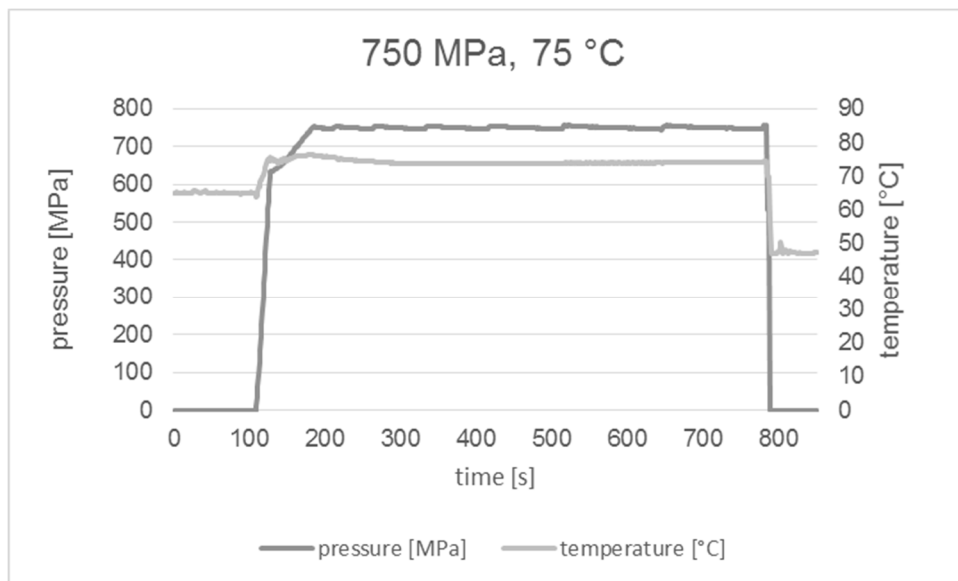


Figure AX: High pressure- temperature-time profile monitored during HPT in the single vessel apparatus U4000. The figure illustrated pressure and temperature profiles as a function of time, when experimental parameters of 750 MPa and 60 °C were applied. Pressure profiles are displayed in black, while temperature profiles are depicted in grey. During pressure holding, mean parameters of 74.05 °C and 750 MPa were monitored in the pressure transferring liquid. Pressure were generated and degenerated by rates of 10.0 and 125.05 MPa/s.

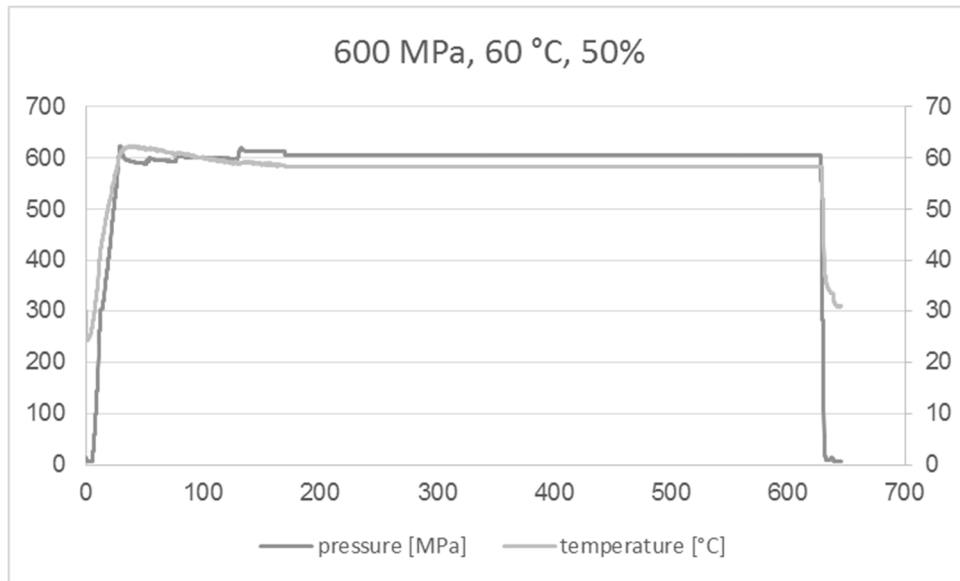


Figure AXI: High pressure- temperature-time profile monitored during HPT in the low temperature vessel U111. The figure illustrated pressure and temperature profiles as a function of time, when experimental parameters of 600 MPa, 60 °C and 50% soybean oil emulsions were used. Pressure profiles are displayed in black, while temperature profiles are depicted in grey. During pressure holding, mean parameters of 60.18 °C and 602.18 MPa were monitored in the emulsion with 50% fat. Pressure were generated and degenerated by rates of 21.65 and 60.22 MPa/s.

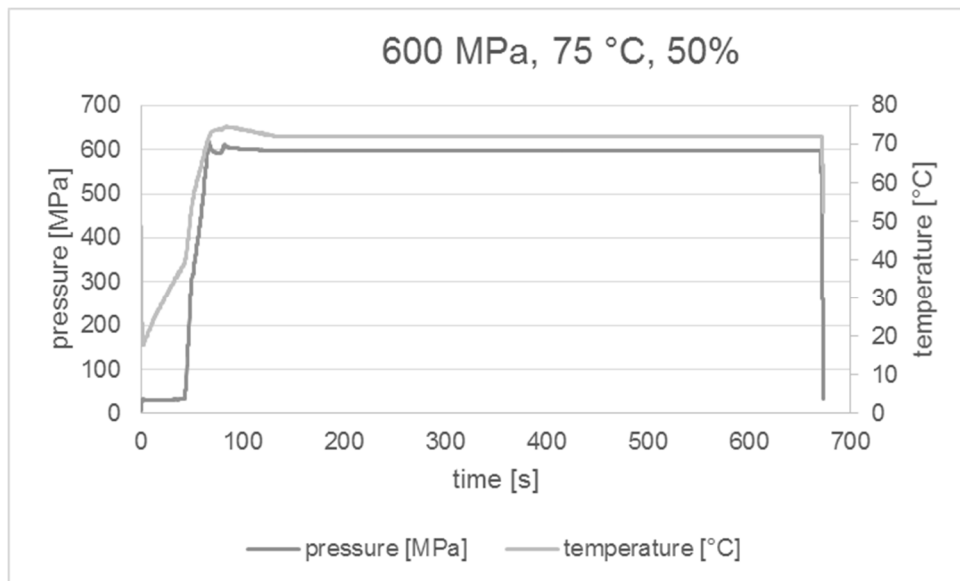


Figure AXII: High pressure- temperature-time profile monitored during HPT in the low temperature vessel U111. The figure illustrated pressure and temperature profiles as a function of time, when experimental parameters of 600 MPa, 75 °C and 50% soybean oil emulsions were used. Pressure profiles are displayed in black, while temperature profiles are depicted in grey. During pressure holding, mean parameters of 72.63 °C and 599.48 MPa were monitored in the emulsion with 50% fat. Pressure were generated and degenerated by rates of 7.49 and 172 MPa/s.

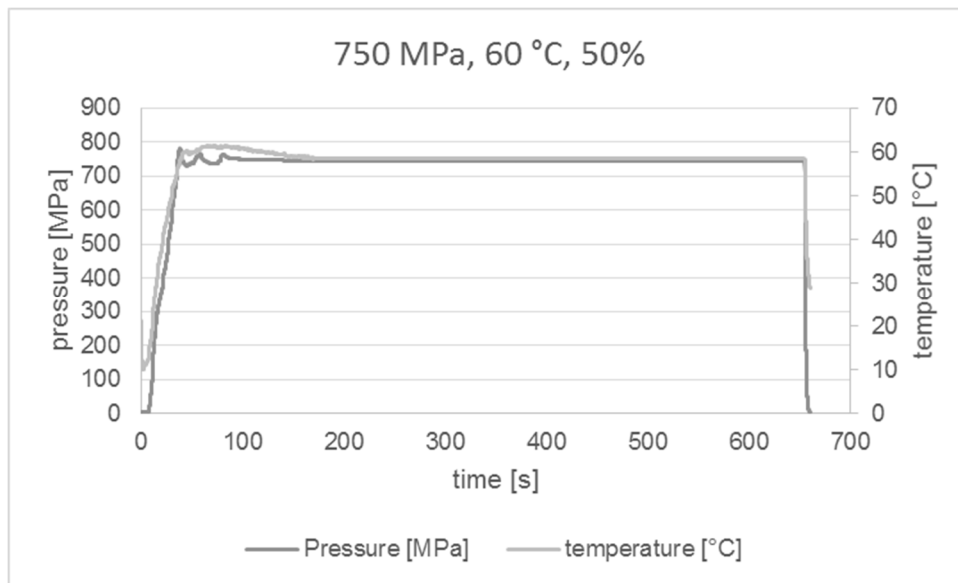


Figure AXIII: High pressure- temperature-time profile monitored during HPT in the low temperature vessel U111. The figure illustrated pressure and temperature profiles as a function of time, when experimental parameters of 750 MPa, 60 °C and 50% soybean oil emulsions were used. Pressure profiles are displayed in black, while temperature profiles are depicted in grey. During pressure holding, mean parameters of 59.64 °C and 747.41 MPa were monitored in the emulsion with 50% fat. Pressure were generated and degenerated by rates of 20.76 and 373.5 MPa/s.

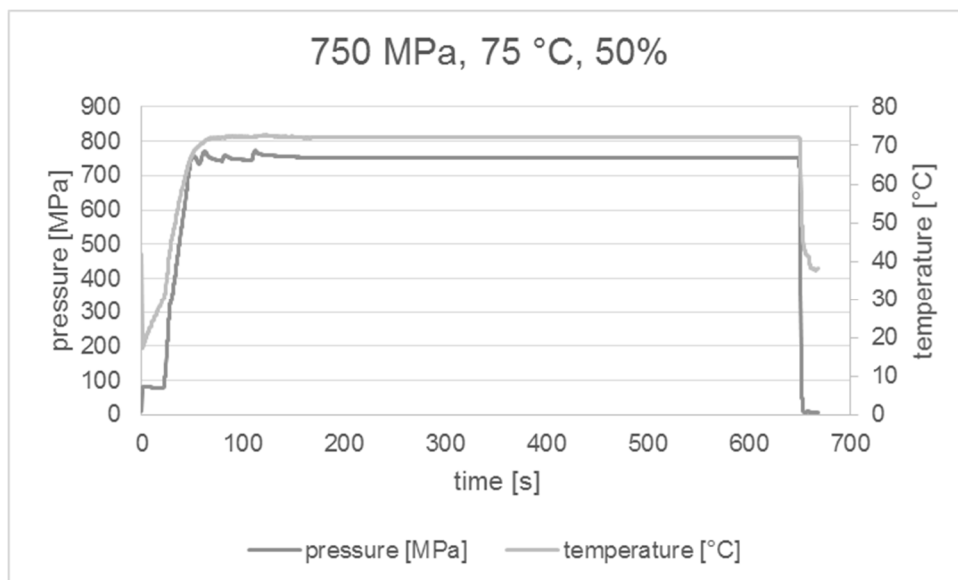


Figure AXV: High pressure- temperature-time profile monitored during HPT in the low temperature vessel U111. The figure illustrated pressure and temperature profiles as a function of time, when experimental parameters of 750 MPa, 75 °C and 50% soybean oil emulsions were used. Pressure profiles are displayed in black, while temperature profiles are depicted in grey. During pressure holding, mean parameters of 71.96 °C and 752.90 MPa were monitored in the emulsion with 50% fat. Pressure were generated and degenerated by rates of 15.36 and 188.22 MPa/s.